A synergy between well-defined homogeneous and heterogeneous catalysts : the case of Ring Opening - Ring Closing Metathesis of cyclooctene

Santosh Kavitake

N° d'ordre

Année 2011

THESE DE L'UNIVERSITE DE LYON

Délivrée par

L'UNIVERSITE CLAUDE BERNARD LYON 1

ECOLE DOCTORALE

DIPLOME DE DOCTORAT

(arrêté du 7 août 2006)

soutenue publiquement le

14 October 2011

par

M. KAVITAKE Santosh

A synergy between well-defined homogeneous and heterogeneous catalysts: the case of Ring Opening - Ring Closing Metathesis of cyclooctene

Directeur de thèse: M. Christophe Copéret
Co-Directeur de thèse: M. Chloé Thieuleux

Jury :
M. Christian Bruneau (University of Rennes)
M. Bert Sels (Katholic University of Leuven)
M. Antoine Gédéon (UPMC, Paris)
M. Christophe Copéret (ETH, Zurich)
M. Chloé Thieuleux (University of Claude Bernard Lyon 1)
M. Daniele Stephane (University of Claude Bernard Lyon 1)
M. Michael Limbach (BASF, Germany)

Rapporteurs:
M. Christian Bruneau
M. Bert Sels

UNIVERSITE CLAUDE BERNARD - LYON 1

Président de l'Université	**M. A. Bonmartin**
Vice-président du Conseil d'Administration	M. le Professeur G. Annat
Vice-président du Conseil des Etudes et de la Vie Universitaire	M. le Professeur D. Simon
Vice-président du Conseil Scientifique	M. le Professeur J-F. Mornex
Secrétaire Général	M. G. Gay

COMPOSANTES SANTE

Faculté de Médecine Lyon Est – Claude Bernard	Directeur : M. le Professeur J. Etienne
Faculté de Médecine et de Maïeutique Lyon Sud – Charles Mérieux	Directeur : M. le Professeur F-N. Gilly
UFR d'Odontologie	Directeur : M. le Professeur D. Bourgeois
Institut des Sciences Pharmaceutiques et Biologiques	Directeur : M. le Professeur F. Locher
Institut des Sciences et Techniques de la Réadaptation	Directeur : M. le Professeur Y. Matillon
Département de formation et Centre de Recherche en Biologie Humaine	Directeur : M. le Professeur P. Farge

COMPOSANTES ET DEPARTEMENTS DE SCIENCES ET TECHNOLOGIE

Faculté des Sciences et Technologies	Directeur : M. le Dr. F. Demareln
Département Biologie	Directeur : M. le Professeur F. Fleury
Département Chimie Biochimie	Directeur : Mme le Professeur H. Parrot
Département GEP	Directeur : M. N. Siauve
Département Informatique	Directeur : M. le Professeur S. Akkouche
Département Mathématiques	Directeur : M. le Professeur A. Goldman
Département Mécanique	Directeur : M. le Professeur H. Ben Hadid
Département Physique	Directeur : Mme S. Fleck
Département Sciences de la Terre	Directeur : Mme le Professeur I. Daniel
UFR Sciences et Techniques des Activités Physiques et Sportives	Directeur : M. C. Collignon
Observatoire de Lyon	Directeur : M. B. Guiderdoni
Ecole Polytechnique Universitaire de Lyon 1	Directeur : M. P. Fournier
Ecole Supérieure de Chimie Physique Electronique	Directeur : M. G. Pignault
Institut Universitaire de Technologie de Lyon 1	Directeur : M. le Professeur C. Coulet
Institut de Science Financière et d'Assurances	Directeur : M. le Professeur J-C. Augros
Institut Universitaire de Formation des Maîtres	Directeur : M. R. Bernard

Acknowledgement

I would like to express my deep and sincere gratitude to my supervisor, Professor Copéret Christophe and Dr. Thieuleux Chloé for their stimulating suggestions and encouragement that motivated me throughout my research and writing of this thesis.

I wish to express my warm and sincere thanks to Laurent Veyre for his valuable technical support throughout my research work.

My special thanks to my friend Samantaray Manoja Kumar for his help in the synthesis of homogeneous catalysts and valuable discussions we had during my research work.

I wish to specially thank my friends Baudouin David and Baffert Mathieu for helping me on my arrival in Lyon. I wish to thank all of my colleagues in our group for creating cooperative and pleasant atmosphere in the lab during the course of my work making me feel at home.

My deepest gratitude goes to my parents, especially my father and my mother for their love and support throughout my life, this dissertation would have been simply impossible without them.

My loving thanks to my wife, Nirmala and my sons, Aditya and Ameya, for their support. Without their encouragement and understanding it would have been impossible for me to finish this work.

I would also like to thank Mr. Michael Limbach, Mr. Richard Dehn and Mr. Stephan Deuerlein from BASF, for their support throughout this project.

Abstract

In the context of the selective formation of cyclic oligomers from cyclooctene, well-defined hybrid organic-inorganic mesoporous materials containing unsymmetrical Ru-NHC units along the pore channel of their silica matrix have been developed and characterized at a molecular level. All systems displayed high activity and selectivity towards the formation of lower cyclic oligomers in the RO-RCM of cyclooctene yielding mainly the dimer and the trimer with 50% and 25% selectivity, respectively, in contrast to classical symmetrical homogeneous analogues (**G-II** and **GH-II**), which yield mainly to polymers. Variation of length and flexibility of the tethers showed that flexible short tethers were critical for high stability of the catalysts during metathesis, which is consistent with the stabilization of Ru-NHC active sites by surface functionalities; this surface interaction was further corroborated by the absence of a PCy_3 ligand coordinated to Ru when short flexible linkers are used. Further investigations using homogeneous symmetrical (**G-II** and **Nolan**) and unsymmetrical (analogues to heterogeneous catalysts) Ru-NHC catalysts clearly showed that the key factor influencing the selectivity towards low cyclic oligomers is the unsymmetrical nature of NHC ligands, which creates dual site configuration in the catalyst architecture thus alternatively favouring one reaction over another, Ring Opening (ROM) *vs.* Ring Closing (RCM) Metathesis (propagation *vs.* backbiting), thus leading to the selective tandem RO-RCM of cyclooctene. Finally, we have also investigated Grubbs Hoveyda-II (**GH-II**) type catalysts immobilized on silica support through adsorption, which showed the same product selectivity as that of the well-defined Ru-NHC materials. This result implies that the adsorbed symmetrical **GH-II** catalyst "becomes unsymmetrical upon adsorption". Adsorbing unsymmetrical molecular **GH II** catalysts did not however improve the performances of these types of catalysts. Overall, the unique property of unsymmetrical NHC Ru catalyst, whether

supported or not, opens new perspectives in the selective synthesis of macrocycles from other cyclic alkenes via metathesis.

Table of contents

Chapter 2: Synthesis of hybrid organic-inorganic, heterogeneous Ru-NHC catalysts and their catalytic performances in RO-RCM of cyclooctene

Chapter 3: Synthesis and catalytic performances of homogeneous unsymmetrical and symmetrical Ru-NHC catalysts

Chapter 4: Synthesis and Catalytic performances of homogeneous and supported symmetrical and unsymmetrical GH-II catalysts

Abbreviations

δ	Chemical shift in NMR downfield from TMS, ppm
Å	Angstrom
BET	Brunauer-Emmett-Teller
BJH	Barret-Joyner-Halenda
°C	Relative temperature in Celsius degree: T = °C + 273.15
CP	Cross-Polarisation
DRIFT	Diffuse reflectance infrared fourier transform
ESI	Electron spray ionization
h	Hour
HRMS	High resolution mass spectrometry
IR	infrared
MAS	Magic angle spinning
P123	Pluronic P123
TON	turn over number, mol.molmetal-1
TOF	turn over frequency, mol.mol metal-1.unit time-1
NMR	nuclear magnetic resonance
RT	room temperature

Introduction

The main objective of this study was to selectively form low cyclic oligomers, in particular dimer via RO-RCM of cyclooctene, using well-defined, heterogeneous Ru-NHC catalysts.

Chapter 1: Reviews the history of olefin metathesis in terms of catalysts developments and olefin metathesis applications. Also deals with the introduction to the mesoporous organic-inorganic hybrid materials.

Chapter 2: Describes the synthesis of well-defined, heterogeneous Ru-NHC catalysts and their catalytic performances in RO-RCM of cyclooctene for selective formation of low cyclic oligomers. The influence of the length and rigidity of the tether in terms of reactivity, stability and selectivity in RO-RCM of cyclooctene has been discussed in this chapter.

Chapter 3: Describes the synthesis of unsymmetrical homogeneous catalysts analogues to the hybrid, heterogeneous Ru-NHC catalysts and their catalytic performances in RO-RCM of cyclooctene. Comparison of the catalytic performances between homogeneous and heterogeneous systems has been studied in order to understand the influence of the unsymmetrical nature of the NHC ligands in the RO-RCM of cyclooctene for selective formation of low cyclic oligomers.

Chapter 4: In this chapter, synthesis, characterization and catalytic performances of GH-II type heterogeneous (symmetrical and unsymmetrical) Ru-NHC complexes adsorbed on silica support, in RO-RCM of cyclooctene has been invetigated. The influence of the silica support (SP Grace) on catalytic performances has been discussed.

Chapter 5: Gives an overall conclusion and possible perspectives.

Chapter 1

Bibliography

1. Introduction

In 2005, three researchers were awarded with the Nobel Prize in Chemistry: Dr. Yves Chauvin, Professor Robert H. Grubbs and Professor Richard R. Schrock "*for the development of the metathesis method in organic synthesis, in which carbon-carbon double bonds are broken and formed catalytically*".[1] Their discoveries had great influence on the development of biologically active heterocyclic compounds leading to development of new drugs, academic research, polymer science and industrial applications.

The metathesis history is immense and composed of olefin metathesis,[2] enyne metathesis,[3] and alkyne metathesis reactions.[4] Since it would be impossible to cover all aspects of this very versatile reaction, we will thus mainly focus on olefin metathesis reaction, some key Ru based catalyst developments, mechanism of olefin metathesis reaction and some selected examples of supported catalyst systems.

1.1. Type of olefin metathesis reactions

The application of olefin metathesis catalysts for performing various transformations with different olefinic substrates and conditions has resulted in the several well-known olefin metathesis reactions, mainly divided in the following reaction types.

1. Ring-opening metathesis polymerization (ROMP)[5]
2. Acyclic diene metathesis polymerization (ADMET)[6]
3. Ring-closing metathesis (RCM)[7]
4. Self and Cross metathesis (CM)[8]

1.1.1. Ring-opening metathesis polymerization (ROMP)

The enthalpic driving force for irreversible ring-opening of ROMP monomers, (norbornene and cyclooctene), is the ring-strain release.[9] Consequently, olefins such as cyclohexene with little ring strain cannot be polymerized easily. Exceptionally, cyclooctene represents an unusual case, as the polymerization is favoured both entropically and enthalpically: it is thus polymerizable at any temperature.[10]

Although, the pathway back to the cyclic compound(s) has to overcome a significant thermodynamic barrier, backbiting to give cyclic oligomers (cyclic dimers, trimers….) remains possible. The formation of cyclic oligomers from cyclic olefins is termed as ring opening-ring closing metathesis (RO-RCM)[11] (Scheme 1).

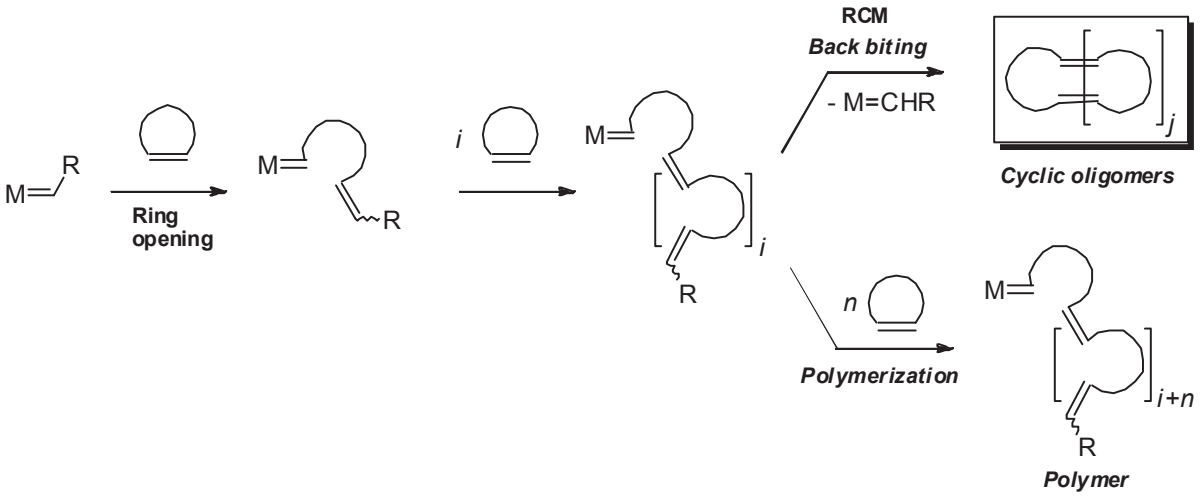

Scheme 1: General representation of polymerization *vs.* backbiting (ROMP *vs.* RO-RCM).

1.1.1.1. ROMP *vs.* RO-RCM

Concentration-dependence is a key feature of these ring-chain equilibria between cyclic oligomers and polymers. With high monomer concentrations ROMP predominates while dilution plays a major role in shifting the equilibrium towards the formation of smaller, cyclic species (RO-RCM) thus favoring backbiting over polymerization.[12] Höcker observed a steady increase in the proportion of cyclic oligomers prior to formation of a measurable amount of polymer[13] and proposed an initial bias toward either cyclic oligomers or linear polymer.[14] The favored pathway was proposed to correlate with the degree of ring strain and the reactivity of the catalyst. Metathesis of high-strain cycloolefins by catalysts of relatively low activity was reported to initially yield high molecular weight polymers, from which cyclic oligomers were subsequently extruded by cyclodepolymerization (*i.e.* backbiting). At the opposite extreme, metathesis of low-strain cycloolefins by highly reactive catalysts gave cyclic oligomers as the kinetic products, with cyclodimers and cyclotrimers being predominant. These cyclic species underwent conversion into high-molecular weight linear polymer through a stepwise chain growth mechanism once the equilibrium concentration of each cyclic oligomer was exceeded.

1.1.2. Acyclic diene metathesis polymerization (ADMET)

ADMET is a condensation polymerization reaction and is essentially the self-metathesis of a diene, usually a terminal diene, to form polymer (Scheme 2).[15] This involves usually equilibrium processes in which the functional groups react in a stepwise fashion to form dimer from two monomers, then trimer, tetramer, and so on to high polymer.

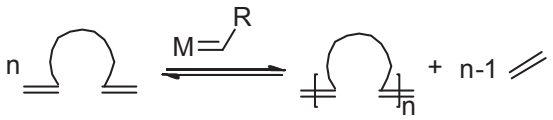

Scheme 2: Acyclic diene metathesis polymerization (ADMET).

1.1.3. Ring-closing metathesis (RCM)

The driving force for RCM is primarily entropic, as one substrate molecule gives two molecules of products (Scheme 3). Furthermore, this reaction is practically irreversible due to the release of volatile small molecules and can therefore proceed to completion.

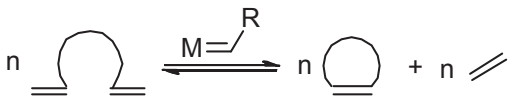

Scheme 3: Ring closing metathesis (RCM).

1.1.3.1. RCM *vs.* ADMET

In both reactions, the loss of ethylene creates a powerful, but indiscriminate, driving force for intra- and intermolecular metathesis.

The key competing reaction in RCM is oligomerization, which can be decreased by lowering the concentration of the diene or by using slow addition of the substrates. Higher temperature also favors ring closure.

ADMET is usually conducted in the absence of solvent to favor polymerization and linear chain extension over cyclization, since high concentration favors intermolecular over intramolecular reactions. Oligomeric cyclics however have also been observed in ADMET polymerization.[16] Acyclic diene metathesis is theoretically capable of cyclizing unimolecularly by the RCM reaction. Thus, monomers that will cyclize to a 5-, 6-, or 7-membered ring yield RCM over ADMET products. Monomers that would hypothetically cyclize to give 3- and 4-membered rings or larger than a 7-membered ring, are more rapidly polymerized than cyclized in ADMET conditions (concentrated solutions).

1.1.4. Cross metathesis (CM)

On the other hand, cross metathesis (CM) reaction is more challenging, as it lacks the entropic driving force of RCM and the ring-strain release of ROMP to get the desired cross-products. This reaction can be used for chain extending, chain shortening and functionalization using functional olefins (Scheme 4).

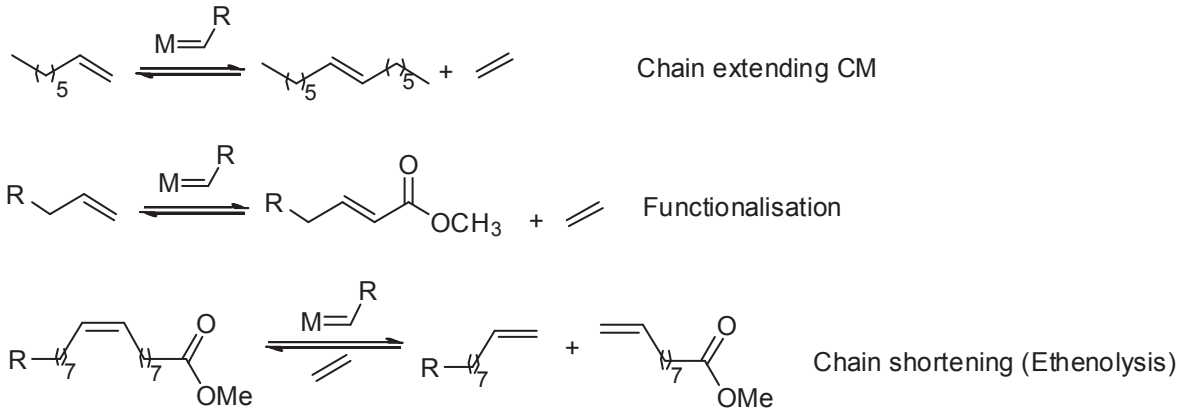

Scheme 4: Cross metathesis (CM) reactions.

1.2. Industrial applications

The olefin metathesis reaction has opened new perspectives in three important fields of industrial chemistry *i.e.* petrochemicals, polymers synthesis and fine chemicals. [17]

1.2.1. Petrochemistry

The applications of metathesis can be found in Shell Higher Olefin Process (SHOP), to produce linear higher olefins from ethylene. The Phillips triolefin process was used to produce ethylene and 2-butene from propylene. Later, a reverse process was used to produce propylene, known as the Olefins Conversion Technology (OCT).

1.2.2. Polymer synthesis

The first commercially made polymer was Norsorex, a polynorbornene compound. A process using a $RuCl_3$/HCl catalyst produces an elastomer which proved useful for oil spill recovery and as a sound or vibration barrier. Degussa-Hüls AG is manufacturing Vestenamer® 8012, a polyoctenamer via ROMP of cyclooctene using tungsten based catalyst. The polymer is used in the rubber industry to manufacture tires, molded rubber articles and roller coatings. The endo-dicyclopentadiene (DCPD), an inexpensive, readily available byproduct of the petrochemical industry, which is now subjected to ROMP to produce linear polymer, also gives cross linked polymers with cyclopentene under specific conditions. These poly-DCPD polymers are used to produce bathroom modules, lawn and garden equipment, construction machinery, body panels for trucks etc. The poly-DCPD was put on the market under the trade names TeleneR and MettonR. In the TeleneR process, molybdenum based precatalyst is activated by a mixture of Et_2AlCl, alcohol and $SiCl_4$ while the MettonR process utilizes a WCl_6 + $WOCl_4$ precursor, which is initiated by the addition of $EtAlCl_2$. Ciba Specialty Chemicals first investigated the ruthenium initiators for producing the poly-DCPD. However,

Materia made it as poly-DCPD resin, which was used in conjunction with glass and thermoplastic microspheres to produce high quality foam products. Later a Japanese company, using ruthenium technology produced a polymer which is used for various applications including bathroom devices.

1.2.3. Fine chemical industry

The development of well-defined and functional-group tolerant ruthenium catalysts has influenced the research in fine chemical research area for the synthesis of complex molecules.[18] Olefin metathesis has been used as one of the key steps in the synthesis of various agrochemicals and pharmaceuticals such as macrocyclic peptides, cyclic sulfonamides, novel macrolides, or insect pheromones.[19] Several ruthenium based metathesis initiators became commercially available at industrial relevant scale during the last couple of years, few examples - (phenylthio)methylene Ru complex 1st and 2nd generation analogues,[20] Hoveyda-derived air stable ZhanR-catalysts,[21] indenylidene based catalysts by Evonik[22] for pharmaceutical applications etc.

2. Olefin Metathesis: Historical overview

2.1. The discovery

Derived from the Greek words *meta* (change) and *thesis* (position), metathesis is the exchange of parts between two substances. Olefin metathesis is a chemical reaction in which two olefins come together in presence of a catalyst and through alkylidene exchange between the two olefins, form two new olefins (Scheme 5).

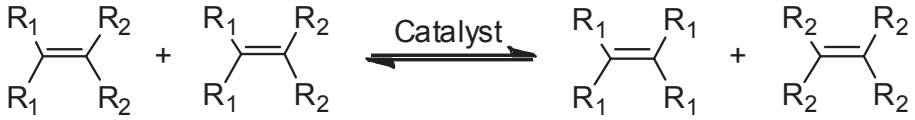

Scheme 5: Olefin metathesis reaction.

The story of olefin metathesis began almost six decades ago, in 1955, the first carbon-carbon double-bond rearrangement reaction, in the titanium-catalyzed polymerization of norbornene was reported by Anderson and Merckling.[23] After few years, Banks and Bailey reported novel transformation – disproportionation of olefins – conversion of propene into ethene and butene upon treatment with a mixture of triisobutylaluminum and molybdenum oxide on alumina.[24] Later, Calderon and co-workers reported further work using other cycloolefins with a mixture of tungsten hexachloride and ethyl aluminum chloride ($WCl_6/EtAlCl_2/EtOH$) as initiator and suggested that the polymerization of cyclic alkenes and the disproportionation of acyclic

alkenes are the same type of reaction and named this metal-catalyzed redistribution of carbon-carbon double bonds as olefin metathesis.[25] These catalytic systems had limited applications in organic synthesis, because of the harsh reaction conditions and prolonged initiation periods. The mechanism underlying metathesis was not yet discovered and remained a mystery.

2.2. Chauvin mechanism and first well-defined systems

In 1971, the first generally accepted mechanism for olefin metathesis was proposed by Prof. Yves Chauvin and his student Jean-Louis Hérisson.[26] Of course, the synthesis of $(CO)_5W=C(CH_3)(OCH_3)$ by Prof. Fischer was an important detail for Prof. Chauvin that led him to his hypothesis.[27] In this mechanism, olefin metathesis proceeds via generation of the metallacyclobutane intermediate, by the coordination of the olefin(s) to a metal alkylidene, via a series of alternating [2 + 2]-cycloadditions and cycloreversions. The mechanism has also experimental support by Prof. Grubbs, T. J. Katz, Schrock and others and is now generally accepted as *the* mechanism for metathesis.[28]

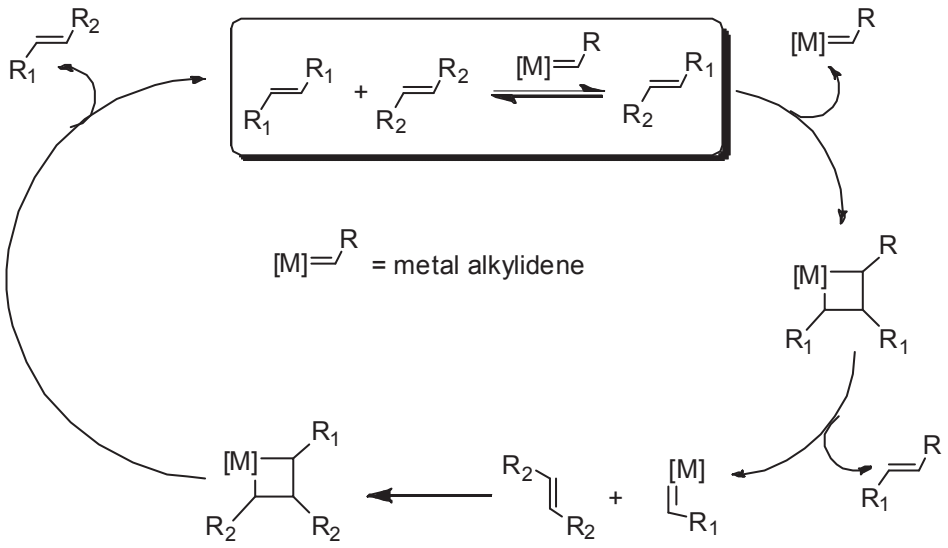

Scheme 6: Chauvin's mechanism of Olefin Metathesis.

However, an equilibrium mixture of olefins is obtained, due to the reversibility of all individual steps in the catalytic cycle. For the metathesis to be productive, it is necessary to shift the equilibrium in one direction.

Importantly, this mechanism, with a metal alkylidene initiating metathesis, indicated that metal-alkylidene complexes can act as catalysts for the metathesis reaction with olefins. The attempts to synthesize metal alkylidenes and eventually metallacyclobutanes led to the first single component metathesis catalysts, based upon tungsten, titanium and tantalum–

$[(CO)_5WdCPh_2$,[29] bis(cyclopentadienyl) titanocyclobutanes,[30] tris(aryloxide) tantalacyclobutanes[31] and various dihaloalkoxide-alkylidene complexes of tungsten].[32]

Later, Prof. Schrock and his group produced stable molecular molybdenum- and tungsten-alkylidene complexes of the general formula [M (=$CHMe_2Ph$) (=N-Ar) (OR_2)], R being bulky groups (figure 1).[33]

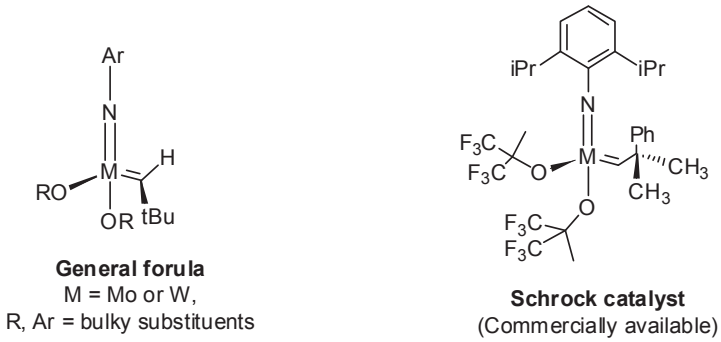

Figure 1: Schrock's Mo and W catalysts.

Unfortunately, the use of these highly active, early transition-metal catalysts was restricted due to their high sensitivity toward oxygen and moisture and to their limited functional group tolerance.[34, 35]

Even though, the problem of functional group tolerance can be handled using functional group protection strategy, it is time consuming and a tedious job.

Although, the structure and reactivity relationship was well-defined using above well-defined systems, it was important to develop catalysts which react preferentially with olefins in the presence of heteroatomic functionalities.

2.3. Why Ru? : Functional group tolerance

Now, if we look at titanium, tungsten, molybdenum, and ruthenium, these catalysts react more selectively with olefins as the metal centers were varied from left to right and bottom to top on the periodic table.

Titanium	Tungsten	Molybdenum	Ruthenium
Acids	Acids	Acids	**Olefins**
Alcohols, Water	Alcohols, Water	Alcohols, Water	Acids
Aldehydes	Aldehydes	Aldehydes	Alcohols, Water
Ketones	Ketones	**Olefins**	Aldehydes
Esters, Amides	**Olefins**	Ketones	Ketones
Olefins	Esters, Amides	Esters, Amides	Esters, Amides

Increasing Reactivity

Figure 2: Functional group tolerance of early and late transition metal olefin metathesis catalysts.[35]

Titanium and tungsten are more reactive towards esters, ketones than olefins, while molybdenum being more reactive towards olefins than these systems, cannot tolerate

aldehydes or alcohols. In comparison to the early transition metals, the later transition metals, such as ruthenium show preferential and increased reactivity towards olefins.[36]

2.4. From ill-defined to well defined Ruthenium alkylidene complexes

First, in the 1960s the ROMP of norbornene derivatives with $RuCl_3$(hydrate) in refluxing ethanol and under aqueous emulsion conditions was carried out but albeit with low yields.[37] Later, in 1980s, $RuCl_3$(hydrate) investigation showed that the ROMP reactions are slower when performed in organic solvents,[38, 39] in contrast to the reactions in aqueous solution. Thus, suggesting tolerance towards alcohols and water. Further developments led to $Ru(H_2O)_6$(*p*-toluenesulfonate)$_2$,[40] which catalyzed ROMP of functionalized norbornene, including hydroxyl-, carboxyl-, alkoxy-, and carboximide-substituted derivatives, However, the activity of $RuCl_3$(hydrate) or $Ru(H_2O)_6$-(*p*-toluenesulfonate)$_2$ is limited to more highly strained substrates. Also, $RuCl_3$(hydrate) and $Ru(H_2O)_6$-(*p*-toluenesulfonate)$_2$ catalyst solutions containing ruthenium olefin adducts were recyclable.[41]

Importantly, addition of acyclic olefins led to their incorporation at the ends of the polymer chains during ROMP[42] suggesting that the active species was a ruthenium alkylidene. Furthermore, the addition of ethyldiazoacetate to $Ru(H_2O)_6$-(*p*-toluenesulfonate)$_2$ to generate Ru-alkylidene, produced a species with higher activity than that of $Ru(H_2O)_6$-(*p*-toluenesulfonate)$_2$.[43] This catalysts, showed promising reactivity towards the ROMP of monomers being less strained than norbornene (cyclooctene for instance).

Based on this, the first metathesis active Ru-alkylidene complex **1**,[44] was prepared applying similar methodology to that used for the synthesis of tungsten alkylidenes.[45]

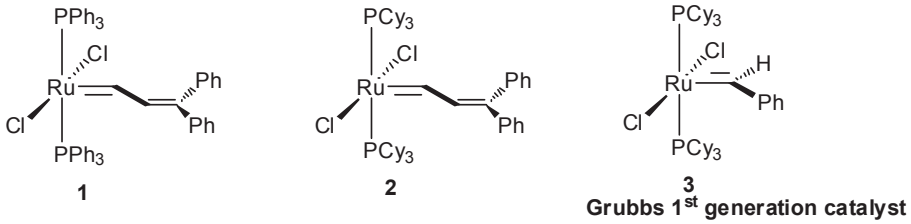

Figure 3: Ruthenium catalysts containing phosphine ligands.

Further development led to catalysts **2**, which showed an improved activity towards low strain cyclic monomers. The catalytic activity of these complexes increases with the basicity of the phosphines in the order PPh_3, P^iPr_3 < PCy_3. The catalyst **2** showed functional group tolerance[46] and was air-stable as a solid, retaining its activity even when exposed to water, alcohols, or acids. Because of difficulties in the synthesis of this catalysts, further developments resulted in the preparation of the benzylidene complex **3**, commonly known as Grubb's 1st generation catalyst (**Grubbs-I**).[47] in the same period, the bis(substituted)N-

heterocyclic carbene (NHC) complex **4** was reported by Prof. Hermann and co workers,[48] which showed slightly better activity than **Grubbs-I**. However, due to less labile nature of NHC ligands, the dissociation of one NHC ligand was difficult. To address this issue further development work to prepare monosubstituted NHC derivative of **Grubbs-I** complex was carried out, which resulted in catalyst **5** with unsaturated NHC backbone, as reported by Prof. Nolan's group and Prof. Grubbs group.[49] Soon after, Prof. Grubbs reported more active catalyst **6** with saturated NHC backbone, known as Grubbs 2nd generation catalyst (**Grubbs-II**).[50] Remarkably, **Grubbs-II** was effective with loadings as low as 0.05 mol % for RCM reactions and 0.0001 mol % (monomer: catalyst= 1,000,000) for ROMP.[51]

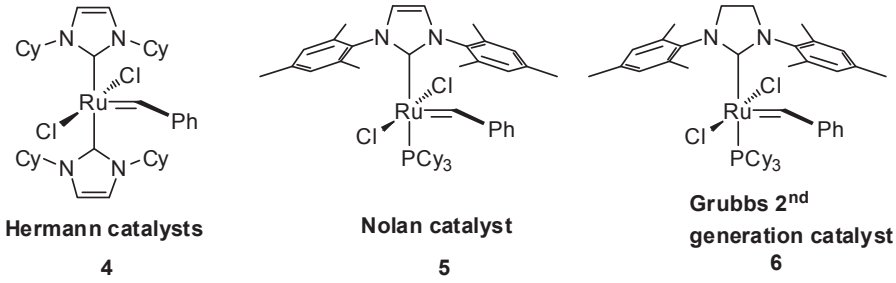

Figure 4: Ruthenium catalysts containing *N*-heterocyclic carbene ligands.

The slow initiation step of **Grubbs-II** catalyst was improved by replacement of the phosphine with weakly bound ligands such as pyridine. This 18-electron bis-pyridine adduct referred as the Grubbs 3rd generation catalyst (**Grubbs-III**) had a very high initiation rate. The mono-pyridine complex could be formed by decoordination of one pyridine under vaccum (Figure 5).[52]

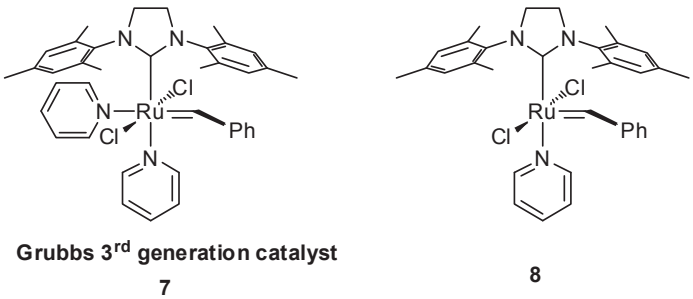

Figure 5: Grubbs 3rd generation catalysts.

The discovery of the Grubbs complexes triggered the search for other active ruthenium based metathesis catalysts. Another breakthrough example is the Hoveyda 1st generation catalyst **9** (**GH-I**) (Figure 6), which was discovered in 1999 during mechanistic studies of Ru-catalyzed styrenyl ether to chromene transformations.[53] This catalyst was found to be exceptionally robust and was isolated in high yield by air-driven silica gel chromatography. Importantly, it forms the same active species as those of **Grubbs-I**. The 2nd generation analogue **10** (**GH-II**) (Figure 6) was a more active catalyst, with similar efficiencies to those of **Grubbs-II**, but

providing selectivity levels for CM and RCM better than the latter.[54] In due course, Prof. Blechert developed an improved synthesis and patented the catalysts with a number of phenyl vinyl ethers and various substitution patterns on the aromatic ring, for example complex **11** (Figure 6). [55] Studies indicated that the presence of steric bulk adjacent to the chelating unit were critical.[56] Electronic effects in the isopropoxystyrene ligand sphere were investigated by Grela *et. al.* The introduction of a strong electron-withdrawing group led to complex **12** (Figure 6), which was equally stable but spectacularly more reactive than **GH-II**.[57] A decrease in electron density of the isopropoxy oxygen atom was expected to reduce its chelating ability, thereby facilitating formation of the 14-electron catalytically active species, while suppressing reassociation to the Ru center. These findings clearly demonstrated that small variations in the ligand structure could result in considerably different catalytic activities.[58]

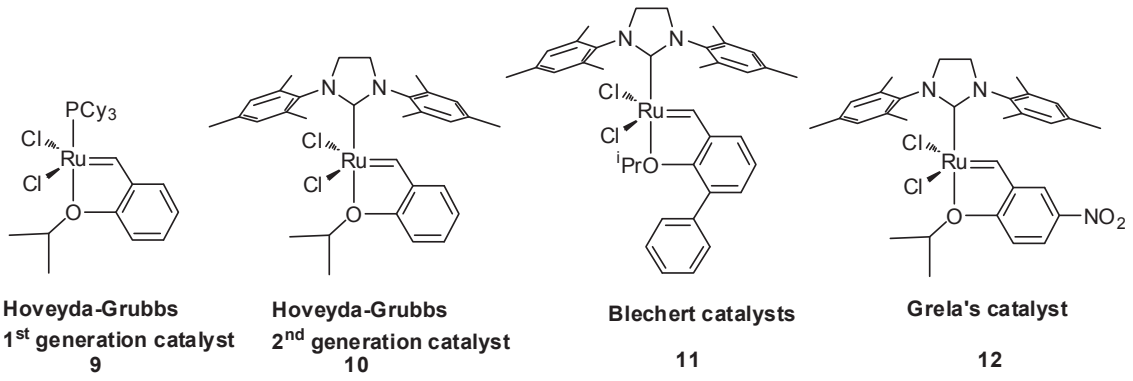

Figure 6: Hoveyda-type catalysts.

Over the last decade, a constant improvement in the Grubbs, Schrock and Hoveyda classes of catalysts, allowed the widespread use of olefin metathesis in organic syntheses as it could replace advantageously many of the traditional synthetic tools.[59]

2.5. NHC – *N*-heterocyclic carbene in Ru Metathesis catalysts:

The *N*-heterocyclic carbenes (NHC) are singlet carbenes with excellent stability.[60] They can act as two electron donor ligands towards almost any element in the periodic table and they derive their excellent stability from their unique electronic structure. The carbene carbon atom is sp^2-hybridised featuring two σ-bonds to the adjacent nitrogen atoms ("pull" stabilization due to large electronegativity of nitrogen) and an electron lone pair in the remaining sp^2-hybrid orbital. Two $\pi_N \rightarrow \pi_C$ donor interactions from the electron lone pairs of nitrogen into the "empty" p-orbital of the carbene carbon atom complete the electron configuration on the carbene carbon atom ("push" stabilization) and gives the NHC its stability (Figure 7)

Due to their electronic structure, NHCs are strong σ-donor but only weak π-acceptor ligands. They bind strong to many transition metals and afford metal-carbon bonds that are usually less labile than the related metal-phosphine bonds. [61,62,63] This decreased lability of carbenes, improve the air and thermal stability of the corresponding organometallic complexes making them more resistant to oxidation. The electronic and steric properties of NHC can be easily modified, by changing the substituents to fine-tune the catalytic properties of the corresponding organometallic complexes.

The stability of cyclic diaminocarbenes NHCs such as imidazolin-2-ylidenes, 1, 2, 4-triazolin-5-ylidenes and benzimidazolylidenes (Figure 7)[64,65] was assigned to their steric bulk which prevents dimerization. For unsaturated NHCs, a further stabilization was associated with their 4n+2 aromatic Hückel configuration.[66] Later, it was found that steric protection was not a decisive factor and sterically less demanding carbenes can be isolated.[67]

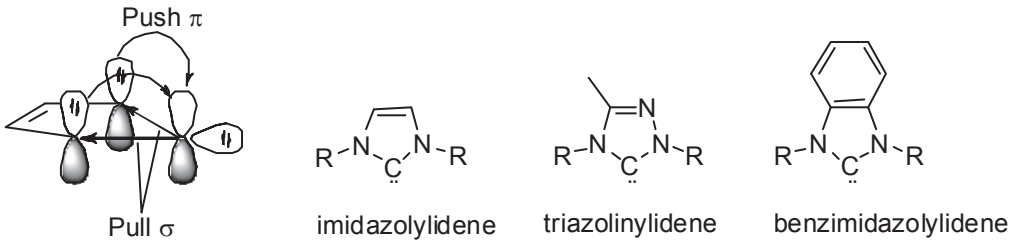

Figure 7: Push-pull stabilization in NHC and diaminocarbenes.

For instance, the saturated imidazolin-2-ylidenes (or imidazolylidenes), were isolated and were thought to be more electron donating than their unsaturated counterparts. However, studies showed that the basicity of NHC ligands had little to do with the saturated or unsaturated nature of the imidazole backbone.[68,69] While imidazolin-2-ylidenes dimerized under special circumstances,[70] in case of saturated systems the steric constraints of the N-substituents determined their existance as either monomeric carbenes or as the enetetramine dimers (Wanzlick equilibrium). The free carbene with sustituents directly bonded (like ^{t}Bu or larger) to the *N*-atoms were stable while smaller groups led to dimerization (Figure 8).[71]

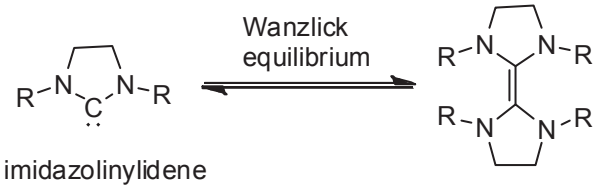

Figure 8: Wanzlick equilibrium.

Profs. Öfele and Wanzlick and Prof. Lappert *et. al.* reported the synthesis of carbene coordinated organometallic complexes **13**, **14** (Figure 9).[72,73,74,75] However, the isolation of

the first stable naked NHC **15** (Figure 9)[76] by Prof. Arduengo *et. al.* triggered the use of heterocyclic carbenes in organometallic chemistry[77] and in organocatalysis.[78]

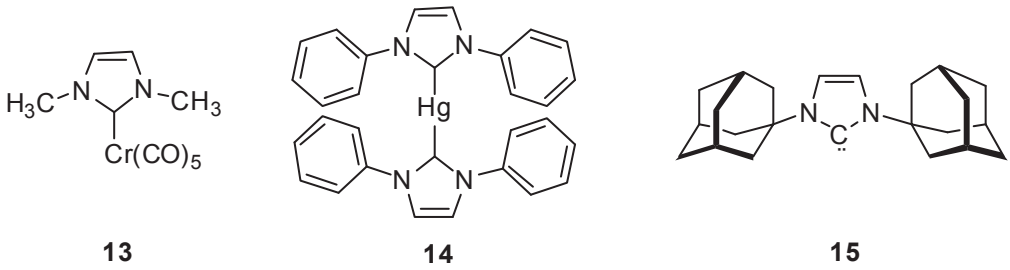

Figure 9: First reported NHC-coordinated organometallic complexes and isolable carbene.

Although, four,[79] six and seven membered[80,81] NHC ligands can be prepared, the five-membered NHC ligands are the most commonly used.

The heterocyclic carbene precursors can be easily prepared via various synthetic routes.[82] Although, many are stable enough to be isolated, their in-situ generation and their subsequent coordination with the desired metal source is more straightforward and popular.

Most common methods used for the preparation of the Ruthenium precatalyst complexes using NHC as ligands comprise

1) The deprotonation of imidazolium or imidazolinium salts with a strong base, such as potassium hexamethyldisilazane (KHMDS) or potassium *tert*-butoxide (KO^tBu), to generate free NHCs[83,84,85,86] which, on subsequent coordination to the appropriate ruthenium precursor, affords the targeted organometallic complex. This is usually achieved by displacing one (or more) phosphine or pyridine ligands.
2) The use of Ag_2O to form the corresponding heterocyclic carbene-Ag complexes (when the in situ generated carbenes tend to dimerize),[87] and their subsequent transmetallation with the metal precursor to afford the desired organometallic complex.

Today, several homogeneous metathesis catalysts are commercially available and as a result, new perspectives are opening up in the amazing research field of olefin metathesis, attracting a vast amount of interest both from industry and academia.[88] The most successful and well-studied ruthenium catalysts bear either symmetrical or unsymmetrical imidazoles or imidazolin-2-ylidenes. We will focus on the ruthenium complexes with symmetrical and unsymmetrical imidazolylidene and imidazolin-2-ylidenes ligands.

2.6. Ruthenium complexes with symmetrical imidazolylidene and imidazolin-2-ylidenes ligands:

In the above section, we have looked at the development of some popular Ru complexes bearing symmetrical *N, N*-dimesityl saturated and unsaturated NHC ligands. However several other Ru based complexes with other symmetrical NHCs were successfully prepared and studied First, sterically demanding NHCs were used and the influence of the bulkiness on the catalytic activity of the corresponding complexes (complexes **16-18**, Figure 10) was investigated.[89] Second, NHCs with ortho fluorinated *N*-bound aryl rings (complexes **19, 20**, Figure 10) were investigated as new ligands and the differences in reactivity was found in the case of Grubbs and Hoveyda type catalysts. This was explained based on the presence of fluorine-ruthenium interactions.[90] Third, NHCs without *o*-substituents on the *N*-bound aryl rings were used to generate complexes **21-23** (Figure 10)[91] and an increased efficiency for the formation of tetrasubstituted olefins starting from sterically demanding substrates Fourth, catalysts with *N*-arylsubstituted NHC without *ortho*-substituents on the *N*-aryl groups were prepared and they were found to be prone to degradation compared to complexes bearing *ortho*-substituted *N*-aryl NHCs.[92,93] Such a lack of stability was attributed to an easier rotation of the *N*-aryl groups in the former. Such rotation allowed the complex degradation through C-H bond activation because of the close vicinity of the ortho C-H bond to Ru. To restrict such a rotation and to make the decomposition pathway unfavorable, NHC substituted catalysts with the bulky substituents on the backbone (complexes **24, 25**, Figure 10) were prepared and were efficient catalysts in RCM, CM and ROMP.[94,95] Fifth, saturated and unsaturated symmetrical NHCs[96] were prepared to investigate the putative presence of intramolecular π-π interactions and their influence on the electronic density at the ruthenium center with the corresponding complexes (complex type **26**, Figure 10) and the catalytic ability of the later complexes was also investigated.[97] Further, catalysts with pH-responsive NHC ligand (complex **27**) was used to favor the removal of residual ruthenium from RCM reaction mixtures by acidification and subsequent filtration. Sixth, catalysts with bulky NHC ligands (complexes **28, 29**, Figure 10) were synthesized to increase the diastereoselectivity of ring rearrangement metathesis reactions.[98,] Although, complexes **28** and **29** showed improvements in the diastereoselectivty, were found to less stable in solutions. Complex **30** was found to be an efficient RCM catalyst.[99] Seventh, catalysts bearing saturated NHCs with two aliphatic side groups[100] (complexes **31, 32**, Figure 10) were successfully isolated and were found to be highly active in ROMP but less active in model RCM and CM reactions. This low efficiency was explained

based on the increased steric bulk of the alkyl groups relative to that of the usual aromatic groups.

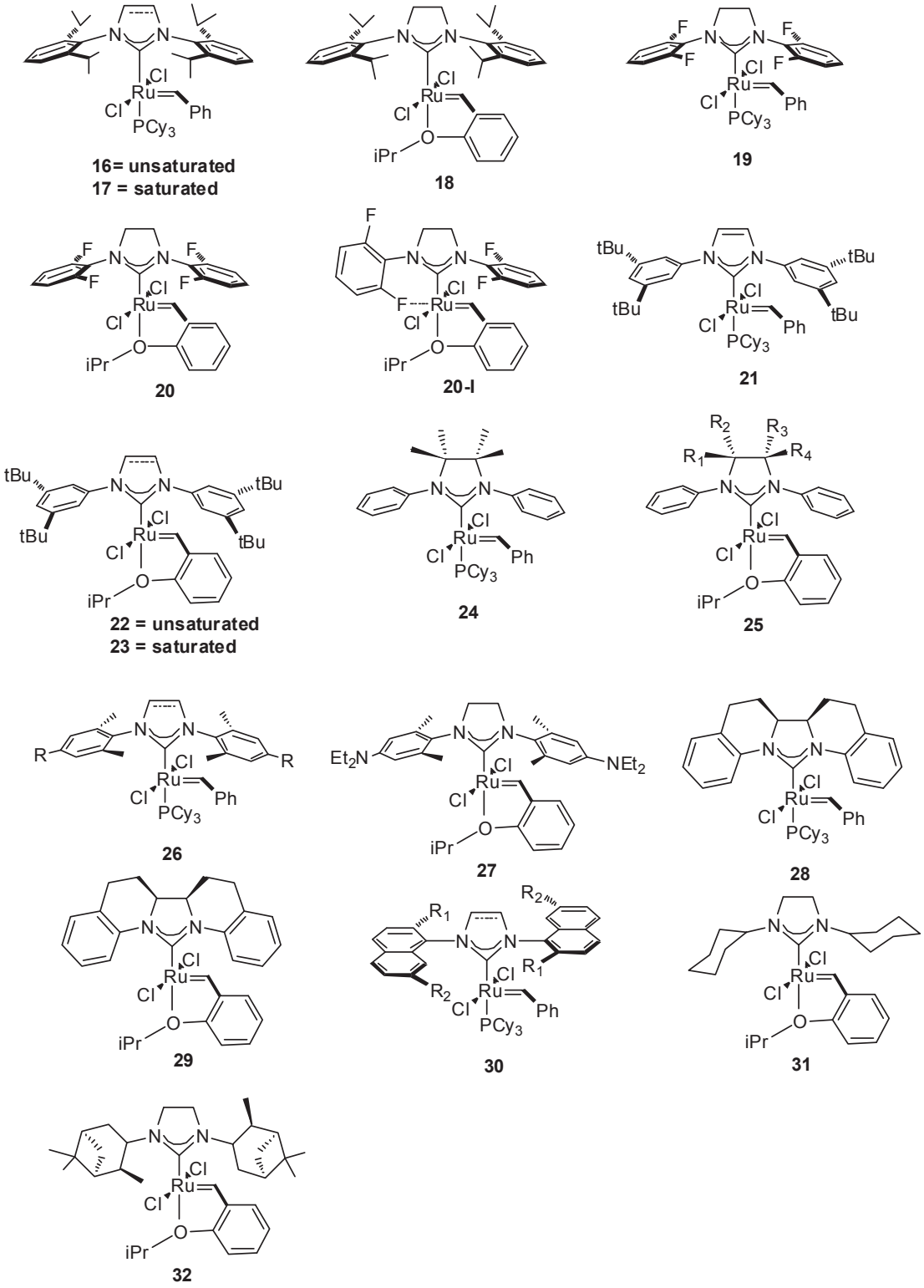

Figure 10: symmetrical Ru-NHC catalysts with different NHC ligands.

2.7. Ruthenium complexes with unsymmetrical imidazolyl- and imidazolin-2-ylidenes:

The first synthesis of Ru-complexes with unsymmetrical NHC ligands was reported by Prof. Fürstner *et. al.* in 2001.[101] Complexes **33-35** (Figure 11) were found to be efficient in the formation of tetrasubstituted olefins *via.* RCM of *N*,*N*-dimethallyl-*N*-tosylamide. Prof. Mol and co-workers attempted the synthesis of complex **37** (Figure 11) to enhance the steric bulk and the electron donating ability of the NHC. Although, the attempts to prepare symmetrical NHC complex failed, probably due to the increased bulkiness of the adamantyl ligand, the unsymmetrical complex **38** (Figure 11) was isolated in good yield.[102] The very low activity in ROMP of norbornene was explained based on the steric hindrance of the adamantyl substituent on the NHC. Unsymmetrical complex **36** (Figure 11) was synthesized to immobilize on various supports.[103] However, rearrangement of the complex during immobilization on silica gel was observed and attributed to the terminal hydroxyl groups. Complexes **38, 39** (R = Me, Et) (Figure 11) were synthesised with the intentions to increase catalyst activity and improve *E/Z* selectivity in CM reactions and improvement of diastereoselectivity in RCM reactions.[104] These catalysts indeed showed improved *E/Z* ratios in selected CM reactions and selectivities in a diastereoselective RCM reaction than symmetrical catalysts. With the same idea, several various *N*-alkyl-*N*-aryl-substituted NHCs ruthenium complexes were synthesized and evaluated. (complexes **40, 41** for insatance, Figure 11).[105,106,107] Consecutively, Prof. Grubbs and co-workers reported the synthesis of ruthenium complexes containing unsymmetrical NHCs with fluorinated *N*-aryl groups (complexes **43, 44** Figure 11). [108,109] These complexes showed higher *E/Z* selectivity in CM reactions. The influence of unsymmetrical NHC ligand on the initiation rate of the irreversible reaction with butyl vinyl ether was also studied. For phosphine-containing catalysts, a dissociative phosphine mechanism was suggested, while an associative mechanism was indicated for phosphine-free catalysts. In 2008, phosphine-containing complexes **42** (Figure 11), coordinated with unsymmetrical bis (*N*-aryl)-substituted NHCs, were also reported.[110]

Prof. Collins and co-workers prepared another family of ruthenium catalysts with unsymmetrical chiral monodentate NHC ligands (complexes **45**, **46**, Figure 11).[111,112] These catalysts showed high reactivities and high enantiomeric excess in representative ARCM reactions. In 2008, Prof. Buchmeiser, Blechert and Grisi reported the synthesis of complexes **47, 48**[113,114] (Figure 11). The pyridine derivatives of complex **47** were studied in alternating

copolymerizations reactions. Further study using complexes **48** with different substitutions for asymmetric induction in ARCM, showed that the chiral substitution on the NHC backbone was a key for asymmetric induction.

Prof. Hoveyda and co-workers have reported the first catalysts in which the chiral information of the NHC ligand was transferred directly to the ruthenium center, using binaphtholate moieties (complex **49**, Figure 11).[115] These complexes were isolated in high diastereo- and enantiomeric purity without resolution. They were found to be recylable and stable towards air and moisture but their activity was low due to the less electronegative nature and the increased steric bulk of the ligand compared to the initial chlorido ligand. The activity was enhanced by increasing the electronegativity of the naphtholate using trifluoromethyl-substituted chiral NHC ligand. The most significant drawback of binaphthyl-based catalysts was their lengthy, chiral auxiliary directed synthesis. Such an issue was addressed by synthesis of biphenolate, NHC-coordinated complexes.[116,117]

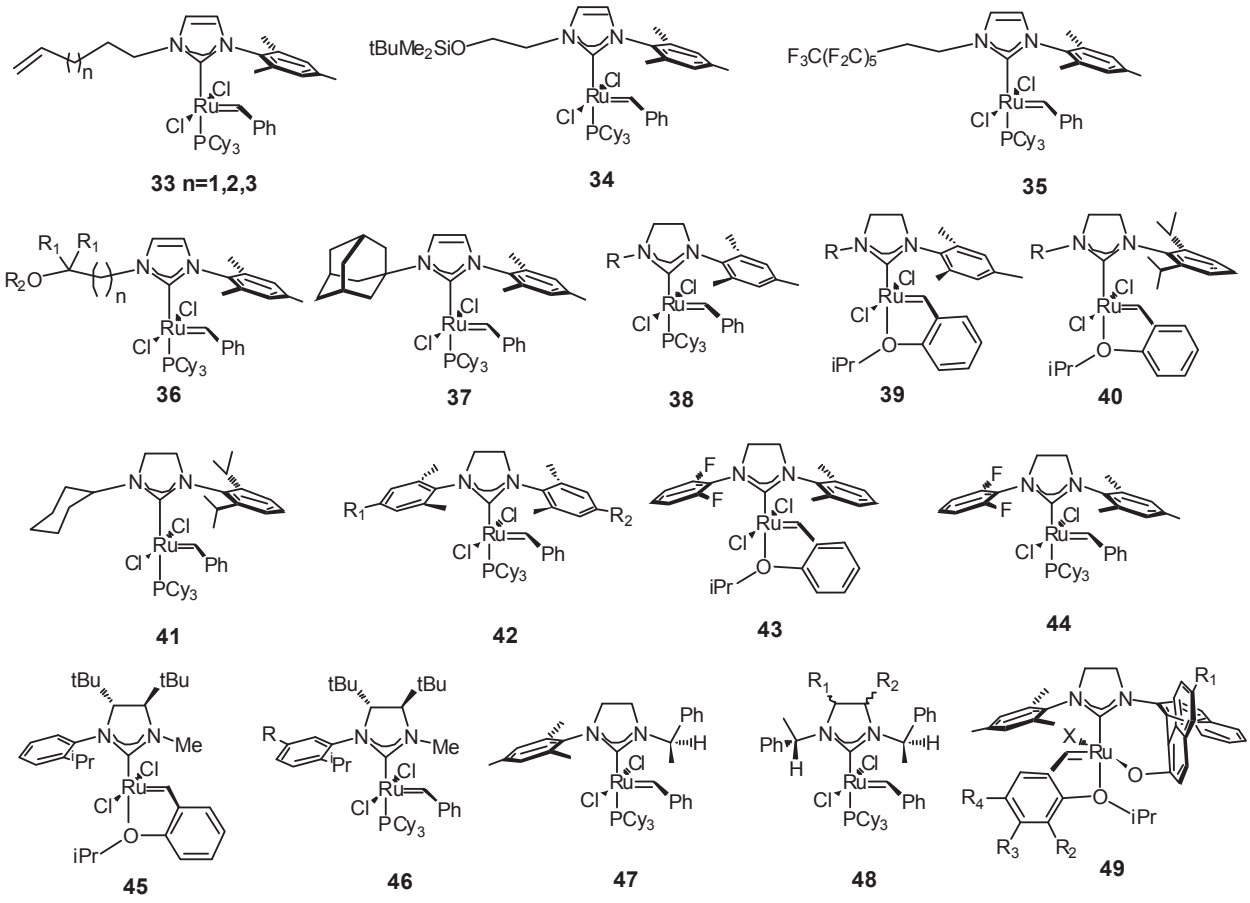

Figure 11: l Ru-NHC catalysts with different unsymmetrical NHC ligands.

Recently, several reports dealing with the utilization of these unsymmetrical catalysts particularly to improve the *E/Z* selectivities, diastereoselectivities, alternative copolymerization and selective ethenolysis were also published.

2.8. Mechanism of olefin metathesis reactions with Ru-NHC complexes

The mechanism using ruthenium 1st and 2nd generation complexes was deeply investigated, and was shown to proceed via an initial dissociation of a phosphine ligand to form a 14-electron intermediate,[118] which coordinates to the olefinic substrate to form a 16-electron complex. The complex, through the coupling of the olefin and the ruthenium alkylidene forms a metallacyclobutane ring within the ruthenium coordination sphere. The Ru(IV) metallacycle breaks down in a productive way to form a new olefin and a new alkylidene complex, or in an unproductive way to regenerate the starting compound (Scheme 7)

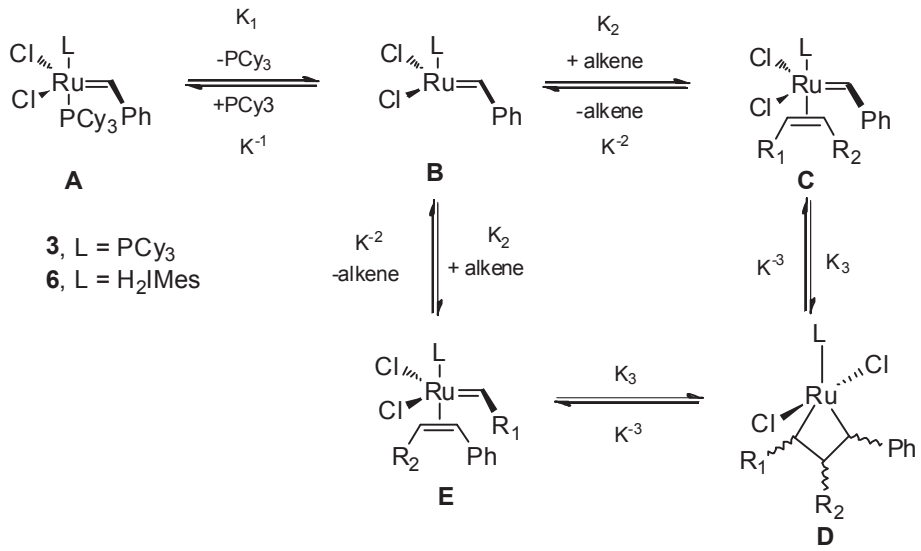

Scheme 7: Proposed dissociative mechanism for Grubbs catalysts.

This dissociative pathway is strongly supported by experimental investigations,[119] computational investigations,[120] direct isolation of a ruthenium coordinated to olefin. Prof. Chen *et. al.* confirmed the identification of the 14- electron active species (B)[121] using mass spectrometry[122] while recently Piers *et. al.* directly observed the ruthenacyclobutane (D) which also provided evidence for *trans* binding mechanism.[123]

Apart from the catalyst initiation, the site of olefin coordination and metallacyclobutane formation were also studied. The experimental evidences showed both mechanisms: olefin binding either *cis*[124] or *trans*[125] to the L-ligand (Scheme 8). Several computational[126] and experimental[127] investigations supported the *trans* olefin binding.

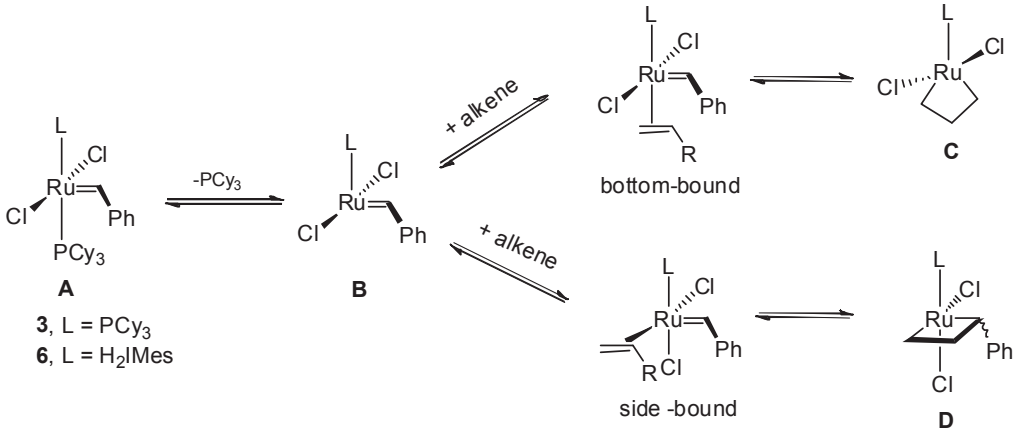

Scheme 8: Coordination of olefin with Ru.

It was also important to note that, calculations by Prof. Cavallo *et. al.* indicated that it was difficult to generalize the conclusion due to the influence of several factors (electronic, steric and even solvent) which could alter the reaction pathway.[128] However, in the presence of steric effects, the reaction mechanism was pushed toward the bottom-bound pathway while in the absence of such steric effects, the side-bound reaction pathway was favored. The *trans* olefin coordination has emerged as the most reliable mechanism in the case of Grubbs catalysts.

The increased activity of the Grubbs-II (**G-II**) *vs.* Grubbs-I (**G-I**) catalysts has also been studied experimentally and theoretically. Initially, faster initiation (dissociation of phosphine) of **G-II** was attributed to the higher electronic *trans*-influence of the NHCs (higher σ-donation properties) as compared to **G-I** and this was assumed to be the reason for higher reactivity of **G-II**. However, mechanistic studies[129,130] and gas-phase experiments[131] proved it wrong. In fact the initiation rate (*k*1) of **G-I** was 2 orders of magnitude higher than that of **G-II**.[132] In contrast, the catalytic activity of **G-II** was about 2 orders of magnitude higher than that of **G-I**.

Such a contradiction led to the proposal that the coordination of the alkene substrate (*k*2) *vs.* the phosphine ligand (*k*-1, return to the resting state of the catalyst), on the intermediate **B**, (Scheme 7), is about 4 orders of magnitude higher for **G-II** relative to **G-I**.[121,122] Such an increased affinity of the NHC substituted ruthenium center for *π*-acidic olefins relative to *σ*-donating phosphines must be the reason for higher activity of **G-II**.

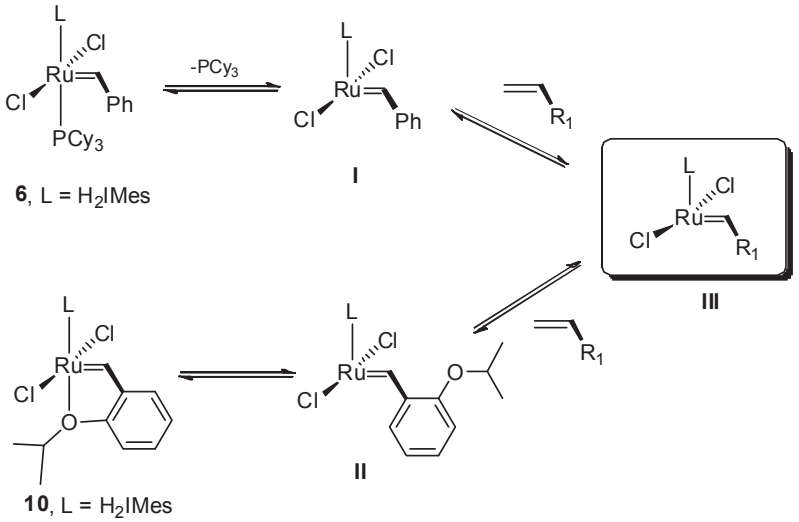

Scheme 9: active 14 electron intermediate after first turnover.

In the case of another breakthrough catalyst namely Grubbs-Hoveyda catalysts (**GH-II,** complex **10**), the proposed catalytic mechanism was slightly different from that for the **G-II** complexes in terms of initiation, but gave same propagating species (**III**, Scheme 9) after a single turnover. Initially, 14-electron intermediate **II** was formed through the dissociation of the benzylidene ether chelating group (Scheme 9). The further coordination of the alkene substrate, followed by metathesis, led to the formation of the catalytically active species **III** and the release of the isopropoxystyrene derivative. Therefore, once the olefin was completely consumed, the catalyst may return to its resting state by rebinding of isopropoxystyrene (release/return mechanism).[133] However, recent reports by Plenio *et. al.* showed that the return phenomenon was not common as previously thought.[134]

Importantly, an activity enhancement similar to that of Grubbs complexes was observed when the phosphine ligand was replaced by the NHC ligand in the Hoveyda-Grubbs 2nd generation catalyst.

2.9. Immobilization of Ru alkylidene complexes

Heterogenization of homogeneous complexes is expected to provide the advantages of homogeneous catalysis, (*i.e.* high catalytic performances and reliable structure activity relationship) and heterogeneous catalysis, (*i.e.* catalyst recycling and ease of separation from the reaction mixture).[135] Several strategies have been therefore developed for immobilization of olefin metathesis catalysts on solid supports. [136] The main strategies are 1) surface organometallic chemistry (SOMC), 2) supported homogeneous catalysts *i.e.* grafting of silylated organometallic complexes/or parent precursors onto supports and 3) adsorption of complexes onto supports. However, we will mainly discuss here about the first two strategies.

2.9.1. Surface organometallic chemistry (SOMC) [137]

In this approach, the organometallic complex is directly attached to the oxide support like silica or alumina: via either a covalent/ionic bond or a Lewis acid–Lewis base interaction. In these systems, the surface is considered as a ligand and is thus directly involved in the coordination sphere of the metal. This approach requires a detailed understanding of the structure of the surface and a control care of the grafting step.

Various well-defined alkylidene systems supported on silica (Figure 12) were prepared in our laboratory and a complete characterization of the supported surface species allowed the understanding of their mechanism of formation and of their reactivity with alkanes and alkenes.[138,139] The alkylidene complexes based on Re (complex **51**, Figure 12),[140] Mo and W (complexes **52**, **53**, Figure 12)[141] have shown better performances than their homogeneous counterparts. The better reactivity and stability was attributed in part by their site isolation on the support, preventing the catalysts decomposition by dimerization pathways.[142] Recent works performed in the laboratory in collaboration with Prof. Schrock provided the significant contribution for the understanding of these types of well-defined systems.[143]

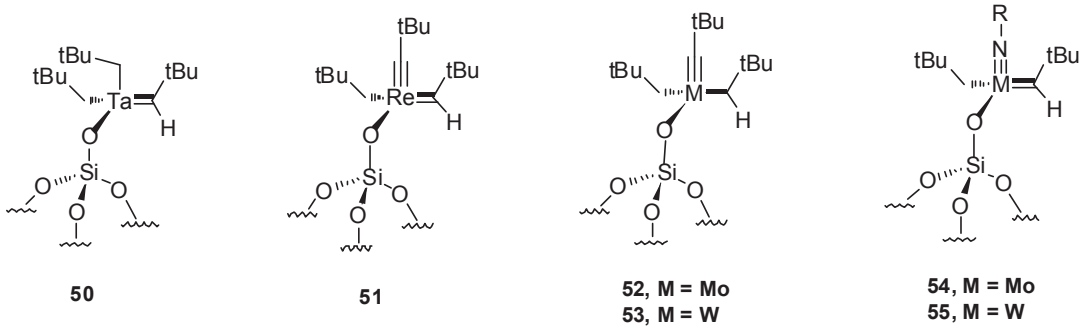

Figure 12: Well-defined alkylidene systems supported on silica**.**

Recently, the research group of Prof. Marciniec also reported the preparation of heterogeneous catalysts based on Ru-NHC sites immobilized on silica through covalent Ru-O-Si bonds (Scheme 10).[144]

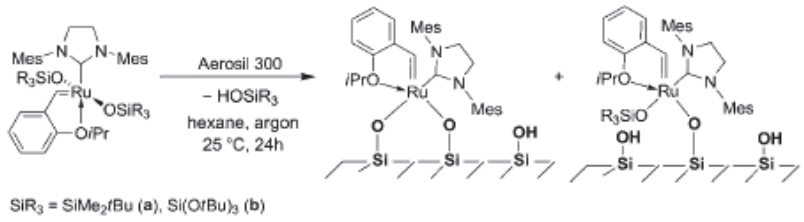

Scheme 10: Immobilization of Hoveyda-Grubbs catalysts on silica through Ru-O-Si bonds.[144]

2.9.2. Supported homogenous catalysts[145]

In this approach, immobilization of homogeneous catalysts is carried out by attaching the complex itself or one of its ligands via a organic linker, with usually a covalent bond to a support/carrier (oxide, polymer, dendrimer). Using this approach, several reports for the immobilization of olefin metathesis catalysts on various supports were published.[145,147] The Grubbs type catalysts were mainly immobilized through (a) halide ligands, (b) the alkylidene ligand, (c) phosphine or NHC ligands.

2.9.2.1. Immobilization through halide exchange

Prof. Grubbs *et. al.* have reported the preparation of carboxylic acid derivatives of the first-generation Grubbs catalyst by chloride replacements.[146] Using this methodology, the group of Prof. Mol *et. al.* reported immobilization of Grubbs I catalyst (**56**, Figure 13) on Merrifield resins functionalised with perfluorated dicarboxylates.[147] Prof. Buchmeiser *et. al.* reported a series of first- and second generation Grubbs and Grubbs-Hoveyda-type catalysts immobilized on Merrifield supports (**57-59**, Figure 13).[148] Monolith-supported version of this catalyst was also used in a continuous flow setup (**60**, Figure 13). Prof. Blechert's group used trialkoxysilyl-substituted fluorinated carboxylates for immobilizing Grubbs catalysts on silica.[149] Based on similar strategy Grubbs-Hoveyda complex was immobilized on SBA-15.[150]

These catalysts displayed good performances in RCM and Ru leaching was extremely low, (*i.e.* <100 ppb/g). Application of these catalysts in a continuous flow reactor was also achieved, with high TON (up to several thousands). However, their performances are still very low compared to their homogeneous analogues and deactivation was still a problem.

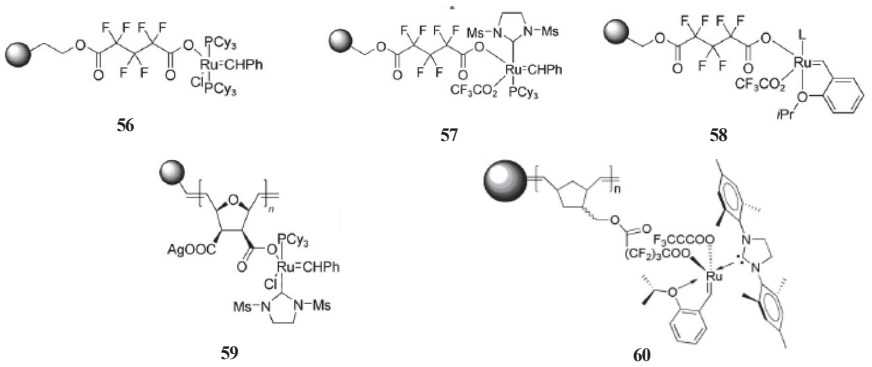

Figure 13: Few examples of catalysts immobilized through halide exchange.[145, 147c]

2.9.2.2. Immobilization through the alkylidene ligands

In principle, the idea of catalyst immobilization through its alkylidene ligand is based on the release of the active complex during catalysis and its return onto the support at the end of the reaction (boomrang concept). Although, immobilization of Grubbs I [151] or Grubbs II [152] catalysts can be achieved by reaction with a macroporous polystyrene or poly-DVB resin having pendant vinyl groups, the fast decrease of the catalyst activity was observed, preventing effective recycling. Prof. Hoveyda *et. al.* provided full evidence for the general applicability of the boomerang concept,[153] which was further confirmed by work of Prof. Barrett *et. al.* and Prof. Nolan *et. al.*[154] Because of this, further investigations were directed at immobilizing these types of complexes through the alkylidene ligands on different supports like polyethyleneglycol (PEG) (**61,** Figure 14),[155] dendrimer (**62** Figure 14),[156] polymer ,[157] Wang resin,[158] silica via organic linkers (**64**, Figure 14)[159] and via polymer linkers.[160]
Even though these immobilized systems are claimed to be active because of the so called boomerang-concept, recent work by Pleino *et. al.* showed that it was probably not so obvious and that the catalyst could be purely homogeneous with no return in its original form.[161] Overall, these supported systems have never out-performed the homogeneous systems but they have definitely reduced the Ru leaching in organic samples.

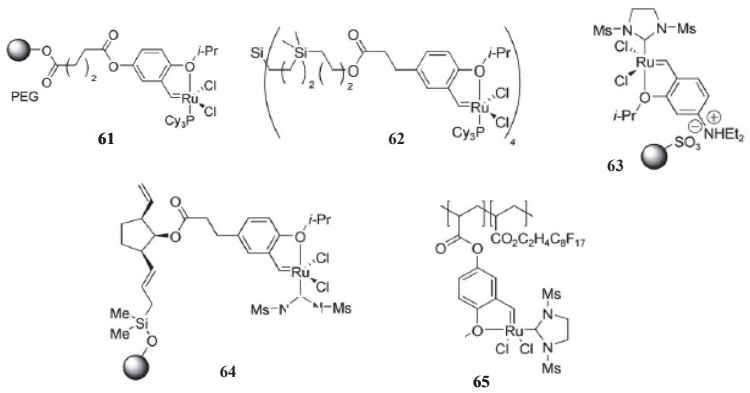

Figure 14: Examples of catalysts immobilized via alkylidene.[145]

2.9.2.3. Immobilization through phosphine ligands

The first attempt to immobilize the Grubbs I catalyst by exchanging its phosphine ligands was reported by the group of Prof. Grubbs *et. al.,* using phosphine incorporated polystyrene-divinylbenzene polymers (PS-DVB).[162] However these systems showed much lower performances than their homogeneous counterparts. Improvement in the performances was observed when using MCM-41 supported phosphine ligands (**67**, Figure 15)[163] probably because of the larger pores, which do not limit the diffusion of reactants (problem usually

encountered with polymers). Prof. Gatard *et. al.* have reported immobilization of Grubbs I catalysts on dendrimer, by replacing both PCy_3 ligands with a bidendate phosphine attached to the dendrimer.[164] However, supported Ru metathesis catalysts with phosphine ligands bound to the support suffer from metal leaching occurring when ligand dissociation takes place.

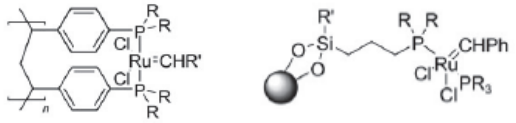

66 **67**

Figure 15: Examples of catalysts immobilized via phosphine.[145]

2.9.2.4. Immobilization through NHC ligands

As NHC ligands are strongly attached to Ru, no dissociation is observed and this characteristic could be advantageously used to permanently anchor the Ru complex via NHC ligand to the support. Several Grubbs II and Grubbs-Hoveyda II immobilized catalysts (Figure 16) were thus prepared via anchoring of NHC units on different supports. Prof. Blechert *et. al.* used Merrifield resin (PS-DVB 1%) and derivatized it to the corresponding imidazolium containing resin before conversion into the corresponding supported Ru-NHC catalyst (**68**). [165] Prof. Hoveyda *et. al.* immobilized the Grubbs-Hoveyda catalyst on monolithic silica rods (**69**)[166] while Prof. Buchmeiser and Fürstner *et. al.* reported on the immobilization of a Grubbs-type catalyst on a ROMP-derived monolith (**70**).[167] In 2005, Prof. Grubbs *et. al.* reported on the synthesis of a water-soluble Grubbs-type catalyst bound to poly(ethylene glycol) (PEG).[168] Weck *et. al.* reported poly (norborn-2-ene)-supported version of a Grubbs-type catalyst.[169] Immobilizations of modified Grubbs II catalyst on SBA silica supports are also reported (**71**).[170] These catalysts have been mainly used in RCM and related reactions with good catalytic performances, recyclability and lower Ru-contamination but the performance is not as good as those of their homogeneous counterparts.

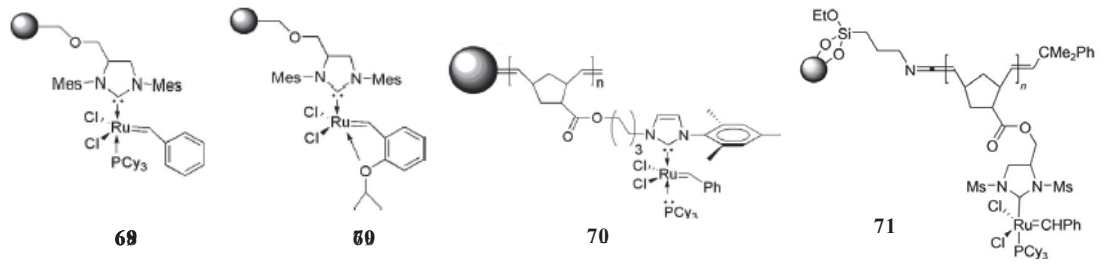

68 **69** **70** **71**

Figure 16: Examples of catalysts immobilized via NHC ligand. [145, 147c]

2.9.2.5. Other immobilized Ru alkylidene catalysts

Kobayashi *et. al.* described a poly(styrene)-supported Ru catalyst bound to the polymer arene ligand, which was found to be active in RCM of various dienes.[171] Prof. Kirschning and Grela *et. al.* also reported an appealing alternative concept for immobilization of a Grubbs-Hoveyda catalyst based on noncovalent interactions[172] between the support and the catalyst:[173] here the amine tagged Hoveyda type catalysts was immobilized on sulfonic acid functionalized Rasching ring support. Recently, the convenient method for the immobilization of Hoveyda–Grubbs catalyst directly on silica gel was also reported.[174] There are also reports on immobilization of an ionically tagged catalyst into an ionic liquid.[175]

Although, organic polymers have been mainly used, the inorganic silica materials are often considered as better supports (in terms of thermal and chemical stability) for the immobilization of homogeneous catalysts. In recent years, tremendous efforts are directed towards the use of mesoporous materials for immobilization of catalysts.[176]

3. Hybrid organic-inorganic mesoporous silica materials[177]

3.1. Introduction

A hybrid material is defined here as a material which contains two different components at the molecular level. When these components are inorganic and organic, the solid is considered as organic inorganic hybrid material (OIH material). We will mainly focus on this latter class solid in the following paragraphs. For the development of OIH materials, the sol-gel process is one of the methods of choice because it allows formation of oxide based materials at temperature compatible with introduction of organics. The sol-gel process is based on the hydrolysis and condensation of the metal alkoxide precursors to form the corresponding oxide. In the particular case of silica based solids their functionalization with organics implies the cohydrolysis and cocondensation of tetraalkoxysilane precursor with organosilanes; the stability of the Si—C bond being an advantage to produce organically modified silica network ion one step. Depending on the predominant pore size, the porous materials are classified by IUPAC into three classes:[178] (1) microporous, having pore sizes below 2.0 nm, (2) macroporous, with pore sizes exceeding 50.0 nm, (3) mesoporous, with intermediate pore sizes between 2.0 and 50.0 nm.

3.2. The sol-gel process [179]

The word "sol-gel" corresponds to the abbreviation of "solution-gelification". The sol-gel process is a versatile chemical process initially used for the preparation of inorganic materials such as glasses and ceramics of high purity and homogeneity. It involves the transition of a system from a liquid "sol" into a solid "gel" phase.

Sols are dispersions of colloidal particles in a liquid. *Colloids* are solid particles with diameters of 1-100 nm. A gel is an interconnected, rigid network with pores of submicrometer dimensions and polymeric chains whose average length is greater than a micrometer. This process involves hydrolysis of metal alkoxide $M(OR)_4$ (tetramethyl orthosilicate (TMOS) or tetraethyl orthosilicate (TEOS)), with water under acidic or basic conditions to the form silanol groups Si-OH. These silanol groups condense to form siloxane Si-O-Si groups. As the hydrolysis and condensation reactions continue, viscosity increases until the "sol" ceases to flow and form the "gel". For example, the main reaction occuring during the formation of a silica gel are presented in scheme 12.

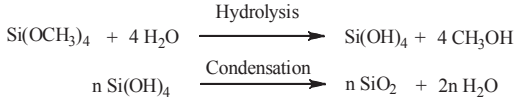

Scheme 12: silica gel formation .

Tremendous progresses in both fundamental understanding of the sol-gel process and the development of new organic-inorganic hybrid materials has been made and extensively reviewed.

In 1992, the first highly ordered mesoporous molecular sieves M41S (pore size in the range 2-10 nm), were reported by Mobile oil company.[180] The long chain cationic surfactants were used as the template (structure directing agents) during the hydrothermal sol-gel synthesis. Depending on the starting components and varying synthesis conditions, different mesoporous silica based oxides with an ordered structuration of their porous network were formed, the structuration being hexagonal (MCM-41), cubic (MCM-48) or laminar (MCM-50) (Figure 17).[181]

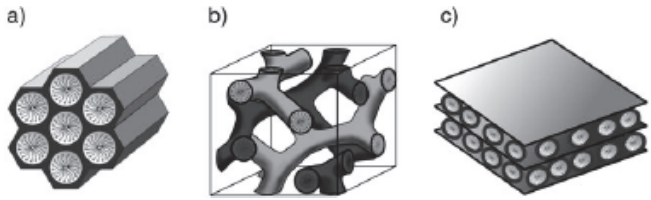

Figure 17: Different structures of mesoporous MCM41S materials a) MCM-41 (2D Hexagonal), b) MCM-48 (cubic), and c) MCM-50 (lamellar).[191]

Two different mechanisms were proposed for the formation of these materials (Scheme 11): 1) the true liquid-crystal templating (TLCT) mechanism, where the presence of the alkoxysilane precursor [normally tetraethyl- (TEOS) or tetramethylorthosilica (TMOS)] is not required for the formation of liquid crystalline phase because the surfactant is already organized in compact mesophases and this high concentration of surfactant is needed,[182] 2) the second mechanism is based on a cooperative assembly between the silica precursor and the surfactant, the latter being introduced in the low concentration if compared to the TLCT concentrations.[183] Recently, the hard sphere packing (HSP) mechanism is described for the synthesis of cubic mesoporous materials.[184] In 1998, silica based Santa Barbara Amorphous type materials (SBA) or SBA-15[185] with larger 4.6 to 30 nanometer pores with hexagonal porous network were produced at the University of California using the cooperative self assembly mechanism. These materials are generally prepared using non-ionic triblock copolymers based on poly(ethylene oxide)–poly(propylene oxide)–poly(ethylene oxide) (PEO-PPO-PEO). Such materials have thick silica walls as compared to the thinner walled MCM-41 structures made with conventional cationic surfactants and this characteristic is responsible for their greater hydrothermal stability.

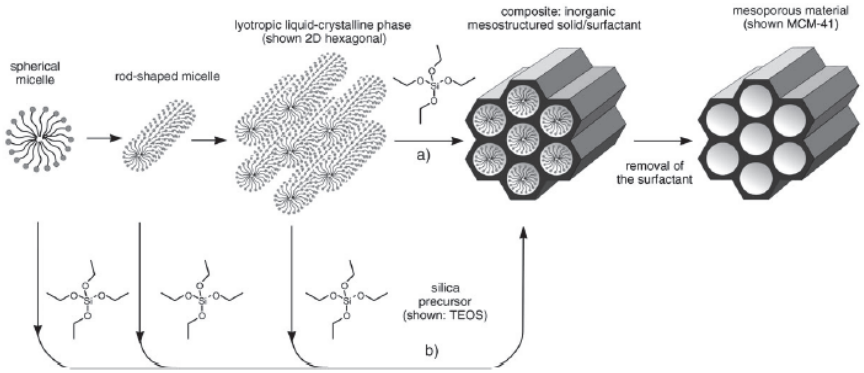

Scheme 11: Formation of mesoporous materials by structure-directing agents: a) true liquid-crystal template mechanism, b) cooperative liquid crystal template mechanism.[191]

3.3. Organically functionalized mesoporous silica

Organic-inorganic hybrid silica based materials are considered to posssess both the properties of their organic and inorganic building blocks and thus offer the possibility to combine enormous functional variations. Such materials, with the advantages of a thermally stable and robust inorganic part are particularly applicable to heterogeneous catalysis. Different strategies were used for the synthesis of organic functionalized porous hybrid materials based on organosilica units: 1) the classical post functionalization (grafting approach), 2) the direct synthesis of organic inorganic hybrid materials with the selective localization of the organic units either in the pores or in the walls of the silica matrix.

3.3.1. Grafting

Grafting is the modification of the inner surfaces of solids (in particular mesostructured silica) by reaction of organosilanes $(R'O)_3SiR$, or less frequently chlorosilanes $ClSiR_3$ or silazanes $HN(SiR_3)_3$, with the free hydroxyl groups of the oxide surfaces (Scheme 13). The process of grafting is frequently called immobilization.

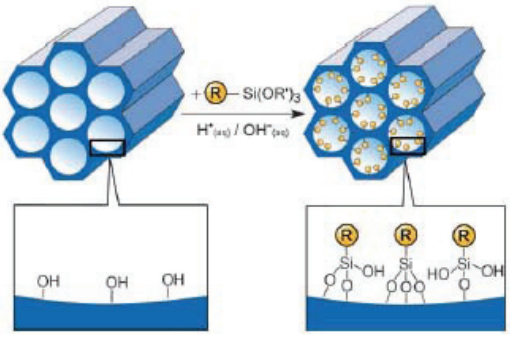

Scheme 13: Post synthetic functionalization of a mesoporous silica with organosilanes $(R'O)_3SiR$. R=organic functional group.[191]

However, such a grafting generally leads to a nonhomogeneous distribution of the organic groups within the pores depending upon the size of the organic residue and the degree of

occupation. In extreme cases (*e.g.* with very bulky organic groups), this can lead to complete closure of the pores (pore blocking). Moreover, the control over the condensation of the organic part on the silica surface is not secured (surface species being mono-, bi- or tripodal – Scheme 18).

3.3.2. Direct synthesis

In this one-pot synthesis method, the materials containing organic residues anchored covalently to their pore walls are formed by the co-hydrolysis and co-condensation of tetraalkoxysilanes [$(RO)_4Si$ (TEOS or TMOS)] and organotrialkoxyorganosilane precursors $(R'O)_3SiR$ in the presence of structure-directing agents (*i.e.* surfactants) (Scheme 14).

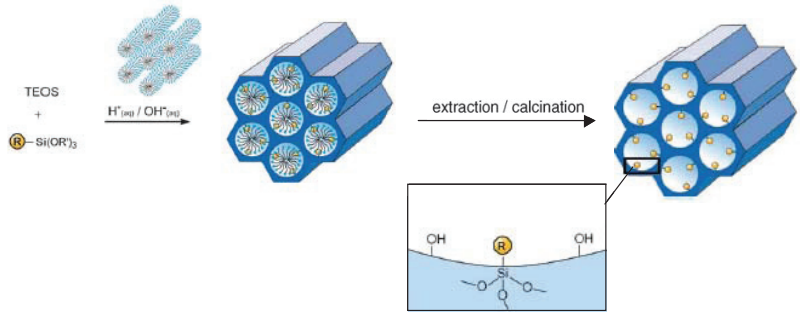

Scheme 14: Co-condensation method (direct synthesis), for the synthesis of organically functionalized mesoporous silica phases. R=organic functional group[191]

Via this synthetic procedure, the organic units are regularly distributed along the pore channels of the silica matrix (different from classical grafting approach) with a control over the condensation of the organic surface species.

These two methodologies (grafting *vs.* direct synthesis) present their own advantages and disadvantages: the post-grafting approach is convenient to introduce rapidly all kinds of organic moieties in solids but it does not permit either the control of the distribution of the functional groups in the final material or the nature of the surface species (Figure 18). This lack of control, during the grafting step, can be a major problem for obtaining homogeneous functionalized material, and this could explain the poorer activity of supported homogeneous catalysts, prepared by this method, compared to their homogeneous analogues.

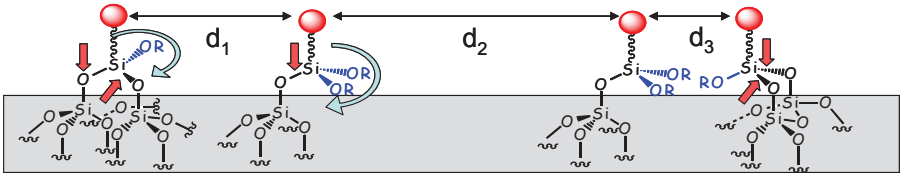

Figure 18: Grafted material: a simplified view of the surface oxide after the grafting reaction.

In contrast, the direct synthesis provide highly mesostructured functionalized materials containing regularly distributed organic moieties along their channel pores[186] and being fused

within the inorganic framework (Figure 19). However, the experimental procedures are more difficult to handle and optimization is often needed when the organosilane precursor is changed.

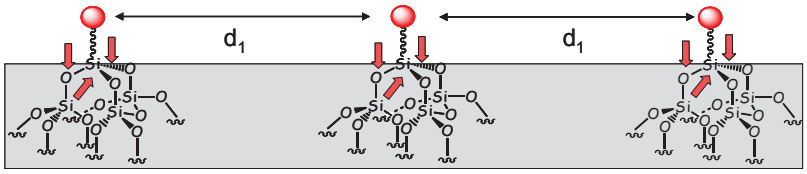

Scheme 19: Hybrid organic-inorganic material: a simplified view of the inner surface of the channel pores.

We reported recently immobilization of Grubbs-type catalyst in SBA-15 hybrid material.[187] Herein the active species remains attached to the support during reaction as the catalyst is permanently grafted via one of the NHC substituent. This catalyst was mainly used in self-metathesis with impressive catalytic performances, recyclability and no Ru-contamination. Prof. Pleixats *et. al.* also reported the immobilization of Grubbs-Hoveyda type catalysts in mesoporous silica,[188] in this case the catalysts is anchored via an alkylidene ligand into the mesoporous silica via direct synthesis approach and then further transformed into catalyst. In this case the active species is released in the solution during the reaction and thus needs to be recaptured after the reaction. These catalysts were tested in the RCM reactions with good activity and recyclability but leaching of Ru was not mentioned. An extension of this work was also performed by directly synthesizing the mesoporous material using silylated Grubbs-Hoveyda ruthenium-alkylidene complex via direct synthesis approach.[189] However, catalyst prepared by this method showed lower performances compared to those prepared by earlier method.

4. Aim

Here the main objective of the study was to selectively form low cyclic oligomers (in particular cyclooctene dimer) in RO-RCM of cyclooctene using metathesis catalysts. The strategy was to develop well-defined, mesoporous, hybrid, organic-inorganic, heterogeneous materials containing Ru-NHC units along the pore channels of their silica matrix. The idea was to use the pore confinement to constrain the formation of cyclic structures over polymers, *i.e.* to favor backbiting over polymerization.

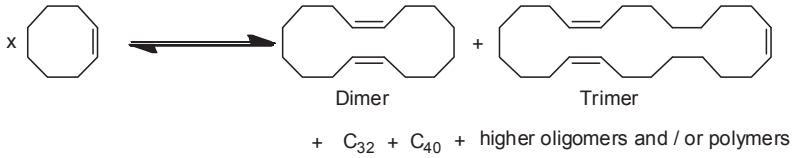

Scheme 15: Metathesis of cyclooctene

In the literature, metathesis of cyclic alkenes or acyclic dienes had already been investigated, and that cyclic oligomers were obtained along with polymers, *albeit* in low yields (Scheme 16).[190] They were obtained via back-biting of the growing chain on the propagating carbene. Although it is a challenge to control back-biting over polymerisation for the selective formation of specific cyclic structure, it could be addressed by using a cavity to constrain the formation of cyclic structures over polymers. Indeed, such confinement effects are known in heterogeneous catalysis, and can be obtained when the active sites is included in a cavity of given controlled size (shape selective catalysis).[191]

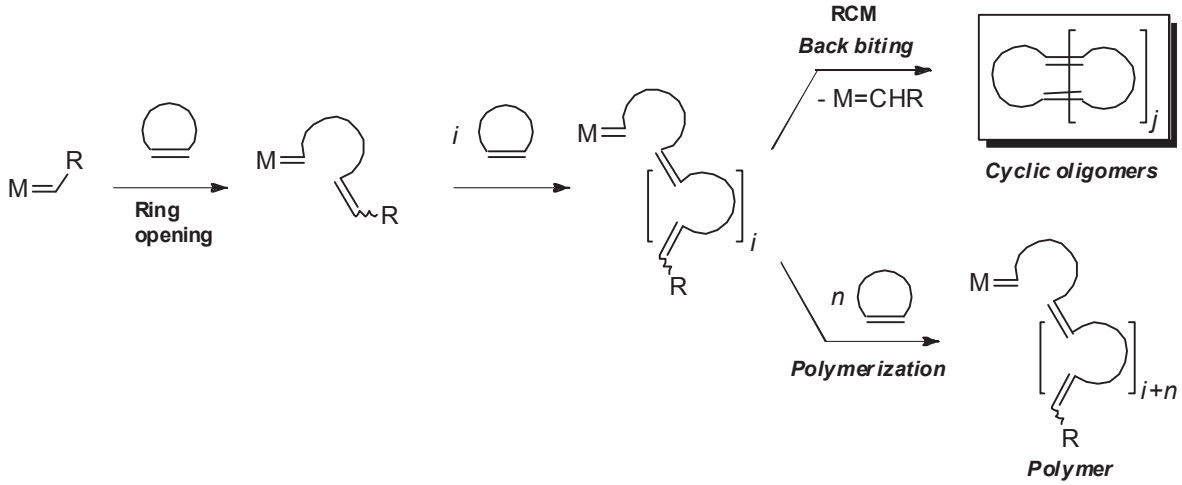

Scheme 16: Ring opening-Ring Closing Metathesis (RO-RCM) reaction *vs.* Ring Opening Metathesis Polymerization (ROMP).

Our group has already developed[187] and protected[192] new well-defined heterogeneous catalysts containing Ru-NHC units regularly distributed through the pore channels of the inorganic matrix. These Ru-NHC heterogeneous catalysts were used in the self-metathesis of ethyl- oleate and showed very high catalytic performances (in terms of rate and TON).

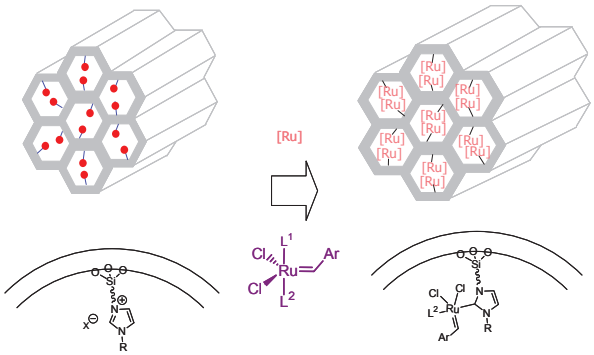

Scheme 17: Mesoporous heterogeneous inorganic matrix containing Ru-NHC units in the pore channels.

Thus, we decided to use and optimize the properties of such mesoporous well-defined Ru-NHC systems to generate selective catalysts for the formation of cyclic oligomers over polymers, in the RO-RCM of cyclooctene.

5. References:

1. For the 2005 Nobel Prize in Chemistry Lectures, see: (a) Chauvin, Y. *Angew. Chem. Int. Ed.* **2006**, *45*, 3740. (b) Schrock, R. R. *Angew. Chem. Int. Ed.* **2006**, *45*, 3748. (c) Grubbs, R. H. *Angew. Chem. Int. Ed.* **2006**, *45*, 3760.

2. (a) Fürstner, A. *Angew. Chem. Int. Ed.* **2000**, 39, 3012. (b) Grubbs, R. H. *Tetrahedron* **2004**, 60, 7117.

3. (a) Diver, S. T.; Giessert, A. J. *Chem. Rev.* **2004**, *104*, 1317. (b) Diver, S. T. *Coordin. Chem. Rev.* **2007**, *251*, 5-6, 671. (c) Villar, H.; Frings, M.; Bolm, C. *Chem. Soc. Rev.,* **2007**, *36*, 1, 55-66.

4. (a) Brizius, G.; Kroth, S.; Bunz, U. H. F. *Macromolecules* **2002**, *35*(13), 5317. (b) Ghalit, N.; Poot, A. J.; Fürstner, A.; Rijkers, D. T. S.; Liskamp, R. M. J. *Org. Lett.* **2005**, *7* (14), 2961. (c) Xian, W.; Matthias, T. *Beilstein J. Org. Chem.* **2011**, *7*, 82.

5. (a) Bielawski, C. W.; Grubbs, R. H. *Prog. Polym. Sci.* **2007**, *32*, 1. (b) Walker, R.; Conrad, R. M.; Grubbs, R. H. *Macromolecules* **2009***, 42,* 599. (c) Leitgeb, A.; Wappel, J.; Slugovc, C. *Polymer* **2010**, *51*, 2927.

6. Baughman, T. W.; Wagener, K. B. *Adv. Polym. Sci.* **2005**, *176*, 1.

7. (a) Conrad, J. C.; Eelman, M. D.; Silva, J. A. D.; Monfette, S.; Parnas, H. H.; Snelgrove, J. L.; Fogg, D. E. *J. Am. Chem. Soc.* **2007***, 129,* 1024. (b) Monfette, S.; Fogg, D. E. *Chem. Rev.* **2009**, *109,* 3783. (c) Monfette, S.; Eyholzer, M.; Roberge, D.; Fogg, D. E. *Chem. Eur. J.* **2010***, 16,* 11720.

8. (a) Connon, S. J.; Blechert, S. *Angew. Chem. Int. Ed.* **2003**, *42*, 1900. (b) Fischmeister, C.; Bruneau, C. *Beilstein J. Org. Chem.* **2011,** *7,* 156.

9. Wiberg, K. B. *Angew. Chem., Int. Ed.* **1986**, *25*, 312.

10. Höcker, H.; Reimann W.; Reif, L.; Riebel, K. *J. Mol. Catal.* **1980**,*8*, 191.

11. (a) Zuercher, W. J.; Hashimoto, M.; Grubbs,R. H. *J. Am. Chem. Soc.* **1996,** *118,* 6634. (b) Harrity, J. P. A.; La, D. S.; Cefalo, D. R.; Visser, M. S.; Hoveyda, A. H. *J. Am. Chem. Soc.* **1998**, *120,* 2343. (c) Stapper, C.; Blechert, S. *J. Org. Chem.* **2002**, *67*, 6456. (d) Jackson, K. L.; Henderson, J. A.; Motoyoshi, H.; Phillips, A. J. *Angew. Chem. Int. Ed.* **2009**, *48*, 2346.

12. Chauvin, Y.; Commereuc, D.; Zaborowski, G. *Makromol. Chem.* **1978**, *179*, 1285.

13. Höcker, H.; Reimann, W.; Riebel, K.; Szentivanyi, Z. *Makromol. Chem.* **1976**, *177*, 1707.

14. Höcker, H. *J. Mol. Catal.* **1991**, *65*, 95–99.

15. Schwendeman, J. E.; Church, C. A.; Wagener, K. B. *Adv. Synth. Catal.* **2002**, *344*, 597.

16. Wagener, K. B.; Smith, Jr., D. W. *Macromolecules* **1991**, 24, 6073.

17. Mol, J. C. *J. Mol. Cat. A* **2004**, 213, 39.

18. (a) Fürstner, A. *Angew. Chem. Int. Ed.* **2000**, 39, 3012. (b) Felpin, F. X.; Lebreton, J. Eur. *J. Org. Chem.* **2003**, 3693.

19. Bicchielli, D.; Borguet, Y.; Delaude, L.; Demonceau, A.; Dragutan, I.; Dragutan, V.; Jossifov, C.; Kalinova, R.; .Nicks, F.; Sauvage, X. Recent Applications of Alkene Metathesis in Fine Chemical Synthesis, *Green Metathesis Chemistry, Great Challenges in Synthesis, Catalysis and Nanotechnology* **2010**, 207–274.

20. (a) van der Schaaf, P. A.; Kolly, R.; Kirner, H.-J.; Rime, F.; Mühlebach, A.; Hafner, A. *J. Organomet. Chem.* **2000**, 606, 65. (b) EP993465, US6407190, WO9900396. (c) Katayama, H.; Nagao, M.; Ozawa, F. *Organometallics* **2003**, 22, 586.

21. Patents CN1907992A, US 2007/0043180 A1, PCT WO 2007/003135 A1

22. Patent US 6635768

23. (a) Anderson, A. W.; Merckling, N. G. (Du Pont de Nemours & Co.) **1955**, U.S. Patent 2,721,189. (b) Eleuterio, H.S. *J. Mol. Catal.* **1991**, *55*, 65 and references therein.

24. Banks, R. L.; Bailey, G. C. *Ind. Eng. Chem. Prod. Res. Dev*. **1964**, *3*, 170.

25. Calderon, N.; Chen, H. Y.; Scott, K. W. *Tetrahedron Lett*. **1967**, 3327. (b) Calderon, N. Ofstead, E. A.; Ward, J. P.; Judy, W. A.; Scott, K. W. *J. Am. Chem. Soc*. **1968**, 90, 4133. (c) Mol, J. C.; Moulijn, J. A.; Boelhouwer, C. *Chem. Commun*. **1968**, 633. (d) Calderon, N. *Acc. Chem. Res*. **1972**, 5, 127.

26. Hérisson, J.-L.; Chauvin, Y. *Makromol. Chem.* **1971**, *141*, 161.

27. (a) Fischer, E. O.; Kollmeier, H. J. *Ang. Chem. Int. Ed.* **1970**, *9*, 309. (b) Fischer, E. O.; Winkler, E.; Kreiter, C.; Huttner, G. G.; Krieg, B. *Ang. Chem., Int. Ed.* **1971**, *10*, 922. (d) Fischer, E. O.; Fischer, H.; Werner, H. *Ang. Chem. Int. Ed.* **1972**, *11*, 644. (e) Fischer, E. O.; Winkler, E.; Kreiter, C.; Huttner, G. G.; Regler, D. *Ang.Chem. Int. Ed.* **1972**, *11*, 238.

28. (a) Katz, T. J.; McGinnis, J. *J. Am. Chem. Soc.* **1975**, *97*, 1592. (b) Grubbs, R. H.; Burk, P. L.; Carr, D. D. *J. Am. Chem. Soc.* **1975**, *97*, 3265. (c) Katz, T. J.; Rothchild, R. *J. Am. Chem. Soc.* **1976**, *98*, 2519. (d) Grubbs, R. H.; Carr, D. D.; Hoppin, C.; Burk, P. L. *J. Am. Chem. Soc.* **1976**, *98*, 3478. (e) Katz, T. J.; McGinnis, J. *J. Am. Chem. Soc.* **1977**, *99*, 1903.

29. (a) Katz, T. J.; Sivavec, T. M. *J. Am. Chem. Soc.* **1985**, *107*, 737. (b) Katz, T. J.; Lee, S. J.; Acton, N. *Tetrahedron Lett.* **1976**, *47*, 4247.

30. (a) Tebbe, F. N.; Parshall, G. W.; Reddy, G. S. *J. Am. Chem. Soc.* **1978**, *100*, 3611. (b) Grubbs, R. H.; Tumas, W. *Science* **1989**, *243*, 907.

31. Wallace, K. C.; Liu, A. H.; Dewan, J. C.; Schrock, R. R. *J. Am. Chem. Soc.* **1988**, *110*, 4964.

32. (a) Kress, J.; Osborn, J. A.; Greene, R. M. E.; Ivin, K. J.; Rooney, J. J. *J. Am. Chem. Soc.* **1987**, *109*, 899. (b) Kress, J., Aguero, A., Osborn, J. A. *J. Mol. Catal*. **1986**, *36*, 1. (c) Quignard, F., Leconte, M., Basset, J.-M. *J. Chem. Soc., Chem. Commun.***1985**, 1816.

33. (a) Murdzek, J. S.; Schrock, R. R. *Organometallics*, **1987**, *126*, 1373. (b) Schrock, R. R.; Krouse, S. A.; Knoll, K.; Feldman, J.; Murdzek, J.S.; Yang, D.C. *J. Mol. Catal*., **1988**, *46*, 243. (c) Schrock, R. R.; Murdzek, J. S.; Barzan, G. C.; Robbins, J., DiMare M., O`Regan, M. *J. Am. Chem. Soc.*, **1990**, *112*, 3875. (h) Bazan, G.C.; Oskam, J.H.; Cho, H.-N.; Park L.Y.; Schrock, R. R.; *J. Am. Chem. Soc*., **1991**, 113, 6899. (i) For reviews of this area, see: (1) Schrock, R. R. *Tetrahedron* **1999**, *55*, 8141. (2) Schrock, R. R. *Acc. Chem. Res.* **1990**, *23*, 158. (j) for detail historical development also see Schrock, R.R. *Angew. Chem. Int. Ed.* **2006**, *45*, 3748.

34. Armstrong, S. K. *J. Chem. Soc., Perkin Trans. 1* **1998**, 371.

35. Trnka, T. M.; Grubbs, R. H. *Acc. Chem. Res.* **2001**, *34*, 18.

36. Grubbs, R. H. *J. Macromol. Sci.-Pure Appl. Chem.* **1994**, *A31*, 1829.

37. (a) Michelotti, F. W.; Keaveney, W. P. *J. Polym. Sci.* **1965**, *A3*, 895. (b) Rinehart, R. E.; Smith, H. P. *Polym. Lett.* **1965**, *3*, 1049.

38. Novak, B. M.; Grubbs, R. H. *J. Am. Chem. Soc.* **1988**, *110*, 960.

39. Several other groups subsequently published related results: (a) Zenkl, E.; Stelzer, F. *J. Mol. Catal.* **1992**, *76*, 1. (b) Lu, S.-Y.; Quayle, P.; Heatley, F.; Booth, C.; Yeates, S.G.; Padget, J. C. *Macromolecules* **1992**, *25*, 2692. (c) Feast, W. J.; Harrison, D. B. *J. Mol. Catal.* **1991**, *65*, 63.

40. (a) Hillmyer, M. A.; Lepetit, C.; McGrath, D. V.; Novak, B. M.; Grubbs, R. H. *Macromolecules* **1992**, *25*, 3345. (b) Novak, B. M.; Grubbs, R. H. *J. Am. Chem. Soc*. **1988**, *110,* 7542.

41. McGrath, D. V.; Grubbs, R. H.; Ziller, J. W. *J. Am. Chem. Soc*. **1991**, *113*, 3611.

42. France, M. B.; Grubbs, R. H.; McGrath, D. V.; Paciello, R. A. *Macromolecules* **1993**, *26*, 4742.

43. France, M. B.; Paciello, R. A.; Grubbs, R. H. *Macromolecules* **1993**, *26*, 4739.

44. Nguyen, S. T.; Johnson, L. K.; Grubbs, R. H.; Ziller, J. W. *J. Am. Chem. Soc*. **1992**, *114*, 3974.

45. Johnson, L. K.; Grubbs, R. H.; Ziller, J. W. *J. Am. Chem. Soc.* **1993**, *115*, 8130.

46. Fu, G. C.; Nguyen, S. T.; Grubbs, R. H. *J. Am. Chem. Soc.* **1993**, *115*, 9856.

47. (a) Schwab, P.; Grubbs, R. H.; Ziller, J. W. *J. Am. Chem. Soc.* **1996**, *118*, 100. (b) Schwab, P.; France, M. B.; Ziller, J. W.; Grubbs, R.H. *Angew. Chem., Int. Ed. Engl*. **1995**, 34, 2039.

48. (a) Weskamp, T.; Schattenmann, W. C.; Spiegler, M.; Herrmann,W. A. *Angew. Chem., Int. Ed.* **1998**, 37, 2490. (b) Herrmann, W.A. et al *Angew. Chem., Int. Ed.* **1999**, 38, 262.

49. (a) Scholl, M.; Trnka, T. M.; Morgan, J. P.; Grubbs, R. H. *Tetrahedron Lett.* **1999**, 40, 2247. (b) Huang, J.; Stevens, E. D.; Nolan, S. P.; Petersen, J. L. *J. Am. Chem. Soc.* **1999***, 121,* 2674.

50. Scholl, M.; Ding, S.; Lee, C. W.; Grubbs, R. H. *Org. Lett.* **1999**, *1*, 953.

51. (a) Stragies, R.; Voigtmann, U.; Blechert, S. *Tetrahedron Lett.* **2000**, *41*, 5465. (b) Smulik, J.A.; Diver, S. T *Org. Lett.* **2000**, *2*, 2271.

52. (a) Sanford, M. S.; Love, J. A.; Grubbs, R. H. *Organometallics* **2001**, 20, 5314. (b) Love, J. A.; Morgan, J. P.; Trnka, T. M.; Grubbs, R. H. *Angew. Chem. Int. Ed.* **2002**, 41, 4035. (c) Choi, T.-L.; Grubbs, R. H. *Angew. Chem. Int. Ed.* **2003**, 42, 1743.

53. (a) Harrity, J. P. A.; Visser, M. S.; Gleason, J. D.; Hoveyda, A. H. *J. Am. Chem. Soc*. **1997**, *119*, 1488. (b) Harrity, J. P. A.; La, D. S.; Cefalo, D. R.; Visser, M. S.; Hoveyda, A. H. *J. Am. Chem. Soc.* **1998**, *120*, 2343. (c) Kingsbury, J. S.; Harrity, J. P. A.; Bonitatebus, P. J.; Hoveyda, A. H. *J. Am. Chem. Soc.* **1999**, *121*, 791.

54. (a) Garber, S. B.; Kingsbury, J. S.; Gray, L. B.; Hoveyda, A. H. *J. Am. Chem. Soc.* **2000**, *122*, 8168. (b) Gessler, S.; Randl, S.; Blechert, S. *Tetrahedron Lett.* **2000**, *41*, 9973.

55. US patent number US2003/0220512 A1, **2003**.

56. (a) Wakamatsu, H.; Blechert, S. *Angew. Chem. Int. Ed*. **2002**, *41*, 2403. (b) Dunne, A. M.; Mix, S.; Blechert, S. *Tetrahedron Lett.* **2003**, *44*, 2733.

57. (a) Grela, K.; Harutyunyan, S.; Michrowska, A. *Angew. Chem. Int. Ed.* **2002**, *41*, 4038. (b) Michrowska, A.; Bujok, R.; Harutyunyan, S.; Sashuk, V.; Dolgonos, G.; Grela, K. *J. Am. Chem. Soc.* **2004**, *126*, 9318. (c) Gulajski, L.; Michrowska, A.; Bujok, R.; Grela, K. *J. Mol. Cat. A*. **2006**, *254*, 118. (d) Bieniek, M.; Michrowska, A.; Gulajski, L.; Grela, K. *Organometallics* **2007**, 26, 1096.

58. Zaja, M.; Connon, S. J.; Dunne, A. M.; Rivard, M.; Buschmann, N.; Jiricek, J.; Blechert, S. *Tetrahedron* **2003**, *59*, 6545.

59. Nicolaou, K. C.; Bulger, P. G.; Sarlah, D. *Angew. Chem. Int. Ed.* **2005**, *44*, 4490.

60. (a) Herrmann, W. A.; Köcher, C. *Angew. Chem. Int. Ed.* **1997**, *36*, 2162. (b) Arduengo, A. J. *Acc. Chem. Res.* **1999**, *32*, 913.(c) Bourissou, D.; Guerret, O.; Gabbaí, F. P.; Bertrand, G. *Chem. Rev.* **2000**, *100*, 39.

61. (a) Huang, J.; Stevens, E. D.; Nolan, S. P.; Peterson, J. L. *J. Am. Chem. Soc.* **1999**, 121, 2674. (b) Dorta, R.; Stevens, E. D.; Scott, N. M.; Costabile, C.; Cavallo, L.;Hoff, C. D.; Nolan, S. P. *J. Am. Chem. Soc.* **2005**, 127, 2485.

62. Herrmann, W. A.; Köcher, C. *Angew. Chem., Int. Ed. Engl.* **1997**, *36*, 2162.

63. (a) Cardin, D. J.; Cetinkaya, B.; Lappert, M. F. *Chem. Rev.* **1972**, *72*, 545. (b) Hu, X.; Castro-Rodriguez, I.; Olsen, K.; Meyer, K. *Organometallics* **2004**, *23*, 755. (c) Süner, M.; Plenio, H. *Chem.Commun.* **2005**, 5417. (d) Cavallo, L.; Correa, A.; Costabile, C.;Jacobsen, H. *J. Organomet. Chem.* **2005**, *690*, 5407. (e) Jacobsen, H.; Correa, A.; Costabile, C.; Cavallo, L. *J. Organomet. Chem.* **2006**, *691*, 4350.

64. Arduengo III, A. J.; Goerlich, J. G.; Marshall,W. *J. Am. Chem. Soc.* **1991**,113, 361.

65. Enders, D.; Breuer, K.; Raabe, G.; Runsink, J.; Teles, J. H.; Melder, J.-P.; Ebel, K.; Brode, S. *Angew. Chem. Int. Ed.* **1995**, 34, 1021.

66. Denk, M. K.; Rodezno, J. M.; Gupta, S.; Lough, A. J. *J. Organomet.Chem.* **2001**, 617-618, 242.

67. Arduengo III, A. J.; Dias, H. V. R.; Harlow, R. L.; Kline, M. *J. Am. Chem. Soc.* **1992**, *114*, 5530.

68. Dorta, R.; Stevens, E. D.; Scott, N. M.; Costabile, C.; Cavallo, L.;Hoff, C. D.; Nolan, S. P. *J. Am. Chem. Soc.* **2005**, *127*, 2485.

69. Magill, A. M.; Cavell, K. J.; Yates, B. F. *J. Am. Chem. Soc.* **2004**, *126*, 8717.

70. Taton, T. A.; Chen, P. *Angew. Chem. Int. Ed.* **1996**, *35*, 1011.

71. (a) Alder, R. W.; Blake, M. E.; Chaker, L.; Harvey, J. N.; Paolini, F.;Schütz, J. *Angew. Chem. Int. Ed.* **2004**, *43*, 5896. (b) Denk, M. K.; Thadani, A.; Hatano, K.; Lough, A. J. *Angew. Chem. Int. Ed.* **1997**, *36*, 2607 (c) Cetinkaya, E.; Hitchcock, P. B.; Jasim, H. A.; Lappert, M. F.; Spyropoulos, K. J. *J. Chem. Soc. Perkin Trans. 1* **1992**, 561. (d) Hahn, F. E.; Paas, M.; Le Van, D.; Fröhlich, R. *Chem. Eur. J.* **2005**, 11, 5080 (e) Denk, M. K.; Hezarkhani, A.; Zheng, F.-L. *Eur. J. Inorg. Chem.* **2007**, 3527.

72. (a) Öfele, K *J. Organomet. Chem.* **1968**, *12*, 42. (b) Wanzlick, H. W.; Schönherr, H. J. *Angew. Chem., Int. Ed. Engl.* **1968**, *7*, 141

73. (a) Cardin, D. J.; Cetinkaya, B.; Lappert, M. F. *Chem. Rev.* **1972**, *72*, 545. (b) Cardin, D. J.; Doyle, M. J.; Lappert, M. F. *J. Chem. Soc., Chem. Commun.* **1972**, 927.

74. Silvia Gonzàlez, D.; Marion N.; Nolan, S. P. *Chem. Rev.* **2009,** *109,* 3612–3676.

75. Lin, J. C. Y.; Huang, R. T. W.; Lee, C. S.; Bhattacharyya, A.; Hwang, W. S., Lin, I. J. B. *Chem. Rev.* **2009,** *109,* 3561.

76. (a) Arduengo, A. J. III; Harlow, R. J.; Kline, M. *J. Am. Chem. Soc.***1991**, *113*, 361. (b) Arduengo, A. J., III; Kline, M.; Calabrese, J. C.; Davidson, F. *J. Am. Chem. Soc.* **1991**, *113*, 9704. (c) Igau, A.; Grutzmacher, H.; Baceiredo, A.; Bertrand, G. *J. Am. Chem. Soc.* **1988**, *110*, 6463. (d) Igau, A.; Baceiredo, A.; Trinquier, G.; Bertrand, G. *Angew. Chem. Int. Ed. Engl.* **1989**, *28*, 621. For two excellent review articles on stable carbenes, see (e) Bourissou, D.; Guerret,O.; Gabbai, F. P.; Bertrand, G. *Chem. Rev.* **2000**, *100*, 39. (f) Canac, Y.; Soleilhavoup, M.; Conejero, F.; Bertrand, G. *J. Organomet. Chem.* **2004**, *689*, 3857.

77. Representative review articles: (a) Herrmann, W. A.; Köcher, C. *Angew. Chem. Int. Ed. Engl.* **1997**, *36*, 2162. (b) Herrmann, W. A. *Angew. Chem. Int. Ed.* **2002**, *41*, 1290. (c) Perry, M. C.; Burgess, K. *Tetrahedron Asymmetry* **2003**, *14*, 951. (d) Hahn, F. E. *Angew.Chem. Int. Ed.* **2006**, *45*, 1348. (e) Kantchev, E. A. B.; O'Brien, C. J.; Organ, M. G. *Angew. Chem. Int. Ed.* **2007**, *46*, 2768. (f) *Coordination Chemistry Reviews* a special issue on the organometallic chemistry of NHCs: **2007**, *251* (5-6), 595-896. (g) *Chemical Reviews* a special issue on carbenes: **2009**, *109* (8), 3209-3884. (h) *European Journal of Inorganic Chemistry* has devoted a special issue on *N*-heterocyclic carbene complexes: **2009**, (13), 1663-2007.

78. Representative review articles: (a) Enders, D.; Balensiefer, T. *Acc. Chem. Res.* **2004**, *37*, 534. (b) Nair, V.; Bindu, S.; Sreekumar, V. *Angew. Chem., Int. Ed.* **2004**, *43*, 5130. (c) Marion, N.; Díez-González, S.; Nolan, S. P. *Angew. Chem., Int. Ed.* **2007**, *46*, 2988.

79. (a) Despagnet-Ayoub, E.; Grubbs, R. H. *J. Am. Chem. Soc.* **2004**, *126*, 10198.
(b) Despagnet-Ayoub, E.; Grubbs, R. H. *Organometallics* **2005**, *24*, 338.

80. (a) Bazinet, P., Yap, G. P. A., Richeson, D. S. *J. Am. Chem. Soc.* **2003**, *125*, 13314.
(b) Alder, R. W.; Blake, M. E.; Bortolotti, C.; Bufali, S.; Butts, C. P.; Linehan, E.; Oliva, J. M.; Orpen, A. G.; Quale, M. *J. Chem. Commun.***1999**, 241. (c) Yun, J.; Marinez, E. R.; Grubbs, R. H. *Organometallics* **2004**, *23*, 4172. (d) Ozdemir, I.; Demir, S.; Cetinkaya, B.; Cetinkaya, E. *J. Organomet. Chem.* **2005**, *690*, 5849. (e) Mayr, M.; Wurst, K.; Ongania, K. H.; Buchmeiser, M. R. *Chem. Eur. J.* **2004**, *10*, 1256. (f) Herrmann,W. A.; Schneider, S. K.; Öfele, K.; Sakamoto, M.; Herdtweck, E. *J. Organomet. Chem.* **2004**, *689*, 2441. (g) Zhang, Y.; Wang, D.; Wurst, K.; Buchmeiser, M. R. *J. Organomet. Chem.* **2005**, *690*, 5728. (h) Schneider, S. K.; Herrmann, W. A.; Herdtweck, E. *J. Mol. Catal. A: Chem.* **2006**, *245*, 248.

81. (a) Scarborough, C. C.; Grrady, M. J. W.; Guzei, I. A.; Gandhi, B. A.; Bunel, E. E.; Stahl, S. S. *Angew. Chem. Int. Ed.* **2005***, 44*, 5269. (b) Scarborough, C. C.; Popp, B. V.; Guzei, I. A.; Stahl, S. S. *J. Organomet.Chem.* **2005**, *690*, 6143.

82. Benhamou, L.; Chardon, E.; Lavigne, G.; Bellemin-Laponnaz, S.; César, V. *Chem. Rev.* **2011**, *111*, 2705–2733.

83. Scholl, M.; Ding, S.; Lee, C. W.; Grubbs, R. H. *Org. Lett.* **1999**, *1*,953.

84. Garber, S. B.; Kingsbury, J. S.; Gray, B. L.; Hoveyda, A. H. *J. Am.Chem. Soc.* **2000**, *122*, 8168.

85. (a) Herrmann, W. A.; Kocher, C.; Goossen, L. J.; Artus, G. R. *Chem.Eur. J.* **1996**, *2*, 1627. (b) Arduengo, A. J., III; Krafczyk, R.; Schmutzler, R.; Craig, H. A.; Goerlich, J. R.; Marshall, W. J.;Unverzagt, M. *Tetrahedron* **1999**, *55*, 14523. (c) Weskamp, T.;Bo¨hm, V. P. W.; Herrmann, W. A. *J. Organomet. Chem.* **2000**, *600*, 12. (d) Enders, D.; Gielen, H. *J. Organomet. Chem.* **2001**, *617-618*, 70. (e) Altenhoff, G.; Goddart, R.; Lehmann, C.; Glorius, F. *J. Am. Chem. Soc.* **2004**, *126*, 15195.

86. Trnka, T. M.; Morgan, J. P.; Sanford, M. S.; Wilhelm, T. E.; Scholl,M.; Choi, T. L.; Ding, S. D.; Day, M. W.; Grubbs, R. H. *J. Am.Chem. Soc.* **2003**, *125*, 2546.

87. (a) Wang, H. M. J.; Lin, I. J. B. *Organometallics* **1998**, *17*, 972. (b) Lin, I. J. B.;Vasam, C. S. *Comments Inorg. Chem.* **2004**, *25*, 75. (c) de Frémont, P.; Scott, N. M.; Stevens, E. D.; Ramnial, T.; Lightbody, O. C.; Macdonald, C. L. B.; Clyburne, J. A. C.; Abernethy, C.D.;Nolan, S. P. *Organometallics* **2005**, *24*, 6301. (d) Garrison, J. C.;Youngs, W. J. *Chem. Rev.* **2005**, *105*, 3978. (e) Yu, X. Y.; Patrick, P. O.; James, B. R. *Organometallics* **2006**, *25*, 2359.

88. (a) Ivin, K. J.; Mol, J. C. *Olefin Metathesis and Metathesis Polymerization*;Academic Press: San Diego, CA, **1997**.(b) Grubbs, R. H. *Handbook of Metathesis*; Wiley-VCH: Weinheim, Germany, **2003.**

89. (a) Jafarpour, L.; Stevens, E. D.; Nolan, S. P. *J. Organomet. Chem.* **2000**,*606*, 49.(b) Fürstner, A.; Ackermann, L.; Gabor, B.; Goddard, R.; Lehmann,C. W.; Mynott, R.; Stelzer, F.; Thiel, O. R. *Chem. Eur. J.* **2001**, *7*,3236.(c) Dinger, M. B.; Mol, J. C. *Ad*V. *Synth. Catal.* **2002**, *344*, 671. (d) Courchay, F. C.; Sworen, J. C.; Wagener, K. B. *Macromolecules* **2003**, *36*, 8231.

90. Ritter, T.; Day, M. W.; Grubbs, R. H. *J. Am. Chem. Soc.* **2006**, *128*,11768.

91. (a) Berlin, J. M.; Campbell, K.; Ritter, T.; Funk, T. W.; Chlenov, A.; Grubbs, R. H. *Org. Lett.* **2007**, *9*, 1339.(b) Stewart, I. C.; Ung, T.; Pletnev, A. A.; Berlin, J. M.; Grubbs, R. H.;Schrodi, Y. *Org. Lett.* **2007**, *9*, 1589.

92. Hong, S. H.; Chlenov, A.; Day, M. W.; Grubbs, R. H. *Angew. Chem.,Int. Ed.* **2007**, *46*, 5148.

93. Hong, S. H.; Wenzel, A. G.; Salguero, T. T.; Day, M. W.; Grubbs,R. H. *J. Am. Chem. Soc.* **2007**, *129*, 7961.

94. Chung, C. K.; Grubbs, R. H. *Org. Lett.* **2008**, *10*, 2693.

95. Kuhn, K. M.; Bourg, J.-B.; Chung, C. K.; Virgil, S. C.; Grubbs, R. H.*J. Am. Chem. Soc.* **2009**, *131*, 5313.

96. Leuthäu*ß*er, S.; Schmidts, V.; Thiele, C. M.; Plenio, H. *Chem. Eur. J.* **2008**, *14*, 5465.

97. (a) Balof, S. L.; P'Pool, S. J.; Berger, N. J.; Valente, E. J.; Shiller, A. M.; Schanz, H. J. *Dalton Trans.* **2008**, 5791. (b) Balof, S. L.; Yu, B.; Lowe, A. B.; Ling, Y.; Zhang, Y.; Schanz, H. J. *Eur. J. Inorg.Chem.* **2009**, 1717.

98. Vehlow, K.; Gessler, S.; Blechert, S. *Angew. Chem., Int. Ed.* **2007**,*46*, 8082.

99. Luan, X.; Mariz, R.; Gatti, M.; Costabile, C.; Poater, A.; Cavallo,L.; Linden, A.; Dorta, R. *J. Am. Chem. Soc.* **2008**, *130*, 6848.

100. Ledoux, N.; Linden, A.; Allaert, B.; Mierde, H. V.; Verpoort, F. *Adv. Synth. Catal.* **2007**, *349*, 1692.

101. Fürstner, A.; Ackermann, L.; Gabor, B.; Goddard, R.; Lehmann,C. W.; Mynott, R.; Stelzer, F.; Thiel, O. R. *Chem. Eur. J.* **2001**, *7*,3236.

102. Dinger, M. B.; Nieczypor, P.; Mol, J. C. *Organometallics* **2003**, *22*, 5291.

103. Prühs, S.; Lehmann, C. W.; Fürstner, A. *Organometallics* **2004**, *23*, 280.

104. Vehlow, K.; Maechling, S.; Blechert, S. *Organometallics* **2006**, *25*, 25.

105. Ledoux, N.; Linden, A.; Allaert, B.; Mierde, H. V.; Verpoort, F. *Adv.Synth. Catal.* **2007**, *349*, 1692.

106. Ledoux, N.; Allaert, B.; Pattyn, S.; Mierde, H. V.; Vercaemst, C.;Verpoort, F. *Chem.Eur. J.* **2006**, *12*, 4654.

107. Ledoux, N.; Allaert, B.; Linden, A.; van der Voort, P.; Verpoort, F.*Organometallics* **2007**, *26*, 1052.

108. Vougioukalakis, G. C.; Grubbs, R. H. *Organometallics* **2007**, *26*, 2469.

109. Vougioukalakis, G. C.; Grubbs, R. H. *Chem. Eur. J.* **2008**, *14*, 7545.

110. Leuthaüβer, S.; Schmidts, V.; Thiele, C. M.; Plenio, H. *Chem.Eur.J.* **2008**, *14*, 5465.

111. Fournier, P. A.; Collins, S. K. *Organometallics* **2007**, *26*, 2945.

112. (a) Fournier, P. A.; Savoie, J.; Stenne, B.; Be´dard, M.; Grandbois, A.; Collins, S. K. *Chem. Eur. J.* **2008**, *14*, 8690. (b) Grandbois, A.;Collins, S. K. *Chem. Eur. J.* **2008**, *14*, 9323.

113. Vehlow, K.; Wang, D.; Buchmeiser, M. R.; Blechert, S. *Angew.Chem., Int. Ed.* **2008**, *47*, 2615.

114. Grisi, F.; Costabile, C.; Gallo, E.; Mariconda, A.; Tedesco, C.; Longo, P. *Organometallics* **2008**, *27*, 4649.

115. van Veldhuizen, J. J.; Garber, S. B.; Kingsbury, J. S.; Hoveyda, A. H. *J. Am. Chem. Soc.* **2002**, *124*, 4954.

116. van Veldhuizen, J. J.; Campbell, J. E.; Giudici, R. E.; Hoveyda, A. H. *J. Am. Chem. Soc.* **2005**, *127*, 6877.

117. Funk, T. W.; Berlin, J. M.; Grubbs, R. H. *J. Am. Chem. Soc.* **2006**, *128*, 1840.

118. Dias, E. L.; Nguyen, S. T.; Grubbs, R. H. *J. Am. Chem. Soc.* **1997**, 119,3887-3897.

119. (a) Ulman, M.; Grubbs, R. H. *Organometallics* **1998**, *17*, 2484. (b) Sanford, M. S.; Love, J.; Grubbs, R. H. *J. Am. Chem. Soc.* **2001**, *123*, 6543. (c) Sanford, M. S.; Ulman, M.; Grubbs, R. H. *J. Am. Chem. Soc.* **2001**, *123*, 749.(d) Hinderling, C.; Adlhart, C.; Chen, P. *Angew. Chem. Int. Ed.* **1998**, *37*, 2685. (e) Volland, M. A. O.; Adlhart, C.; Kiener, C. A.; Chen, P.; Hofmann, P. *Chem. Eur. J.* **2001**, *7*, 4621.

120. (a) Vyboishchikov, S. F.; Bühl, M.; Thiel, W. *Chem. Eur. J.* **2002**, *8*, 3962. (b) Fomine, S.; Vargas, S. M.; Tlenkopatchev, M. A. *Organometallics* **2003**, *22*, 93. (c) Bernardi, F.; Bottoni, A.; Miscione, G. P. *Organometallics* **2003**, *22*, 940.(d) van Rensburg,W. J.; Steynberg, P. J.; Meyer,W. H.; Kirk, M. M.; S., F. G. *J. Am. Chem. Soc.* **2004**, *126*, 14332. (e) Adlhart, C.; Chen, P. *J. Am. Chem. Soc.* **2004**, *126*, 3496. (f) Jordaan, M.; van Helden, P.; Sittert, C. G. C. E.; Vosloo, H. C. M. *J. Mol.Cat. A* **2006**, *254*, 145. (g) Cavallo, L. *J. Am. Chem. Soc.* **2002**, *124*, 8965.(h) Aagaard, O. M.; Meier, R.; Buda, F. *J. Am. Chem. Soc.* **1998**, *120*, 7174.

121. Tallarico, J. A.; Bonitatebus, P. J.; Snapper, M. L. *J. Am. Chem. Soc.* **1997**, *119*, 7157.

122. Adlhart, C.; Hinderling, C.; Baumann, H.; Chen, P. *J. Am. Chem. Soc.* **2000**, *122*, 8204.

123. Romero, P. E.; Piers, W. E. *J. Am. Chem. Soc.* **2005**, *127*, 5032.

124. (a) Trnka, T. M.; Day, M. W.; Grubbs, R. H. *Organometallics* **2001**, *20*, 3845.
(b) Anderson, D. R.; Hickstein, D. D.; O'Leary, D. J.; Grubbs, R. H. *J. Am. Chem. Soc.* **2006**, *128*, 8386.

125. Berlin, J. M.; Goldberg, S. D.; Grubbs, R. H. Angew. Chem. Int. Ed. **2006**, *45*, 7591.

126. Costabile, C.; Cavallo, L. *J. Am. Chem. Soc.* **2004**, *126*, 9592.

127. Wenzel, A. G.; Grubbs, R. H. *J. Am. Chem. Soc.* **2006**, *128*, 16048.

128. (a) Benitez, D.; Goddard, W. A. I. *J. Am. Chem. Soc.* **2005**, *127*, 12218. (b) Correa, A.; Cavallo, L. *J. Am. Chem. Soc.* **2006**, *128*, 13352.

129. Sanford, M. S.; Love, J. A.; Grubbs, R. H. *J. Am. Chem. Soc.* **2001**,*123*, 6543.

130. Sanford, M. S.; Ulman, M.; Grubbs, R. H. *J. Am. Chem. Soc.* **2001**,*123*, 749.
131. Adlhart, C.; Chen, P. *Helv. Chim. Acta.* **2003**, *86*, 941.

132. (a) Getty, K.; Delgado-Jaime, M. U.; Kennepohl,P. *J. Am. Chem. Soc.* **2007**, *129*, 15774. (b) Antonova, N. S., Carbo´, J. J., Poblet, J. M. *Organometallics* **2009**, *28*, 4283.

133. (a) Kingsbury, J. S.; Harrity, J. P. A.; Bonitatebus, P. J., Jr.; Hoveyda,A. H. *J. Am. Chem. Soc.* **1999**, *121*, 791.(b) Garber, S. B.; Kingsbury, J. S.; Gray, B. L.; Hoveyda, A. H. *J. Am.Chem. Soc.* **2000**, *122*, 8168. (c) Kingsbury, J. S.; Hoveyda, A. H. *J. Am. Chem. Soc.* **2005**, *127*, 4510.

134. Tim Vorfalt, Klaus J. Wannowius, Vasco Thiel, Herbert Plenio *Chem. Eur. J.* **2010**, *16*, 12312.

135. D. E. De Vos, M. D., Sels, B. F.; Jacobs, P. A. *Chem. Rev.* **2002**, *102,* 3615.

136. Coperet, C.; Basset, J.-M. *Adv. Synth. Catal.* **2007**, *349*, 78.

137. (a) Coperet, C.; Chabanas, M.; Saint-Arroman, R. P. Basset, J-M. *Angew. Chem. Int. Ed.* **2003**, *42*, 156. (b) Basset, J-M.; Baudouin, A.; Bayard, F.; Candy, J. P.; Coperet, C.; De Mallmann, A.; Godard, G.; Kuntz, E.; Lefebvre, F.; Lucas, C.; Norsic, S.; Pelzer, K.; Quadrelli, A.; Santini, C.; Soulivong, D.; Stoffelbach, F.; Taoufik, M.; Thieuleux, C.; Thivolle-Cazat, J.; Veyre, L.; *Modern Surface Organometallic Chemistry* (Eds.: Basset, J-M.; Psaro, R.; Roberto, D.; Ugo, R.) Wiley-VCH, Weinheim, **2009**, Chap. 3.8.

138. Lesage, A.; Emsley, L.; Chabanas, M.; Copéret, C.; Basset, J.-M. *Angew. Chem. Int. Ed*. **2002**, *41*, 4535

139. Rendón, N.; Blanc, F.; Copéret, C. *Coord. Chem. Rev.* **2009***, 253,* 2015.

140. (a) Chabanas, M.; Quadrelli, E. A.; Fenet, B.; Copéret, C.; Thivolle-Cazat, J.; Basset, J.-M.; Lesage, A.; Emsley, L. *Angew. Chem. Int. Ed.* **2001**, *40*, 4493. (b) Chabanas, M.; Baudouin, A.; Copéret, C.; Basset,J.-M. *J. Am. Chem. Soc.* **2001**, *123*, 2062. (c) Chabanas, M.; Baudouin, A.; Copéret, C.; Basset,J.-M.; Lukens, W.; Lesage, A.; Hediger, S.; Emsley, L.; *J. Am.Chem. Soc.* **2003**, *125*, 492. (d) Chabanas, M. ; Copéret, C. ; Basset, J.-M. *Eur. J. Chem*. **2003**, 9, 971. (e) Copéret, C. *New. J. Chem.* **2004**, 28, 1.(f) Toreki, R.; Schrock, R. R. *J. Am. Chem. Soc.* **1990**,*112*, 2448. (g) Toreki, R.; Vaughan, G. A.; Schrock, R. R.; Davis, W. M. *J. Am. Chem. Soc.* **1993**, *115*, 127.

141. (a) Blanc, F.; Coperet, C.; Thivolle-Cazat, J.; Basset, J.-M.; Lesage, A.; Emsley, L.; Sinha, A.; Schrock, R. R.; *Angew. Chem. Int. Ed.* **2006**, *45*, 1216. (b) Rhers, B.; Salameh, A.; Baudouin, A.; Quadrelli, E. A.; Taoufik, M.; Copéret, C.; Lefebvre, F.; Basset, J.-M.; Solans-Monfort, X.; Eisenstein, O.; Lukens, W. W.; Lopez, L. P. H.; Sinha, A.; Schrock, R. R. *Organometallics* **2006**, *25*, 3554. (c) Poater, A.; Solans-Monfort, X.; Clot, E.; Copéret, C.; Eisenstein, O. *Dalton Trans.* **2006**, 3077. (d) Feher, F. J.; Tajima, T. L. *J. Am. Chem. Soc.* **1994**, *116*, 2145.

142. (a) Lopez, L. P. H.; Schrock, R. R. *J. Am. Chem. Soc.* **2004**, *126*, 9526. (b) Sinha, A; Lopez, L. P. H.; Schrock, R. R.; Hock,A. S.; Mueller, P. *Organometallics* **2006**, *25*, 1412.

143. (a) Blanc, F.; Thivolle-Cazat, J.; Basset, J. M. J.; Copéret, C.; Hock, A. S.; Tonzetich, Z. J.; Schrock, R. R. *J. Am. Chem. Soc.* **2007**, *129*,1044. (b) Copéret, C. *Dalton Trans.* **2007**, 5498. (c) Blanc, F.; Rendón, N.; Berthoud, R.; Basset, J.-M.; Copéret, C.; Tonzetich, Z. J.; Schrock, R. R. *Dalton Trans.* **2008**, 3156. (d) Blanc, F.; Salameh, A.; Thivolle-Cazat, J.; Basset, J. M.; Coperet, C.; Sinha, A.; Schrock, R. R. *C. R. Chim* .**2008**, *11*, 137. (e) Rendón, N.; Berthoud, R.; Blanc, F.; Gajan, D.; Maishal, T.; Basset, J. M.; Coperet, C.; Lesage, A.; Emsley, L.; Marinescu, S. C.; Singh, R.; Schrock, R. R. *Chem. Eur. J.* **2009**, *15*, 5083.;

144. Marciniec B.; Rogalski, S.; Potrzebowski, M. J.; Pietraszuk, C. *ChemCatChem* **2011**, *3,* 904.

145. (a) Buchmeiser, M. R. *New J. Chem*. **2004**, *28*, 549 (b) H. Clavier, K. Grela, A. Kirschning, M. Mauduit, S. P. Nolan, *Angew. Chem. Int.Ed.* **2007**, *46*, 6786 (c) Buchmeiser, M. R. *Chem. Rev*. **2009**, *109*,303.

146. (a) Wu, Z.; Nguyen, S. T.; Grubbs, R. H.; Ziller, J. W. *J.Am. Chem. Soc.* **1995**, 117, 5503. (b) Buchowicz, W.; Ingold, F.; Mol, J. C.; Lutz, M.; Spek, A. L. *Chem.Eur. J.* **2001**, *7*, 2842.

147. (b) Nieczypor, P.; Buchowicz, W.; Meester, W. J. N.; Rutjes, F. P. J. T.; Mol, J. C. *Tetrahedron Lett.* **2001**, *42*, 7103.

148. (a) Krause, J. O.; Lubbad, S. H.; Nuyken, O.; Buchmeiser M. R. *Macromol. Rapid Commun.* **2003**, 24, 875. (b) Yang, L.; Mayr, M.; Wurst, K.; Buchmeiser, M. R. *Chem. Eur. J.* **2004**, 10, 5761. (c) Krause, J. O.; Nuyken, O.; Buchmeiser M. R. *Chem.Eur. J.* **2004**, 10, 2029. (d) Halbach, T. S.; Mix, S.; Fischer, D.; Maechling, S.; Krause, J. O.;Sievers, C.; Blechert, S.; Nuyken, O.; Buchmeiser, M. R. *J. Org.Chem.* **2005**, *70*, 4687.

149. Vehlow, K.; Kohler, K.; Blechert, S.; Dechert, S.; Meyer, F. *Eur. J. Inorg. Chem.* **2007**, 2727.

150. David Bek, Naděžda Žilkova, Jiří Dědeček, Jan Sedláček, Hynek Balcar *Top Catal* **2010**, *53,* 200.

151. (a) Ahmed, M.; Barrett, A. G. M.; Braddock, D. C.; Cramp, S. M.; Procopiou, P. A. *Tetrahedron Lett.* **1999**, *40*, 8657. (b) Ahmed, M.; Arnauld, T.; Barrett, A. G. M.; Braddock, D. C.; Procopiou, P. A. *Synlett* **2000**, 1007. (c) Fuchter, M. J.; Hoffman, B. M.; Barrett, A. G. M. *J. Org. Chem.* **2006**, *71*, 724. (d) Cetinkaya, S.; Khosravi, E.; Thompson, R. *J. Mol.Catal. A: Chem.* **2006**, *254*, 138.

152. (a) Jafarpour, L.; Nolan, S. P. *Org. Lett.* **2000**, *2*, 4075. (b) Jafarpour, L.; Heck, M.-P.; Baylon, C.; Lee, H. M.; Mioskowski, C.; Nolan, S. P. *Organometallics* **2002**, *21*,671.

153. (a) Kingsbury, J. S.; Harrity, J. P. A., Jr.; Hoveyda, A. H. *J. Am. Chem. Soc.* **1999**, *121*, 791. (b) Kingsbury, J. S.; Hoveyda, A. H. *J. Am. Chem. Soc.* **2005**, *127*, 4510.

154. (a) Ahmed, M.; Arnauld, T.; Barrett, A. G. M.; Braddock, D. C.;Procopiu, P. A. *Synlett* **2000**, 1007. (b) Nolan, S. P.; Jafarpour, L. *Chem. Abstr.* **2005**, *143*, 133542; U.S.Patent US 6.921.736 B1, 2005.

155. (a) Yao, Q. *Angew. Chem. Int. Ed.* **2000**, *39*, 3896.(b) Yao, A.; Rodriguez Motta, *Tetrahedron Lett.* **2004**, *45*, 2447.

156. Garber, S. B.; Kingsbury, J. S.; Gray, B. L.; Hoveyda, A. H. *J. Am. Chem. Soc.* **2000**, *122*, 8168.

157. (a) Grela, K.; Tryznowski, M.; Bieniek, M. *Tetrahedron Lett.* **2002**, *43*, 9055. (b) Connon, S. J.; Dunne, A. M.; Blechert, S. *Angew.Chem. Int. Ed.* **2002**, *41*, 3835. (c) Yao, Q.; Zhang, Y. *J. Am. Chem. Soc.* **2004**, *126*, 74. (d) Michrowska, A.; Mennecke, K.; Kunz, U.; Kirschning, A.; Grela, K. *J. Am. Chem. Soc.* **2006**, *128*, 13261.

158. Randl, S.; Buschmann, N.; Connon, S. J.; Blechert, S. *Synlett* **2001**, 1547.

159. (a) Kingsbury, J. S.; Garber, S. B.; Giftos, J. M.; Gray, B. L.; Okamoto, M. M.; Farrer, R. A.; Fourkas, J. T.; Hoveyda, A. H. *Angew. Chem. Int. Ed.* **2001**, *40*, 4251. (b) Kingsbury, J. S.; Hoveyda, A. H. *J. Am. Chem. Soc.* **2005**, 127, 4510. (c) Fischer, D. ; Blechert, S. *Adv. Synth. Catal.* **2005**, 347,1329.

160 Michalek, F.; Maedge, D.; Ruehe, J.; Bannwarth, W. *Eur. J. Org. Chem.* **2006**, 577.

161. (a) Vorfalt, T.; Wannowius, K. J.; Thiel V.; Plenio H. *Chem. Eur. J.* **2010**, *16*, 12312. (b) Vorfalt, T.; Wannowius, K. J.; Thiel V.; Plenio H. *Angew. Chem. Int. Ed.* **2010**, *49*, 5533.

162. Nguyen, S. T.; Grubbs, R. H. *J. Organomet. Chem.* **1995**, *497*, 195.

163. Melis, K.; De Vos, D.; Jacobs, P.; Verpoort, F. *J. Mol.Catal. A: Chem.* **2001**, *169*, 47.

164. (a) Gatard, S.; Nlate, S.; Cloutet, E.; Bravic, G.; Blais, J.-C.; Astruc, D. *Angew. Chem. Int. Ed.* **2003**, *42*, 452.(b) Gatard, S.; Kahlal, S.; Mery, D.; Nlate, S.; Cloutet, E.; Saillard, J.-Y.; Astruc, D. *Organometallics* **2004**, *23*, 1313. (c) Astruc, D.; Heuze, K. Gatard, S.; Mery, D.; Nlate, S.; Plault, L. *Adv. Synth. Catal.* **2005**, *347*, 329.

165. Schurer, S. C.; Gessler, S.; Buschmann, N.; Blechert, S. *Ang. Chem. Int. Ed.* **2000**, *39*, 3898.

166. Kingsbury, J. S.; Garber, S. B.; Giftos, J. M.; Gray, B. L.; Okamoto, M. M.; Farrer, R. A.; Fourkas, J. T.; Hoveyda, A. H. *Angew. Chem.* **2001**, *113*, 4381.

167. Mayr, M.; Wang, D.; Kröll, R.; Schuler, N.; Prühs, S.; Fürstner, A.;Buchmeiser, M. R. *Adv. Synth. Catal.* **2005**, *347*, 484.

168. (a) Gallivan, J. P.; Jordan, J. P.; Grubbs, R. H. *Tetrahedron Lett.* **2005**, *46*, 2577. (b) Hong, S. H.; Grubbs, R. H. *J. Am. Chem. Soc.* **2006**, *128*, 3508.

169. Sommer, W. J.; Weck, M. *Adv. Synth. Catal.* **2006**, *348*, 2101.

170. (a) Prühs, S.; Lehmann, C. W.; Fürstner, A. *Organometallics* **2004**, *23*,280. (b) Li, L.; Shi, J.-l. *Adv. Synth. Catal.* **2005**, *347*, 1745. (c) Sommer, W. J.; Weck, M. *Adv. Synth. Catal.* **2006**, *348*, 2101. (d) Allen, D. P.; Van Wingerden, M. M.; Grubbs, R. H. *Org. Lett.* **2009**, 11, 1261.

171. Akiyama, R.; Kobayashi, S. *Angew. Chem.* **2002**, *114*, 2714.

172. Horn, J.; Michalek, F.; Tzschucke, C. C.; Bannwarth, W. *Top. Curr. Chem.* **2004**, *242*, 43.

173. (a) Michrowska, A.; Mennecke, K.; Kunz, U.; Kirschning, A.; Grela, K. *J. Am. Chem. Soc.* **2006**, *128*, 13261. (b) Michrowska, A.; Gulajski, L.; Kaczmarska, Z.; Mennecke, K.;Kirschning, A.; Grela, K. *Green Chem.* **2006**, *8*, 685.

174. Van Berlo B.; Houthoofd K.; Sels, B. F.; Jacobs, P. A. *Adv. Synth. Catal.* **2008**, 350, 1949.

175. (a) Yao, Q., Zhang, Y. *Angew. Chem., Int. Ed.* **2003**, *42*, 3395. (b)Yao, Q.; Sheets, M. *J. Organomet. Chem.* **2005**, *690*, 3577.(c) Thurier, C.; Fischmeister, C.; Bruneau, C.; Olivier-Bourbigou, H.; Dixneuf, P. H. *J. Mol. Catal. A: Chem.* **2007**, *268*, 126. (d) Keraani, A.; Rabiller-Baudry, M.; Fischmeister, C.; Bruneau C.; *Catalysis Today* **2010**, *156*, 268.

176. (a) Moreau, J. J. E.; Wong Chi Man, M. *Coord. Chem. Rev*. **1998**, *178-180*, 1073. (b) Wight, A. P.; Davis, M. E. *Chem. Rev.* **2002,** *102,* 3589. (c) De Vos, D. E.; Dams, M.; Sels, B. F.; Jacobs, P. A. *Chem. Rev.* **2002,** *102,* 3615. (d) Zamboulis, A.; Moitra, N.; Moreau, J. J. E.; Cattöen, X.; Wong Chi Man, M. *J. Mater. Chem*., **2010**, *20*, 9322.

177. Hoffmann, F.; Cornelius, M.; Morell, J.; Fröba M. *Angew. Chem. Int. Ed.* **2006**, *45*, 3216.

178. Sing, K. S. W.; Everett, D. H.; Haul, R. H. W.; Moscou, L.; Pierotti, R. A.; Rouquerol, J.; Siemieniewska, T. *Pure Appl. Chem*. **1985**, *57*, 603.

179. Hench, L. L.; West, J. K. *Chem. Rev.* **1990**, *90. 33.*

180. Kresge, C. T.; Leonowicz, M. E.; Roth, W. J.; Vartuli, J. C.; Beck, J. S.; *Nature*, **1992**, *359*, 710.

181. (a) Beck, J. S.; Vartuli, J. C.; Roth, W. J.; Leonowicz, M. E.; Kresge, C. T.; Schmitt, K. D.; Chu, C. T.-W.; Olson, D. H.; Sheppaard, E. W.; McCullen, S. B.; Higgins, J. B.;Schlenker, J. L. *J. Am. Chem. Soc*. **1992**, *114*, 10834. (b) Monnier, A.; Schüth, F.; Huo, Q.; Kumar, D.; Margolese, D.; Maxwell, R. S.; Stucky,G. D.; Krishnamurty, M.; Petroff, P.; Firoouzi, A.; Janicke, M.; Chmelka, B. F.*Science* **1993**, *261*, 1299.

182. Attard, G. S.; Glyde, J. C.; Göltner, C. G. *Nature* **1995**, *378*, 366.

183. Monnier, A.; Scheth, F.; Huo, Q.; Kumar, D.; Margolese, D.; Maxwell, R. S.; Stucky, G.; Krishnamurty, M.; Petroff, P.; Firouzi, A.; Janicke, M.; Chmelka, B.; *Science* **1993**, *261*, 1299.

184. Tang, J.; Zhou, X.; Zhao, D.; Lu, G. Q.; Zou, J.; Yu, C. *J. Am. Chem. Soc*. **2007**, 129, 9044.

185. Zhao, D.; Feng, J.; Huo, Q.; Melosh, N.; Fredrickson, G. H.; Chmelka, B. F.; Stucky, G. D. *Science* **1998**, *279* , 548.

186. (a) Corriu R. J. P. *Chem. Commun*., **2000**, 71. (b) Guari,Y.; Thieuleux, C.; Mehdi, A.; Reyé, C.; Corriu, R. J. P.; Gomez-Gallardo, S.; Philippot, K.; Chaudret, B.; Dutartre, R. *Chem. Commun***. 2001**, *15*, 1374. (c Guari,Y.; Thieuleux, C.; Mehdi, A.; Reyé, C.; Corriu, R. J. P.; Gomez-Gallardo, S.; Philippot, K.; Chaudret, B. *Chem. Mater.* **2003**, *15*, 2017. (d) Corriu, R. J. P.; Mehdi, A.; Reyé, C.; Thieuleux, C.; Frenkel, A.; Gibaud, A. *New J. Chem.* **2004**, *28*, 156. (e) Corriu, R. J. P.; Mehdi, A.; Reyé, C.; Thieuleux, C. *Chem. Mater.* **2004**, *16*, 159. (f) Corriu, R. J. P.; Mehdi, A.; Reyé, C. *J. Mater. Chem.* **2005**, *15*, 4285. (g) Mouawia, R.; Mehdi, A.; Reyé, C.; Corriu, R. J. P. *New J. Chem.* **2006**, *1*, 1077

187. Karame, I.; Boualleg, M.; Camus, J. M.; Maishal, T. K.; Alauzun, J.; Basset, J. M.; Coperet, C.; Corriu, R. J. P.; Jeanneau, E.; Mehdi, A.; Reye, C.; Veyre, L.; Thieuleux, C. *Chem. Eur. J.* **2009**, 15, 11 820.

188. (a) Elias, X.; Pleixats, R.; Wong Chi Man, M.; Moreau, J. J. E. *Adv. Synth. Catal.* **2006**, *348*, 751. (b) Elias, X.; Pleixats, R.; Wong Chi Man, M.; Moreau, J. J. E. *Adv. Synth. Catal.* **2007**, *349*, 1701. (c) Elias, X.; Pleixats, R.; Wong Chi Man, M. *Tetrahedron* **2008**, *64*, 6770.

189. Borja, G.; Pleixats, R.; Alibés, R.; Cattoën, X.; Wong Chi Man, M. *Molecules* 2010, *15*, 5756.

190. (a) Arlie,J.-P.; Chauvin, Y.; Commereuc, D.; Soufflet, J.-P. *Makromol. Chem*. **1974**, *175*, 861. (b) Pampus, G.; Lehnert, G. *Makromol. Chem.* **1974**, *175*, 2605. (c) Höcker, H.; Reimann, W.; Reif, L.; Riebel, K. *Makromol. Chem.* **1976**, *177*, 1707.

191. Derouane, E. G. *J. Mol. Cat. A*. **1998**, *134*, 29.

192. Thieuleux, C.; Coperet, C.; Veyre, L.; Corriu, R.; Reye, C.; Mehdi, A.; Basset, J. M.; Maishal, T.; Boualleg, M.; Karame, I.; Camus, J. M.; Alauzun, J. US 2011/0160412 A1, WO 2009/092814 A1, EP 2082804 A1.

Chapter 2

Synthesis of hybrid organic-inorganic, heterogeneous Ru-NHC catalysts and their catalytic performances in RO-RCM of cyclooctene

In the present chapter we have described the following points:

1. The synthesis of hybrid organic-inorganic heterogeneous unsymmetrical Ru-NHC catalysts
    i. Five well-defined, heterogeneous unsymmetrical Ru-NHC catalysts with different tethers namely propyl (*short-flexible)*, benzyl (*semi-rigid)*, hexyl (*long-flexible)*, phenyl mesityl (*long-rigid)* and dimethyl phenyl (*short-rigid)* were prepared and fully characterized.
2. The catalytic performances of these catalysts in the RO-RCM of cyclooctene for the selective formation of cyclic oligomers (in particular dimer of cyclooctene) were studied.
3. A kinetic investigation was perfomed to determine the nature of products (primary *vs.* secondary products) during the RO-RCM of cyclooctene and dimer of cyclooctene.

Five targeted heterogeneous catalysts are listed below:

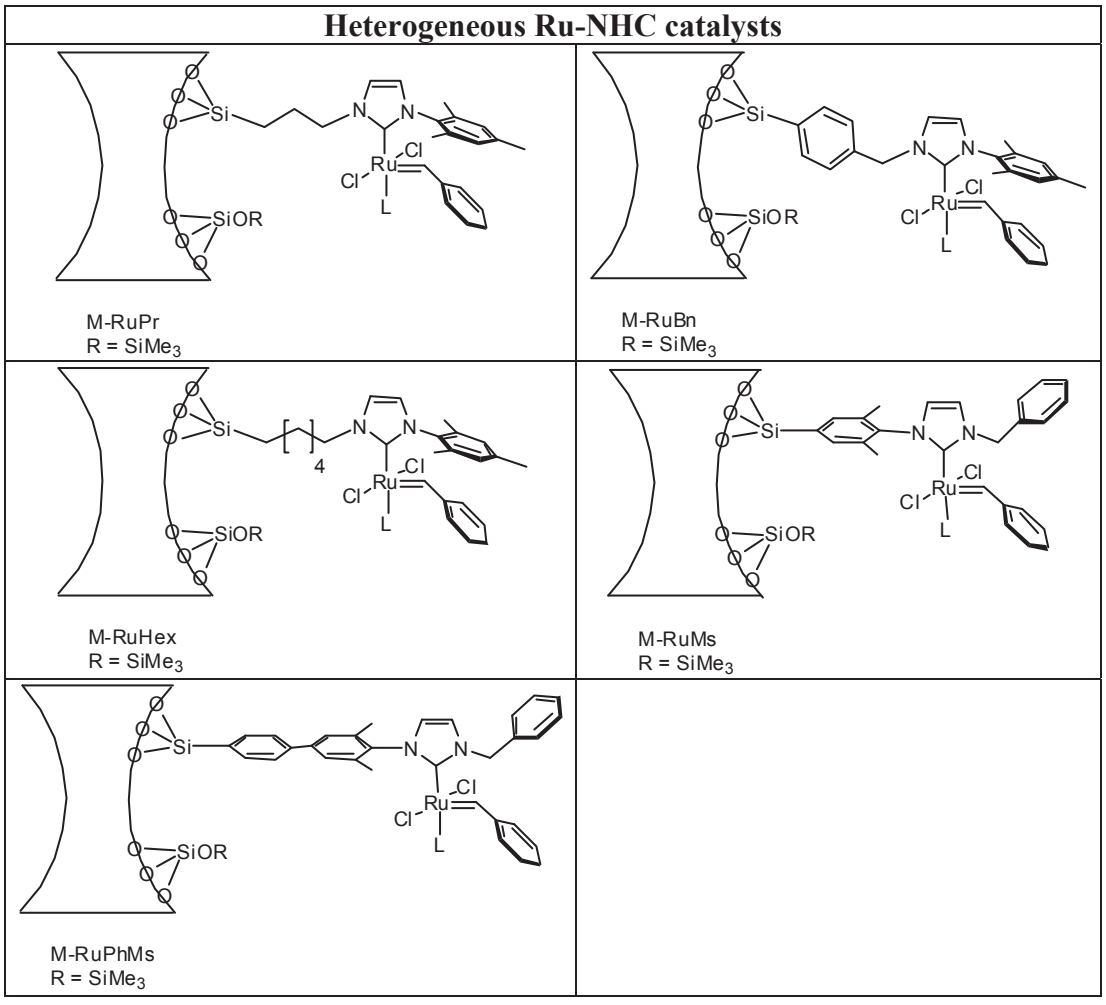

Figure 1: Well-defined heterogeneous unsymmetrical Ru-NHC catalysts.

1. Introduction

Low molecular weight cyclic oligomers (C15-17 cyclic alkenes) are important intermediates in the fragrance and perfume industry to prepare macrocyclic musks.[1] Our objective was thus the selective formation of low molecular weight cyclic oligomers (in particularly dimer-C16) from cyclooctene through the tandem Ring Opening - Ring Closing Metathesis (RO-RCM) reactions, which to date remains a challenge. One of the key problems is the competitive polymerization of cyclooctene *via* Ring Opening Metathesis Polymerisation (ROMP), which is favoured both entropically and enthalpically at any temperature.[2]

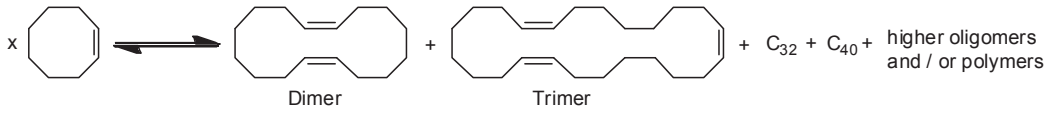

Scheme 1: Tandem Ring Opening - Ring Closing Metathesis (RO-RCM) of cyclooctene.

RO-RCM of cyclooctene has been reported previously using Re_2O_7/Al_2O_3 catalysts pre-activated with tin compounds for the synthesis of macrocyclic dienes.[3] Recently, heterogenized methyltrioxorhenium (MTO) species were used for the synthesis of low molecular weight cyclic oligomers.[4] However, higher activity and better selectivity in lower cyclic-oligomers still remain a challenge.

One parameter to favour the selective formation of specific cyclic structure is the control of back-biting over polymerisation. One approach in the context of heterogeneous catalysis can consist in using confinement effects (shape selective catalysis)[5] to impose constrain for the preferred formation of cyclic structures over polymers.

Our research group has recently developed a new class of heterogeneous catalysts based on regularly distributed surface M-NHC units (M = Ir, Ru, Au) through the pore channels of the mesostructured inorganic matrix. [6] Such well-defined and fully controlled Ru-NHC based materials - obtained by sol-gel process *via* a templating route - display unprecedented high activity and stability in the self-metathesis of ethyl oleate.[7]

Thus, we decided to use these mesoporous materials as catalysts, tuning advantage of their structuration to generate confinement effects as well as a favorable interaction of the Ru-center with the surface to yield mostly cyclic structures over polymers. In this context, we prepared several Ru-NHC hybrid heterogeneous catalysts with different length and flexibility of tethers [**M-RuPr** *(short-flexible tether)*, **M-RuBn** *(semi-rigid tether)*, **M-RuHex** *(long-flexible tether)*, **M-RuPhMs** *(long-rigid tether)* and **M-RuMs** *(short-rigid tether)*] (Figure 1) and we tested their catalytic performances for the selective formation of cyclic oligomers (particularly cyclic dimer) in RO-RCM of cyclooctene.

2. Results and discussion

2.1. General strategy for the synthesis of hybrid materials containing Ru-NHC units

2D hexagonal mesostructured materials were prepared by sol-gel process *via* a templating route[8], *i.e. via* cohydrolysis and co-polycondensation of tetraethyl-orthosilicate (TEOS) and an organotrialkoxysilane RSi-$(OR)_3$ in the presence of a surfactant (used as structure-directing agent), namely the triblock copolymer, Pluronic 123, $EO_{20}PO_{70}EO_{20,}$ [poly(ethyleneoxide)-poly(propyleneoxide)-poly(ethyleneoxide)]. The surfactant was then removed by non destructive solvent extraction thus liberating the material porosity (Figure 2).

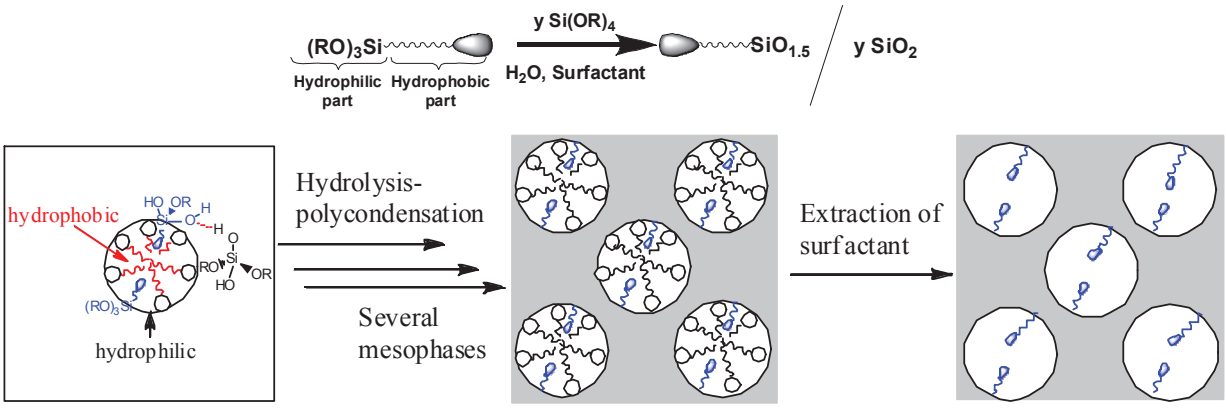

Figure 2: Synthesis of hybrid materials with organic functionalities inside the pores.

Using this templating route, we synthesized five different hybrid materials as shown in Figure 3.

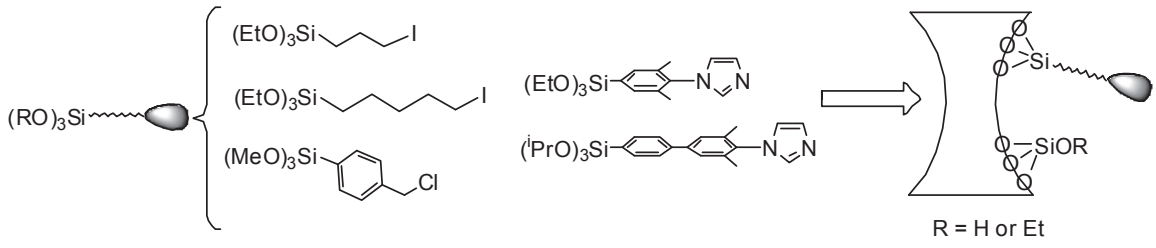

Figure 3: Hybrid materials with different organic tethers.

In general, after removal of the surfactant, these materials are quantitively transformed into imidazolium units by reaction with mesityl-imidazole in toluene under reflux for 48 h. The materials are further treated with 2.0 M acid solution at 45 °C for 2 - 3 h, in order to transform the surface alkoxy silane groups into silanols. Materials are further extracted with aqueous pyridine/HCl solution for the removal of trace amounts of surfactant.[9] Then, the materials silanol surface groups are passivated into trimethylsilyl units using Me_3SiBr in presence of triethylamine. This material is then treated with KHMDS to generate a NHC-carbene unit, and

contacted with the Grubbs-I complex, thus yielding the targetted Ru-NHC heterogeneous catalyst (Figure 4).

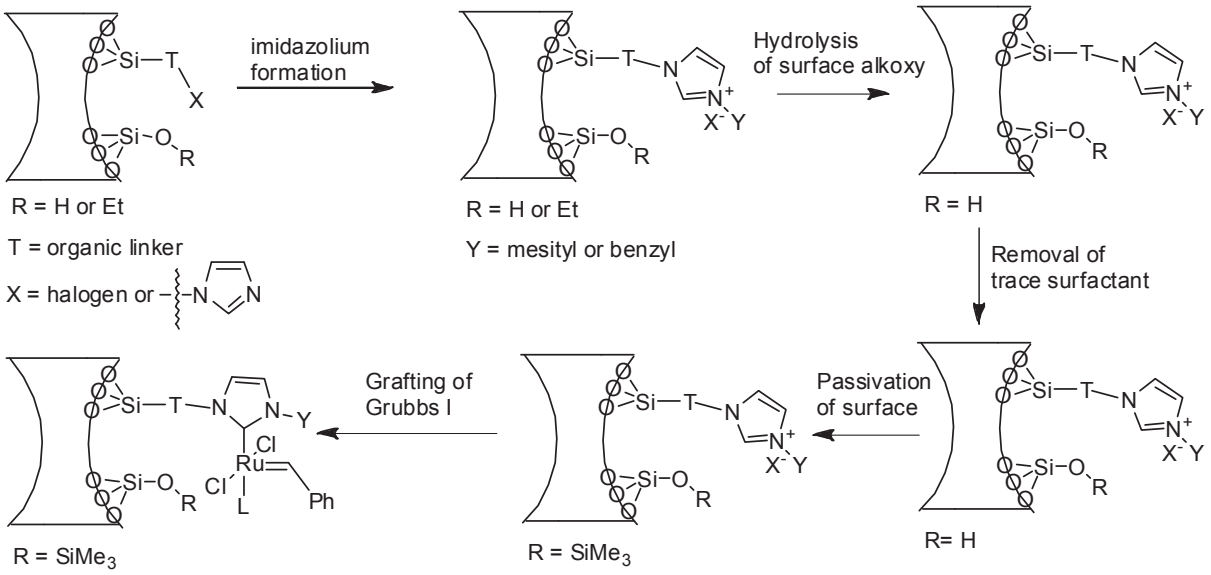

Figure 4: Methodology for the synthesis of Ru-NHC materials.

Using this methodology, we prepared several Ru-NHC based heterogeneous catalysts [**M-RuPr** *(short-flexible tether)*, **M-RuBn** *(semi-rigid)*, **M-RuHex** *(long-flexible)*, **M-RuPhMs** *(long-rigid)* and **M-RuMs** *(short-rigid)*]. The synthesis of these functionalized materials is described in the experimental section; only specific features will be discussed here.

The catalysts **M-RuPr** and **M-RuHex** contain identical Ru-NHC species attached to the silica surface *via* a linear carbon chain: C3 and C6 carbons respectively. Such high flexible tethers should allow the Ru sites to interact with the surface functionalities. While in case of **M-RuBn**, Ru-NHC units are attached to the silica surface *via* semi flexible benzyl tether having a phenyl rigid part, but a "flexible" -CH_2 group close to the NHC. This semi-rigid tether could allow the Ru centre to interact with the surface functionality but in a less significant manner than in **M-RuPr**/**M-RuHex**. Finally, **M-RuMs** and **M-RuPhMs** were prepared to generate isolated Ru sites from the silica surface, using rigid tethers phenyl and biphenyl, respectively.

The effect of tether length and flexibility were indeed observed and is discussed below, first in terms of chemical structures of Ru-NHC sites (first and second coordination sphere) and then in terms of low cyclic oligomers selectivity and productivity.

2.2. Interaction of surface functionality with Ru-NHC - Effect of flexibility and length of tether

A key feature of the Ru-NHC pre-catalyst is the presence of a coordinated PCy_3 ligand, which is liberated to generate the active 14 electron species (Scheme 2). For Ru-NHC pre-catalysts the ratio P/Ru is 1. The elemental analysis of the supported pre-catalysts also revealed the ratio P/Ru of *ca.* 1. We thus investigated the nature of the supported pre-catalysts by ^{31}P NMR in order to get a better understanding of the structure of these Ru-NHC supported systems, in particular because proton and ^{13}C solid-state NMR, even using ^{13}C labelled samples, failed to provide much information about their structures.

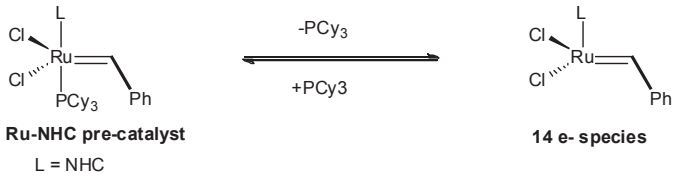

Scheme 2: Dissociation of phosphine to generate 14 e^- species.

It is noteworthy that for **M-RuPr**, **M-RuBn** and **M-RuMs** no signal was observed in the 32-36 ppm region in the ^{31}P NMR spectra as expected for PCy_3 coordinated to Ru-NHC species. This result indicated that the Ru centre was not coordinated to PCy_3 and thus probably stabilized by surface functionalities, *e.g.* siloxane oxygen (Figures 6a-c). The only - large - signal observed at 49 ppm corresponds to a pentavalent phosphorous compound, probably a tricyclohexylphosphine oxide resulting from side-reactions of PCy_3 with surface functionalities.[10,11] For **M-RuHex** *(long-flexible tether),* the major signal still appears at 49 ppm, but it is possible to observe a *weak signal* at 32 ppm (Figure 6d), suggesting that either some Ru centres have kept a coordinated PCy_3 or phosphonium species are generated.[11] In contrast, for **M-RuPhMs (***long rigid tether) a strong signal* at 36 ppm appears along with the signal at 49 ppm (Figure 6e), suggesting that besides the formation of pentavalent phosphorus compound, a large number of Ru centres (most) are coordinated to PCy_3. The shoulder peak at around 25 ppm is probably due to the presence of a phosphonium surface species (Figure 6e).

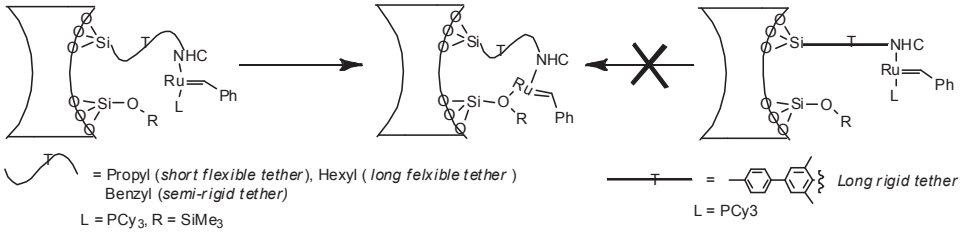

Figure 5: Presence or absence of interactions between the surface functionality and the Ru phosphine complex depending on the tether.

This result shows that the nature of the tether has indeed a major influence on the structure of supported Ru-NHC pre-catalysts, the interaction with surface functionalities being more prominent with the *shorter flexible tethers* than with the *long rigid tethers i.e.*; Pr ~ Bn ~ Ms > Hex >> PhMs (Figure 5).

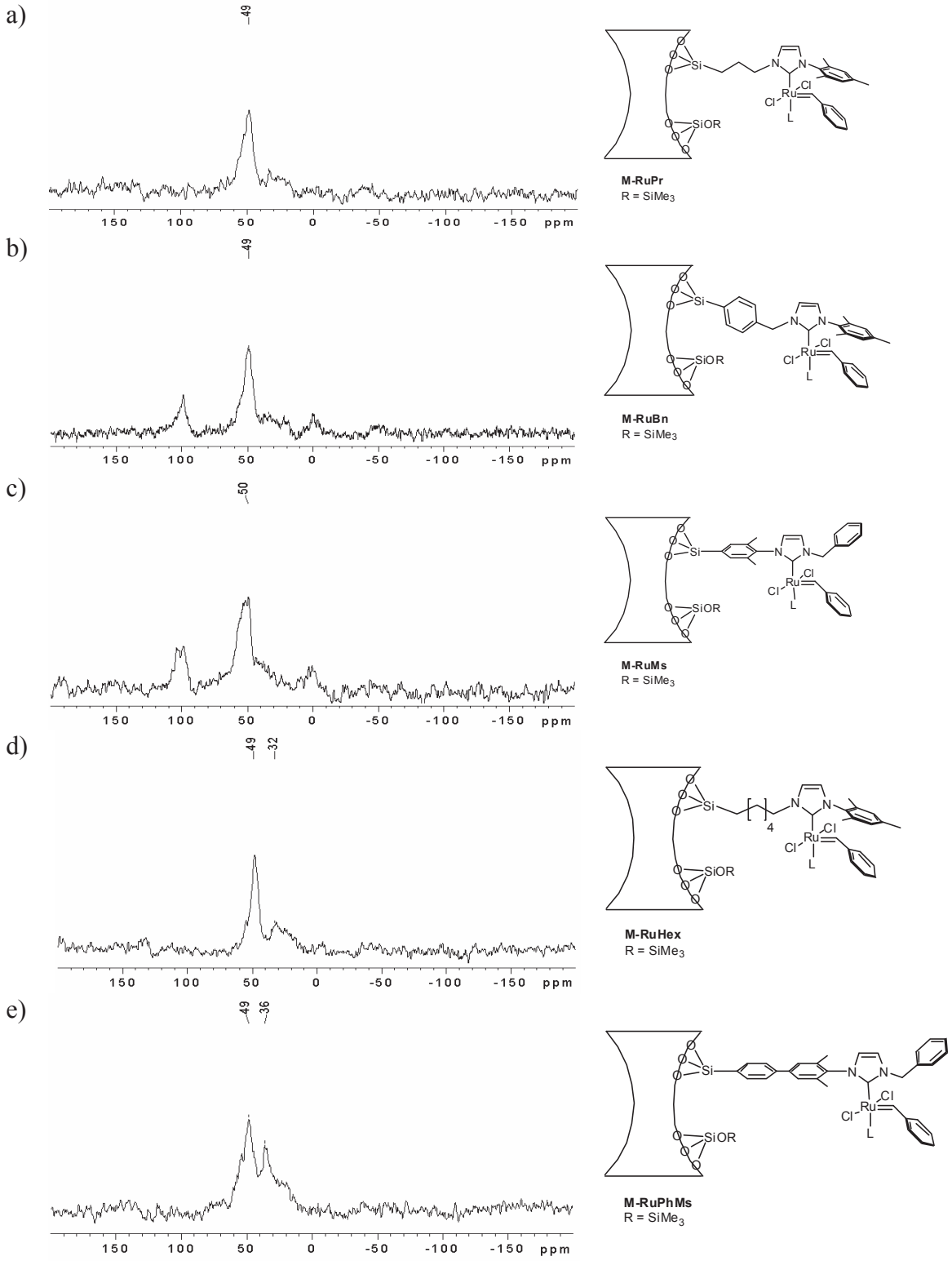

Figure 6: ^{31}P NMR for heterogeneous Ru-NHC catalysts, peaks at 0 and 100 ppm are spinning side bands

2.3. Evaluation of catalytic performances as a function of the tether

All the catalytic reactions were carried out in toluene with a ratio cyclooctene / Ru = 10,000 using ≈ 20 mM solution of cyclooctene in toluene at room temperature unless otherwise noted. Conversion and selectivities were monitored using eicosane as internal standard. Sample at 0 min was taken before the addition of catalyst and considered as reference point. All selectivities are defined as follows:

S_i = (number of mole of cyclooctene converted in product i) / (total number of cyclooctene converted).

The response ratio (cyclooctene and dimer) with respect to eicosane (internal standard) were measured and used to monitor their concentration as a function of time during the catalytic test (Appendix section 5.1). For the higher cyclic oligomers (trimer, tetramer & pentamer), the concentrations were measured with respect to the internal standard assuming that the response factor of n-mers is n times the response factor of cyclooctene (use of FID detector and assuming that there is no segregation in the injector as observed for the dimer).

Oligomers greater than pentamers were not detected by GC with the present method and only in small amounts by direct injection in MS.

2.3.1. Catalytic Performances of Ru-NHC containing hybrid material M-RuPr for the selective RO-RCM of cyclooctene

The reaction was performed under standard conditions, *i.e.* with a ratio of cyclooctene / Ru = 10000 and ~21 mM cyclooctene. Results concerning conversion of cyclooctene, product selectivities and mass balance in the cyclo-oligomerisation of cyclooctene are summarized in Figures 7, 8 (details can be found in the appendix - Table 4).

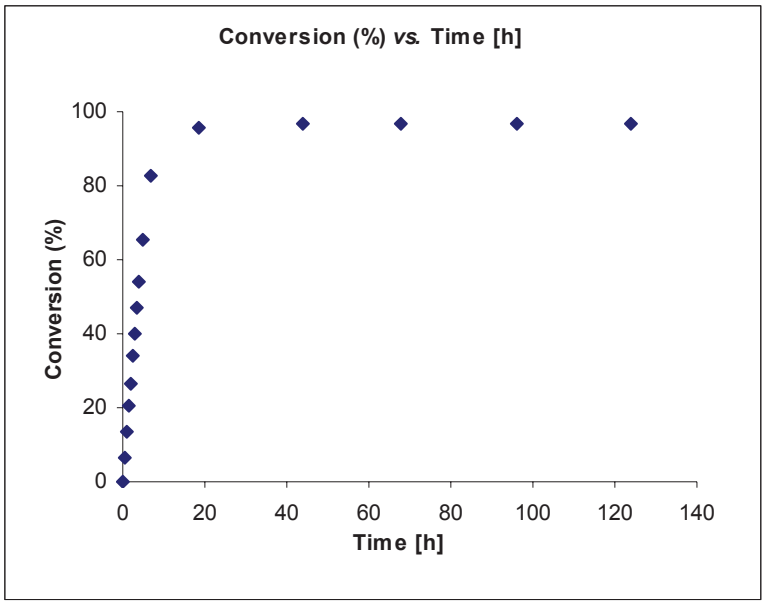

Figure 7: Conversion of cyclooctene (%) *vs.* time [h] using **M-RuPr**.

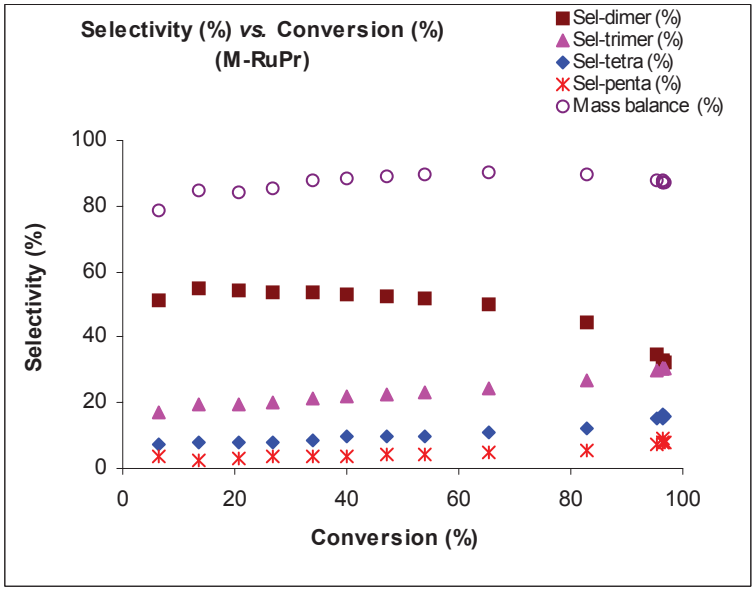

Figure 8: Selectivity of cyclic products (%) *vs.* conversion of cyclooctene (%) using **M-RuPr**.

In the case of M-RuPr (flexible propyl tether), high conversion of cyclooctene (83% within 7 h) was obtained with an initial rate of *ca. 1360* mol/mol Ru/h; the conversion reaching ca. 96% after 20 h (Figure 7).

The mass balance was high at all reaction times: it increased from 79% at low conversion to reach a steady maximum of 87-90% (Figure 8). The main detected products were the dimers and trimers of cyclooctene along with smaller amounts of tetramers and pentamers; higher oligomers up to octamers were detected in small amount (<2%) by mass spectrometry only *via* direct introduction of the reaction mixtures. The selectivity in dimer was observed to vary from 50% to 54% up to 60-65% conversion of cyclooctene and then decreased slowly to 32-33% from 65-95% conversion of cyclooctene. Concomitantly the selectivity in trimer (17-31%), tetramer (7-16%) and pentamers (3-8%) increased throughout the catalytic test (Figure 8). The correlation between the decrease of selectivity in dimer and the increase of selectivity in higher oligomers along with a constant mass balance of ca. 87-90% is consistent with the conversion of dimer into other oligomers at higher conversions.

Overall, it is noteworthy that **M-RuPr** displayed the selective formation of lower cyclic oligomers, in particular dimer, with constant mass balance even at higher cyclooctene conversions and the current data suggested that nearly no polymers are formed during the catalytic test and that low cyclic oligomers are mainly obtained with high selectivity.

Moreover, the selectivity at low conversions indicates that all oligomers are possibly formed as primary products, but also *via* secondary processes.

2.3.2. Comparison of catalytic Performances of Ru-NHC containing hybrid materials

With such promising results in obtaining the selective formation of lower cyclic oligomers (in particular dimer) for **M-RuPr**, we investigated the catalytic performances of **M-RuBn, M-RuHex, M-RuMs** and **M-RuPhMs** using the same reaction conditions, *i.e.* ratio of cyclooctene / Ru = 10000 and ~21 mM cyclooctene. Comparison of results of these catalysts to that of **M-RuPr** in terms of i) conversion of cyclooctene, ii) dimer selectivities and iii) mass balance in the RO-RCM of cyclooctene are summarized in Figures 9-12 (details for each catalyst performance can be found in the appendix section - Tables 5-8, Figures 59-66).

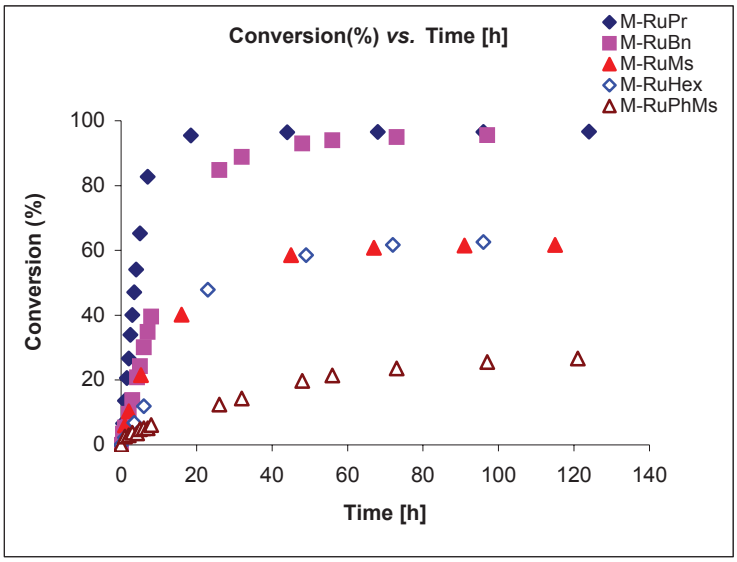

Figure 9: Comparison of conversion of cyclooctene (%) *vs.* time [h] using various heterogeneous catalysts.

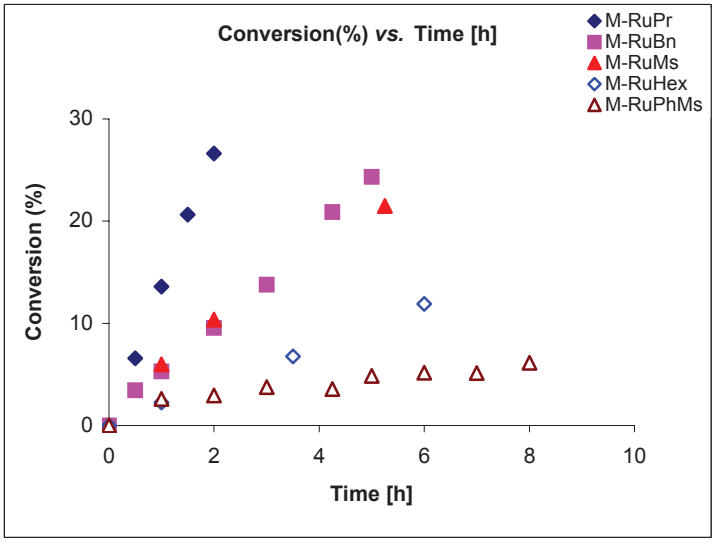

Figure 10: Zoom for initial 10 h, comparison of conversion of cyclooctene (%) *vs.* time [h] using various heterogeneous catalysts.

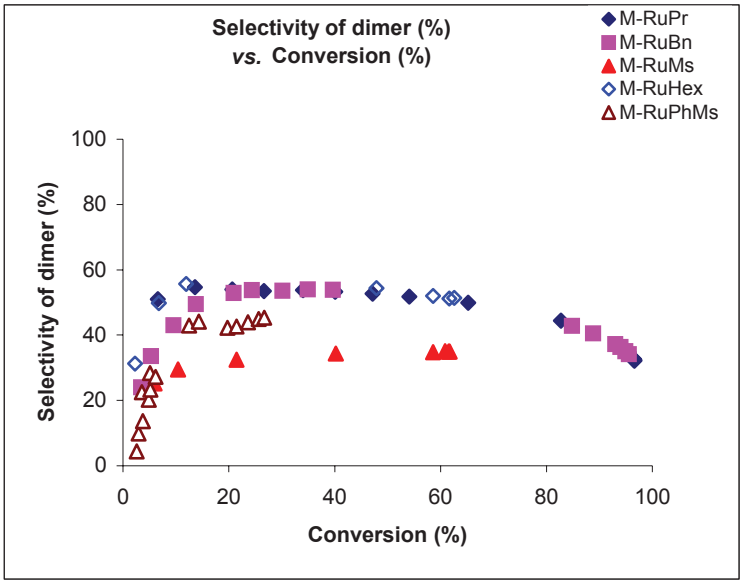

Figure 11: Selectivity of cyclic products (%) *vs.* conversion of cyclooctene (%) using various heterogeneous catalysts.

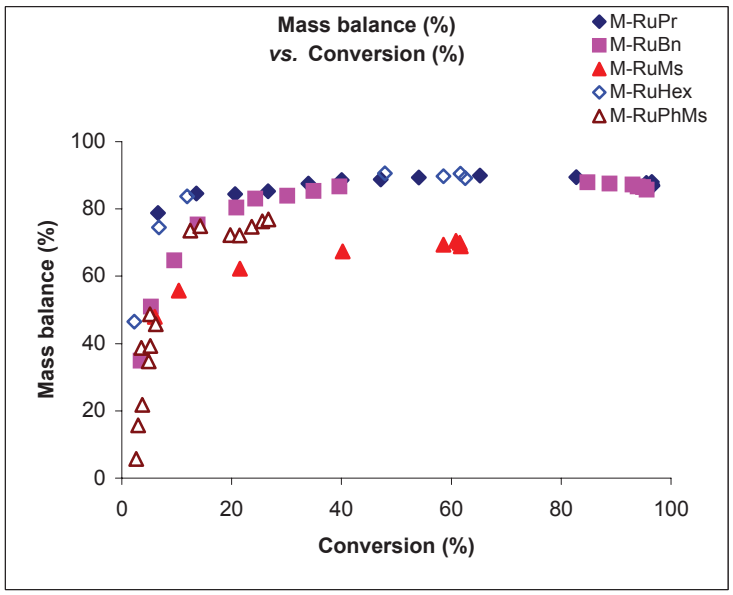

Figure 12: Mass balance (%) *vs.* conversion of cyclooctene (%) using various heterogeneous catalysts.

With respect to initial rates, the reactivity of the catalysts for cyclooctene conversion is of order: **M-RuPr** > **M-RuMs** > **M-RuBn** > **M-RuPhMs** > **M-RuHex** (Figure 10, Table 1). This result indicates that the catalysts with shorter tethers are more active than those with the longer ones.

In terms of final conversion, the performances of **M-RuPr** and **M-RuBn** were observed to be similar (Table 1) where as the performances of **M-RuMs** are similar to those of **M-RuHex**, the latter catalysts showing an initiation period and a rapid deactivation with a maximum conversion of 60-65%. **M-RuPhMs** was found to be the worst catalysts: it displayed an initiation period and a lower maximum conversion (ca. 20-25% after 95-100 h). For this specific catalysts it is noteworthy that (long rigid tether), ^{31}P NMR (Figure 6e) showed the

presence of coordinated phosphine on Ru. This result could explain the presence of an initiation period (the phosphine decoordination from Ru). The faster deactivation of **M-RuMs** because stabilising interactions between the Ru-NHC active site and the surface functionalities are not favored.

Overall, the trend in terms of stability is: **M-RuPr** (*short-flexible)* > **M-RuBn** (*semi-rigid)* > **M-RuHex** (*long-flexible)* > **M-RuMs** (*short-rigid)* > M-**RuPhMs** (*long-rigid),* showing that the stability depends mainly on the flexibility and then on the length of the tether.

In terms of selectivity, catalysts with flexible tethers (**M-RuPr**, **M-RuBn** and **M-RuHex**) showed similar performances, in particular dimer selectivity of 50-54% and mass balance of 85-90%. In contrast, catalysts with rigid tethers and in particular **M-RuMs** displayed much lower selectivity of dimer (30-35%) and mass balance (65-70%); **M-RuPhMs** being slightly more active than **M-RuMs** with the dimer selectivity of 40-45% and a mass balance of 75-80% (Figure 11, 12). Thus presence of a long rigid tether and a phosphine coordinated to Ru seems to be detrimental to catalytic performance, thus illustrating the influence of the interactions between the metal centre and the passivated silica surface.

The slow increase in the selectivity of trimer, tetramer and pentamers throughout the catalytic test was also observed for all the catalysts (Figures for selectivity of all the cyclic products and mass balance can be found in the appendix section), where as the decrease of selectivity in dimer was observed only after conversion of cyclooctene reached 60-65% (Figure 11), for the catalysts **M-RuPr** and **M-RuBn**.

Table 1: Comparison of selectivity of cyclic products, at 30-40% conversion of cyclooctene and constant mass balance. Also in terms of initial rate and final conversion of cyclooctene

Catalyst	Initial rate [mol/mol Ru/h]	Final conversion (%)	Selectivity (%)				Mass balance (%)
			Dimer	Trimer	Tetramer	Pentamer	
M-RuPr	1360	95-96	53	22	10	4	85-90
M-RuBn	529	95-96	54	20	8	3	85-90
M-RuHex	215	60-65	54	24	9	3	85-90
M-RuPhMs	260	20-25	45	19	8	4	75-80
M-RuMs	598	60-65	34	17	10	6	65-70

Overall, catalysts with short flexible tethers were found to be better in terms of rate and selective formation of dimer in RO-RCM of cyclooctene.

2.4. Kinetic Investigation - primary *vs.* secondary products

2.4.1. RO-RCM of Cyclooctene

Kinetic investigation was carried out in order to have a deeper understanding of the reaction mechanism for selective formation of cyclic oligomers. To know if these cyclic products are primary products or secondary products, reactions with varying concentrations of cyclooctene (from 5 to 20 mM) at constant cyclooctene / Ru ratio (10000) were carried out using **M-RuPr** as the reference catalyst. Results concerning the rate of reaction, selectivity of products and productivity of cyclic products are summarized in Figures 13-18. (Details can be found in appendix section Tables 9-14)

2.4.1.1. Effect of concentration on reaction rate

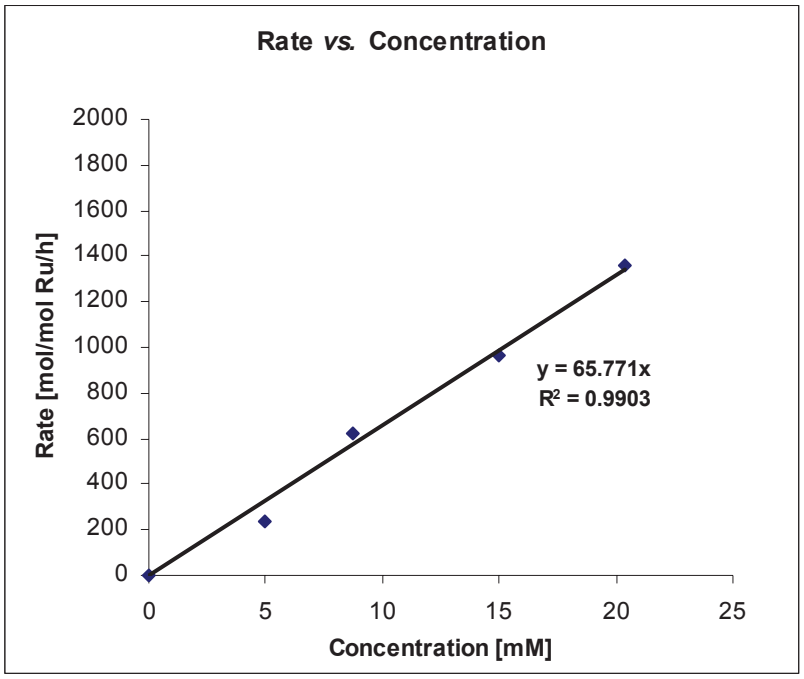

Figure 13: Rate [mol/mol Ru/h] *vs.* Concentration [mM]. Effect of cyclooctene concentration on rate of reaction in COM of cyclooctene.

We can observe here that the rate of conversion is roughly proportional to the concentration of cyclooctene, thus indicating that the reaction is 1st order with respect to cyclooctene (Figure 13).

$$\text{Rate} = k\,[\text{cyclooctene}]^1$$

2.4.1.2. Effect of concentration on selectivity of products

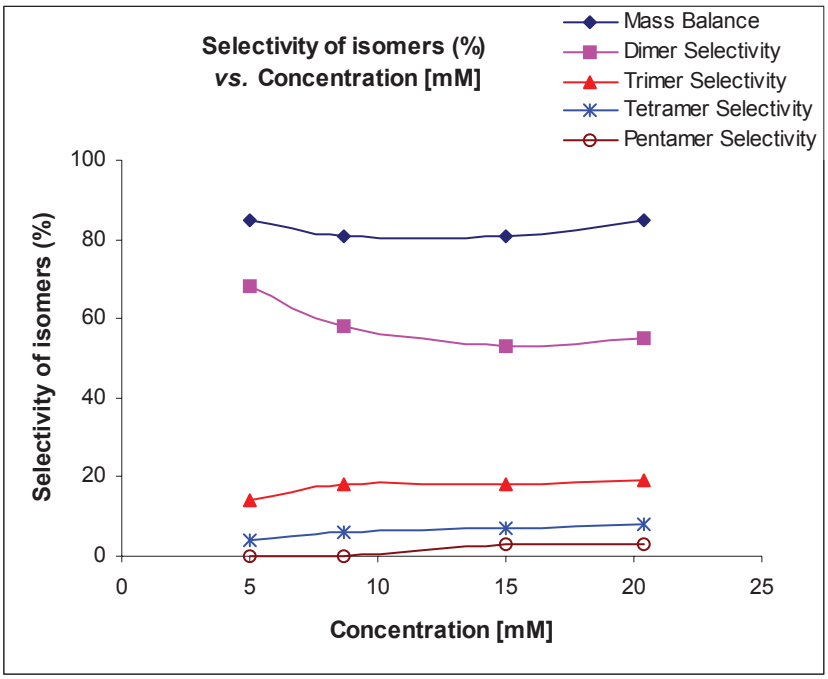

Figure 14: Selectivity of isomers (%) *vs.* Concentration [mM] at 13-15% conversion of cyclooctene Effect of cyclooctene concentration on the selectivity of products in COM of cyclooctene.

The experimental data show that product selectivities, at similar conversion (13-15%) and mass balance (81-85%) (Figure 14), are also affected by cyclooctene concentration: Selectivity of dimer increases with the decrease of cyclooctene concentration whereas the selectivity of other products (trimer up to pentamer) decreases. This further supports that dimer is indeed a primary product, where as other oligomers are also formed *via* secondary processes (COM of dimer).

2.4.1.3. Nature of products (primary *vs.* secondary)

To have a closer look at the the effect of concentration of cyclooctene variations on the formation of each cyclic oligomer (dimer to pentamer), *i.e.* to have better understanding of the nature of the products (primary and secondary processes involved in their formation). We decided to plot products productivity dimer, trimer, tetramer and the pentamer oligomers (cumulated TON in each product) as a function of cyclooctene conversion. This analysis was performed

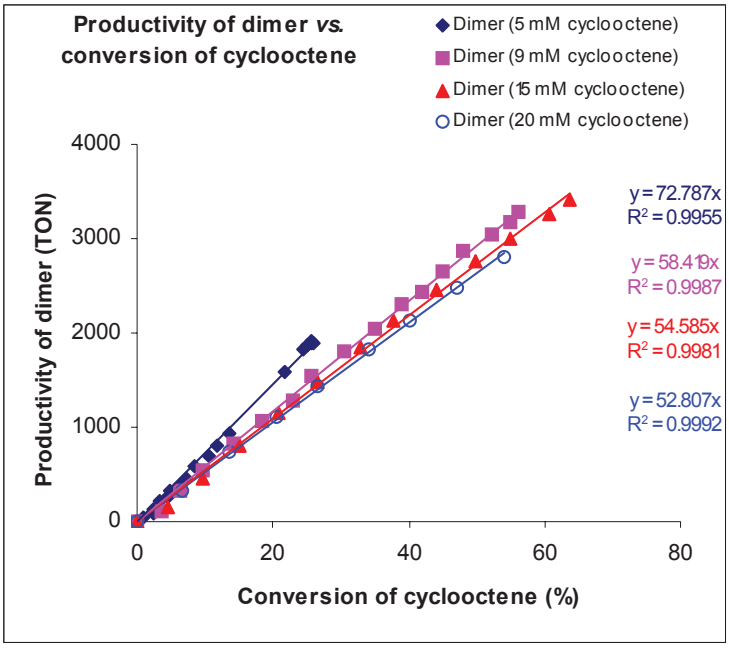

Figure 15: Productivity of dimer at 50-60% conversion of cyclooctene.

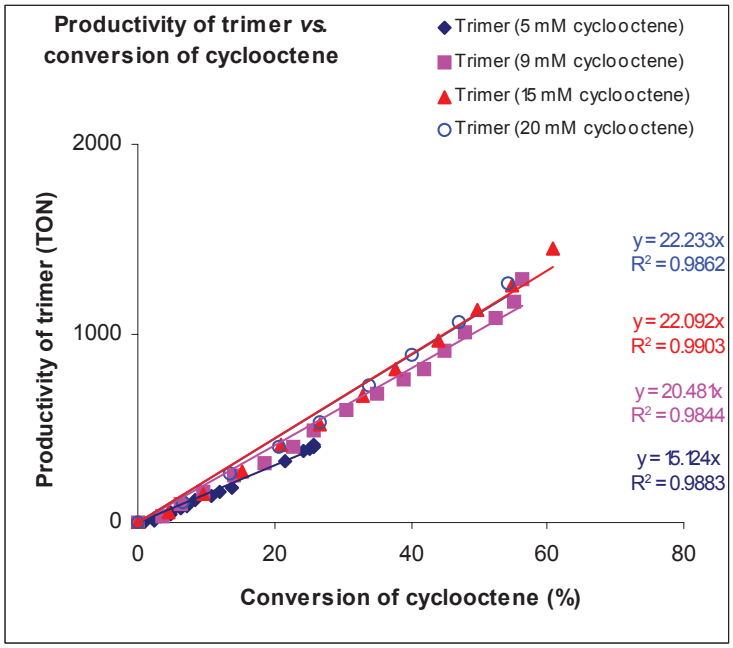

Figure 16: Productivity of trimer at 50-60% conversion of cyclooctene.

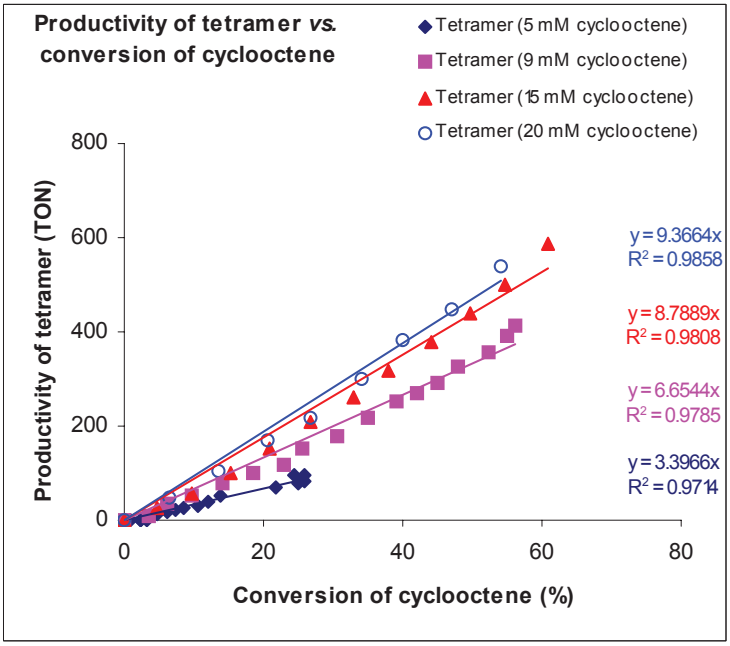

Figure 17: Productivity of tetramer at 50-60% conversion of cyclooctene.

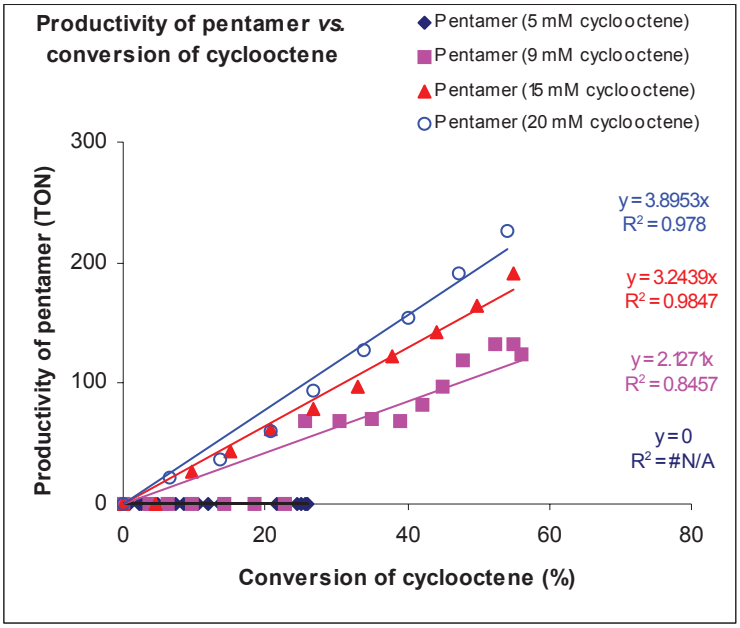

Figure 18: Productivity of pentamer at 50-60% conversion of cyclooctene.

We can therefore see a linear increase in the product productivities with conversion (for the first 50-60% conversion), thus suggesting that they were all primary products. However, comparison of the slopes for the reactions carried out at different concentrations of cyclooctene, indicated that the dimer and the trimer formations, were not as much affected by concentrations of cyclooctene if compared to tetramer and pentamer formations (Figure 14-18).

Further analysis of productivity at higher conversion of cyclooctene (> 60%) showed the decrease in the productivity of dimer which was consistent with the fact that dimer is primary product. It is noteworthy that the productivity of trimer was almost unaffected and showed minor increase compared to the increase in productivity of the tetramer and the pentamer products. This indicates that trimer mainly comes from cyclooctene and thus it can be primary product, while tetramer and pentamer are formed *via* secondary processes involving dimer and are likely secondary products. (Details in appendix section, Figures 67-70).

2.4.2. RO-RCM of cyclooctene dimer

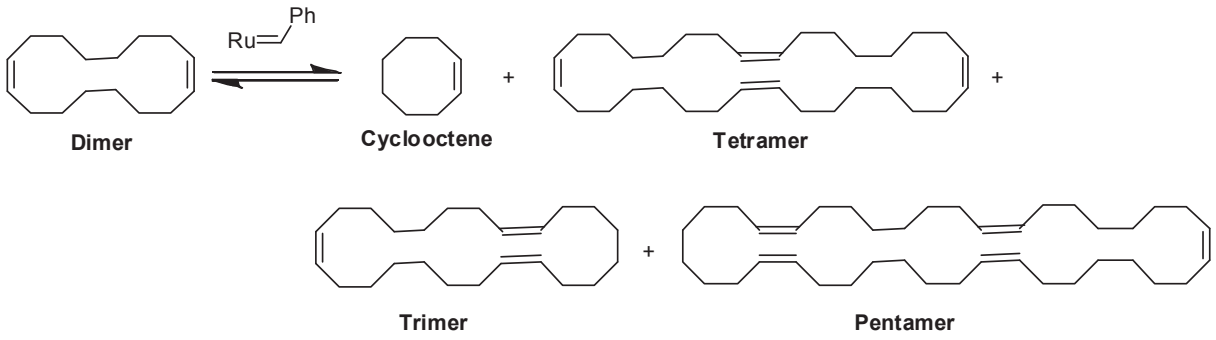

Scheme 3: RO-RCM of cyclooctene dimer.

2.4.2.1. RO-RCM of dimer

Because of the decrease in the productivity of dimer during the RO-RCM of cyclooctene, we decided to perform the RO-RCM of cyclooctene dimer as a key experiment for understanding the formation of cyclic products. The reaction was carried out with a ratio of dimer / Ru = 5000 and ~10 mM dimer solution in toluene. These conditions were chosen because they correspond to the maximum possible concentration of dimer to be reached considering a selective and quantitative conversion of ~20 mM cyclooctene in its cyclic dimer.

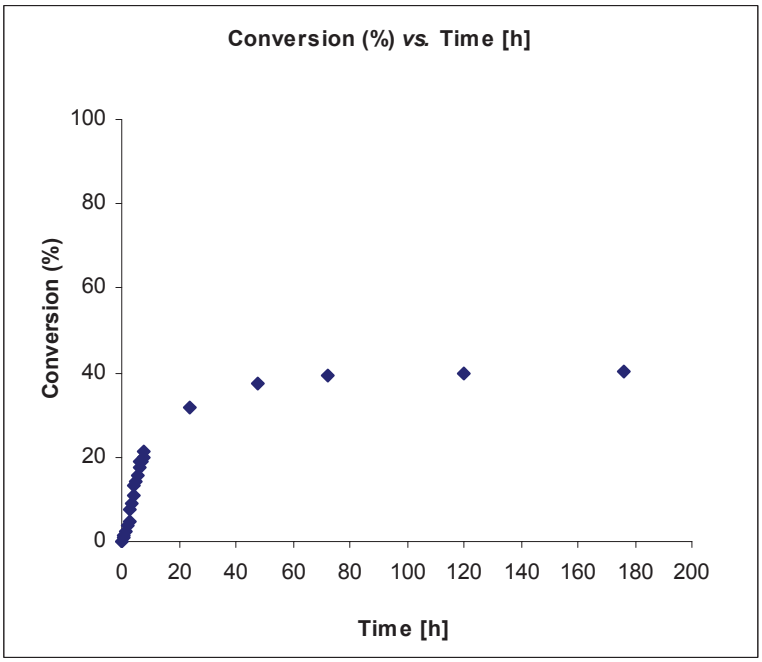

Figure 19: Conversion (%) *vs.* time [h] using **M-RuPr**.

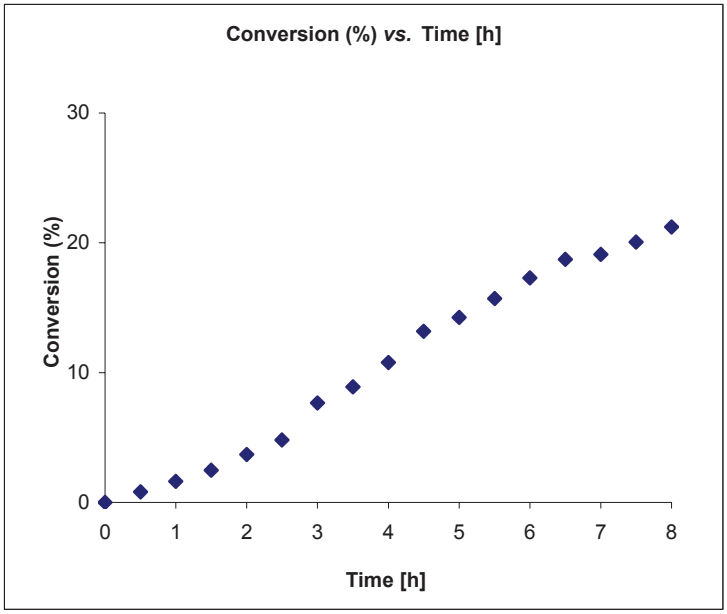

Figure 20: Zoom of conversion for initial 8 h using **M-RuPr**.

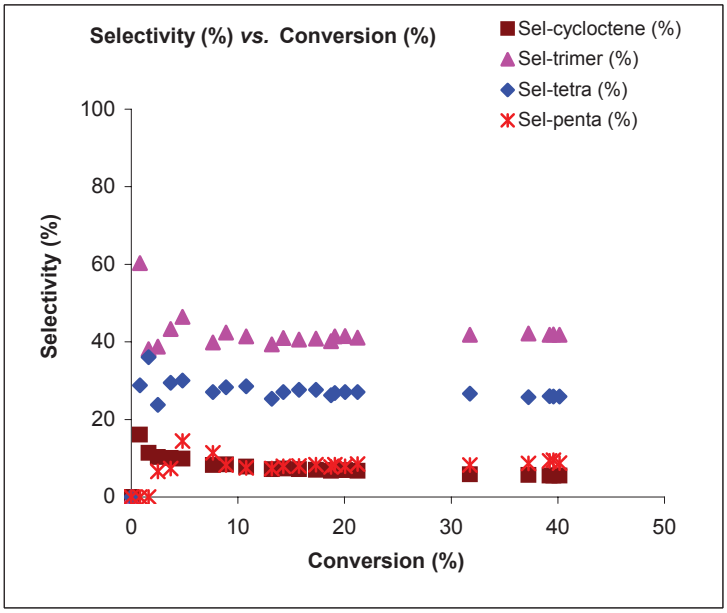

Figure 21: Selectivity (%) *vs.* conversion (%) using **M-RuPr**.

The conversion of dimer was found to be slow for the first 1-2 h with the initial rate of *ca. 80* mol/mol Ru/h and it slowly increased from 2 - 8 h (Figure 19, 20) before slowing down to reach a maximum conversion of 38-39% (Figure 19). At low conversion, RO-RCM of the dimer gave cyclooctene, trimer and tetramer as primary products with high selectivities in trimer and tetramer (Figure 21). The pentamer selectivity was null at low conversion (Figure 21, which is consistent with its formation as at least a secondary product (tetramer + cyclooctene or trimer + dimer). This preliminary data, in particular the formation of cyclooctene, was consistent with a relatively fast back-biting reaction *vs.* polymerisation.

At low conversions we have observed the increase and decrease of selectivities for trimer, tetramer and pentamer (Figure 21) but this could not give a clear insight in the nature of those products. In contrario, the selectivity for cyclooctene was found to be decreasing from 8-3% and remained almost constant throughout the reaction (Figure 21) thus indicating that the cyclooctene was observed as a primary product. In order to have a deeper understanding of the influence of cyclooctene formed during the metathesis of dimer, we carried out further experiments with addition of cyclooctene during the dimer metathesis reactions.

2.4.2.2. Effect of cyclooctene concentration

2.4.2.2.1. Effect of cyclooctene addition on the rate of reaction

The influence of cyclooctene during the metathesis of cyclooctene dimer (C16) is studied here by addition of cyclooctene during the metathesis of dimer. The reactions were performed using **M-RuPr** with a ratio of cyclooctene / Ru = 5,000 and ~10 mM dimer of cyclooctene with no addition of cyclooctene (0 mM), 2 mM cyclooctene and 4 mM cyclooctene. The results are summarized in Figures 22-24. (Details can be found in the appendix- Tables 16-19).

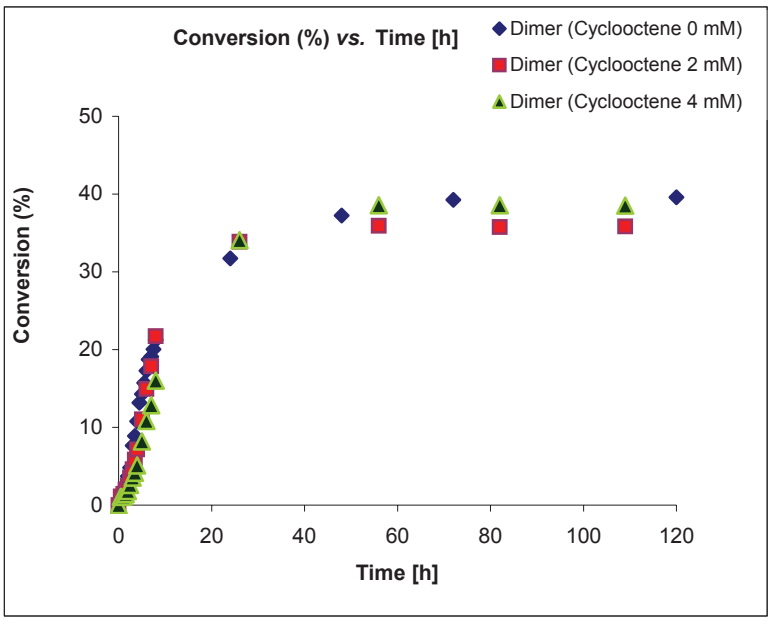

Figure 22: Comparison of Conversion of dimer (%) *vs.* time [h].

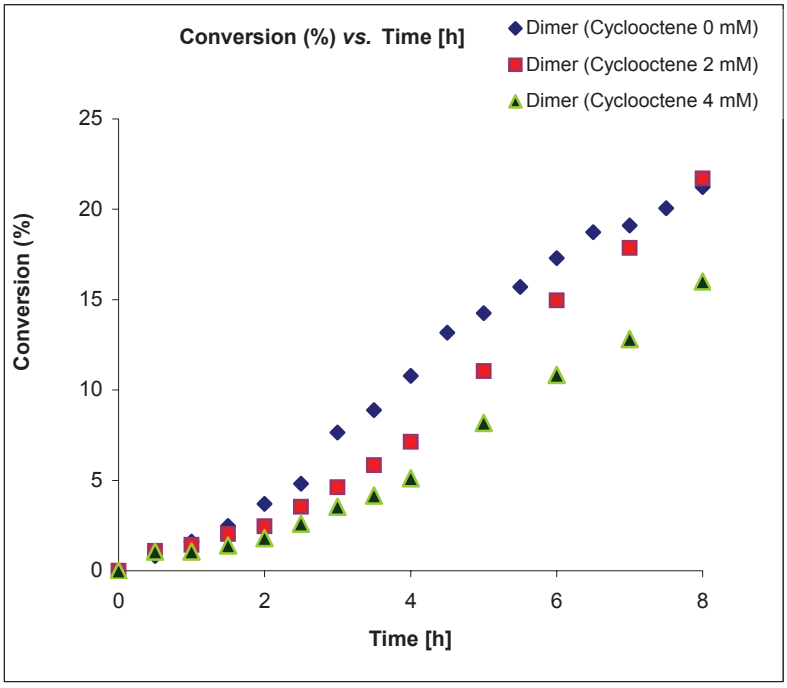

Figure 23: Zoom of comparison of Conversion of dimer (%) *vs.* time [h].

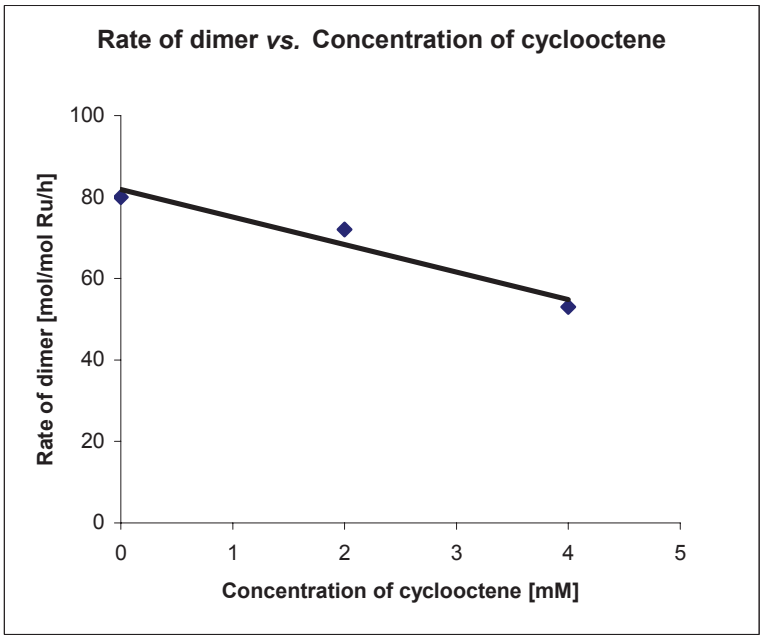

Figure 24: Rate of dimer [mol/mol Ru/h] *vs.* cyclooctene concentration [mM].

First, the decrease of the rate of the conversion of dimer was observed as the concentration of cyclooctene increased (Figure 22-24). This is consistent with the fact that the conversion of cyclooctene was faster than this of the dimer.

2.4.2.2.2. Effect of cyclooctene addition on the productivity of cyclic products

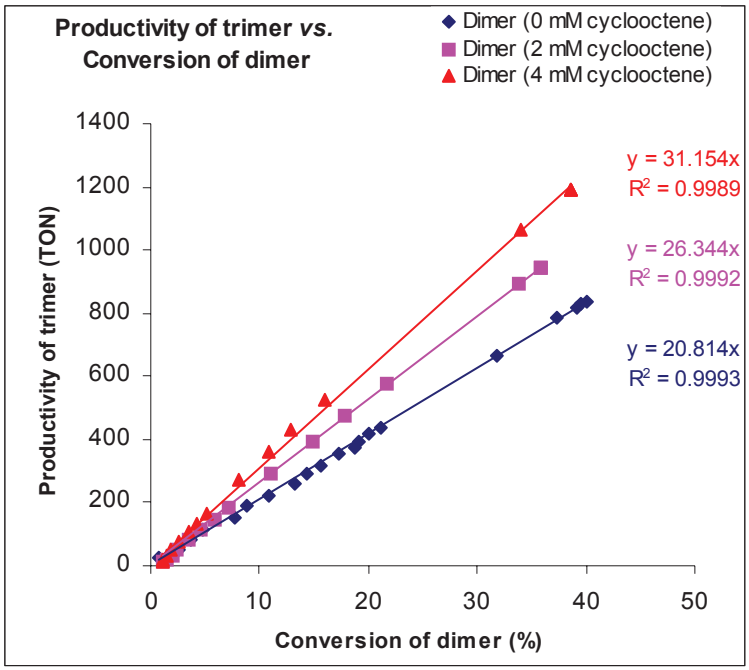

Figure 25: Productivity of trimer *vs.* conversion of dimer (%).

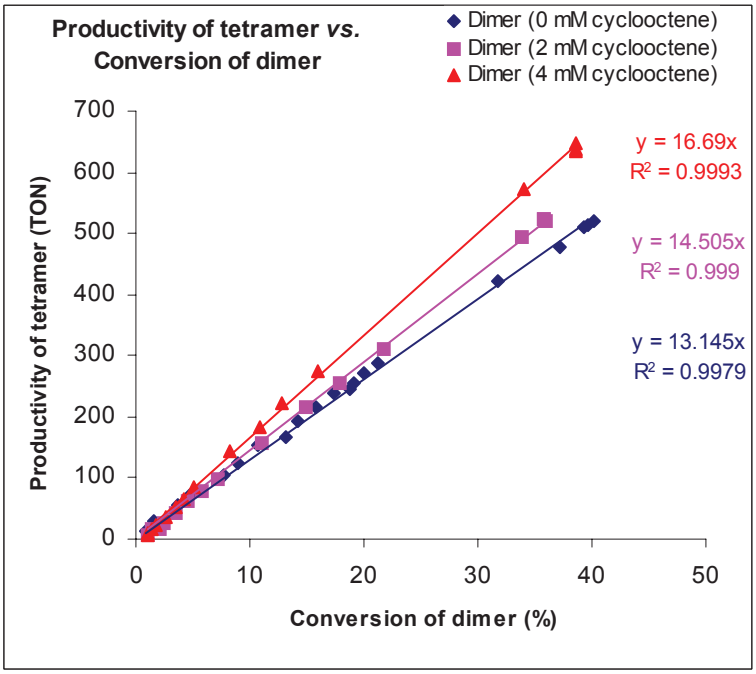

Figure 26: Productivity of tetramer *vs.* conversion of dimer (%).

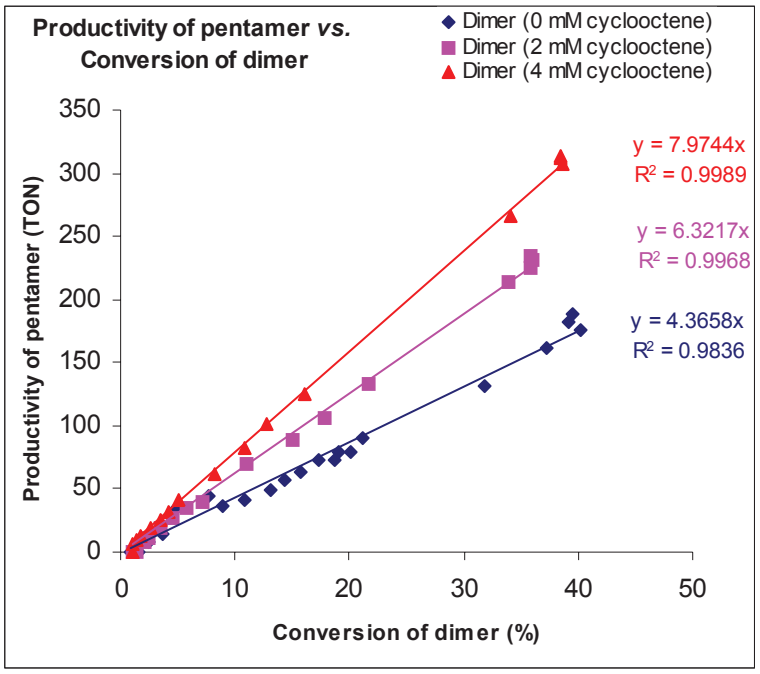

Figure 27: Productivity of pentamer *vs.* conversion of dimer (%).

If we compare now the productivity in product formation, *i.e.* for the trimer, the tetramer and the pentamer (cumulated TON in each product) as a function of dimer conversion, a linear increase is observed thus, indicating that all the low cyclic products are primary products (or formed by processes faster than cyclooctene and dimer metathesis). Moreover, the effect of the concentration of added cyclooctene is noteworthy: comparison of the slope shows that for the tetramer formation, its productivity is not as much affected as for trimer and pentamer formation (Figures 25-27). This is consistent with the fact that the tetramer is mainly produced *via* the dimer only. While the formation of the trimer and the pentamer are resulting from a reaction involving cyclooctene as reactant (Scheme 2). This explains why such products are apparently primary products and formed *via* cross metathesis of the dimer and cyclooctene.

3. Conclusion

- We have developed here five well-defined, heterogeneous Ru-NHC catalysts with different tether length and flexibility.
- Investigation of the structure of the Ru-NHC active sites by ^{31}P NMR of the five materials showed that the flexibility of the tethers and thus the presence of interactions with the silica surface functionalities is an important factor for the stability of active Ru site.
- Catalytic performances showed that catalysts with short-flexible tethers (**M-RuPr** and **M-RuBn**) were better catalysts for RO-RCM of cyclooctene as they provided selectively low cyclic oligomers with high rate.
- The higher catalytic performances observed for **M-RuPr** and **M-RuBn** compared to those of **M-RuHex**, **RuMs** and **M-RuPhMs** could also be explained by the stabilization of the Ru active species by surface functionalities as suggested by ^{31}P NMR observations.
- Further kinetic investigation of the reaction of cyclo-oligomerization with **M-RuPr** showed that this reaction was 1st order in cyclooctene, and that dimer and trimer were primary products, while the tetramer and pentamer were secondary products.
- At this stage the observed selectivity towards lower cyclic oligomers could be attributed either to confinement of pores or to nature of the unsymmetrical NHC ligands (see next chapter).

4. Experimental section

4.1. Synthesis and characterization of hybrid materials

General Information:

All the passivation steps and experiments for introduction of metal complex were carried out under 'Ar' using standard Schlenk techniques, using dry and degassed solvents. Toluene was freshly distilled over NaK under 'Ar' in presence of benzophenone ketyl. Dichloromethane was freshly distilled over P_2O_5. tetraethoxysilane (TEOS) was distilled over Mg under Ar. Triethylamine, Pluronic acid P123, Me_3SiBr (TMSBr), [$K(N(SiMe_3)_2$] (0.5 M in toluene), hexamethyldisilazane and Grubbs I catalyst ($Cl_2(PCy_3)_2Ru(=CHPh)$) were bought from Sigma-Aldrich. Chlorobenzyltriethoxysilane and 3-chloropropyltriethoxysilane from ABCR.
Pluronic P123 from BASF was used for the synthesis of the benzyl chloride containing material to *ca.* 30 g. Elemental analyses were performed at the microanalysis center in Pascher, Germany.

Nuclear Magnetic Resonance Spectroscopy:

Liquid state NMR spectra were recorded using a Bruker AC 300 and solid state NMR spectra were recorded under MAS on a Bruker Avance 300 and 500 MHz spectrometer with a conventional double resonance 4 mm CP-MAS probe.
The MAS frequency was set to 10-10.5 kHz for all of the experiments reported here. The samples were introduced in a 4 mm zirconia rotor in the glove box and tightly closed.

^{29}Silicon NMR

Table 2 : Representative NMR values for different type of silicon

T^3	Q^2	Q^3	Q^4
~ -65 ppm	-90 ppm	-101 ppm	-111 ppm
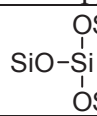	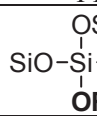	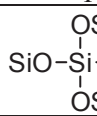	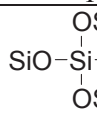

4.1.1. Synthesis of M-RuPr

4.1.1.1. Reaction scheme

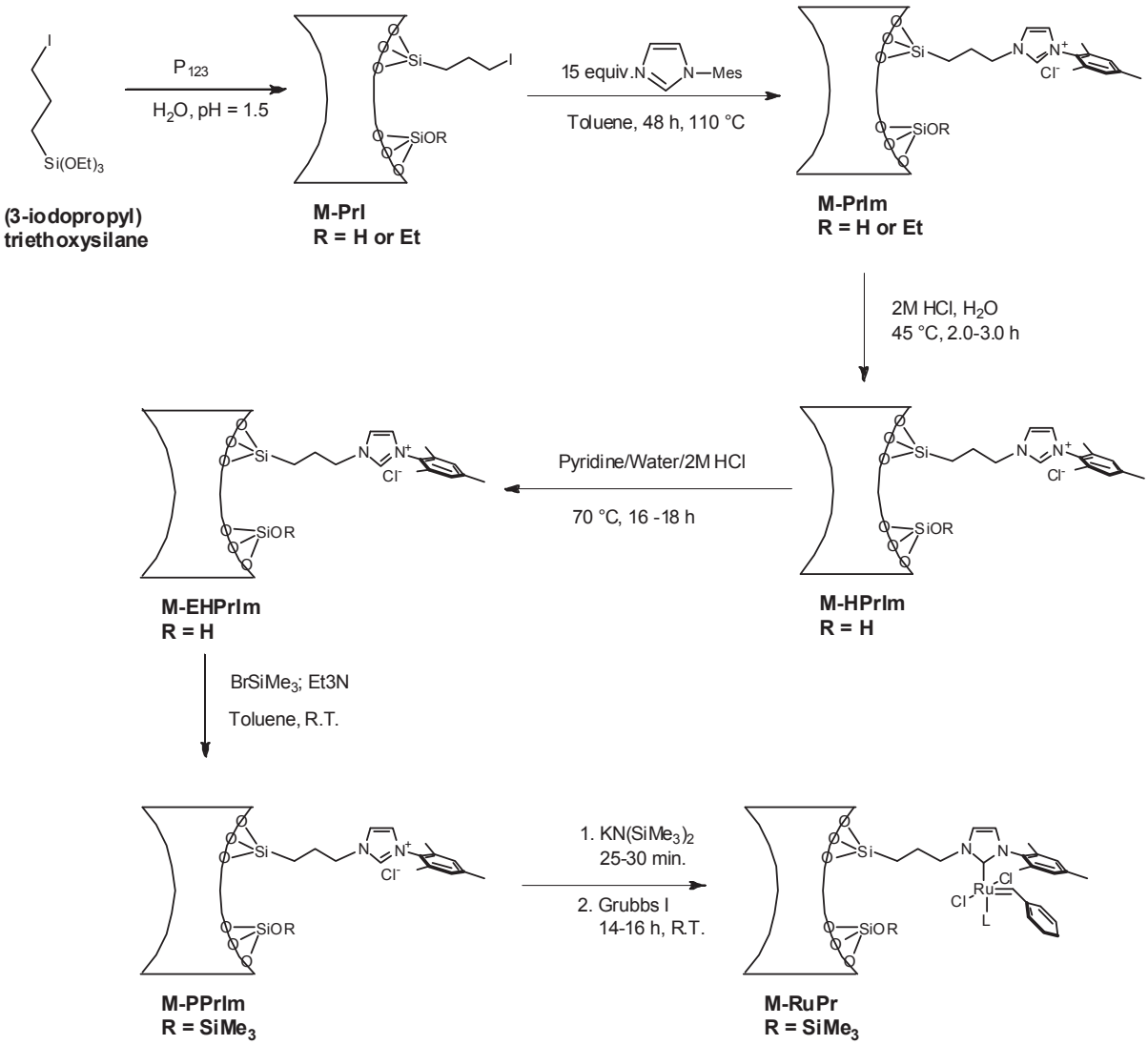

Scheme 4: Synthesis of **M-RuPr**.

4.1.1.2. Synthesis

We have synthesized **M-HPrIm** as described in the previous work.[8]

4.1.1.3. Material M-PrI - Nitrogen adsorption at 77 K

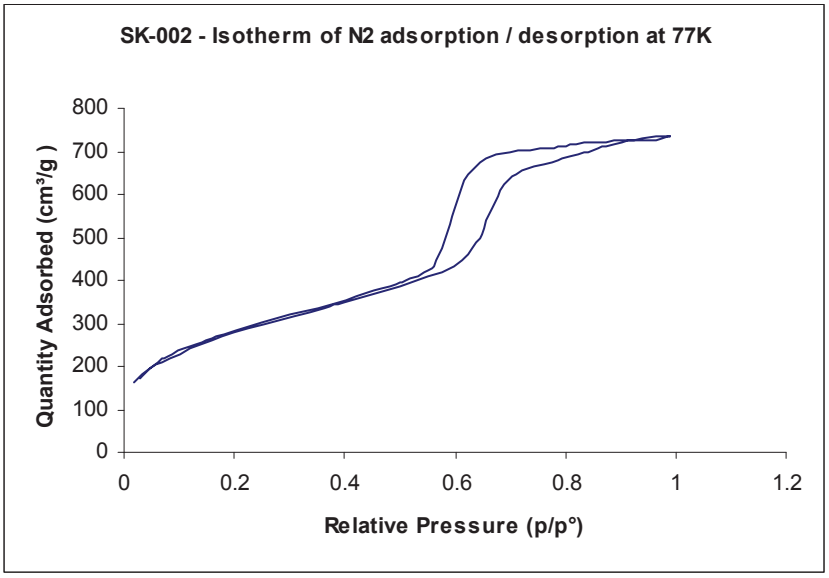

Figure 28: Nitrogen adsorption-desorption isotherm of **M-PrI**.

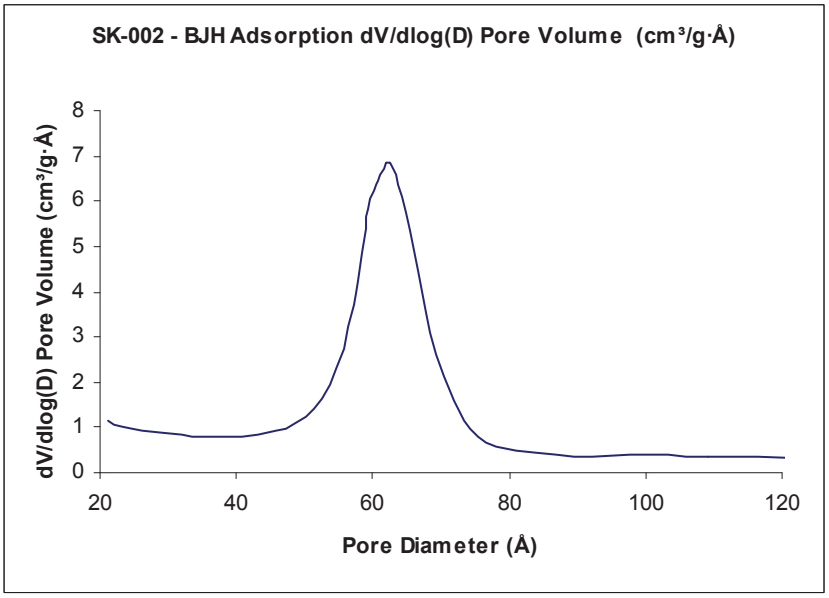

Figure 29: Pore distribution of **M-PrI**.

Isotherm of type IV, characteristic of mesoporous materials with a narrow pore size distribution, S_{BET}: 1010.3 ± 7 m^2/g, Vp: 1.1 cm^3/g and $Dp_{BJHads.}$: 6.2 nm.

4.1.1.4. Synthesis of material M-EHPrIm

To the material **M-HPrIm** (5.6 g) was added a solution of pyridine (42.0 mL), water (42.0mL) and 2 M aqueous HCl (7.0 mL), and the reaction mixture was heated to 70 °C. After stirring for 16-17 h, the solid was filtered and washed successively with water (3 × 200 mL), acetone (3 × 200 mL) diethyl ether (2 × 100 mL). The solid was then dried for 14-16 h under high vacuum (10^{-5} mm Hg) at 135 °C, affording 5.1 g of material.

Elemental analysis: Si: 36.2%; N: 1.22%

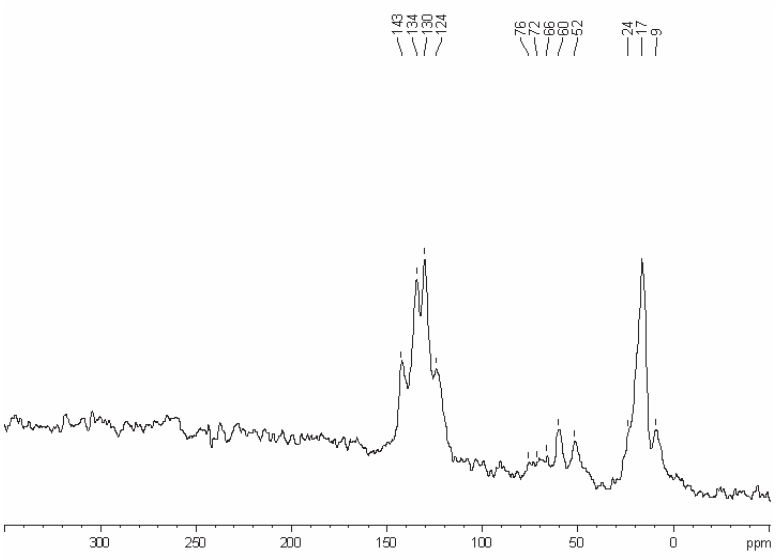

Figure 30: Solid State ^{13}C NMR of **M-HPrIm**.

Peaks at 120-140 ppm are attributed to aromatic and imidazolium carbon atoms, 76-66 ppm to surfactant, 60 ppm to -O<u>C</u>H_2CH_3, 52 ppm to -<u>C</u>H_2N of the propyl, 9 and 24 ppm to -CH_2 of the propyl groups respectively, 17 ppm to methyl groups of mesityl.

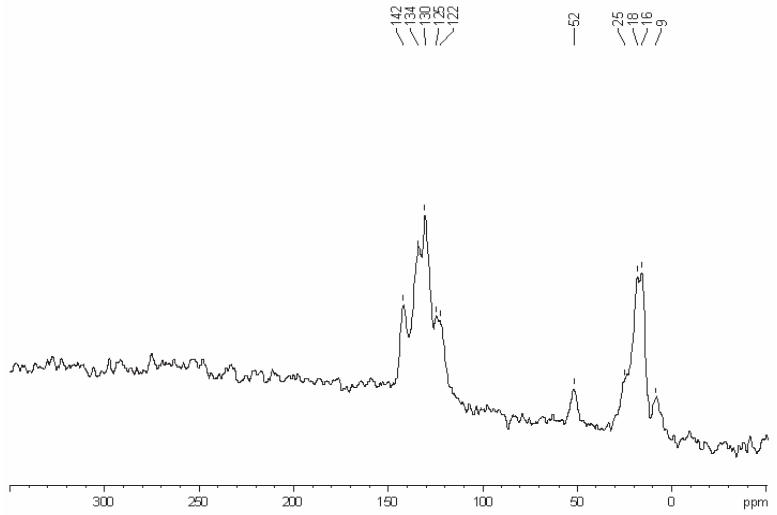

Figure 31: Solid State ^{13}C NMR of **M-EHPrIm**.

Peaks at 120-140 ppm are attributed to aromatic and imidazolium carbons, 52 ppm to -<u>C</u>H_2N of propyl, 9 and 25 ppm to -CH_2 of the propyl group, 17 ppm to methyl groups of mesityl. (Note: peaks at 76-66 ppm (to surfactant) and 60 ppm (to -O<u>C</u>H_2CH_3) are absent. Indicating at complete removal of the surfactant and ethoxy groups on the surface.)

4.1.1.5. Synthesis of material M-PPrIm

To the suspension of **M-EHPrIm** (3.2 g) in toluene (230.0 mL) triethylamine (43.0 mL) and trimethylsilylbromide (20.5 mL) were added at room temperature. After stirring the reaction mixture overnight, the solid was filtered and washed successively with toluene (2 × 30 mL) and dichloromethane (4 × 50 mL). The solid was dried under high vacuum (10^{-5} mm Hg) for 16 h) at 135 °C, affording 3.4 g of material. **Elemental analysis:** Si: 38.8%; N: 1.14%.

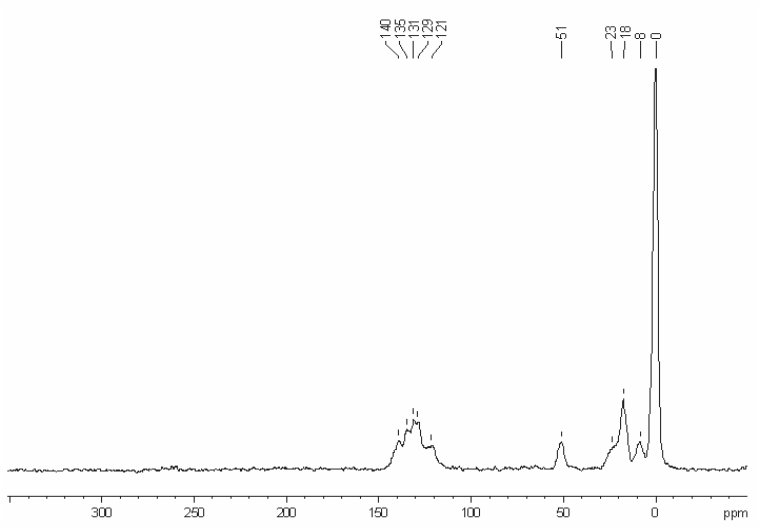

Figure 32: Solid State ^{13}C NMR of **M-PPrIm**.

Peaks at 120-140 ppm are attributed to aromatic and imidazolium carbons, 51 ppm to -$\underline{C}H_2N$ of propyl, 8 and 23 ppm to -CH_2 of the propyl group,17 ppm to methyl groups of mesityl and at 0 ppm to -OSi($\underline{C}H_3$)$_3$.

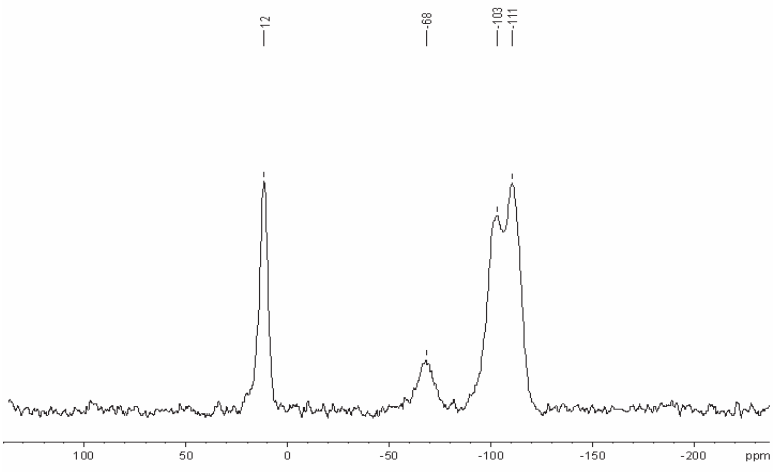

Figure 33: Solid state ^{29}Si NMR of **M-PPrIm**.

Peaks at 12, -68, -103 and -111 ppm are attributed to -O$\underline{Si}$(CH_3)$_3$, T^3, Q^3 and Q^4.

4.1.1.6. Synthesis of material M-RuPr

To the suspension of material **M-PPrIm** (3.15 g, 1.0 equiv) in toluene (10.0 mL) was slowly added at room temperature 3.4 mL of a 0.5 M toluene solution of [K(N(SiMe3)2] (1.2 equiv). After stirring for 30 min., slowly added the solution of $Cl_2(PCy_3)_2Ru(=CHPh)$ (1.41 g, 1.2 equiv) in toluene (20.0 mL) at room temperature and stirred overnight. The solid was then filtered and washed successively with toluene (2 × 20 mL) and dichloromethane (4 × 20 mL) till the filtrate was colourless. The material was dried under high vacuum (10^{-5} mm Hg) at room temperature for 14-16 h to yield 3.1 g of light beige solid.

Elemental analysis: Si: 37.2%; N: 1.04%; Ru: 0.63%, P : 0.17%.

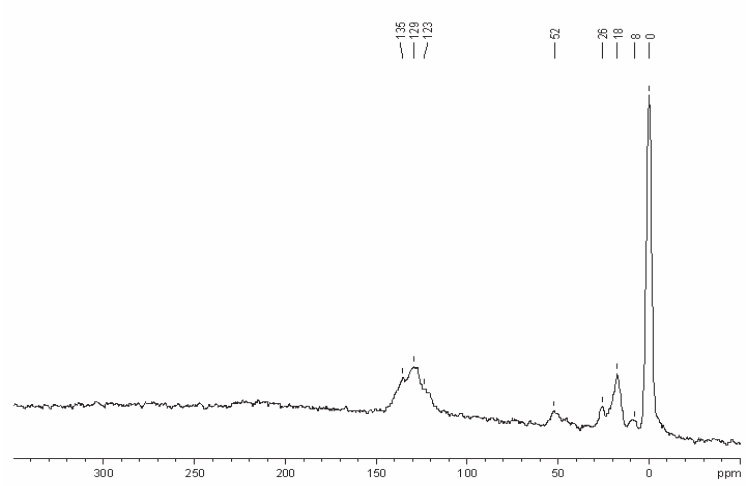

Figure 34: Solid State ^{13}C NMR of **M-RuPr**.

Peaks at 120-135 ppm are attributed to aromatic and imidazolium carbons, 52 ppm to -$\underline{C}H_2N$ of propyl, 26 ppm to -P$\underline{C}y_3$,8 ppm to -$\underline{C}H_2$ of propyl,18 ppm to methyl groups of mesityl and at 0 ppm to -OSi-($\underline{C}H_3)_3$.

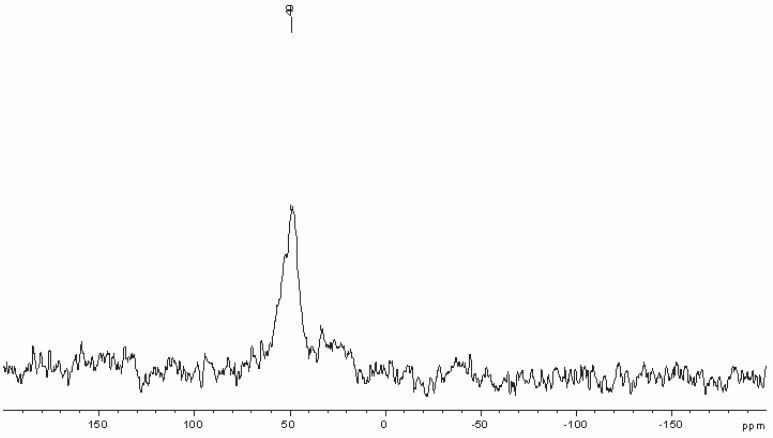

Figure 35: Solid State ^{31}P NMR of **M-RuPr**.

Attribution**:** 49 ppm (phosphine oxide (probably due to further reaction of liberated PCy_3) no signal at 36 ppm (PCy_3 bound to Ru).

4.1.2. Synthesis of M-RuBn

4.1.2.1. Reaction scheme

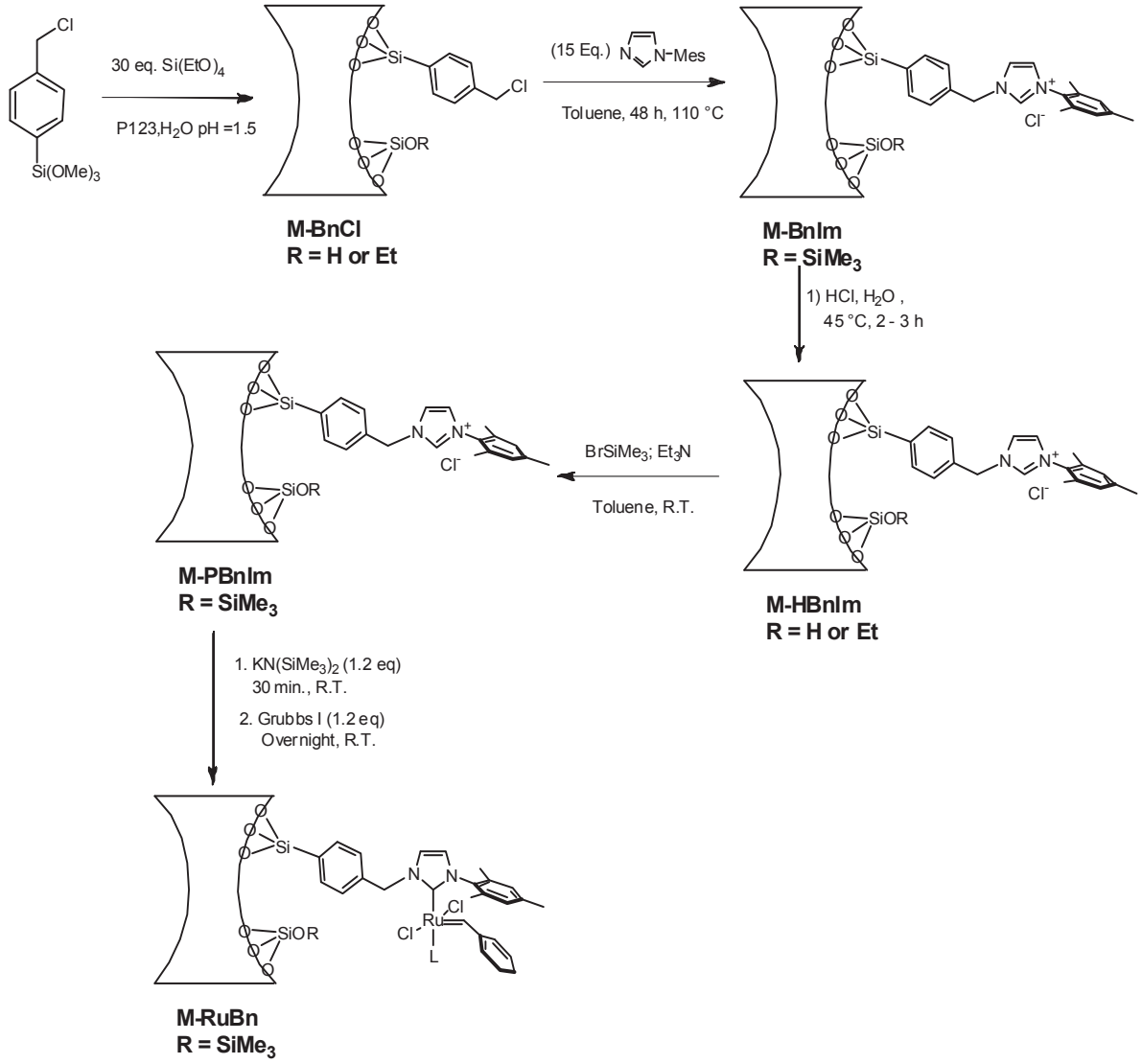

Scheme 5: Synthesis of **M-RuBn.**

4.1.2.2. Synthesis

Synthesis of this catalyst has already been depicted in the previous work.[8]

4.1.2.3. Material M-BnCl - Nitrogen adsorption at 77 K

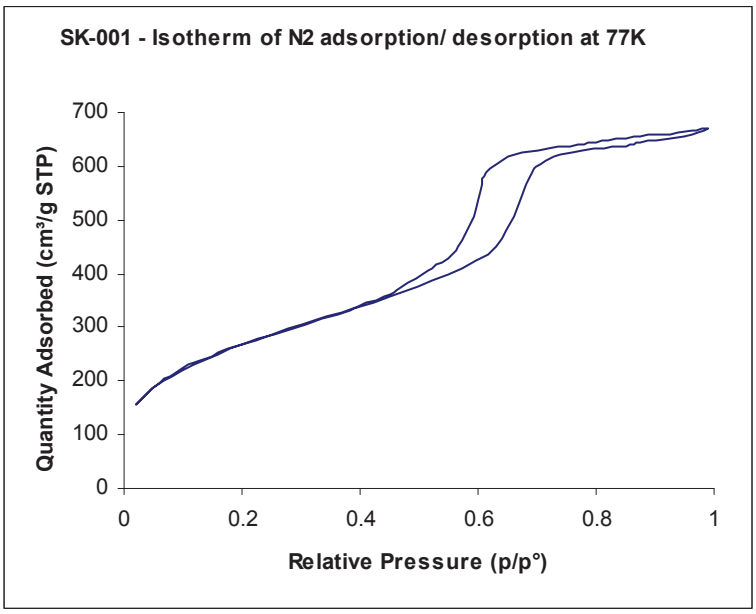

Figure 36: Nitrogen adsorption-desorption isotherm of **M-BnCl**.

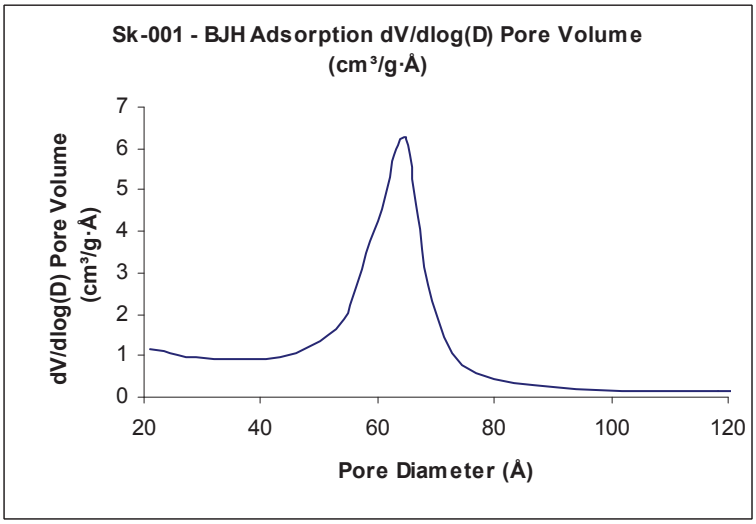

Figure 37: Pore distribution of **M-BnCl**.

Isotherm of type IV, characteristic of mesoporous materials with a narrow pore size distribution, S_{BET}: 971.7 ±5 m^2/g, Vp: 1.0 cm^3/g and $Dp_{BJHads.}$: 6.5 nm.

4.1.2.4. Synthesis of M-RuBn

To the suspension of material **M-PBnIm** (1.5 g, 0.693 mmol, 1.0 eq) in toluene (8.0 mL, 5.3 rel vol), 0.5 M Toluene solution of $[K(N(SiMe_3)_2]$ (1.66 mL, 0.831 mmol, 1.2 mol eq) was slowly added at room temperature. After stirring for 30 min. slowly added the solution of $Cl_2(PCy_3)_2Ru(=CHPh)$ (0.68 g, 0.831 mmol, 1.2 mol eq) in toluene (6.0 ml, 4.0 rel vol) at room temperature. After stirring the reaction mixture for overnight, filtered the solid and washed successively with toluene (3 × 10mL) and dichloromethane (3 × 10mL) till the filtrate was colourless. The material was dried under high vacuum (10^{-5} mm Hg) at room temperature overnight (14-16 h) to yield 1.4 g of a light beige solid.

Elemental analysis: Si: 35.0%; N: 0.87%; Ru: 0.84%; P: 0.24%.

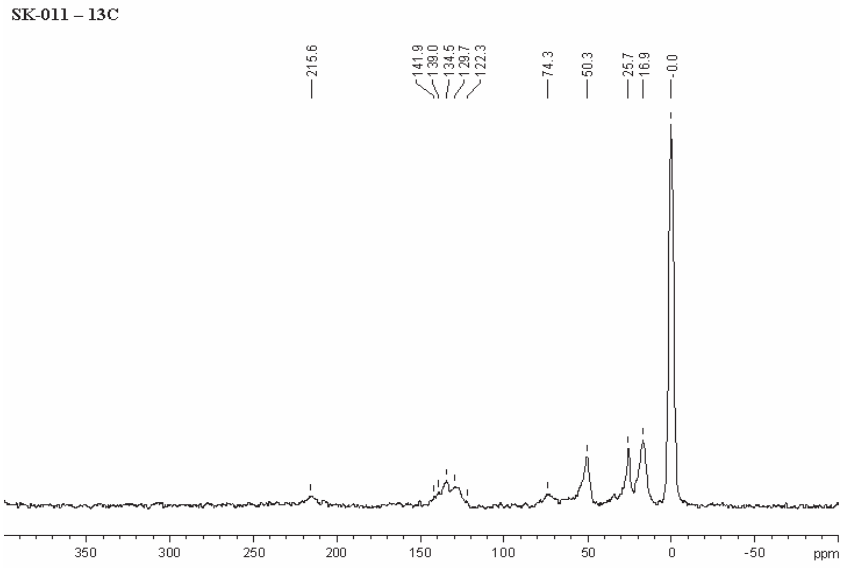

Figure 38: Solid State ^{13}C NMR of **M-RuBn**.

Peaks at 122-141 ppm are attributed to aromatic and imidazolium carbon atoms, 74 ppm to surfactant, 52 ppm to -$\underline{C}H_2N$ of propyl, 26 ppm to -P$\underline{C}y_3$,17 ppm to methyl groups of mesityl and at 0 ppm to -OSi-($\underline{C}H_3)_3$, peaks around 215 ppm are spinning side bands.

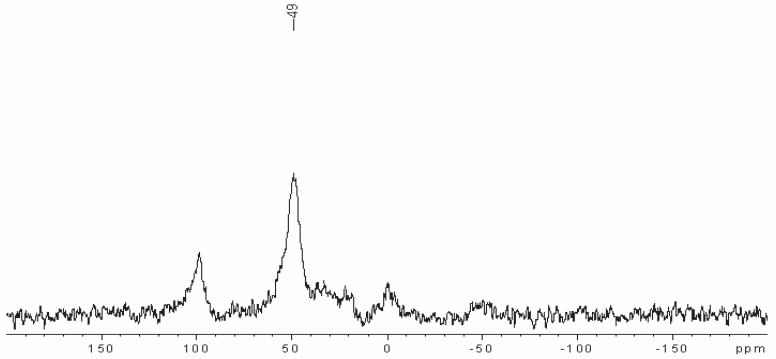

Figure 39: Solid State ^{31}P NMR of **M-RuBn**.

Attribution**:** 49 ppm (phosphine oxide (probably due to further reaction of liberated PCy_3) no signal at 36 ppm (PCy_3 bound to Ru). peaks around 100 and 0 ppm are spinning side bands.

4.1.3. Synthesis of M-RuHex

4.1.3.1. Reaction scheme

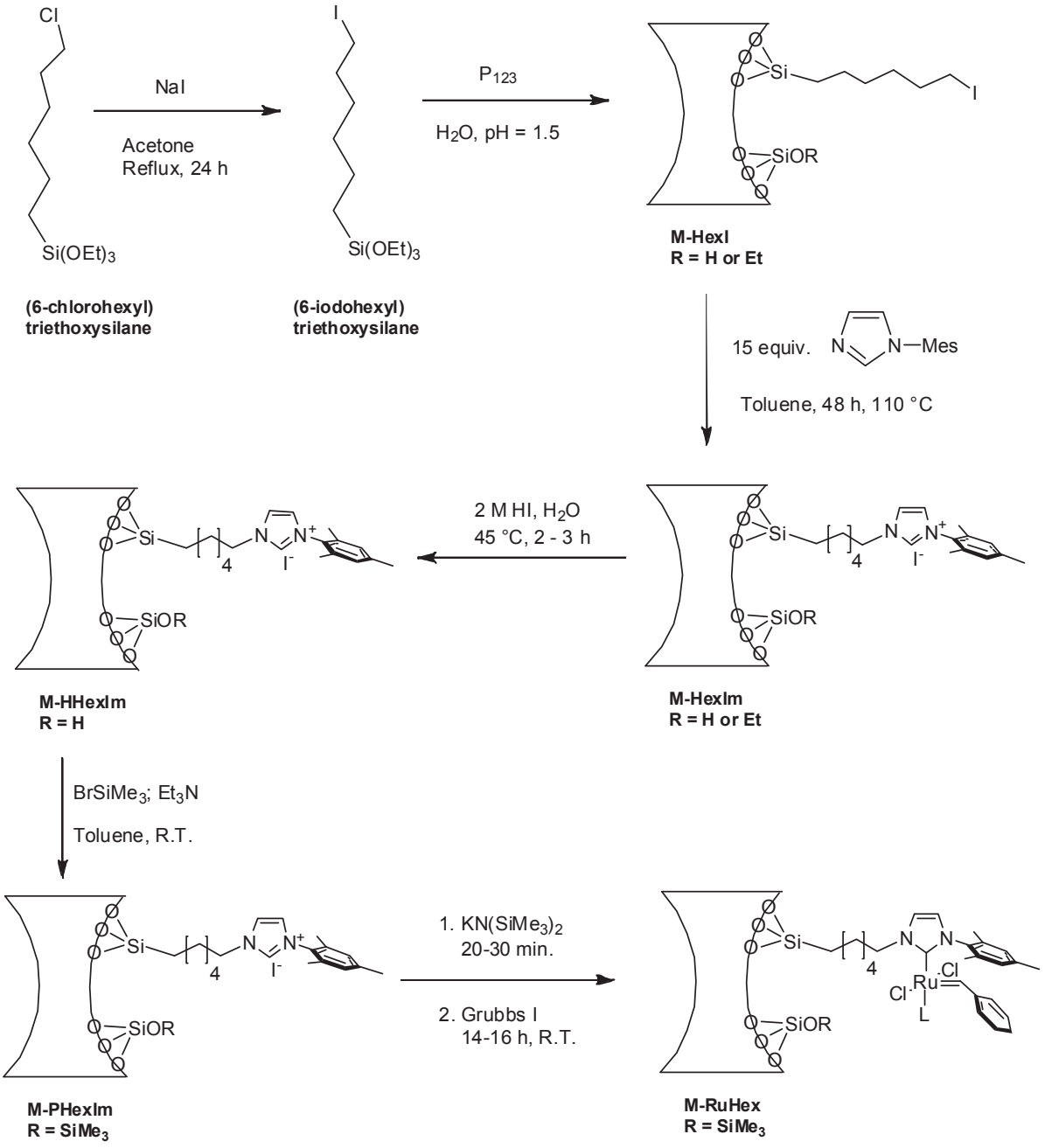

Scheme 6: Synthesis of **M-RuHex.**

4.1.3.2. Synthesis

*Original synthesis and development work for **M-HexIm** was carried out in Montpellier in LCMOS (ICG), in collaboration with our laboratory (ANR PNANO "Nanobiocat") and this work was already published in the CPE patent.*[6]

4.1.3.3. Material M-HexIm Nitrogen adsorption at 77 K

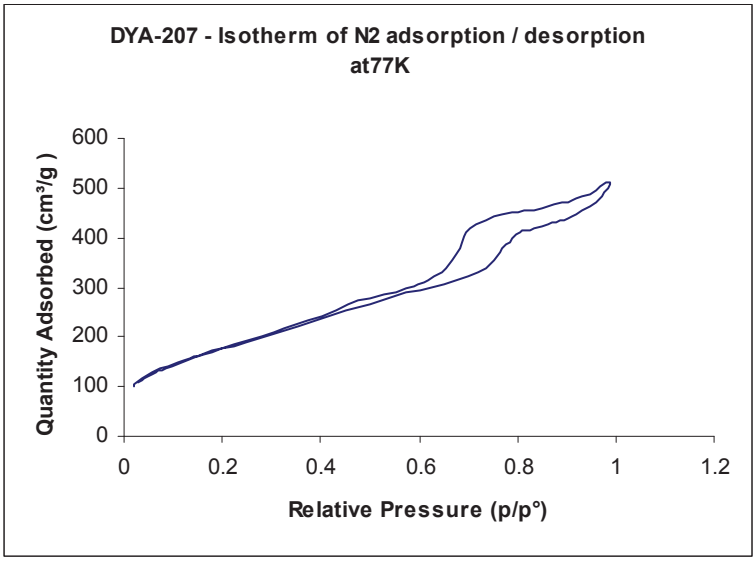

Figure 40: Nitrogen adsorption-desorption isotherm of **M-HexIm.**

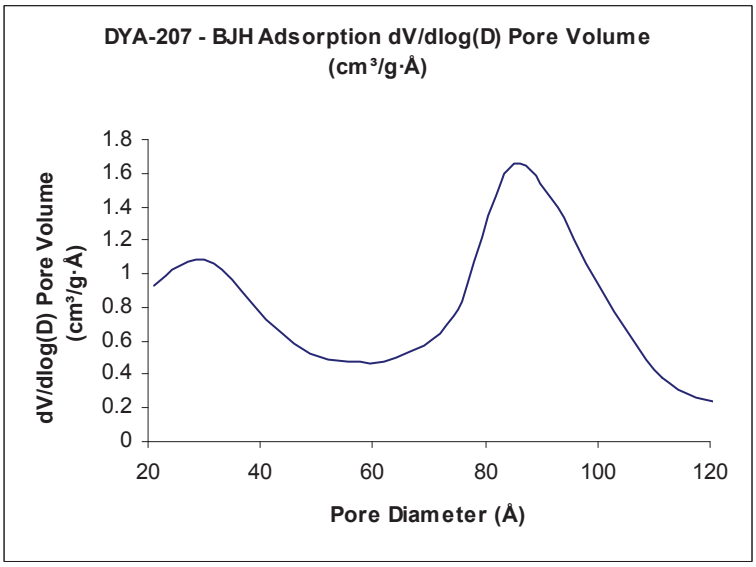

Figure 41: BJH adsorption pore distribution of **M-HexIm**.

Isotherm of type IV, characteristic of mesoporous materials with a narrow pore size distribution, $\mathbf{S_{BET}}$**:** 656.2 ± 2 m^2/g, **Vp:** 0.79 cm^3/g and $\mathbf{Dp_{BJHads.}}$: 8.4 nm.

4.1.3.4. Synthesis of M-HHexIm

The material **M-HexIm** (1.6 g, DYA-207) was stirred in a 2 M aqueous HI solution (160.0 mL), at 45 °C for 2 h. The solid was then filtered and washed successively with water (2 × 100 mL), acetone (2 × 100 mL) & diethyl ether (2 × 100 mL). The solid was dried under high vacuum (10^{-5} mm Hg) for overnight (14-16 h) at 135 °C, affording 1.3 g of material.

4.1.3.5. Synthesis of M-PHexIm

To the suspension of material **M-HHexIm** (1.05 g) in toluene (80.0 mL), triethylamine (13.6 mL) and trimethylsilylbromide (6.3 mL) were added at room temperature. After stirring the reaction mixture overnight, the solid was filtered under 'Ar' and washed successively with toluene (2 × 50 mL) and dichloromethane (2 × 50 mL). The solid was dried under high vacuum (10^{-5} mm Hg) for overnight (14-16 h) at 135 °C, affording 1.1 g of material.

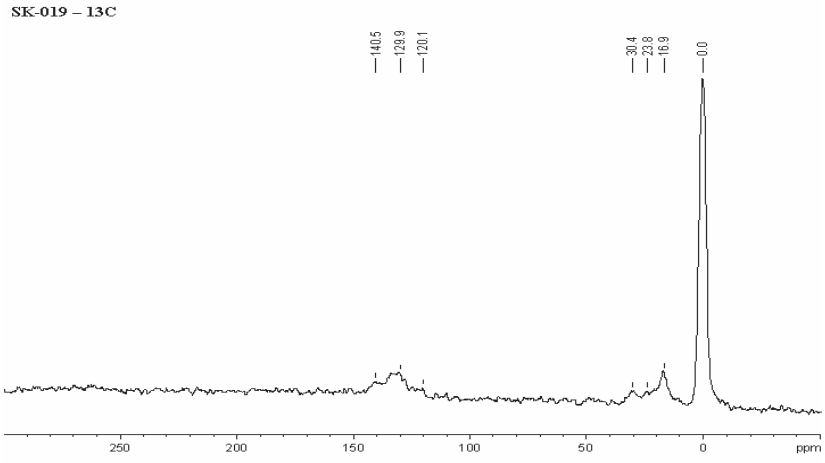

Figure 42: Solid State ^{13}C NMR of **M-PHexIm**.

Peaks at 120-140 ppm are attributed to aromatic and imidazolium carbon atoms, 30, 24 ppm to -CH_2 of Hexyl groups, 17 ppm to methyl groups of mesityl unit and at 0 ppm to -OSi-($\underline{C}H_3$)$_3$.

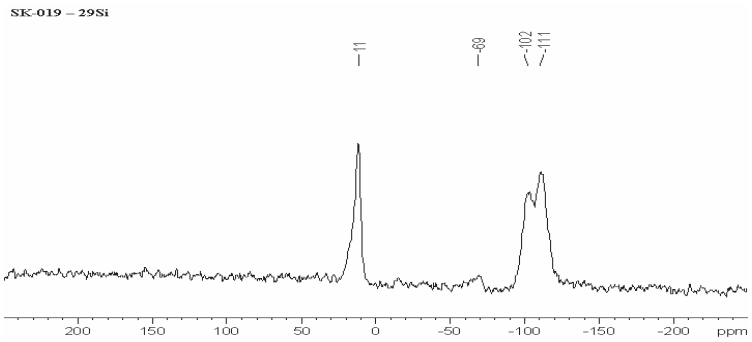

Figure 43: Solid state ^{29}Si NMR of **M-PHexIm**.

Peaks at 11, -69, -102 and -111 ppm are attributed to -O$\underline{Si}$(CH_3)$_3$, T^3, Q^3 and Q^4.

4.1.3.6. Synthesis of M-RuHex

To the suspension of material **M-PHexIm** (0.92 g, 0.409 mmol, 1.0 eq) in toluene (6.0 mL, 5.5 rel vol), 0.5 M toluene solution of [$K(N(SiMe_3)_2$] (1.0 mL, 0.490 mmol, 1.2 mol eq) was slowly added at room temperature. After stirring for 30 min., a solution of $Cl_2(PCy_3)_2Ru(=CHPh)$ (0.40 g, 0.490 mmol, 1.2 mol eq) in toluene (4.0 mL, 3.6 rel vol) was slowly added at room temperature and stirred overnight. The solid was then filtered and washed successively with toluene (3 × 10 mL) and dichloromethane (3 × 10 mL) under 'Ar' till the filtrate was colourless. The material was dried under high vacuum (10^{-5} mm Hg) at room temperature (14-16 h) to yield 0.85 g of light beige solid. **Elemental analysis:** Si: 35.8%; N: 0.80%; Ru: 0.71%; P: 0.20%.

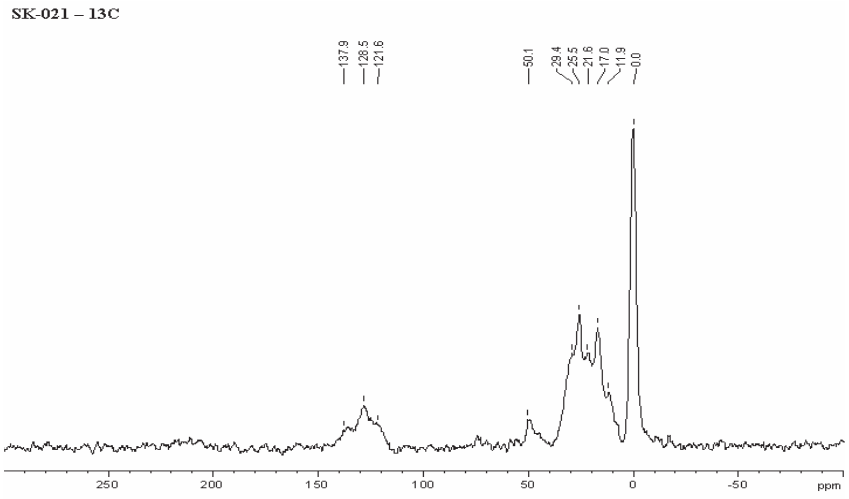

Figure 44: Solid State ^{13}C NMR of **M-RuHex**.

Peaks at 122-139 ppm are attributed to aromatic and imidazolium carbon atoms, 50 ppm to methoxy groups on the surface, 29, 22, 12 ppm to -CH_2 of hexyl groups, 25 ppm to -P$\underline{Cy}_3$ moities, around 17 ppm to methyl groups of mesityl unit, and at 0 ppm to -OSi-($\underline{C}H_3)_3$.

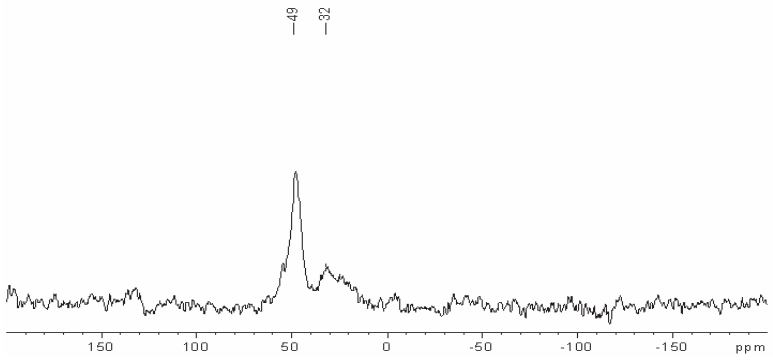

Figure 45: Solid State ^{31}P NMR of **M-RuHex.**

Attribution**:** 49 ppm (phosphine oxide-probably due to further reaction of liberated PCy_3), 32 ppm (weak signal for PCy_3 bound to Ru or phosphonium species).

4.1.4. Synthesis of M-RuPhMs

4.1.4.1. Reaction scheme

4.1.4.1.1. Synthesis of PhMs-precursor

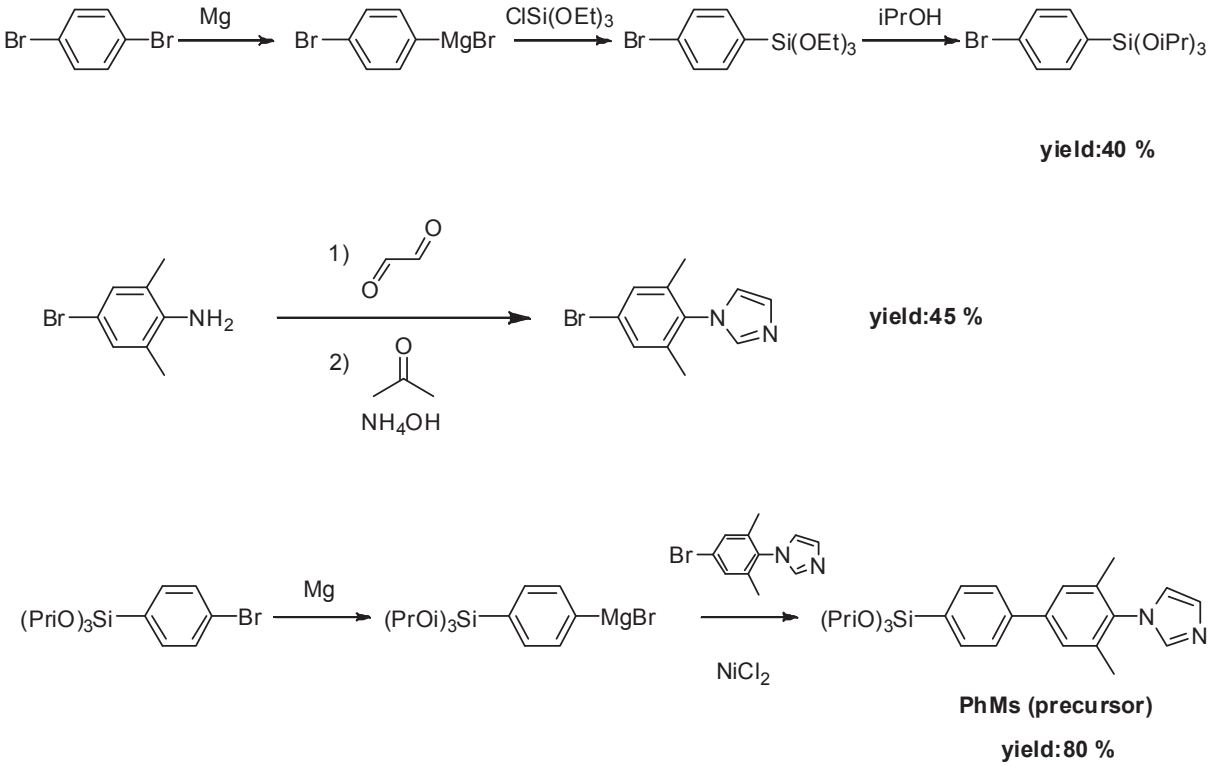

Scheme 7: Synthesis of Precursor **PhMs.**

Overall yield for the synthesis of **PhMs** precursor was 14%.

4.1.4.1.2. Synthesis of M-RuPhMS

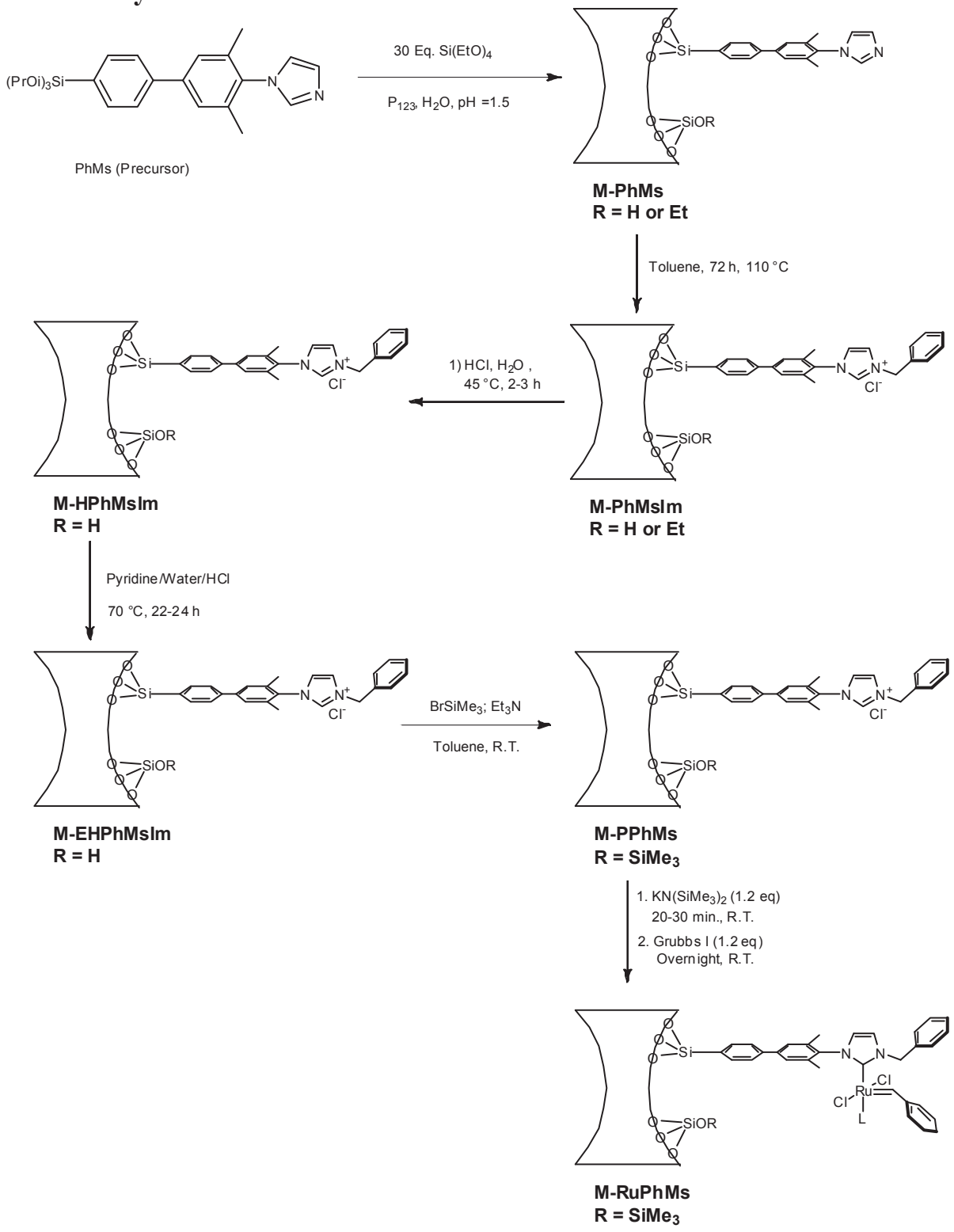

Scheme 8: Synthesis of **M-RuPhMs.**

NOTE: Original synthesis and development work for **PhMs** (precursor) and **M-PhMs** were carried out in Montpellier in LCMOS (ICG), in collaboration with our laboratory (ANR PNANO "Nanobiocat") and this work was already published in the CPE patent.[6]

4.1.4.2. Material M-PhMs - Nitrogen adsorption at 77K

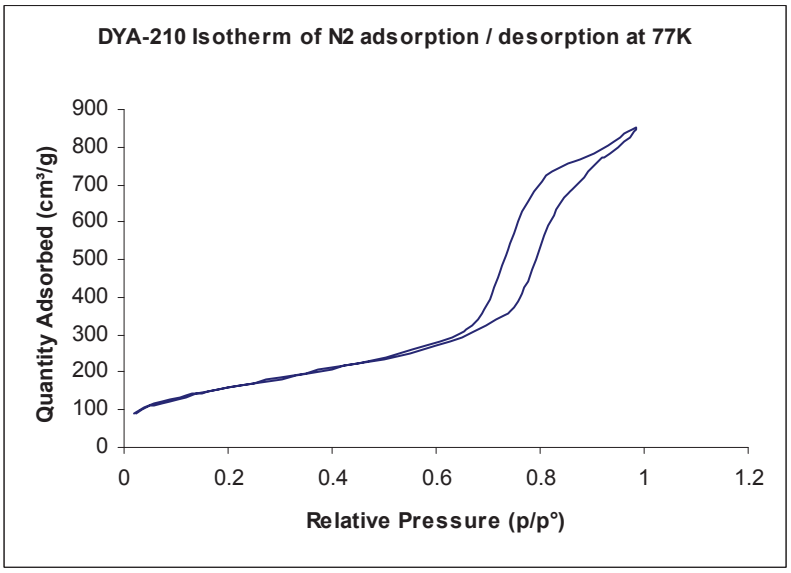

Figure 46: Nitrogen adsorption-desorption isotherm of **M-PhMs.**

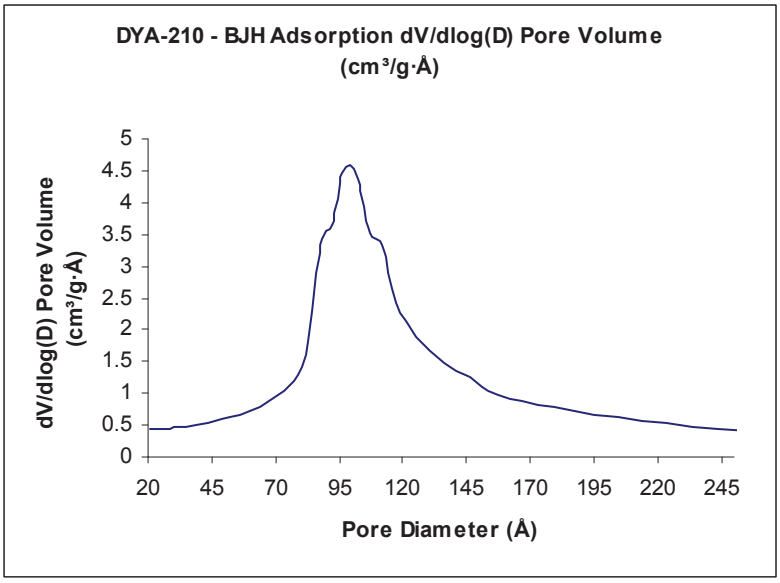

Figure 47: Pore distribution of **M-PhMs.**

Isotherm of type IV, characteristic of mesoporous materials with a narrow pore size distribution, $\mathbf{S_{BET}}$**:** 581.9 ± 2 m^2/g, **Vp:** 1.3 cm^3/g and $\mathbf{Dp_{BJHads}}$.: 9.9 nm.

4.1.4.3. Synthesis of M-PhMsIm

To the material **M-PhMs** (0.8 g, DYA-210) were added toluene (15.0 mL) and benzyl chloride (0.62 mL, 15 equiv.). The reaction mixture was heated up to 110 °C. After stirring, for 70-72 h, the solid was filtered and washed successively with toluene (3 × 100 mL), acetone (3 × 100 mL) and diethyl ether (3 × 50 mL). The solid was then dried for 14-16 h under high vacuum (10^{-5} mm Hg) at 135 °C, affording 0.75 g of product.

Elemental analysis: N: 1.23%, Si: 35.6%.

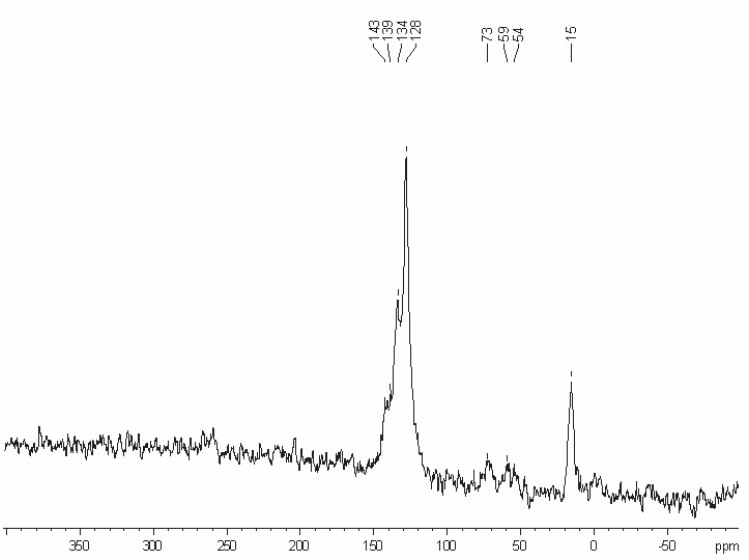

Figure 48: Solid State ^{13}C NMR of **M-PhMsIm.**
Attribution**:**127-142 ppm (aromatic carbon atoms), 73 ppm to surfactant, 59 ppm to -$O\underline{C}H_2CH_3$, 15 ppm (CH_3 of mesityl unit).

4.1.4.4. Synthesis of M-HPhMsIm

To the material **M-PhMsIm** (0.7 g, SK-055) was added 5 mL of a 2 M aqueous HCl. The reaction mixture was heated up to 45 °C. After stirring the reaction mixture for 2 h, the solid was filtered and washed successively with water (3 × 100 mL), acetone (3 × 100 mL) and diethyl ether (3 × 50 mL). The solid was then dried for 5-6 h under high vacuum (10^{-5} mm Hg) at 135 °C, affording 0.6 g of product.

4.1.4.5. Synthesis of M-EHPhMsIm

To the material **M-HPhMsIm** (0.55 g, SK-058) was added a mixture of pyridine (4.1 mL), water (4.1 mL) and 2 M aqueous HCl (0.7 mL). The reaction mixture was heated up to 70 °C. After stirring the suspension for 22-23 h, the solid was filtered and washed successively with

water (3 × 100 mL), acetone (3 × 100 mL) and diethyl ether (3 × 100 mL). The solid was then dried for 14-16 h under high vacuum (10^{-5} mm Hg) at 135 °C, affording 0.5 g of product.

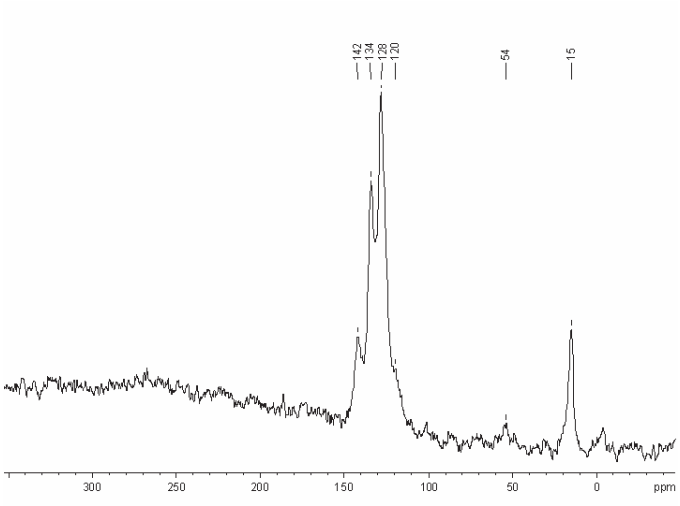

Figure 49: Solid State ^{13}C NMR of **M-EPhMsIm.**

Attribution**:** 128-142 ppm (aromatic carbon atoms), 54 ppm to -N<u>C</u>H_2Ph, of 15 ppm (CH_3 of mesityl unit).

4.1.4.6. Synthesis of M-PPhMsIm

To the suspension of material **M-EPhMsIm** (0.4 g) in toluene (28.0 mL) was added triethylamine (5.1 mL) and trimethylsilylbromide (2.5 mL) at room temperature. The reaction mixture was stirred overnight. The solid was further filtered and washed successively with toluene (3 × 20 mL) and dichloromethane (3 × 20 mL). The solid was dried under high vacuum (10^{-5} mm Hg) overnight (16-18 h) at 135 °C, affording 0.4 g of material.

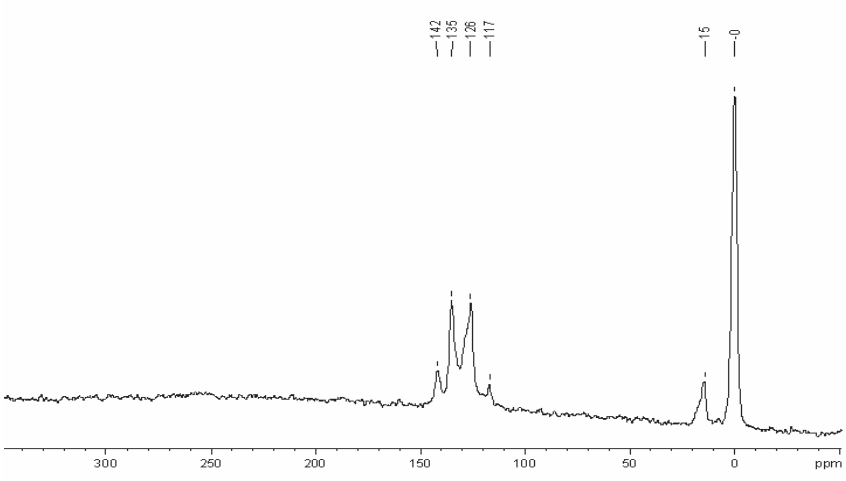

Figure 50: Solid State ^{13}C NMR of **M-PPhMsIm.**

Attribution**:** 128-142 ppm (aromatic carbons), 15 ppm (CH_3 of mesityl), 0 ppm to (-OSi(*Me*)$_3$).

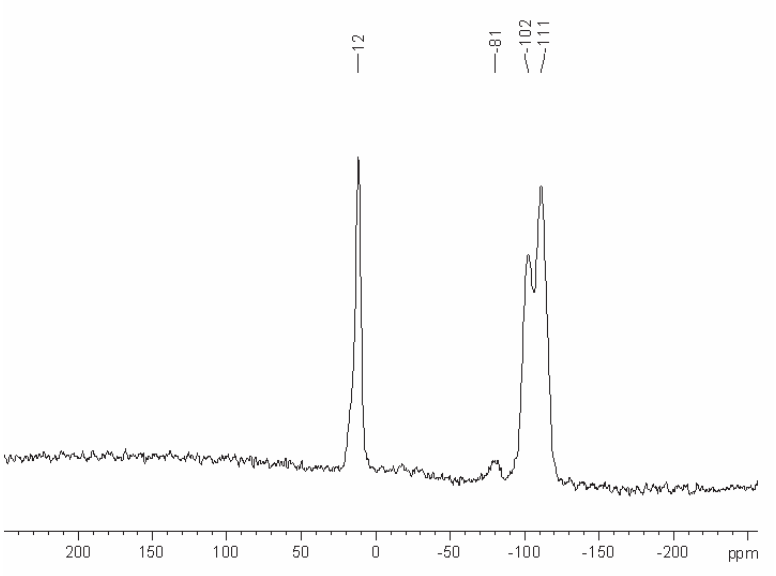

Figure 51: Solid State ^{29}Si NMR of **M-PPhMsIm.**

Attribution**:** -111 ppm (Q^4), -102 ppm (Q^3), -81 ppm (T^3), 12 ppm (-OSi(Me)$_3$).

4.1.4.7. Synthesis of M-RuPhMs

To the suspension of **M-PPhMsIm** (0.38 g, 1.0 equiv) in toluene (2.0 mL) was slowly added a 0.5 M toluene solution of [K(N(SiMe$_3$)$_2$] (0.4 mL, 1.2 mol equiv) at room temperature. After stirring for 30 min, a solution of $Cl_2(PCy_3)_2Ru(=CHPh)$ (0.16 g, 1.2 mol eq) in toluene (4.0 mL) at room temperature was slowly added to the reaction mixture. After stirring the reaction mixture for 20 h, the solid was filtered and washed successively with toluene (2 × 20mL) and dichloromethane (3 × 20 mL) till the filtrate was colourless. The material was dried under high vacuum (10^{-5} mm Hg) at room temperature for 22-24 h to yield 0.35 g of a light greenish solid.

Elemental analysis: N:1.13%; Ru:1.40%., P: 0.40%.

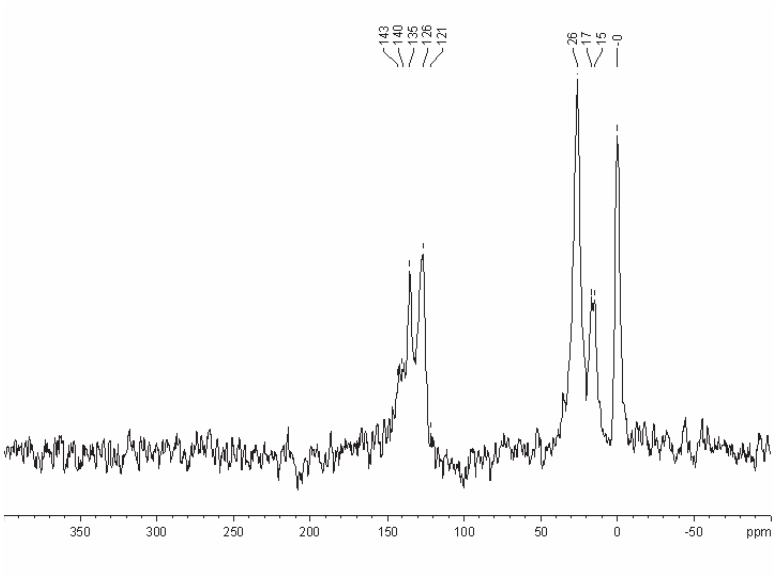

Figure 52: Solid State ^{13}C NMR of **M-RuPhMs.**

Attribution**:** 126-140 ppm (aromatic carbon atoms), 26 ppm ($P\underline{C}y_3$ moieties), 15 ppm (CH_3 of mesityl unit), 0 ppm to (-OSi(*Me*)$_3$).

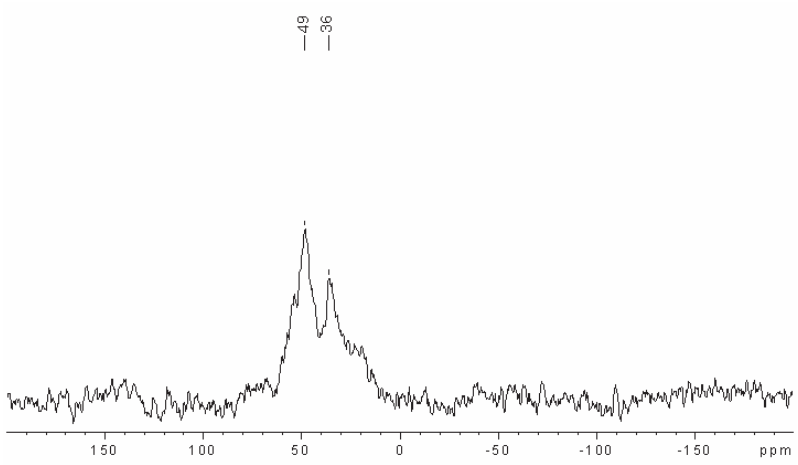

Figure 53: Solid State ^{31}P NMR of **M-RuPhMs.**

Attribution**:** 49 ppm (phosphine oxide-probably due to further reaction of liberated PCy_3) 36 ppm (PCy_3 bound to Ru -first evidence of a coordinated Phosphine on Ru), shoulder peak around 30 ppm (probably due to the phosphonium species).

4.1.5. Synthesis of M-RuMs

4.1.5.1. Reaction scheme

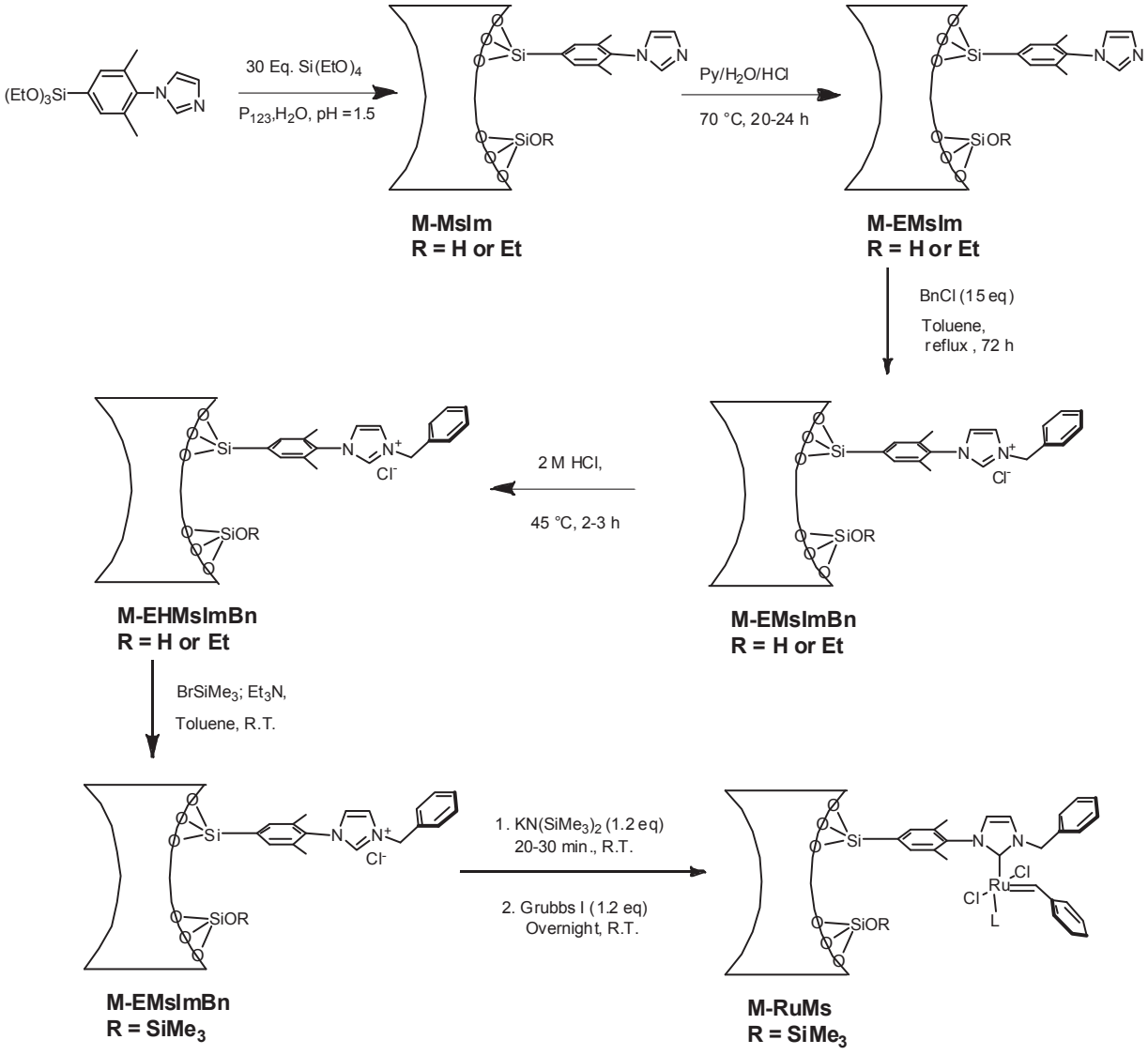

Scheme 9: Synthesis of **M-RuMs.**

4.1.5.2. Synthesis of M-EMsIm

To the material **M-MsIm** (1.08 g), was added a mixture of pyridine (7.5 mL), water (7.5 mL) and 2 M aqueous HCl (1.25 mL). The reaction mixture was heated to 70 °C. After stirring the reaction mixture for 20-24 h, the solid was filtered and washed successively with water (3 × 200 mL), acetone (3 × 200 mL) and diethyl ether (3 × 100 mL). The solid was then dried for 14-16 h under high vacuum (10^{-5} mm Hg) at 135 °C, affording 0.7 g of material.

4.1.5.3. M-EMsImBn

To the material **M-EMsIm** (0.63 g) were added toluene (10.0 mL) and benzyl chloride (0.62 g, 0.56 mL, 20 mol eq.). The reaction mixture was heated up to 110 °C. After stirring the reaction mixture for 70-72 h, the solid was filtered and washed successively with toluene (3 × 100 mL), acetone (3 × 200 mL) and diethyl ether (3 × 100 mL). The solid was then dried for 14-16 h under high vacuum (10^{-5} mm Hg) at 135 °C, affording 0.6 g of material.

4.1.5.4. Synthesis of M-EHMsImBn

To the material **M-EMsImBn** (0.6 g) was added 60 mL of a 2 M aqueous HCl. The reaction mixture was heated up to 45 °C. After stirring the reaction mixture for 2 -2.5 h, the solid was filtered and washed successively with water (3 × 200 mL), acetone (3 × 200 mL) and diethyl ether (3 × 100 mL). The solid was then dried for 5-6 h under high vacuum (10^{-5} mm Hg) at 135 °C, affording 0.4 g of material.

4.1.5.5. Synthesis of M-PMsIm

To the suspension of material **M-EHPhMsIm** (0.4 g) in toluene (28.0 mL), were added triethylamine (4.2 mL, 200 mol eq) and trimethylsilylbromide (2.0 mL, 100 mol eq) at room temperature. The reaction mixture was stirred overnight. The solid was then filtered and washed successively with toluene (3 × 20 mL) and dichloromethaner (3 × 20 mL). The solid was dried under high vacuum (10^{-5} mm Hg) overnight (16-18 h) at 135 °C, affording **0.25 g** of material. **Elemental analysis:** Si: 40%; N: 0.81%.

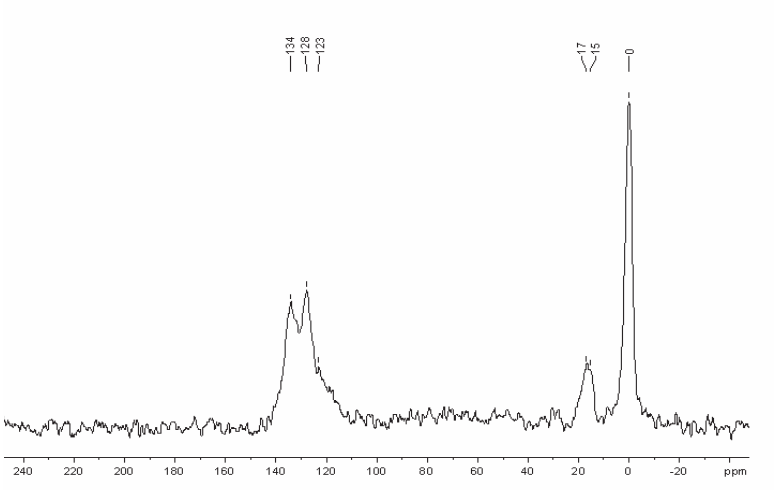

Figure 54: Solid State ^{13}C NMR of **M-PMsIm.**

Attribution**:** 128-134 ppm (aromatic carbon atoms), 15-17 ppm (CH_3 of mesityl unit), 0 ppm to (-OSi(*Me*)$_3$).

4.1.5.6. Synthesis of M-RuMs

To the suspension of **M-PMsIm** (0.2 g, 1.0 equiv) in toluene (2.0 mL), was slowly added a 0.5 M toluene solution of [K(N(SiMe$_3$)$_2$] (0.17 mL, 1.2 mol equiv) at room temperature. After stirring for 30 min, a solution of Cl$_2$(PCy$_3$)$_2$Ru(=CHPh) (0.07 g, 1.2 mol eq) in toluene (2.0 mL) at room temperature was slowly added to the reaction mixture. After stirring the reaction mixture overnight, the solid was filtered and washed successively with toluene (2 × 20mL) and dichloromethane (3 × 20 mL) until the filtrate was colourless. The material was dried under high vacuum (10^{-5} mm Hg) at room temperature for 12-16 h to yield 0.15 g of a light greenish solid. **Elemental analysis:** Si: 36.9%; N:0.86%; Ru: 0.71%, P: 0.19%.

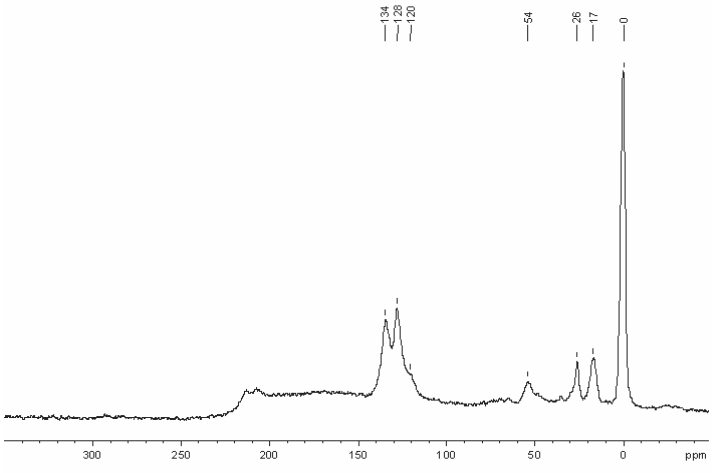

Figure 55: Solid State ^{13}C NMR of **M-RuMs.**

Attribution**:** 120-134 ppm (aromatic carbon atoms), 54 ppm to -N<u>C</u>H$_2$Ph, 26 ppm (-P<u>C</u>y$_3$ moieties), 17 ppm (CH$_3$ of mesityl unit), 0 ppm to (-OSi(*Me*)$_3$), peaks around 210 ppm are spinning side bands.

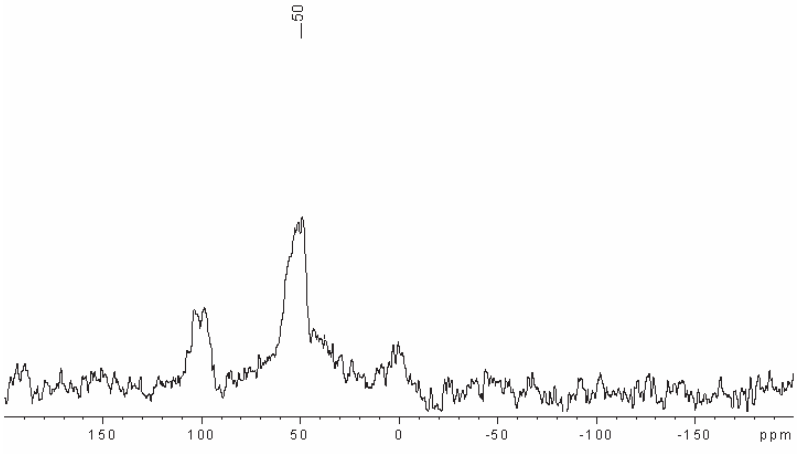

Figure 56: Solid State ^{31}P NMR of **M-RuMs.**

Attribution**:** 49 ppm (phosphine oxide (probably due to further reaction of liberated PCy$_3$), no signal for the PCy$_3$ bound to Ru. peaks around 100 and 0 ppm are spinning side bands.

4.2. Catalytic performances of hybrid materials

General information for catalytic tests:

All metathesis experiments were carried out under an inert atmosphere, in a glove-box. Toluene was dried over NaK and distilled under nitrogen prior to use. Cyclooctene (*cis*-cyclooctene) was purchased from Aldrich, distilled over Na prior to use. Catalysts G-II and GH-II were purchased from Aldrich and catalyst (Nolan) was synthesized according to the literature procedures.

Cyclooctene metathesis experiments with heterogeneous Ru-complexes (*Ratio Cyclooctene/ Ru of c.a. 10,000).*

Representative procedure for heterogeneous catalysts: Eicosane was dissolved in ~20mM toluene solution of cyclooctene. Sample was taken for GC analysis as a reference. Heterogeneous Ru-catalyst was added to the above solution of cyclooctene, at room temperature. The progress of the metathesis reaction was monitored by sampling at suitable intervals. (The samples were immediately quenched by an excess of ethyl acetate). The samples were analysed by GC with a HP5 column.

5. Appendix:

5.1. GC standardization (Response factor using internal standard

Standardization of GC was performed to calculate the response of cyclooctene & dimer with respect to eicosane (standard). Standard solutions were prepared with different concentrations of cyclooctene & dimer keeping the eicosane concentration constant at 8.14 mM. Response ratio for the cyclooctene was 0.368 & for the dimer 0.786 (see Figure 5, 6 and Table S1).

Gas phase analyses (metathesis) were performed on Agilent Technologies 7890A GC apparatus equipped with a FID detector and a HP5 Fame column (30 m × 0.32 mm). Split ratio of GC was set to 50:1. Sample injection was 1 microliter with 10 microliter syringe.(details can be found in Appendix - Table S1).

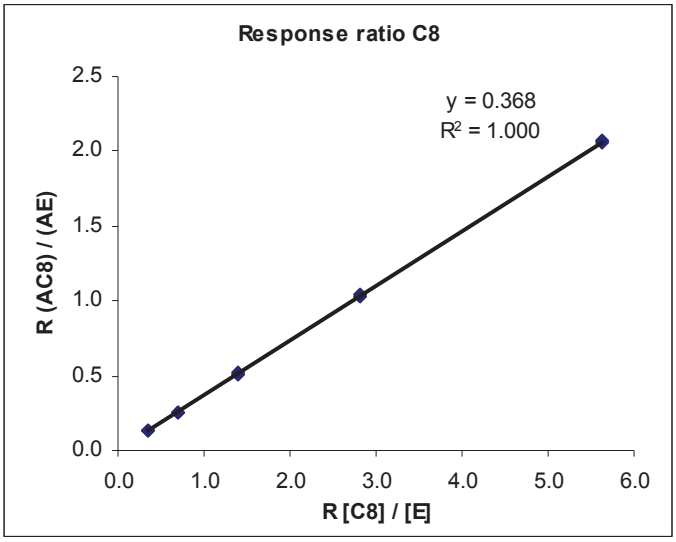

Figure 57: Response ratio of C8 /E.

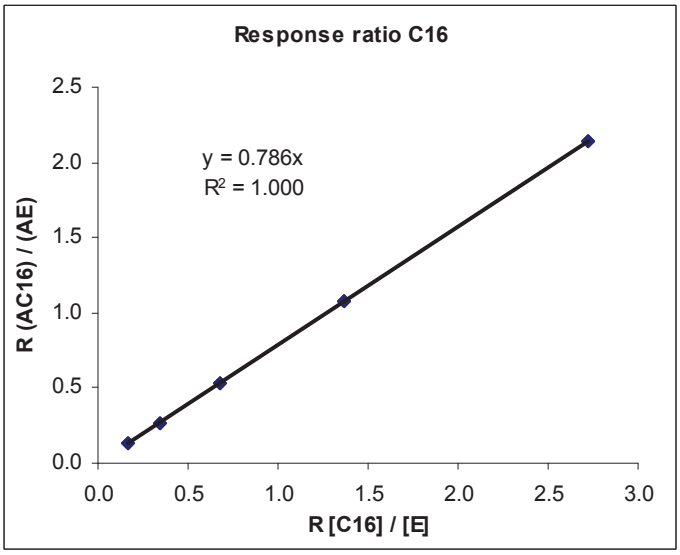

Figure 58: Response ratio of C16/ E.

Table 3: GC standardization for the response of cyclooctene (C8) & dimer (C16) with respect to Eicosane (E) as standard.

[C8]	[C16]	Ratio [C8]/[E]	Ratio [C16]/[E]	(AC8)	(AC16)	Eicosane	R(AC8) /(AE)	R(AC16) /(AE)
2.86	1.39	0.3511	0.1703	139.4	144.2	1092.9	0.13	0.13
		0.3511	0.1703	138.2	142.8	1084.0	0.13	0.13
5.72	2.77	0.7022	0.3406	279.2	285.7	1087.2	0.26	0.26
		0.7022	0.3406	282.5	289.6	1102.9	0.26	0.26
11.43	5.55	1.4045	0.6812	565.9	582.5	1090.3	0.52	0.53
		1.4045	0.6812	570.8	593.4	1111.9	0.51	0.53
22.87	11.09	2.8090	1.3624	1139.0	1172.9	1095.2	1.04	1.07
		2.8090	1.3624	1153.2	1197.7	1116.9	1.03	1.07
45.74	22.18	5.6180	2.7247	2319.0	2397.9	1119.1	2.07	2.14
		5.6180	2.7247	2326.8	2421.8	1132.4	2.05	2.14

[C8] = Concentration of C8 in mM, [C16] = Concentration of C16 in mM, (AC8) = Area of C8, (AC16) = Area of C16, [E] = Concentration of eicosane in mM, (AE) = Area of eicosane.

5.2. Catalytic performance

5.2.1. M-RuPr

Table 4: Catalytic performances of **M-RuPr** in the RO-RCM of cyclooctene.

Time [h]	Conversion (%)	TON	Sel-dimer (%)	Sel-trimer (%)	Sel-tetra (%)	Sel-penta (%)	Mass balance (%)
0.0	0.0	0					
0.5	6.6	658	**51**	17	7	3	79
1.0	13.6	1359	**55**	19	8	3	85
1.5	20.6	2065	**54**	19	8	3	84
2.0	26.6	2663	**53**	20	8	4	85
2.5	34.0	3400	**54**	21	9	4	88
3.0	40.1	4006	**53**	22	10	4	89
3.5	47.1	4713	**53**	22	10	4	89
4.0	54.1	5408	**52**	23	10	4	89
5.0	65.2	6522	**50**	24	11	5	90
7.0	82.7	8274	**44**	27	12	6	89
18.5	95.5	9550	**35**	30	15	7	88
44.0	96.5	9649	**33**	31	15	9	88
68.0	96.6	9656	**33**	31	16	8	87
96.0	96.6	9658	**32**	31	16	8	87
124.0	96.6	9662	**32**	31	16	8	87

5.2.2. Catalytic performance of M-RuBn

Table 5: Catalytic performance of **M-RuBn** in the RO-RCM of cyclooctene.

Time [h]	Conversion (%)	TON	Sel-dimer (%)	Sel-trimer (%)	Sel-tetra (%)	Sel-penta (%)	Mass balance (%)
0.0	0.0	0					
0.5	3.4	345	**24**	8	3	0	35
1.0	5.3	529	**34**	11	4	2	51
2.0	9.5	954	**43**	14	5	3	65
3.0	13.8	1379	**49**	17	6	3	75
4.3	20.9	2087	**53**	18	7	3	80
5.0	24.3	2433	**54**	19	7	3	83
6.0	30.1	3011	**54**	20	7	3	84
7.0	34.9	3489	**54**	20	8	3	85
8.0	39.6	3962	**54**	21	8	4	87
26.0	84.8	8479	**43**	27	12	6	88
32.0	88.8	8883	**41**	28	13	6	88
48.0	93.0	9298	**37**	29	14	7	87
56.0	94.0	9396	**36**	30	14	7	87
73.0	94.9	9493	**35**	30	15	7	86
97.0	95.6	9555	**34**	30	14	7	86

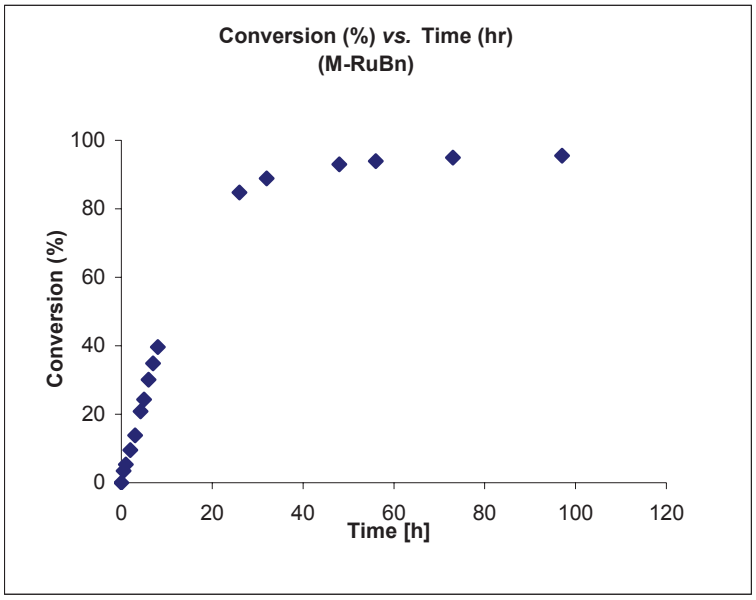

Figure 59 : Conversion of cyclooctene (%) *vs.* time [h] using **M-RuBn.**

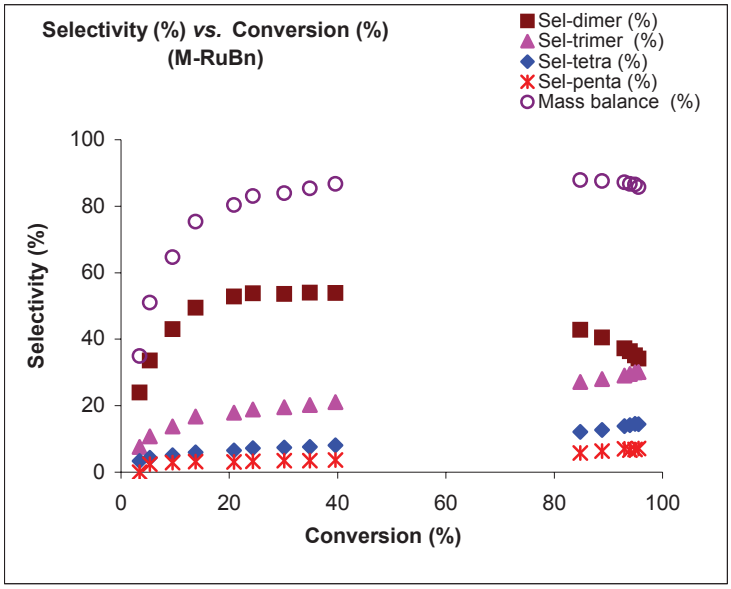

Figure 60 : Selectivity of cyclic products (%) *vs.* conversion of cyclooctene (%) using **M-RuBn.**

5.2.3. Catalytic performance of M-RuHex

Table 6: Catalytic performance of **M-RuHex** in the RO-RCM of cyclooctene.

Time [h]	Conversion (%)	TON	Sel-dimer (%)	Sel-trimer (%)	Sel-tetra (%)	Sel-penta (%)	Mass balance (%)
0.0	0.0	0					
1.0	2.3	226	**31**	11	4	0	47
3.5	6.8	676	**50**	17	6	2	75
6.0	11.9	1190	**56**	19	7	2	84
23.0	47.9	4789	**54**	24	9	3	91
49.0	58.6	5858	**52**	24	10	4	90
72.0	61.7	6165	**51**	25	10	4	90
96.0	62.5	6254	**51**	24	10	4	89

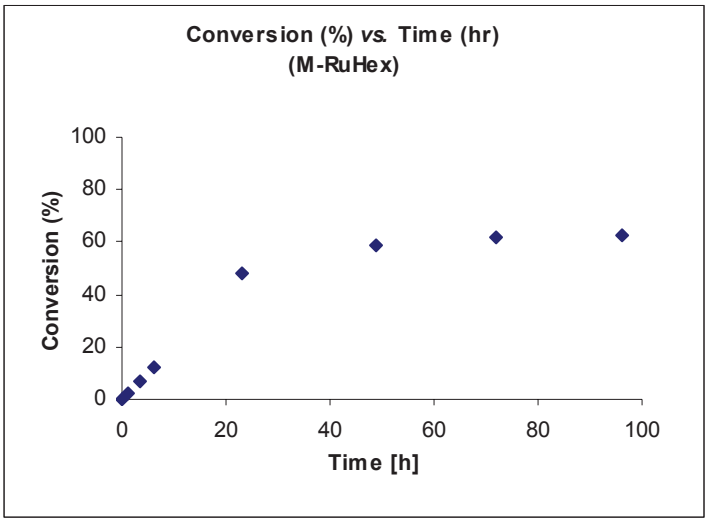

Figure 61: Conversion of cyclooctene (%) *vs.* time [h] using **M-RuHex**.

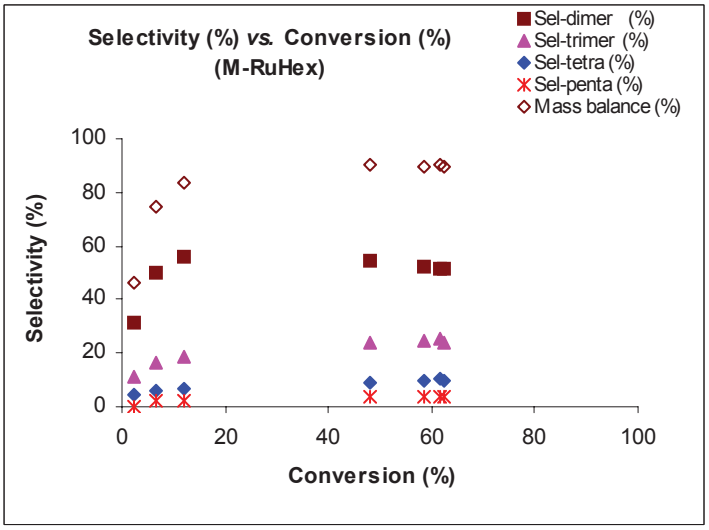

Figure 62: Selectivity of cyclic products (%) *vs.* conversion of cyclooctene (%) using **M-RuHex**.

5.2.4. Catalytic performance of M-RuPhMs

Table 7: Result of catalytic performance of **M-RuPhMs** in the RO-RCM of cyclooctene.

Time [h]	Conversion (%)	TON	Sel-dimer (%)	Sel-trimer (%)	Sel-tetra (%)	Sel-penta (%)	Mass balance (%)
0.0	0.0	0					
1.0	2.6	260	**4**	1	0	0	6
2.0	2.9	294	**10**	3	2	0	16
3.0	3.7	374	**14**	5	3	0	22
4.3	3.6	357	**23**	9	4	3	39
5.0	4.9	487	**20**	8	4	2	35
6.0	5.2	518	**23**	9	4	2	39
7.0	5.1	512	**28**	11	5	4	49
8.0	6.2	615	**27**	11	5	3	46
26.0	12.5	1246	**43**	18	8	5	74
32.0	14.3	1430	**44**	18	8	4	75
48.0	19.8	1976	**42**	18	8	4	72
56.0	21.5	2146	**43**	18	8	4	72
73.0	23.6	2363	**44**	18	8	4	75
97.0	25.6	2561	**45**	19	8	4	76
121.0	26.7	2666	**45**	19	9	4	77

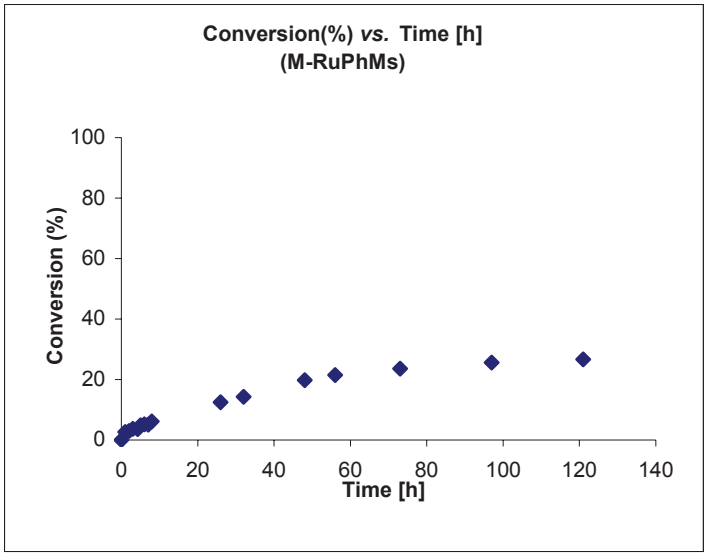

Figure 63 : Conversion of cyclooctene (%) *vs.* time [h] using **M-RuPhMs**.

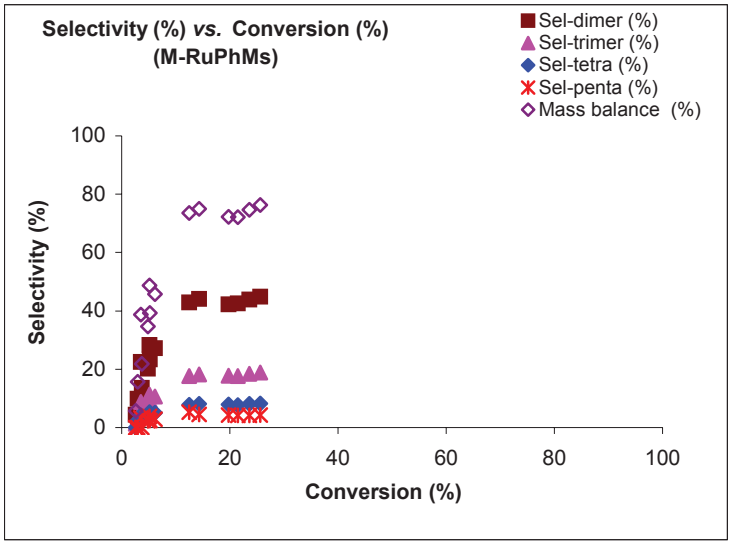

Figure 64 : Selectivity of cyclic products (%) *vs.* conversion of cyclooctene (%) using **M-RuPhMs**.

5.2.5. Catalytic performance of M-RuMs

Table 8: Result of catalytic performance of **M-RuMs** in the RO-RCM of cyclooctene.

Time [h]	Conversion (%)	TON	Sel-dimer (%)	Sel-trimer (%)	Sel-tetra (%)	Sel-penta (%)	Mass balance (%)
0.0	0.0	0					
1.0	6.0	598	**25**	12	7	4	48
2.0	10.4	1036	**29**	14	8	4	56
5.3	21.5	2148	**32**	16	9	5	62
16.0	40.2	4022	**34**	17	10	6	67
45.0	58.6	5859	**35**	19	10	6	69
67.0	60.8	6083	**35**	19	11	6	71
91.0	61.5	6153	**35**	19	10	6	70
115.0	61.7	6171	**35**	19	10	5	69

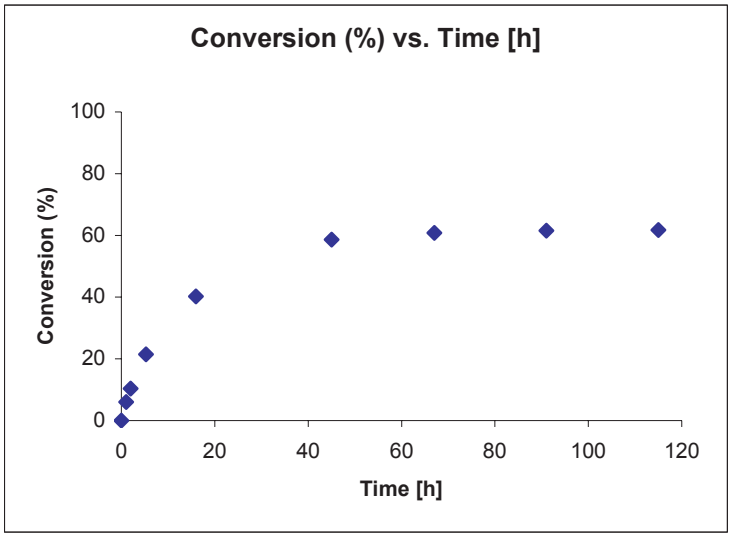

Figure 65 : Conversion of cyclooctene (%) *vs.* time [h] using **M-RuMs**.

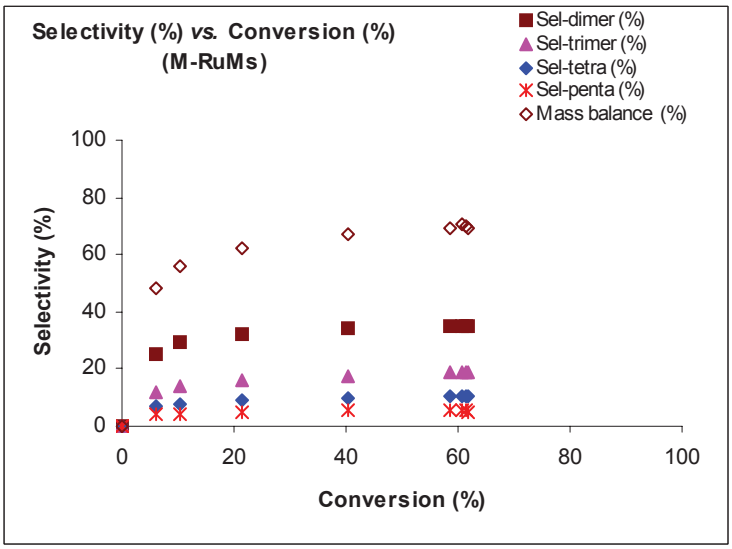

Figure 66 : Selectivity of cyclic products (%) *vs.* conversion of cyclooctene (%) using **M-RuMs**.

5.3. Kinetic investigation

5.3.1. RO-RCM of cyclooctene

Table 9: Rate of reaction for cyclooctene RO-RCM at different concentration using **M-RuPr**.

Concentration [mM]	**5**	**9**	**15**	**20**	**21**
Rate [mol/mol Ru/h]	239	624	963	1359	1696

Table 10: Selectivity of products in RO-RCM of cyclooctene at different concentration with similar conversion (13-15%) and mass balance (80-85%) using **M-RuPr**.

Concentration [mM]	**Conversion (%)**	**Mass Balance (%)**	**Selectivity of products (%)**			
			Dimer	**Trimer**	**Tetramer**	**Pentamer**
0	0	0	0	0	0	0
5	13.7	85	68	14	4	0
9	14.2	81	58	18	6	0
15	15.2	81	53	18	7	3
20	13.6	85	55	19	8	3

Table 11: Productivity of products in RO-RCM of cyclooctene using 5 mM cyclooctene and using **M-RuPr**.

Conversion (%)	**TON**	**TON Dimer**	**TON-trimer**	**TON-tetramer**	**TON-pentamer**	**TON-Sum**	**Mass balance (%)**
0.0	0	0	0	0	0	0	
0.8	83	49	0	0	0	49	59
2.4	239	87	13	0	0	100	42
2.4	244	140	20	0	0	160	65
3.2	319	216	30	0	0	247	77
4.7	465	267	43	12	0	322	69
4.8	480	335	53	15	0	403	84
6.2	619	397	78	16	0	491	79
7.3	731	455	90	23	0	568	78
8.5	846	595	117	28	0	740	87
10.7	1065	703	141	32	0	875	82
11.9	1192	810	164	40	0	1014	85
13.7	1370	925	187	51	0	1164	85
21.7	2166	1587	322	70	0	1978	91
24.4	2437	1821	378	97	0	2297	94
25.1	2514	1866	389	79	0	2334	93
25.8	2578	1896	404	85	0	2385	93
25.8	2584	1901	395	94	0	2390	92
25.7	2570	1909	412	85	0	2406	94

Table 12: Productivity of products in RO-RCM of cyclooctene using 9 mM cyclooctene and using **M-RuPr**.

Time [h]	Conversion (%)	TON	TON-Dimer	TON-trimer	TON-tetramer	TON-pentamer	TON-Sum	Mass balance (%)
0.0	0.0	0	0	0	0	0	0	
0.5	3.6	365	108	33	8	0	149	41
1.0	6.2	624	333	93	34	0	459	74
1.5	9.7	968	546	165	51	0	762	79
2.0	14.2	1423	829	250	79	0	1158	81
2.5	18.4	1844	1055	317	99	0	1471	80
3.0	22.9	2288	1281	401	116	0	1797	79
3.5	25.7	2572	1535	490	152	69	2246	87
4.0	30.5	3054	1806	590	179	68	2643	87
4.5	35.0	3503	2036	681	219	70	3005	86
5.0	39.0	3898	2311	756	253	68	3388	87
5.5	42.0	4202	2440	812	268	82	3602	86
6.0	45.1	4506	2660	911	293	98	3962	88
6.5	47.9	4786	2861	1001	328	119	4310	90
7.0	52.3	5231	3040	1085	355	132	4612	88
7.5	55.0	5501	3174	1166	393	133	4866	88
8.0	56.2	5621	3273	1287	413	124	5097	91
24.0	82.3	8232	4390	2213	794	230	7626	93
48.0	85.3	8530	4432	2378	855	265	7930	93
72.0	86.1	8611	4466	2419	874	273	8031	93
120.0	86.2	8621	4472	2442	843	269	8027	93

Table 13: Productivity of products in RO-RCM of cyclooctene using 15 mM cyclooctene and using **M-RuPr**.

Time [h]	Conversion (%)	TON	TON-Dimer	TON-trimer	TON-tetramer	TON-pentamer	TON-Sum	Mass balance (%)
0.0	0.0	0	0	0	0	0	0	
0.5	4.6	463	160	52	24	0	236	51
1.0	9.6	963	463	149	57	26	695	72
1.5	15.2	1521	807	273	102	44	1226	81
2.0	20.9	2092	1158	408	153	62	1780	85
2.5	26.6	2664	1486	521	208	79	2294	86
3.0	32.9	3289	1848	674	259	97	2878	88
3.5	37.9	3786	2128	808	315	122	3373	89
4.0	44.1	4409	2458	962	377	143	3941	89
4.5	49.8	4984	2753	1124	440	164	4481	90
5.0	54.8	5485	2992	1257	501	191	4942	90
5.5	60.8	6078	3266	1451	585	215	5518	91
6.0	63.8	6378	3411	1556	640	241	5848	92
7.0	72.8	7283	3742	1881	780	311	6714	92
8.0	78.3	7832	3878	2094	885	348	7205	92
23.0	94.1	9407	3745	2911	1348	569	8572	91
50.0	95.4	9539	3599	3022	1425	612	8657	91
78.0	95.6	9562	3597	3031	1438	644	8710	91
110.0	95.7	9571	3554	2837	1220	487	8098	85

Table 14: Productivity of products in RO-RCM of cyclooctene using 20 mM cyclooctene and using **M-RuPr**.

Conversion (%)	TON	TON Dimer	TON-trimer	TON-tetramer	TON-pentamer	TON-Sum	Mass balance (%)
0.0	0	0	0	0	0	0	
6.6	658	335	113	47	23	518	79
13.6	1359	743	264	105	37	1149	85
20.6	2065	1115	399	167	60	1742	84
26.6	2663	1424	534	218	94	2269	85
34.0	3400	1827	721	300	128	2976	88
40.1	4006	2134	881	382	154	3550	89
47.1	4713	2484	1059	448	191	4182	89
54.1	5408	2803	1263	540	226	4832	89
65.2	6522	3253	1598	703	312	5866	90
82.7	8274	3673	2238	1019	471	7402	89
95.5	9550	3316	2875	1472	712	8375	88
96.5	9649	3148	2967	1496	883	8494	88
96.6	9656	3143	2961	1547	763	8414	87
96.6	9658	3124	2970	1566	758	8418	87
96.6	9662	3111	2961	1556	768	8397	87

Representative plots for the productivity of products in RO-RCM of cyclooctene using different concentration of cyclooctene using **M-RuPr**.

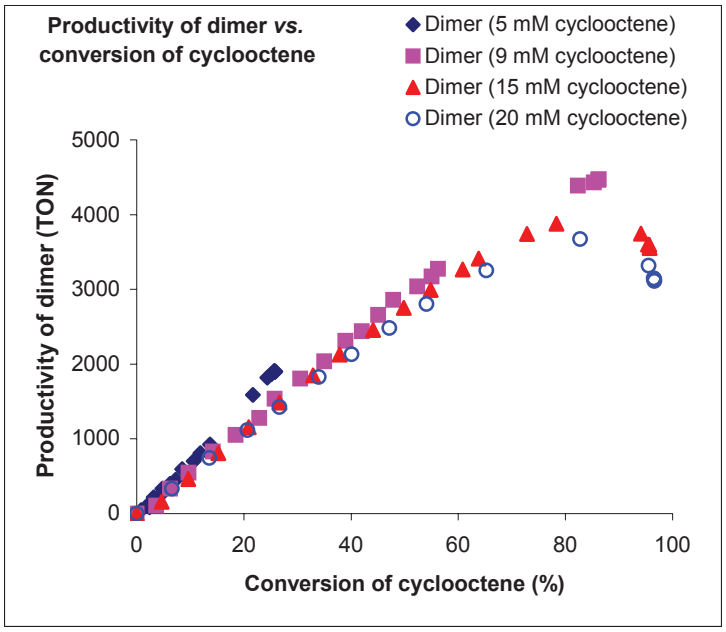

Figure 67: Productivity of dimer for the reactions carried out with different concentration of cyclooctene using **M-RuPr**.

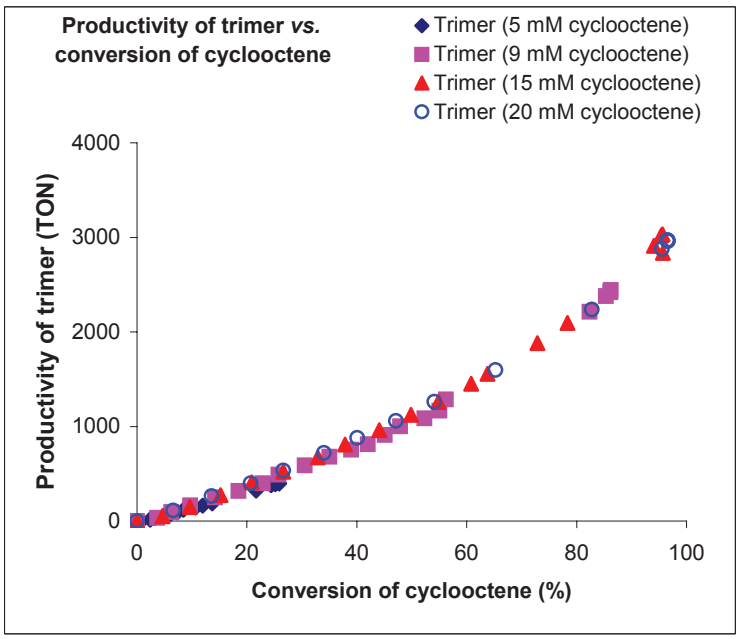

Figure 68: Productivity of trimer for the reactions carried out with different concentration of cyclooctene using **M-RuPr**.

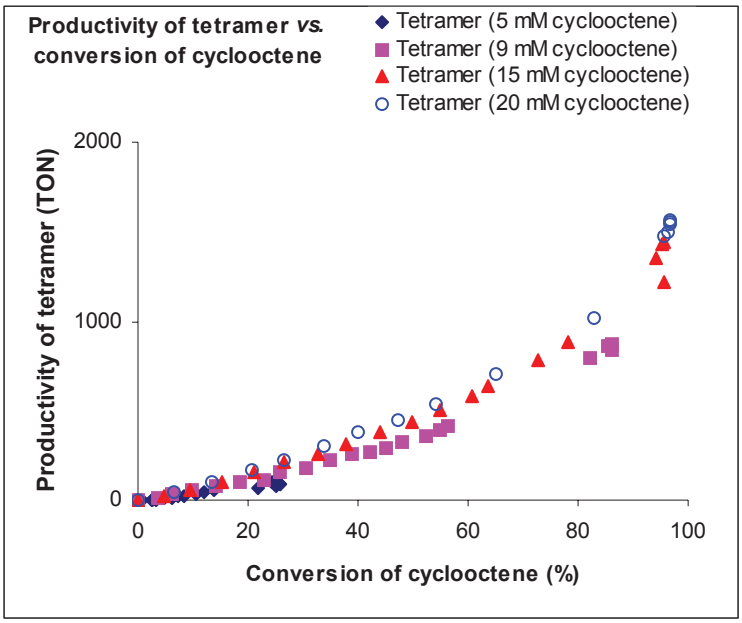

Figure 69: Productivity of tetramer for the reactions carried out with different concentration of cyclooctene using **M-RuPr**.

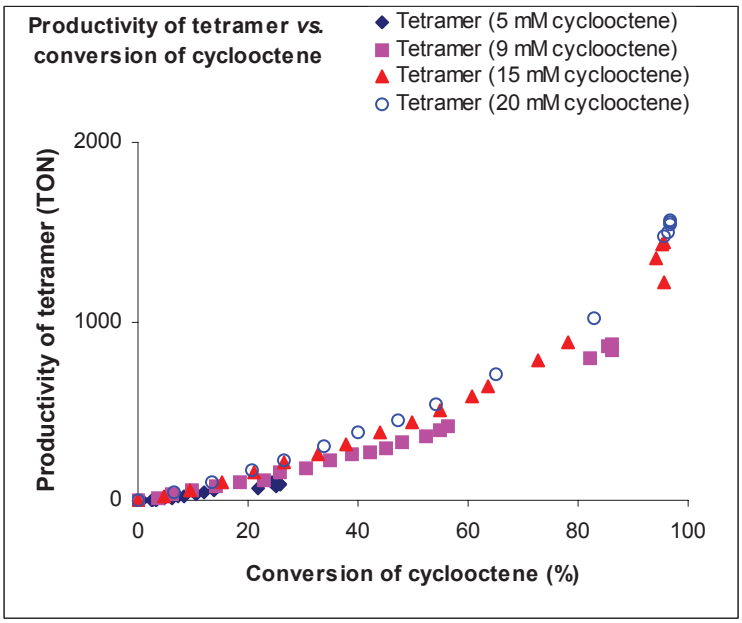

Figure 70: Productivity of pentamer for the reactions carried out with different concentration of cyclooctene using **M-RuPr**.

5.3.2. RO-RCM of dimer

Table 15: Result of catalytic performance for RO-RCM of dimer using **M-RuPr**.

Time [h]	Dimer conversion (%)	Sel-cycloctene (%)	Sel-trimer (%)	Sel-tetra (%)	Sel-penta (%)	Mass balancel (%)
0.5	**0.8**	16	60	29	0	105
1.0	**1.6**	11	38	36	0	86
1.5	**2.5**	10	39	24	7	80
2.0	**3.7**	10	43	29	7	90
2.5	**4.8**	10	46	30	14	101
3.0	**7.7**	8	40	27	11	87
3.5	**8.9**	8	42	28	8	87
4.0	**10.8**	8	41	29	8	85
4.5	**13.2**	7	39	25	7	79
5.0	**14.3**	7	41	27	8	83
5.5	**15.7**	7	41	28	8	83
6.0	**17.3**	7	41	28	8	84
6.5	**18.7**	7	40	26	8	81
7.0	**19.1**	7	41	27	8	84
7.5	**20.1**	7	41	27	8	83
8.0	**21.2**	7	41	27	9	83
24.0	**31.7**	6	42	27	8	83
48.0	**37.2**	6	42	26	9	82
72.0	**39.2**	5	42	26	9	83
120.0	**39.6**	6	42	26	10	83
176.0	**40.1**	5	42	26	9	82

Table 16: Effect of addition of cyclooctene on the rate of metathesis of dimer: addition of 0 mM cyclooctene and using **M-RuPr**.

Time [h]	Dimer (%)	TON Dimer	TON-trimer	TON-tetramer	TON-pentamer	TON-Sum
0.0	**0.0**	**0**	0	0	0	0
0.5	**0.8**	**41**	24	12	0	36
1.0	**1.6**	**80**	31	29	0	60
1.5	**2.5**	**124**	48	30	8	86
2.0	**3.7**	**185**	80	54	14	148
2.5	**4.8**	**241**	112	72	35	219
3.0	**7.7**	**383**	152	104	44	300
3.5	**8.9**	**444**	189	126	37	351
4.0	**10.8**	**539**	223	154	41	418
4.5	**13.2**	**659**	260	167	49	475
5.0	**14.3**	**713**	292	193	56	542
5.5	**15.7**	**786**	319	217	63	598
6.0	**17.3**	**865**	353	239	72	665
6.5	**18.7**	**937**	376	245	73	695
7.0	**19.1**	**955**	396	256	79	731
7.5	**20.1**	**1003**	416	271	79	766
8.0	**21.2**	**1062**	436	287	90	813
24.0	**31.7**	**1587**	663	423	131	1217
48.0	**37.2**	**1862**	784	479	162	1425
72.0	**39.2**	**1962**	820	510	182	1513
120.0	**39.6**	**1979**	829	513	188	1530
176.0	**40.1**	**2007**	839	520	175	1535

Table 17: Effect of addition of cyclooctene on the rate of metathesis of dimer: addition of 2 mM cyclooctene and using **M-RuPr**.

Time [h]	Dimer conversion (%)	TON Dimer	TON-trimer	TON-tetramer	TON-pentamer	TON-Sum
0.0	**0.0**	**0**	0	0	0	0
0.5	**1.1**	**55**	11	5	0	16
1.0	**1.4**	**72**	21	16	0	38
1.5	**2.0**	**101**	34	18	8	60
2.0	**2.5**	**123**	53	27	11	91
2.5	**3.5**	**177**	81	43	19	143
3.0	**4.6**	**231**	116	61	26	203
3.5	**5.8**	**292**	148	79	34	261
4.0	**7.1**	**357**	181	98	40	320
5.0	**11.0**	**552**	294	158	69	522
6.0	**15.0**	**748**	393	215	89	697
7.0	**17.9**	**893**	475	256	107	838
8.0	**21.7**	**1086**	578	312	133	1023
26.0	**33.9**	**1694**	895	495	214	1604
56.0	**35.9**	**1797**	941	519	231	1691
82.0	**35.8**	**1788**	944	524	225	1692
109.0	**35.8**	**1792**	947	525	234	1706

Table 18: Effect of addition of cyclooctene on the rate of metathesis of dimer: addition of 4 mM cyclooctene and using **M-RuPr**.

Time [h]	Dimer (%)	TON Dimer	TON-trimer	TON-tetramer	TON-pentamer	TON-Sum
0.0	**0.0**	**0**	0	0	0	0
0.5	**1.1**	**53**	10	5	0	15
1.0	**1.1**	**53**	22	10	6	38
1.5	**1.4**	**70**	32	16	9	58
2.0	**1.8**	**90**	50	24	12	87
2.5	**2.6**	**130**	75	38	19	132
3.0	**3.5**	**177**	105	53	25	184
3.5	**4.2**	**208**	134	67	31	232
4.0	**5.1**	**256**	165	84	41	289
5.0	**8.2**	**409**	270	143	62	474
6.0	**10.8**	**542**	359	185	83	626
7.0	**12.8**	**641**	428	221	101	750
8.0	**16.0**	**800**	529	276	125	929
26.0	**34.1**	**1704**	1062	571	265	1898
56.0	**38.5**	**1927**	1191	649	313	2152
82.0	**38.6**	**1929**	1190	636	307	2133
109.0	**38.5**	**1927**	1192	638	313	2144

Table 19: Rate of dimer metathesis for reactions carried out with addition of different concentration of cyclooctene using **M-RuPr**.

Dimer Rate [mol/mol Ru/h]	Concentration of added cyclooctene [mM]
80	0
72	2
53	4

6. References

1 . Williams, A. S. *Synthesis* **1999***, 10,* 1707.

2 . Höcker, H.; Reimann, W.; Reif, L.; Riebel, K. *J. Mol. Catal.* **1980***, 8,* 191.

. a) Warwel, S.; Katker, H.; Rauenbusch, C. *Angew. Chem. Int. Ed. Engl. 26 ,***1987***, No. 7,* 702; b) Warwel, S.; Katker, H. *Synthesis,* **1987***,* 935*;* c) Eberle, H.-J.; Kreuzer, F.-H.; Zeitler, N. *US Patent A-4668836,* **1987**; d) Eberle, H.-J.; Csellich, C.; Zeitler, N.; Maixner, G. *European Patent 0343437 B1,* **1989**.

4. Rost, A. M. J.; Schneider, H.; Zoller, J. P.; Herrmann, W. A.; Kühn, F. E. *J. Organometal. Chem. 690 (***2005***)* 4712.

5 . Derouane, E. G. *J. Mol. Cat. A*. **1998**, *134*, 29.

6 . (a) Thieuleux, C.; Coperet, C.; Veyre, L.; Corriu, R.; Reye, C.; Mehdi, A.; Basset, J. M.; Maishal, T.; Boualleg, M.; Karame, I.; Camus, J. M.; Alauzun, J. US 2011/0160412 A1, WO 2009/092814 A1, EP 2082804 A1.(b) Maishal, T. K.; Alauzun, J.; Basset, J. –M.; Copéret, C.; Corriu, R. J. P.; Jeanneau, E.; Mehdi, A.; Reyé, C.; Veyre, L.; Thieuleux, C. *Angew. Chem. Int. Ed.* **2008**, *47*, 8654.

7 . Karame, I.; Boualleg, M.; Camus, J. M.; Maishal, T. K.; Alauzun, J.; Basset, J. M.; Coperet, C.; Corriu, R. J. P.; Jeanneau, E.; Mehdi, A.; Reye, C.; Veyre, L.; Thieuleux, C. *Chem. Eur. J.* **2009**, 15, 11 820.

8 . (a) Corriu R. J. P. *Chem. Commun*., **2000**, 71. (b) Guari,Y.; Thieuleux, C.; Mehdi, A.; Reyé, C.; Corriu, R. J. P.; Gomez-Gallardo, S.; Philippot, K.; Chaudret, B.; Dutartre, R. *Chem. Commun***. 2001**, *15*, 1374. (c Guari,Y.; Thieuleux, C.; Mehdi, A.; Reyé, C.; Corriu, R. J. P.; Gomez-Gallardo, S.; Philippot, K.; Chaudret, B. *Chem. Mater.* **2003**, *15*, 2017. (d) Corriu, R. J. P.; Mehdi, A.; Reyé, C.; Thieuleux, C.; Frenkel, A.; Gibaud, A. *New J. Chem.* **2004**, *28*, 156. (e) Corriu, R. J. P.; Mehdi, A.; Reyé, C.; Thieuleux, C. *Chem. Mater.* **2004**, *16*, 159. (f) Corriu, R. J. P.; Mehdi, A.; Reyé, C. *J. Mater. Chem.* **2005**, *15*, 4285. (g) Mouawia, R.; Mehdi, A.; Reyé, C.; Corriu, R. J. P. *New J. Chem.* **2006**, *1*, 1077

9 . Boullanger, A.; Alauzun, J.; Mehdi, A.; Reyé, C.; Corriu, R. J. P. *New J. Chem.*, **2010**, 34, 738.

10. Blümel J. *Inorg. Chem.* **1994**, *33*, 5050.

11. Staub, H.; Guillet-Nicolas, R.; Even, N.; Kayser, L.; Kleitz, F.; Fontaine, F-G. *Chem. Eur. J.* **2011**, *17*, 4254.

Chapter 3

Synthesis and catalytic performances of homogeneous unsymmetrical and symmetrical Ru-NHC catalysts

In the previous chapter, hybrid heterogeneous Ru-NHC catalysts have promoted the selective formation of cyclic oligomers in RO-RCM of cyclooctene. The particularly high selectivity in low cyclic oligomers could be attributed to various hypotheses: the pore confinement effect and surface interactions or the chemical structure of the Ru-NHC sites bearing unsymmetrical NHC ligands, which could favor backbiting over polymerization.

In order to address these questions, we will first compare the catalytic performances of the classical symmetrical homogeneous Ru-NHC complexes (**G-II** and **N-II**) and unsymmetrical homogeneous Ru-NHC analogues (effect of chemical structure).

Then the catalytic performances of the Ru-NHC unsymmetrical complexes will be compared to those of our hybrid heterogeneous catalysts (effect of pore confinement or surface interactions).

1. Introduction

We have observed that RO-RCM of cyclooctene, using Ru-NHC based heterogeneous catalysts, showed selectivity towards formation of cyclic oligomers. It was thus important to know whether the observed selectivity was due to pore confinement/surface interaction which could impose constrain to favour formation of cyclic oligomers over higher oligomers and /or polymers or to the chemical structure of Ru-NHC sites (dissymmetry of the NHC ligand).

Note that, several reports can be found in the literature concerning synthesis and use of unsymmetrical Ru-NHC for ROMP, RCM and CM reactions.[1] Recently, the research groups of Prof. Chen[2] and Prof. Buchmeiser[3] have developed unsymmetrical catalysts for sequence-selective copolymerization of norbornene (NBE) with *cis*-cyclooctene (COE) and cyclopentene (CPE) by Ring Opening Metathesis Polymerization (ROMP). The observed chemoselectivity was attributed to the dual configuration of catalysts provided by the presence of an unsymmetrical ancillary ligand (phosphine or NHC), which allowed discrimination between two substrates in the same catalytic reaction (ROMP).

Herein, we will discuss the synthesis and catalytic performances of unsymmetrical Ru-NHC catalysts analogues to those contained in our hybrid heterogeneous catalysts, in view of understanding the origin of the selectivities in RO-RCM of cyclooctene.

2. Results and discussion

2.1. General strategy for the synthesis of homogeneous complexes

Homogeneous unsymmetrical Ru-NHC complexes were prepared using the respective unsymmetrical imidazolium salts (Scheme 1). Although several methods were used for the synthesis of symmetrical and unsymmetrical imidazolium salts,[4] we chose to prepare them by quaternisation of mesityl imidazole with alkyl halides in 80-90% isolated yields. For the synthesis of Grubbs-type catalysts, the imidazolium salt was treated with KHMDS (potassium bis(trimethylsilyl)amide) in toluene at RT to generate the corresponding naked carbene. The carbene was further reacted with the Grubbs-I complex at RT yielding the targetted Ru-NHC complex. The detailed synthesis of such complex is described in the experimental section.

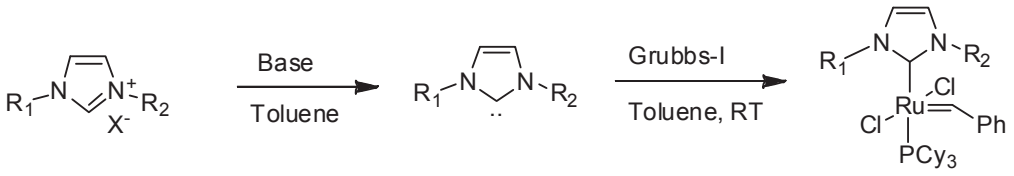

Scheme 1: Methodology for the synthesis of Ru-NHC homogeneous catalysts.

2.2. Structural feature of homogeneous catalysts

Three unsymmetrical homogeneous silylated complexes, namely **RuPr$_{Si}$, RuBn$_{Si}$** and **RuPhMs$_{Si}$** (Figure 1a) were prepared as analogues of the Ru-NHC sites contained in our hybrid heterogeneous catalysts **M-RuPr, M-RuBn** and **M-RuPhMs**. Note that non-silylated unsymmetrical complexes **RuPr** and **RuBn** were also synthesised to get insight in the influence of the silane groups over the selectivity and the activity during the RO-RCM of cyclooctene.

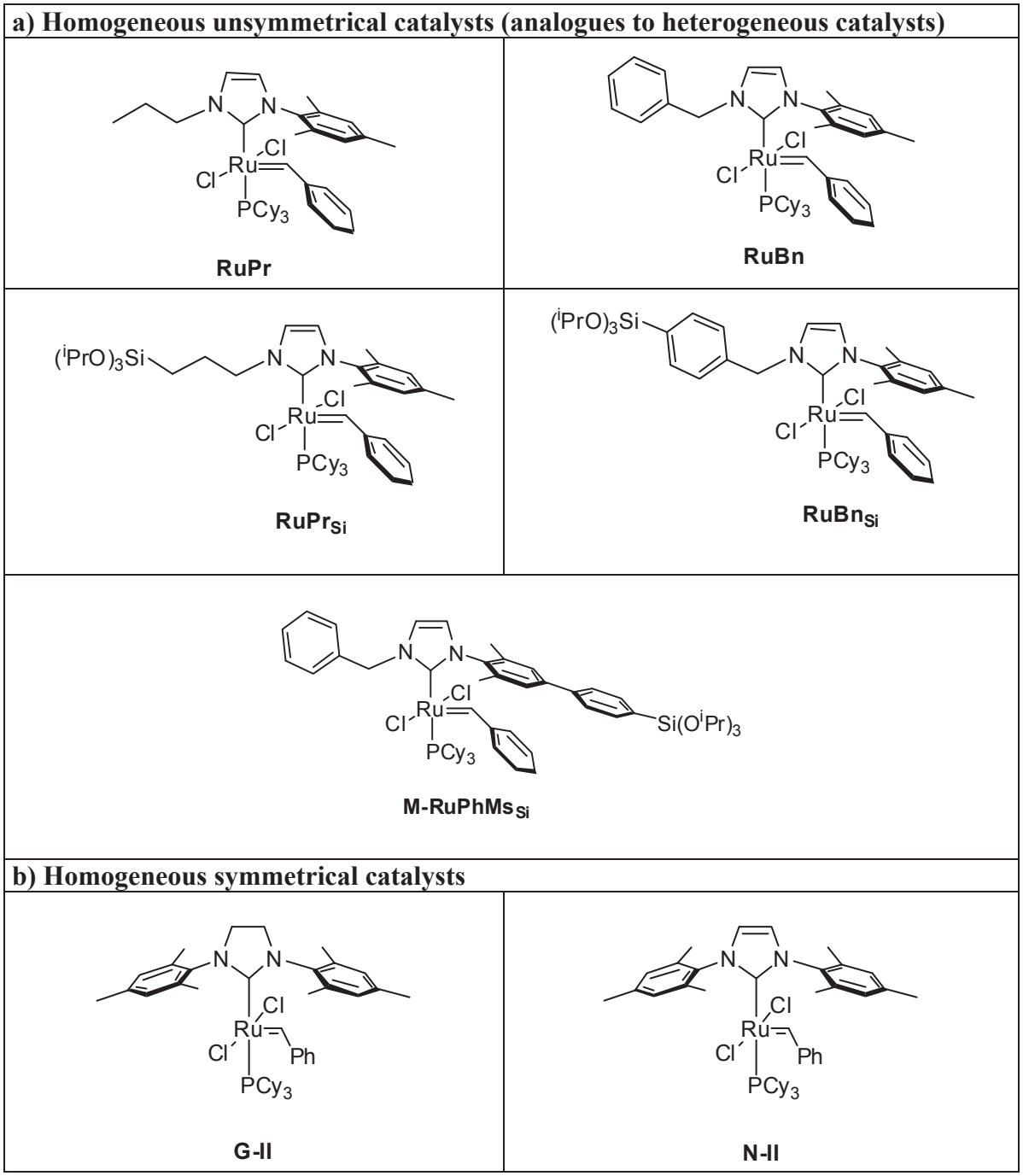

Figure 1: Homogeneous unsymmetrical and symmetrical Ru-NHC pre-catalysts.

The only distinctive feature of these Ru-NHC homogeneous catalysts compared to the classical Ru-NHC catalysts (**G-II** and **N-II**) is the coordination of unsymmetrical NHC ligands on Ru. All these unsymmetrical complexes were obtained in high yield and fully characterized by liquid state NMR and mass spectrometry.

In the specific case of **RuBn**, an X-ray structure was obtained. Note that the **RuBn$_{Si}$** is already reported by our group and the X-ray structure was elucidated.[5] The structural analysis of **RuBn** reveals a square pyramidal coordination with a nearly linear Cl(2)-Ru-Cl(3) angle (165.56 °). However, **RuBn** displays a Ru-C(23) bond distance (1.830 Å) shorter than that in **N-II** (1.841 Å), and an increase in the bond angles (2-4 °) for the NHC substituents with respect to NHC backbone carbon atoms as compared to **N-II**, indicating a slight increase of steric interactions around the metal center.

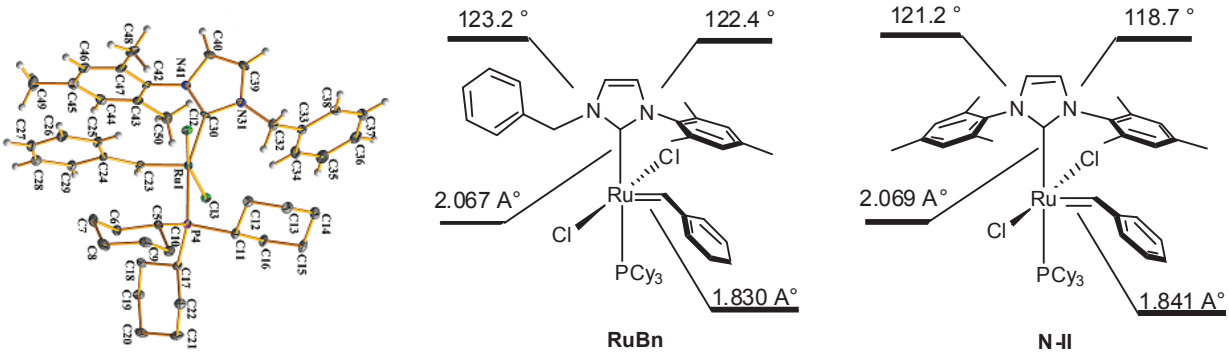

Figure 2: Selected geometrical features of Ru-NHC pre-catalysts **RuBn** and **N-II.**

The carbene unit is perpendicular to the C(30)-Ru-P plane, and the carbene aryl moiety is slightly twisted out of the Cl(2)-Ru-Cl(3)-C(23) plane with the phenyl ring of the apical benzylidene ligand and the N-mesityl substituent of the NHC are almost coplanar, clearly indicating the presence of the π-π interactions, which is also a characteristic feature of symmetrical catalysts reported earlier.[6,7]

Attempts to crytallize **RuPr, RuPr$_{Si}$** and **RuPhMs$_{Si}$** complexes are still under progress. The synthesis and the characterisation of these catalysts is described in the experimental section.

2.3. Evaluation of catalytic performances

All homogeneous catalysts were tested in RO-RCM of cyclooctene using the typical conditions developed for the heterogeneous systems, *i.e.* ratio of cyclooctene / Ru = 10,000 and ≈ 20 mM solution of cyclooctene in toluene at room temperature. Conversion and selectivities were monitored using eicosane as internal standard. Sample at 0 min was taken before the addition of catalyst and considered as the reference point. All selectivities are defined as follows:

S_i.= (number of mole of cyclooctene converted in product i) / (total number of cyclooctene converted).

The response ratio of cyclooctene and dimer with respect to eicosane (internal standard) were measured and used to monitor their concentration as a function of time during the catalytic test. For the higher cyclic oligomers (trimer, tetramer & pentamer), the concentrations were measured with respect to the internal standard assuming that the response factor of n-mers is n times the response factor of cyclooctene (use of FID detector and assuming that there is no segregation in the injector as observed for the dimer).

Oligomers bigger than pentamers have not been detected by GC with the present method.

2.3.1. Comparison of Ru-NHC complexes catalytic performances

2.3.1.1. Effect of unsymmetrical nature of NHC - unsymmetrical *vs.* symmetrical homogeneous Ru-NHC complexes

We have compared here the catalytic performances of unsymmetrical homogeneous catalysts **$RuPr_{Si}$, $RuBn_{Si}$** and **$RuPhMs_{Si}$** with respect to those of symmetrical catalysts **G-II, N-II,** in order to check the influence of the NHC unsymmetry over the selectivity in low cyclic oligomers during the RO-RCM of cyclooctene. Details for individual results can be found in the appendix section.

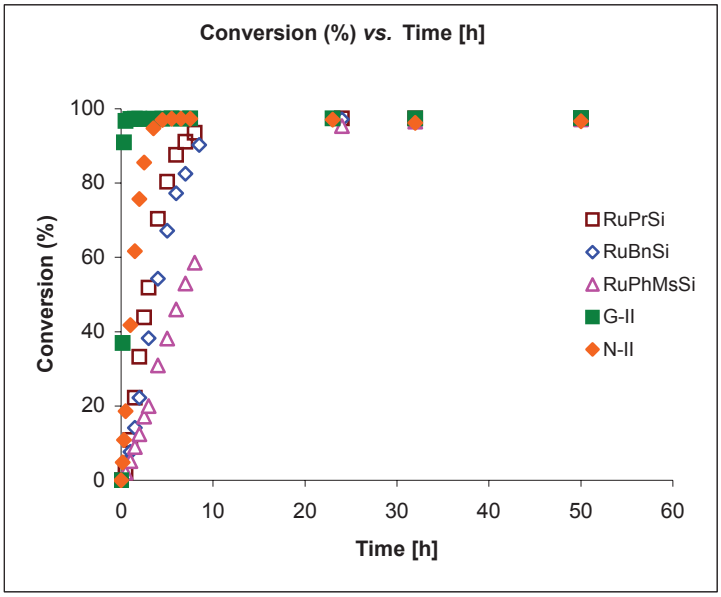

Figure 3: Conversion of cyclooctene (%) *vs.*time [h] using several Ru-NHC complexes.

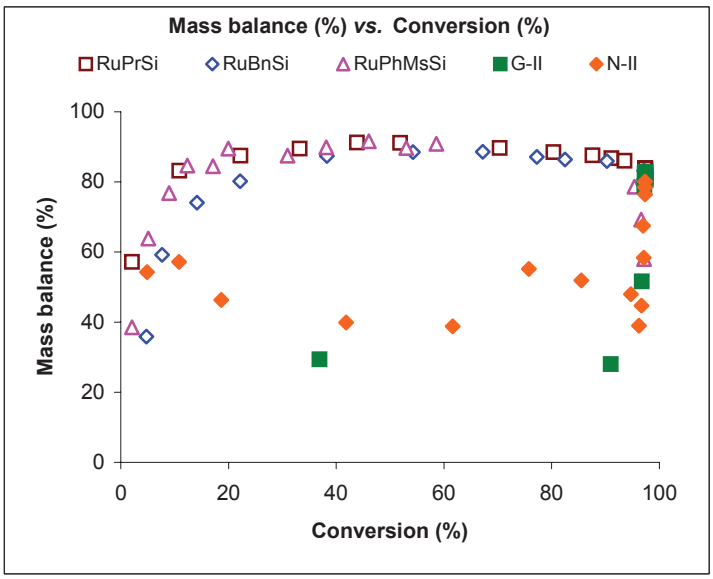

Figure 4: Mass balance (%) *vs.* conversion of cyclooctene (%) using several Ru-NHC complexes.

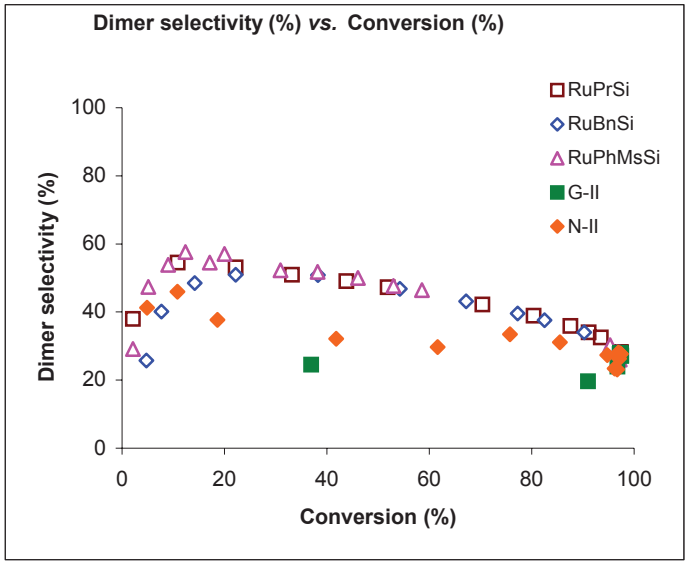

Figure 5: Dimer selectivity (%) *vs.* conversion of cyclooctene (%) using several Ru-NHC complexes.

All the catalysts showed high catalytic activities leading to full conversion of cyclooctene in 24 h (Figure 3). The symmetrical catalysts showed higher activity than the unsymmetrical catalysts, in terms of initial rates with the following order of reactivity: **G-II** (TOF 9721 h^{-1}) > **N-II** (TOF 4181 h^{-1}) > **RuPr$_{Si}$** (TOF 1090 h^{-1}) > **RuBn$_{Si}$** (TOF 570 h^{-1})> **RuPhMs$_{Si}$** (TOF 513 h^{-1}) (Figure 3, Table 1).

However, it is noteworthy that these catalysts displayed very different mass balance and product selectivities. The symmetrical catalysts (**G-II** and **N-II)** exhibit a rather low mass balance (30-40%) up to 90% conversion before a sharp increase up to 80% at high conversion (Figure 4). This is consistent with the formation of polymers (or higher oligomers) first and then their conversion into smaller oligomers *via* backbiting when cyclooctene is consumed (*i.e.* at very high conversion). In sharp contrast, the unsymmetrical catalysts led to a high mass balance reaching a constant value of 80% after 10% conversion and remained constant throughout the reaction (Figure 4). This experimental data clearly shows that the formation of smaller cyclic oligomers (up to pentamers) was favored.

Table 1: Mass balance of cyclic oligomers and their selectivity at 30-40% conversion of cyclooctene.

Catalyst	Initial rate (mol/mol Ru/h)	Selectivity (%)				Mass balance (%)
		Dimer	Trimer	Tetramer	Pentamer	
G-II	9721	25	3	1	1	29
Nolan	4181	32	5	2	1	40
RuPr$_{Si}$	1090	**51**	24	10	4	**90**
RuBn$_{Si}$	770	**51**	23	9	4	**87**
RuPhMs	513	**52**	25	10	4	**90**

In terms of selectivity, the major product was the dimer along with smaller amounts of trimer, tetramer and pentamer cyclic oligomers for all catalysts, in particular the dimer selectivity reached 50% for unsymmetrical catalysts, but only 30% for symmetrical ones (Figure 5, Table 1). It is also noteworthy that for unsymmetrical catalysts the trimer was also produced with a significant yet lower selectivity of 24%, yielding a dimer/trimer ratio of *ca.* 2:1 (Table 1). Interestingly, the selectivity of dimer decreased slowly to 28-30% from 65 to 95% conversion of cyclooctene (Figure 5). The decrease in the selectivity of dimer at higher conversion (with mass balance being constant) indicates the conversion of the dimer into higher oligomers.

In conclusion, the unsymmetrical nature of NHC is indeed a key parameter for the favoured formation of lower cyclic oligomers in RO-RCM of cyclooctene, *i.e.* backbiting is favoured over polymerisation in case of unsymmetrical catalysts but the influence of silicon atom on the selectivity need to be clarified to assess this later comment (vide supra).

These results suggest that the higher dimer selectivity observed in case of hybrid heterogeneous catalysts is not due to pore confinement effect, but it is related to the unsymmetrical nature of the NHC bonded to Ru.

2.3.1.2. Effect of the silane group on the NHC substituent – Comparison of catalytic performances of unsymmetrical homogeneous catalysts (silylated *vs.* non-siloxy silylated)

We have investigated here the effect of silane groups present on the NHC substituents by comparison of the catalytic performances of unsymmetrical homogeneous silylated catalysts **$RuPr_{Si}$, $RuBn_{Si}$** with non silylated **RuPr, RuBn.** Detail results for the individual catalysts can be found in Appendix section.

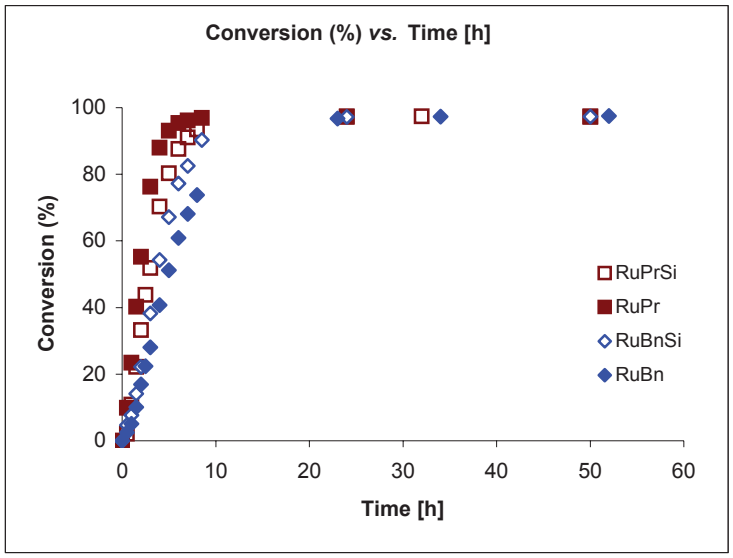

Figure 6: Comparison of conversion of cyclooctene (%) *vs.* time [h] using silylated and non-silylated Ru-NHC complexes.

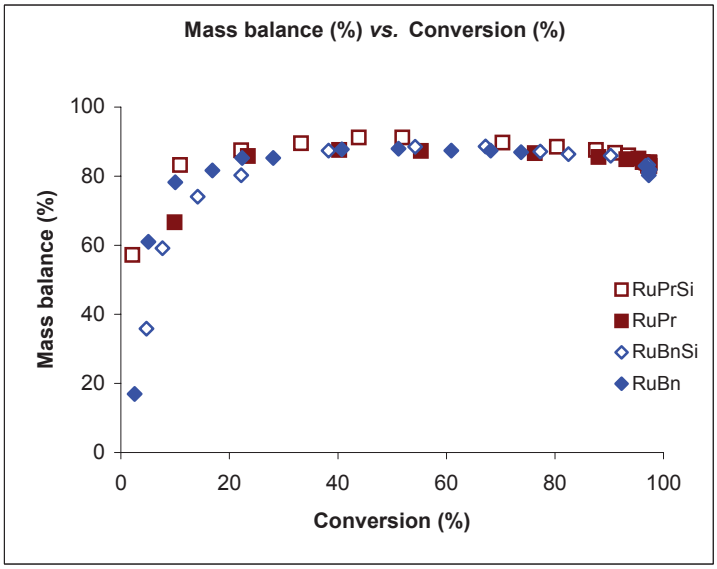

Figure 7: Comparison of mass balance (%) *vs.* conversion of cyclooctene(%) using silylated and non-silylated Ru-NHC complexes.

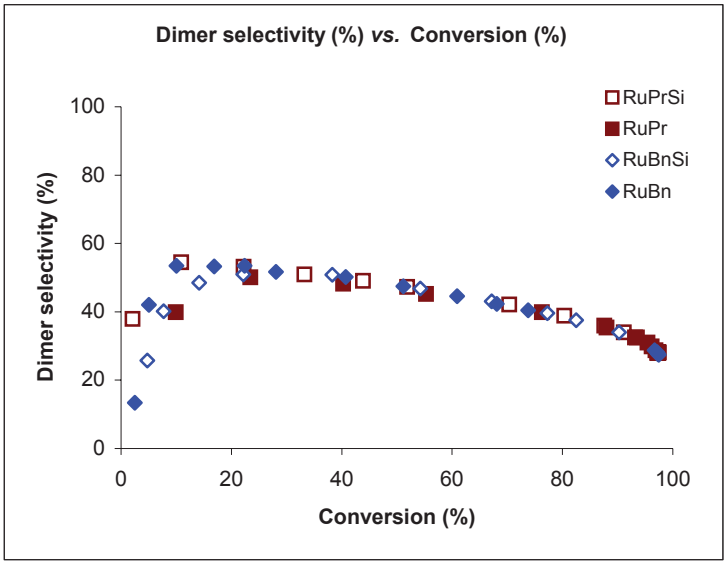

Figure 8: Comparison of dimer selectivity (%) *vs.* conversion of cyclooctene(%) using silylated and non-silylated Ru-NHC complexes.

All the catalysts showed high activity, with different initial rates and the order of reactivity was **RuPr** (TOF 2343 h^{-1}) > **$RuPr_{Si}$** (TOF 1090 h^{-1}) > **$RuBn_{Si}$** (TOF 770 h^{-1})> **RuBn** (TOF 505 h^{-1}) (Figure 6, Table 2). Note that in case of **$RuPr_{Si}$** the silane group lowered the initial rate, in contrast to that was observed for **$RuBn_{Si}$**. Such difference could be mainly due to the difference in the initiation periods of each system.

However, all the catalysts showed similar performances in term of mass balance which increased to 80% within 10-15% conversion and remained constant throughout the reaction (Figure 7). Selectivities in all products, in particular in dimer and trimer, were found to be similar (Figure 8, Table 2)

Table 2: Comparison of selectivity of cyclic products at 30-40% conversion and constant mass balance.

Catalyst	Initial rate (mol/mol Ru/h)	Selectivity (%)				Mass balance (%)
		Dimer	Trimer	Tetramer	Pentamer	
RuPr	2343	48	24	11	5	88
$RuPr_{Si}$	1090	51	24	10	4	90
RuBn	505	50	24	10	4	88
$RuBn_{Si}$	770	51	23	9	4	87

Overall, the comparison of the catalytic performances of silylated **($RuPr_{Si}$** and **$RuBn_{Si}$)** and non-silylated **(RuPr and RuBn)** catalysts indicate that there was no influence of silane group, over the selectivity of cyclic products or over the mass balance during the RO-RCM of cyclooctene, at the exception of slight modification in the initial rates. Thus, the origin of low oligomers selectivity arose exclusively from the unsymmetrical nature of the NHC ligand.

2.3.1.3. Unsymmetrical hybrid heterogeneous catalysts *vs.* unsymmetrical homogeneous homologues

The catalytic performances of both unsymmetrical heterogeneous (**M-RuPr**, **M-RuBn** and **M-RuPhMs**) and homogeneous systems (**$RuPr_{Si}$**, **$RuBn_{Si}$**, and **RuPhMs**) were compared to confirm the single site nature of Ru active sites within our heterogeneous systems and also to calibrate the intrinsic catalytic performances of our materials: are they as active as homogeneous systems?

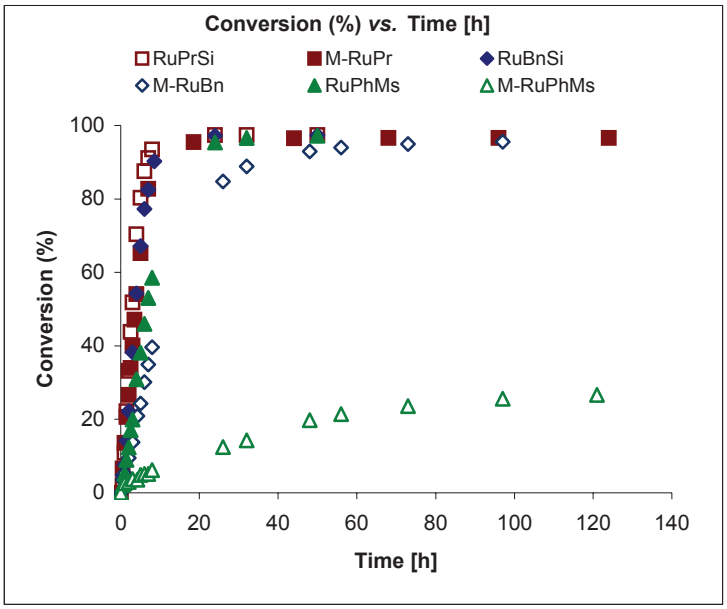

Figure 9: Conversion of cyclooctene (%) *vs.* time [h] using Ru-NHC based heterogeneous and homogeneous complexes.

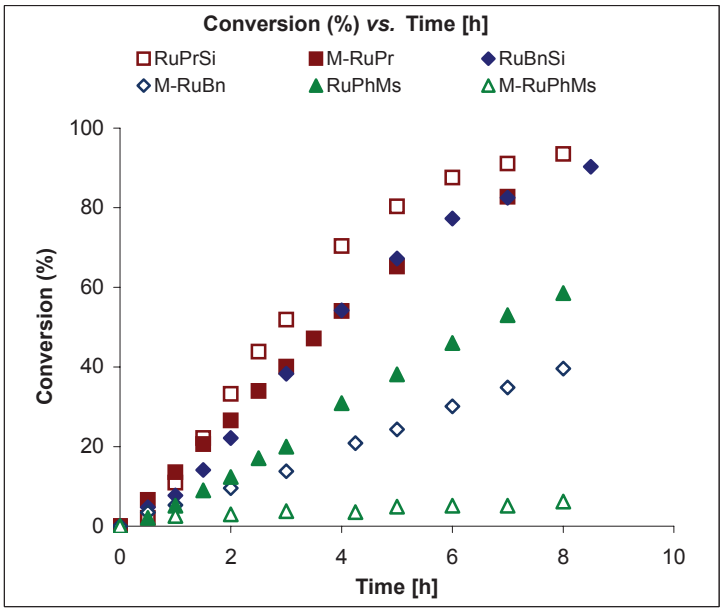

Figure 10: zoom of initial 8h for conversion of cyclooctene (%) *vs.* time [h] using Ru-NHC based heterogeneous and homogeneous complexes.

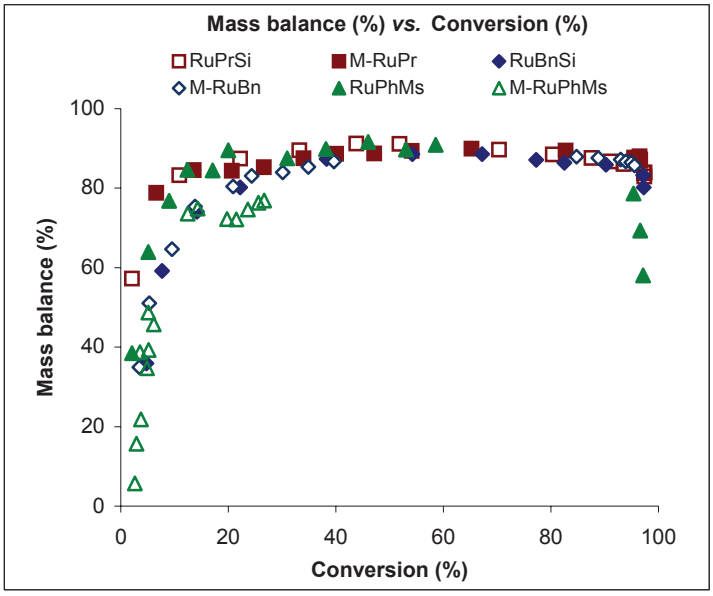

Figure 11: Mass balance (%) *vs.* conversion of cyclooctene (%) using Ru-NHC based heterogeneous and homogeneous complexes.

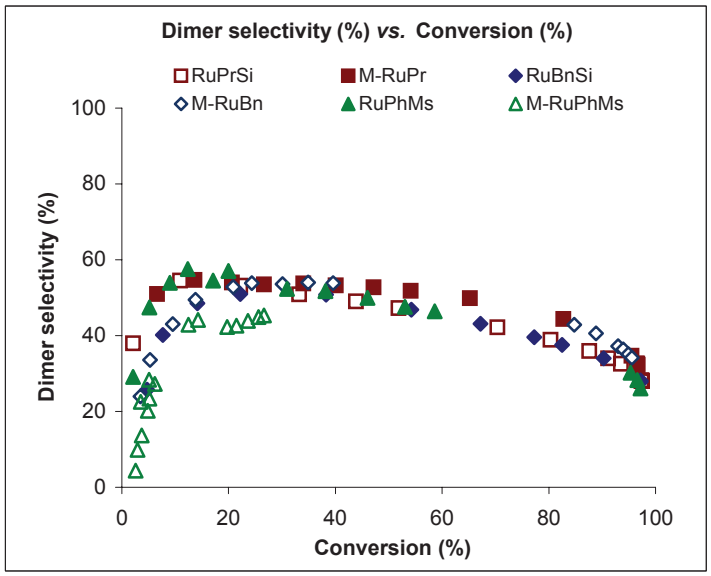

Figure 12: Dimer selectivity (%) *vs.* conversion of cyclooctene (%) using Ru-NHC based heterogeneous and homogeneous complexes.

In RO-RCM of cyclooctene, **M-RuPr** displayed almost similar rate when compared to **RuPr**. For **M-RuBn,** the observed rate is slightly lower than that of the corresponding homogeneous analogue **RuBn** (Figure 9). However, a closer look at the conversion over the first 8 h indicated the presence of a short initiation period and then a slightly higher rate of conversion for homogeneous systems compared to heterogeneous systems (Figure 10). The observation of the absence of initiation period for heterogeneous systems (**M-RuPr** and **M-RuBn**) was consistent with fact that no phosphine was coordinated in **M-RuPr** as well as in **M-RuBn**, (vide supra, Chapter 2). This lack of coordinated phosphine on Ru centre was attributed to the presence of surface functionalities ($SiOSiMe_3$) interacting with the Ru-NHC active sites. The

much lower performances of **M-RuPhMs** compared to those of **RuPhMs$_{Si}$** in terms of rate and productivity (final conversion and TON) could be attributed to the absence of surface interactions stabilizing the Ru-NHC active sites.

Interestingly, in terms of mass balance, all heterogeneous catalysts showed almost similar results to those of their homogeneous analogues (Figure 11, Table 3). The only exception was observed for **RuPhMs$_{Si}$,** for which a decrease in mass balance (from 80% to 60%) was observed at the end of the reaction (conversion between 95-97%), indicating the formation of higher oligomers and/or polymers (Figure 11). This was mainly due to the higher performances of the homogeneous system *vs.* the heterogeneous system.

In terms of dimer selectivity, the heterogeneous and homogeneous catalysts were found to be equivalent. Although, we could observe a slightly faster decrease in dimer selectivity for homogeneous systems (Figure 12), being possibly due to either the faster rate of reaction for the homogeneous systems or the adsorption-desorption problem of the dimer in heterogeneous systems, slowing down the metathesis of dimer in these systems. For trimers, tetramers and pentamers, there was an increase in the selectivity throughout the reaction for all systems.

Table 3: Mass balance of cyclic oligomers and their selectivity at 30-40% conversion of cyclooctene

Catalyst	Initial rate [mol/mol Ru/h)	Selectivity (%)				Mass balance (%)
		Dimer	Trimer	Tetramer	Pentamer	
RuPr$_{Si}$	1090	51	24	10	4	90
M-RuPr	1350	53	22	10	4	89
RuBn$_{Si}$	770	51	23	9	4	87
M-RuBn	529	54	20	8	3	85
RuPhMs	513	52	25	10	4	90
M-RuPhMs	260	45	19	8	4	76

Overall, the performances of our heterogeneous systems were found to be almost similar to those of **the** respective homogeneous analogues, in terms of dimer selectivity and mass balance (Table 3), clearly showing that active sites in both heterogeneous and homogeneous systems were equivalent if not identical, with surface providing stability to active sites of heterogeneous catalysts.

3. Proposed mechanism

Such dramatic selectivity switch due to the presence of unsymmetrical NHC ligand is reminiscent of what was reported regarding the sequence-selective copolymerization of norbornene and cyclooctene using unsymmetrical phosphine or NHC ligands.[2,3] Such chemoselectivity could be explained by the fact that the alkylidene ligand swings between two non-equivalent "positions" (two different configuration associated to two different steric environments) for each metathesis cycle, thus allowing alternating site reactivity.

This sequence selective ROMP, providing alternated cyclooctene/norbonene copolymer, originates from the catalyst architecture having dual-site configuration, which discriminates between two substrates in the same catalytic reaction (ROMP). Such mechanism can also explain here the observed selectivity towards cyclic oligomers in particular the selective formation of dimers and trimers including their ratio in the RO-RCM of a single substrate, cyclooctene, by alternatively favouring one reaction over another, Ring Opening (ROM) *vs.* Ring Closing (RCM) Metathesis (propagation *vs.* backbiting) (Scheme 2).

For illustration, Ru-NHC complexes enter the catalytic cycle by de-coordinating the phosphine ligand to generate a reactive 14-electron complex having the benzylidene unit on the *most* open configuration ($\mathbf{A_{MOST}}$). Further reaction of $\mathbf{A_{MOST}}$ with cyclooctene yields $\mathbf{B_{LESS}}$ *via* ROM with a swing of the propagating alkylidene ligand from the *most* open to the *less* open configuration. At this stage, $\mathbf{B_{LESS}}$ can regenerate $\mathbf{A_{MOST}}$ through backbiting (non-productive) or react with cyclooctene to yield $\mathbf{C_{MOST}}$ *via* ROM with the propagating chain on the *most* open configuration. With this configuration, backbiting is disfavored (steric constrains), while further reaction with cyclooctene is favored giving $\mathbf{D_{LESS}}$. Now the propagating chain is on the *less* open configuration thus favoring backbiting over tandem coordination of cyclooctene and ROM. Here backbiting can occur on the different alkene moieties along the growing chain:

1. When backbiting occurs on the alkene at the terminal position ($\mathbf{BB^3}$), trimer is formed and $\mathbf{A_{MOST}}$ is regenerated.
2. When backbiting occurs on the alkene at the intermediate position ($\mathbf{BB^2}$), dimer is formed and the intermediate $\mathbf{B_{MOST}}$ is formed with the alkylidene on the most open site.
3. When backbiting occurs on the closest alkene ($\mathbf{BB^1}$), it yields back $\mathbf{C_{MOST}}$ and cyclooctene (non-productive).

From $\mathbf{B_{MOST}}$, with the alkylidene in the open configuration, further reaction with cyclooctene leads to $\mathbf{C_{LESS}}$, for which backbiting is favored, releasing dimer and regenerating $\mathbf{A_{MOST}}$.

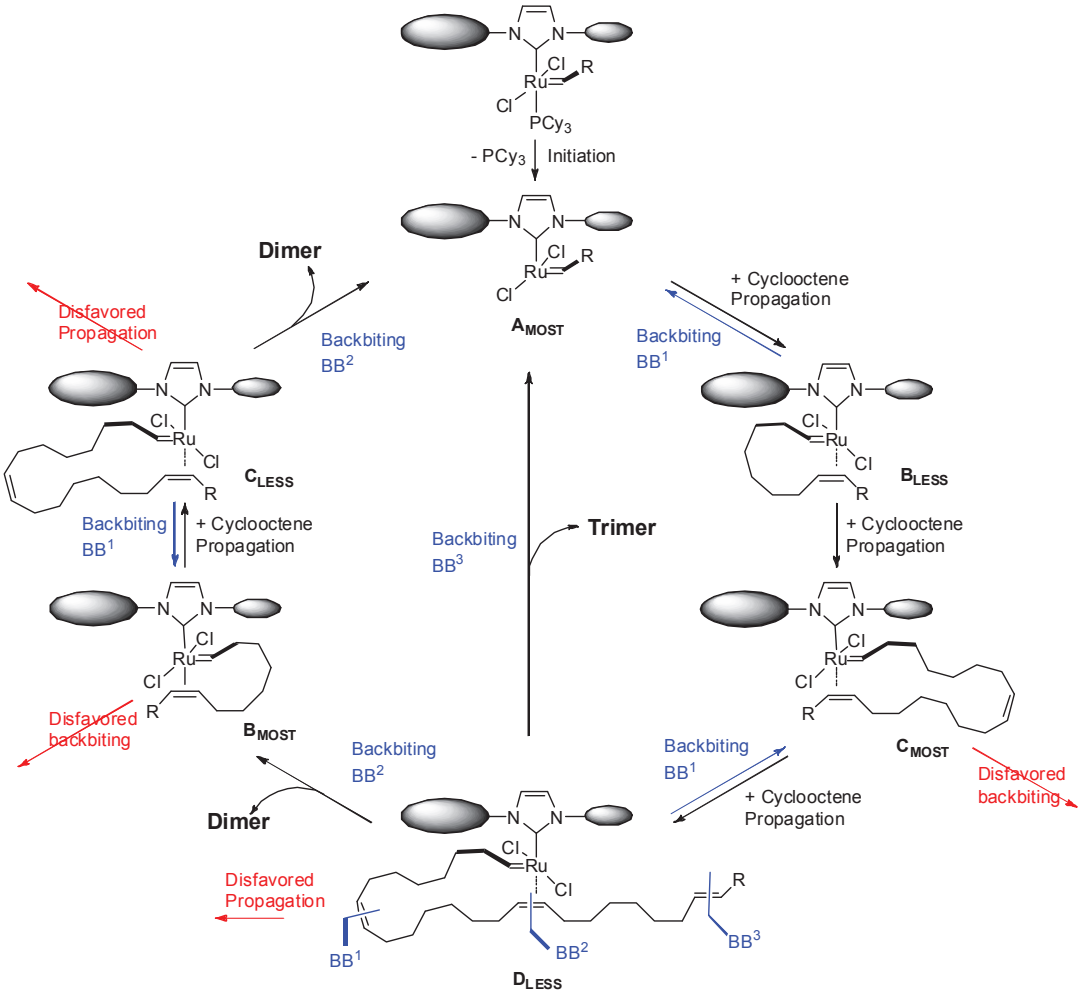

Scheme 2: Proposed mechanism for the tandem Ring Opening-Ring Closing Metathesis of *cis*-cyclooctene, selective formation of dimer and trimer. Mesityl represents the small group while Propyl or Benzyl represent the bulky group. (BB^n = backbiting, n = position of alkene from the carbene carbon).

Such proposed mechanism explains the preferred formation of dimer and trimer products including the observed 2:1 ratio (Table 4), if one considers that all backbiting reactions on remote alkenes from $\mathbf{D_{LESS}}$ are equally favored ($\mathbf{BB^2 \approx BB^3}$).

Table 4: Ratio of dimer to trimer in RO-RCM of cyclooctene using homogeneous/heterogeneous catalysts.

Catalyst	Selectivity (%)		Ratio of dimer/trimer	
	Dimer	Trimer	Experimental	Expected
RuPr	48	24	2	2
$RuPr_{Si}$	51	24	2.1	2
M-RuPr	53	22	2.4	2
RuBn	50	24	2.1	2
$RuBn_{Si}$	51	23	2.1	2
M-RuBn	54	20	2.7	2
$RuPhMs_{Si}$	52	25	2.1	2
M-RuPhMs	45	19	2.4	2
M-RuMs	34	17	2	2
M-RuHex	54	24	2.2	2

In conclusion, we have shown that Ru-alkylidene metathesis catalysts bearing unsymmetrical NHC-units provide selectively small cyclic oligomers – dimer and trimer – over polymers from cyclooctene. This is in sharp contrast with symmetrical homologues, which lead mainly to polymers. This unexpected selectivity is due to a controlled tandem RO-RCM reaction, where one configuration favors intramolecular backbiting and the other one coordination of an additional substrate (intermolecular), thus leading to RO-RCM.

4. Conclusion

- Ru-alkylidene metathesis catalysts bearing unsymmetrical NHC-units provide selectively small cyclic oligomers dimer and trimer – over polymers from cyclooctene. This is in sharp contrast with symmetrical homologues, which lead mainly to polymers.
- Silane functionalities in homogeneous systems does not have any effect on their catalytic performances in terms of dimer selectivity and mass balance. The unsymmetrical nature of NHC is thus the key for the selective formation of lower cylic oligomers over higher oligomers and/or polymers.
- There is no evidence for pore confinement or/surface effect in the mesoporous, hybrid heterogeneous catalysts over the selectivity in low cyclic oligomers.
- The active Ru-NHC sites in both heterogeneous and homogeneous systems are identical (similar performances in terms of selectivity of dimer and mass balance), with surface interactions providing stability to the active Ru-NHC sites in case of heterogeneous catalysts.
- The proposed mechanism based on the catalyst architecture having dual-site configuration is consistent with the observed selectivity towards cyclic oligomers in particular the selective formation of dimers and trimers.

5. Experimental section

5.1. Synthesis of homogeneous catalysts

5.1.1. Synthesis of RuPr

5.1.1.1. Reaction scheme

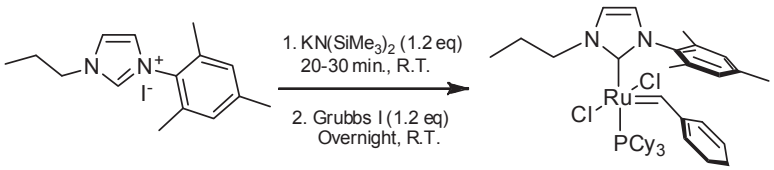

PrIm **RuPr**

5.1.1.2. Synthesis of RuPr

To a solution of 1-mesityl-3-propyl-imidazolium iodide (0.5 g, 1.4 mmol) in 5 mL of toluene, was added 2.8 mL (1.4 mmol) of a 0.5 M toluene solution of $[K(N(SiMe_3)_2]$. A white precipitate was formed after stirring for 20 min. Then a solution of $Cl_2(PCy_3)_2Ru(=CHPh)$ (0.98 g, 1.2 mmol) in 10 mL of toluene was added. The reaction mixture, was stirred for 3 h and then filtered over Celite. The solvent was removed under vacuum and the residual solid product was crystallized in toluene and pentane yielding 0.64 g of **RuPr**. ^{1}H NMR (CD_2Cl_2, 300 MHz): δ (ppm) = 19.26 (s, 1H), 7.9 (br, 1H), 7.45 (t, 1H, *J* = 7.5 Hz), 7.3 (d, 1H, *J* = 1.8 Hz), 7.16 (m, 2H), 6.88 (d, 1H, *J* =1.8Hz), 6.3 (br, 2H), 4.7 (t, 2H, *J* = 7.5 Hz), 2.4-2.2 (m, 6H), 1.96 (s, 6H), 1.94 (s, 3H), 1.66 (m, 16H), 1.17-1.39 (m, 18H), ^{31}P NMR (CD_2Cl_2, 300 MHz): δ (ppm) = 33.7 (s, 1P). ^{13}C NMR (CD_2Cl_2, 75 MHz): δ (ppm) = 187.5 (C_{NHC}=Ru, J_{P-C} = 82 Hz), 152.2 C_{ar}, 139.3 C_{ar}, 137.2 C_{ar}, 136.9 C_{ar}, 131 C_{ar}, 129.9 C_{ar}, 129.4 C_{ar}, 129.0 C_{ar}, 128.8 $C_{ar,}$ 124.4 $C_{ar,}$ 121.8 $C_{ar,}$ 53.1 (CH_2-N), 32.5 (d, J_{P-C} = *16.5 Hz, ipso*-C_{Cy}), 30.4 (*meta*-C_{Cy}), 28.7 (d, J_{P-C} = *9.75 Hz ortho*-C_{Cy}), 27.5 (*para*-C_{Cy}), 24.8 (-CH_2), 21.6 (Ar-CH_3), 18.9 (Ar-CH_3) , 12.2 (-CH_3) HRMS (ESI+): m/z 735.3150 $[M]^+$ *i.e.* calculated 735.3150.

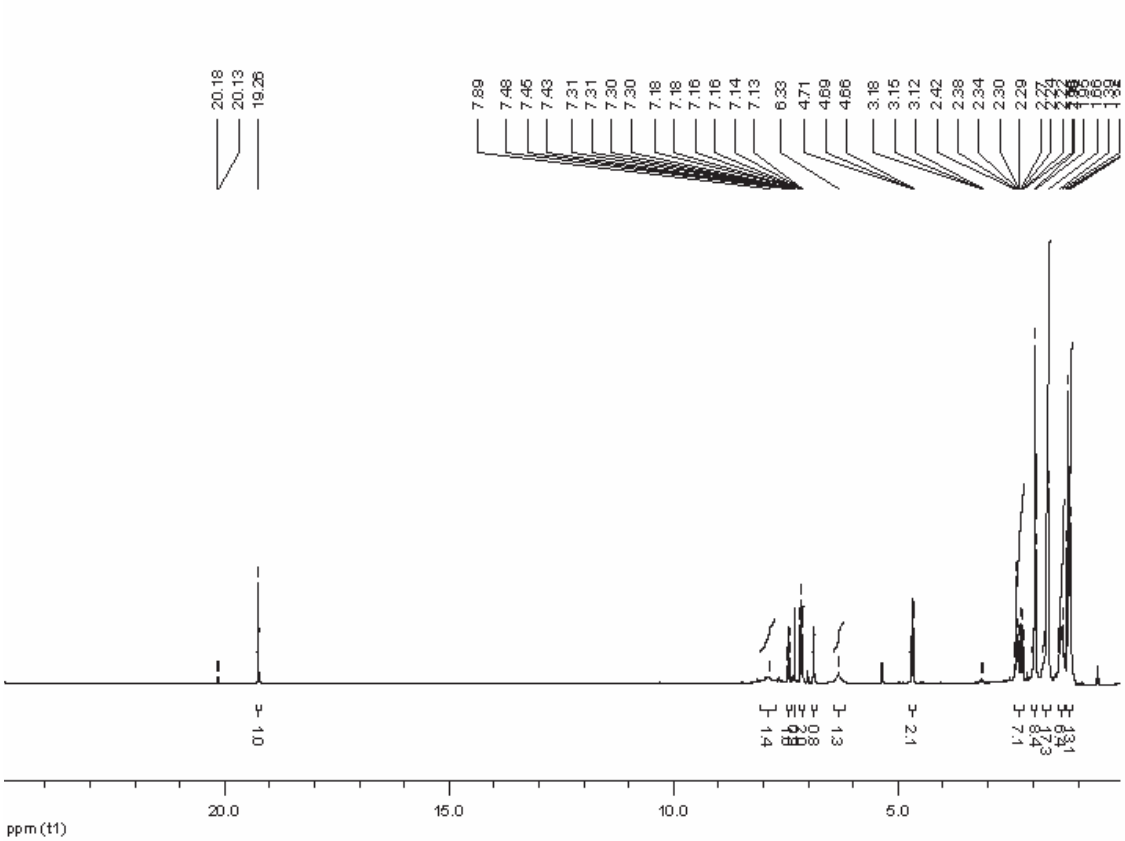

Figure 13: ^{1}H NMR of **RuPr**

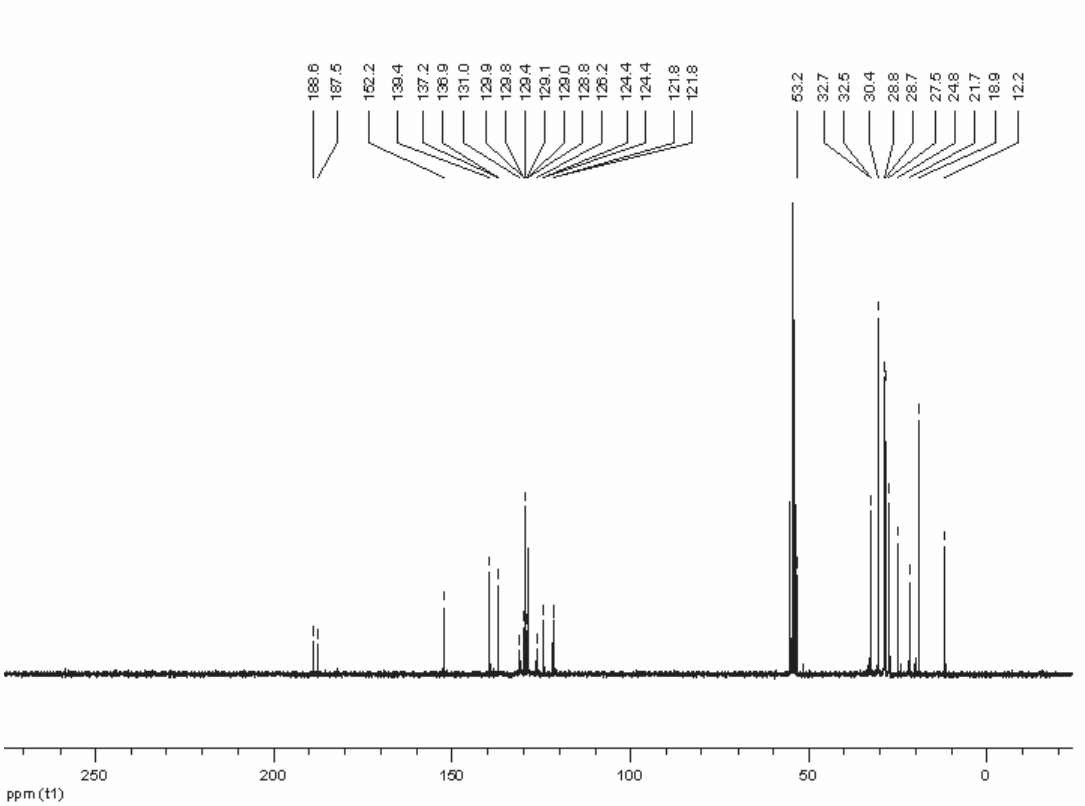

Figure14: ^{13}C NMR of **RuPr**

a) High resolution mass spectrum (ESI+) of **RuPr**

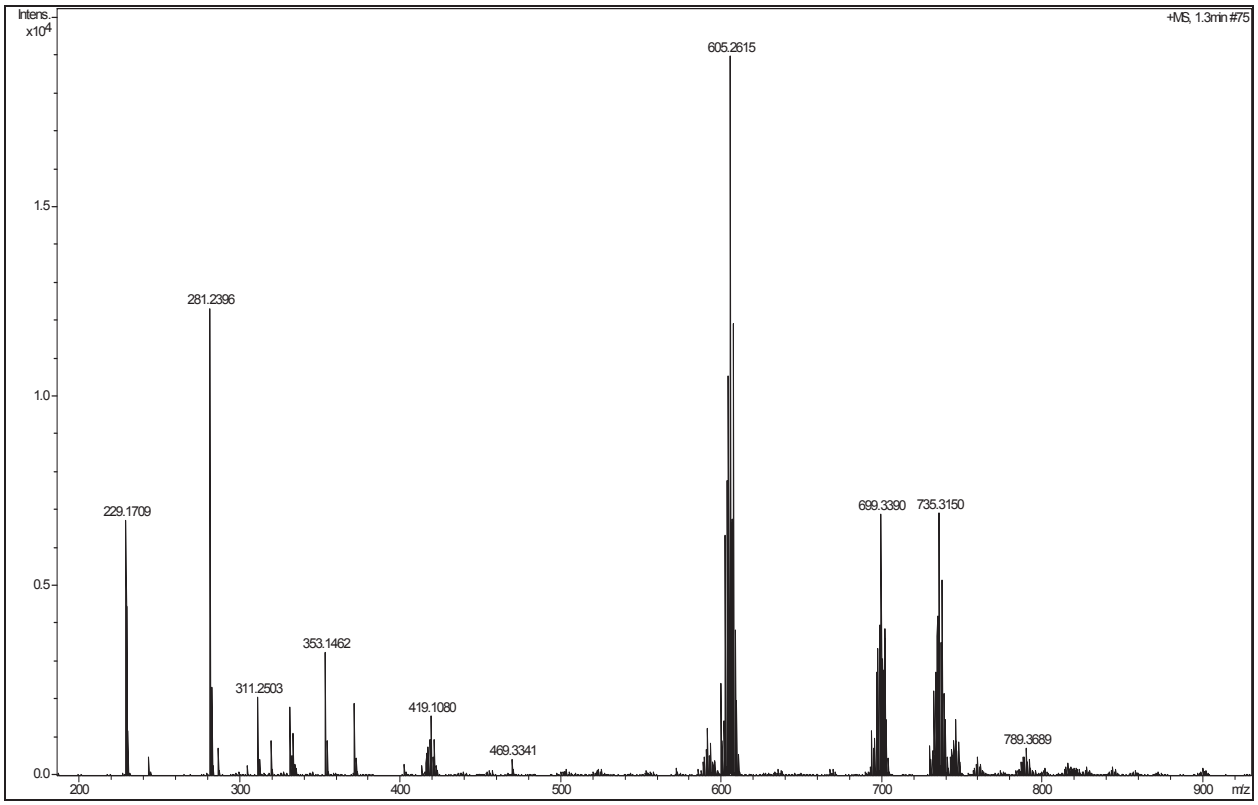

b) Experimental molecule ion spectrum

c) Simulated spectrum.

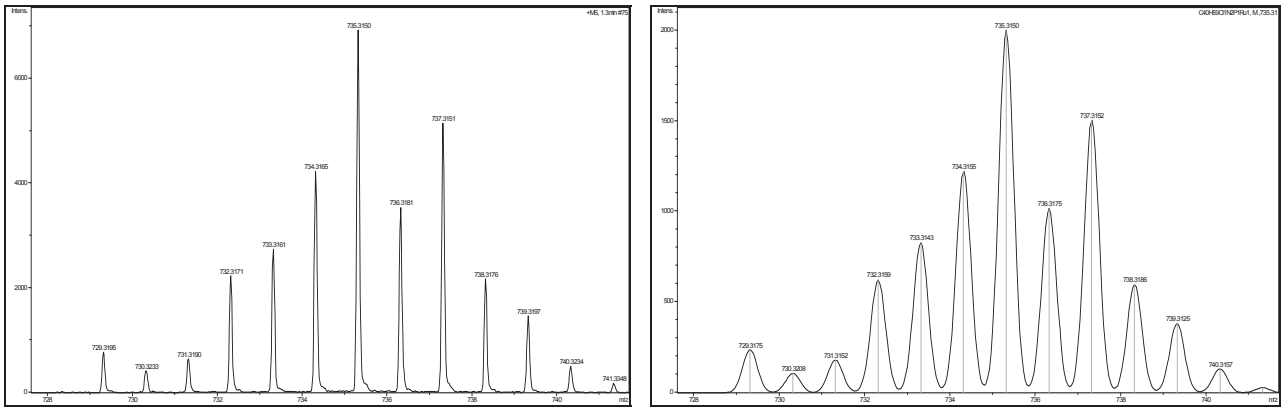

Figure 15: a) High resolution mass spectrum (ESI+) of **RuPr**. b) Experimental molecule ion spectrum. c) Simulated spectrum.

5.1.2. Synthesis of $RuPr_{Si}$

5.1.2.1. Reaction scheme

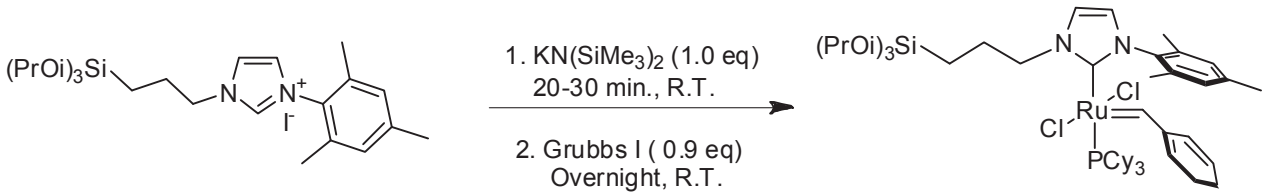

$PrIm_{Si}$ **$RuPr_{Si}$**

5.1.2.2. Synthesis

The catalysts has been synthesized previously.[10]

5.1.3. Synthesis of RuBn

5.1.3.1. Reaction scheme

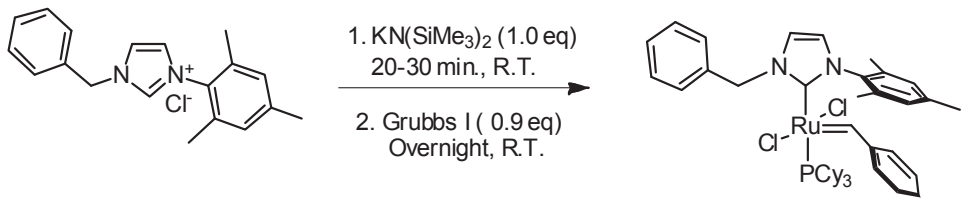

BnIm **RuBn**

5.1.3.2. Synthesis of RuBn

To 1-mesityl-3-benzyl imidazolium chloride (0.3 g, 0.96 mmol) in 5 mL of toluene, was added 1.92 mL (0.96 mmol) of a 0.5 M toluene solution of $[K(N(SiMe_3)_2]$. After stirring for 20 min, a solution of $Cl_2(PCy_3)_2Ru(=CHPh)$ (0.67 g, 0.82 mmol) in 10 mL of toluene was added. The reaction mixture was stirred for 3 h and filtered over celite. The solvent was removed under vacuum, and the residual solid product was crystallized in toluene and pentane giving 0.46 g of **RuBn**. ^1H NMR (CD_2Cl_2, 300 MHz): δ (ppm) = 19.21 (s, 1H), 7.96 (br, 1H), 7.72 (dd, 1H, *J* = 1.8 Hz), 7.47 (t, 2H, *J* = 7.5 Hz), 7.16 (t, 2H, *J* = 7.5 Hz), 6.98 (d, 1H, *J* =1.8Hz), 6.86 (d, 1H, *J* =1.8Hz), 6.37 (br, 2H), 5.9 (s, 2H), 2.4-2.2 (m, 4H), 2.0 (s, 3H), 1.98 (s, 6H), 1.62 (m, 16H), 1.11-1.36 (m, 14H), ^{31}P NMR (CD_2Cl_2, 300 MHz): δ (ppm) = 36.9 (s, 1P). ^{13}C NMR (CD_2Cl_2, 75 MHz): δ (ppm) = 187.5 (C_{NHC}=Ru, J_{P-C} = 82 Hz), 152.2 C_{ar}, 138.8 C_{ar}, 136.5 $C_{ar,}$ 136.3 C_{ar}, 135.8 C_{ar}, 130.56 C_{ar}, 129.7 C_{ar}, 129.2 C_{ar}, 129.0 C_{ar}, 128.9 C_{ar}, 128.5 $C_{ar,}$128.3 $C_{ar,}$124.4 $C_{ar,}$ 121.9 $C_{ar,}$ 55.3 (CH_2-N), 31.7 (d, J_{P-C} = *16.5 Hz, ipso*-C_{Cy}), 29.9 (*meta*-C_{Cy}), 28.07 (d, J_{P-C} = *9.8 Hz ortho*-C_{Cy}), 26.9 (*para*-C_{Cy}), 21.07 (Ar-CH_3), 18.3 (Ar-CH_3). HRMS (ESI+): m/z 783.3149 $[M-Cl]^+$ *i.e.* calculated 783.3151

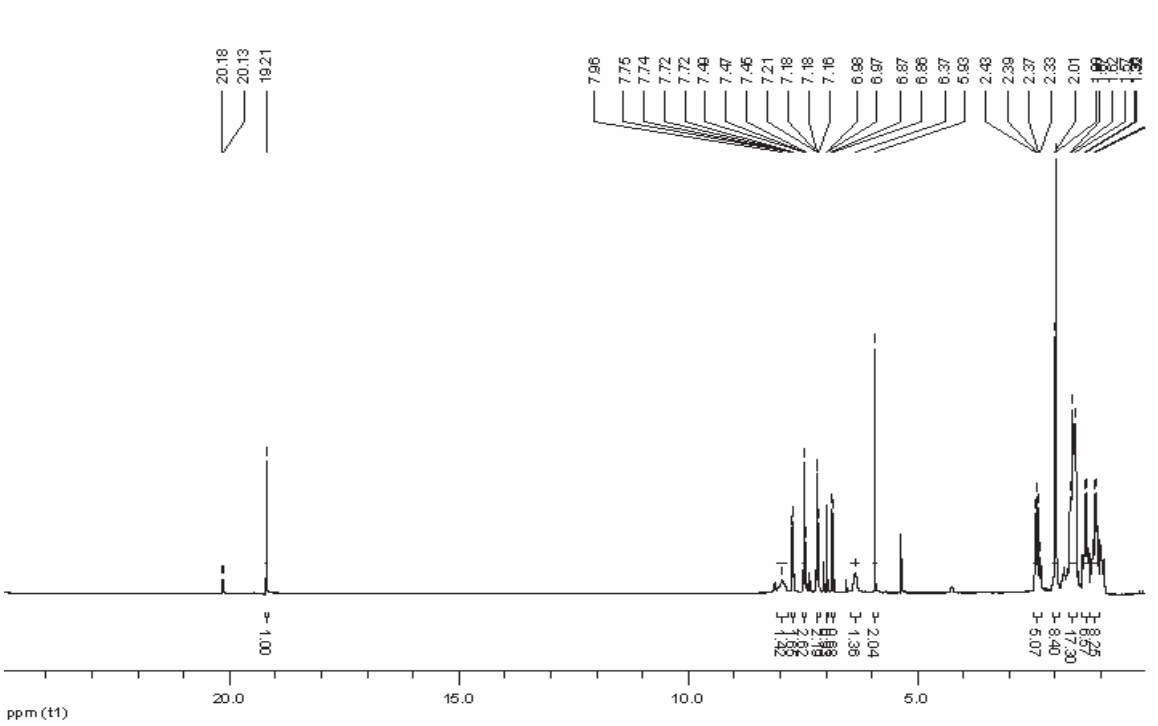

Figure 16 : ^{1}H NMR of **RuBn**

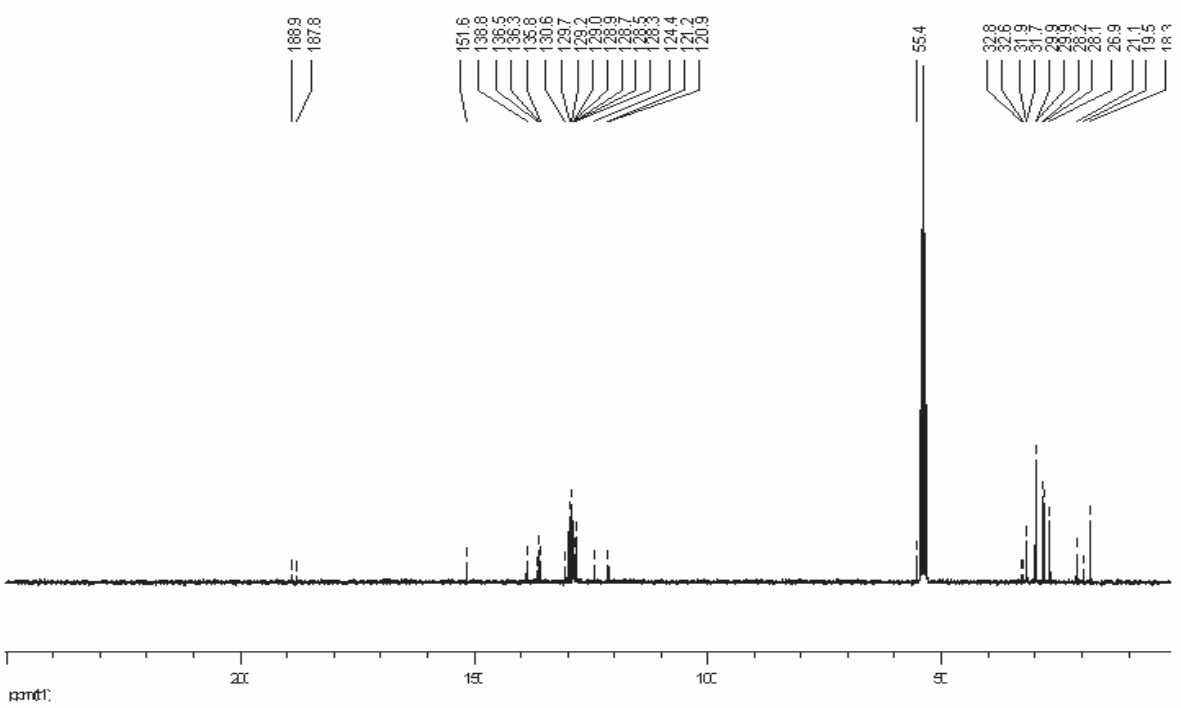

Figure 17: ^{13}C NMR of **RuBn**.

a) High resolution mass spectrum (ESI+) of **RuBn**.

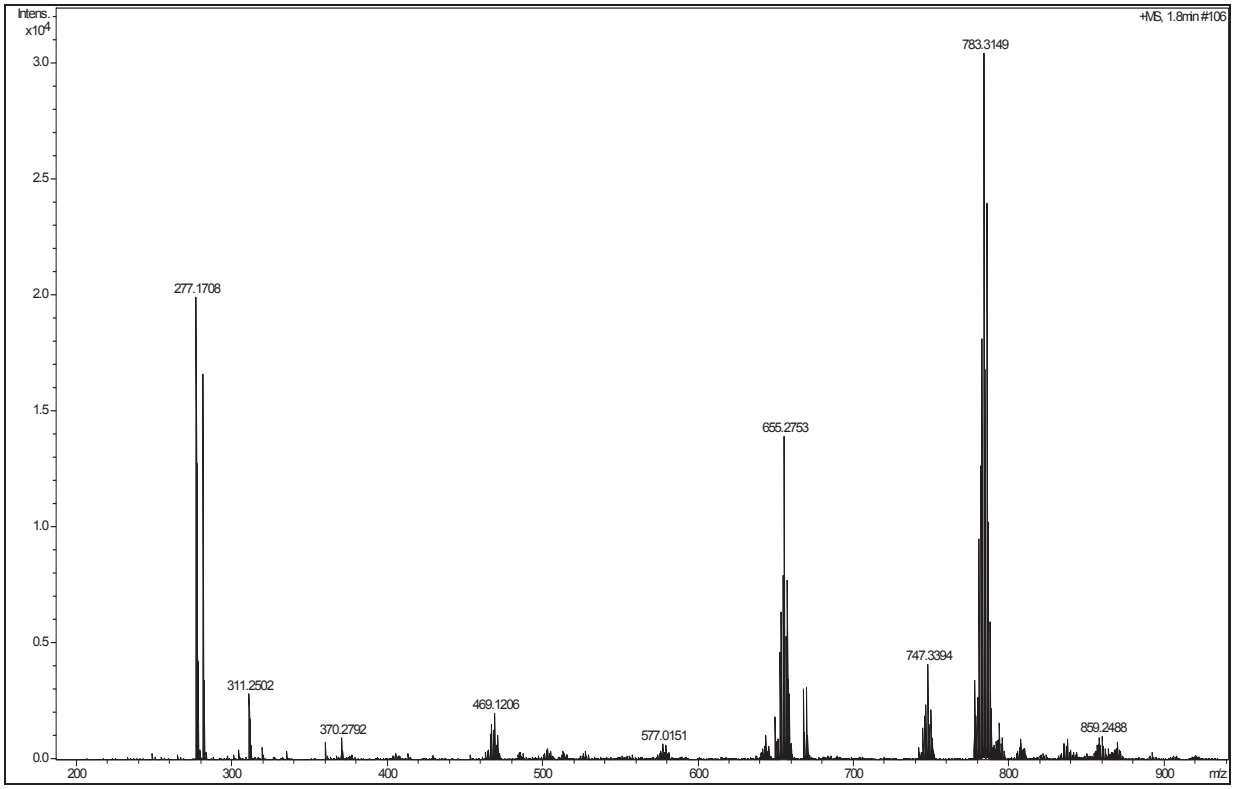

b) Experimental molecule ion spectrum

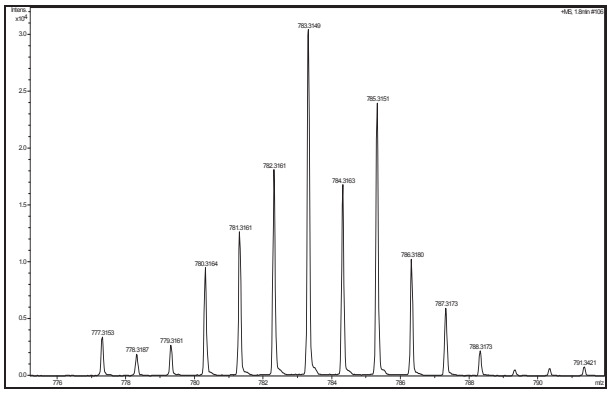

c) Simulated spectrum.

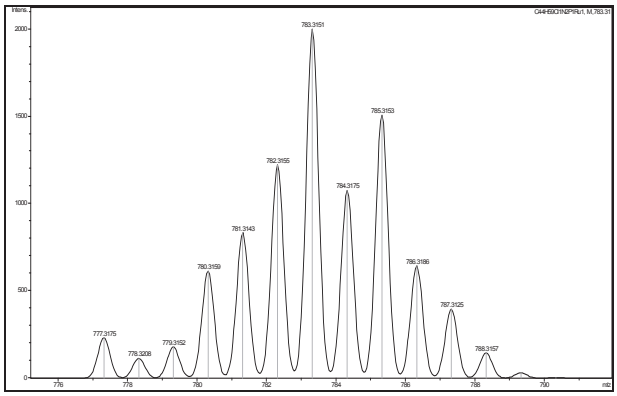

Figure 18: a) High resolution mass spectrum (ESI+) of **RuBn**. b) Experimental molecule ion spectrum. c) Simulated spectrum.

5.1.4. Synthesis of $RuBn_{Si}$

5.1.4.1. Reaction scheme

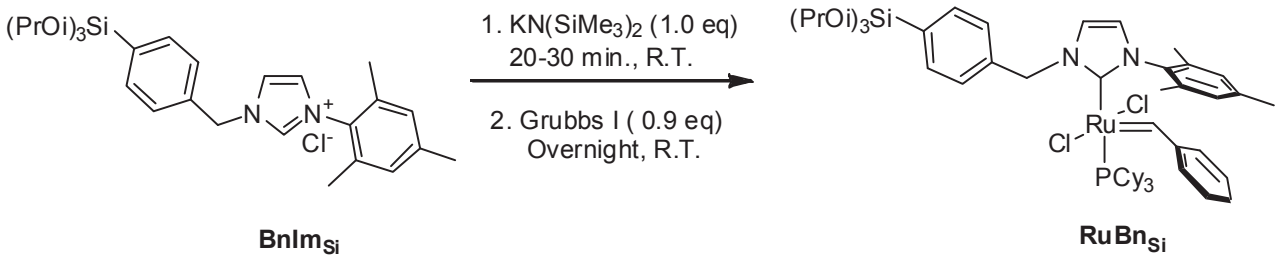

$BnIm_{Si}$ **$RuBn_{Si}$**

5.1.4.2. Synthesis

The catalysts has been synthesized previously.[10]

5.1.5. Synthesis of $RuPhMs_{Si}$

5.1.5.1. Reaction scheme

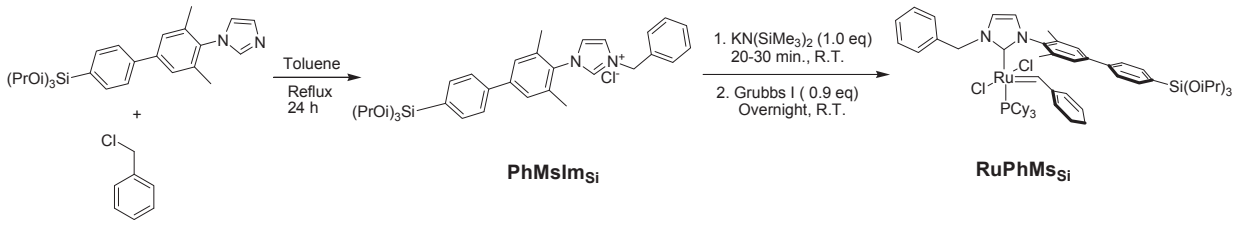

$PhMsIm_{Si}$ **$RuPhMs_{Si}$**

5.1.5.2. Synthesis of ($PhMsIm_{Si}$)

To the solution of triisopropoxysilylphenylmesityl imidazole (0.63 g) in toluene (10.0 mL) was added benzyl chloride (0.21 g, 1.2 mol eq), and the reaction mixture was heated to reflux. After stirring for 24 h the solid was filtered and washed with pentane (20.0 mL). Viscous liquid was dried at 50 °C under vaccum to afford 0.7 g of the **$PhMsIm_{Si}$**. The product was characterized by NMR. ^{1}H NMR (CD_2Cl_2, 300 MHz): δ (ppm) = 1.25 (d, J_{HH} = 6Hz, 18H, (-$CH(C\boldsymbol{H}_3)_2)_3$, 2.24 (s, 6H, -$ArCH_3$), 4.33 (m, 3H, -$C\boldsymbol{H}(CH_3)_2$), 5.97 (s, 2H, -$CH_2Ph$), 7.26 (s, 1H), 7.46-7.50 (m, 5H), 7.63-7.66 (m, 5H), 7.79 (d, J_{HH} = 9 Hz , 2H), 11.23 (s, 1H). ^{13}C NMR (CD_2Cl_2, 75 MHz): δ (ppm) = 143.7 C_{ar}, 140.7 $C_{ar,}$ 139.3 C_{ar}, 136.4 C_{ar}, 136.3 C_{ar}, 136.2 C_{ar}, 133.8 C_{ar}, 129.4 C_{ar}, 129.3 C_{ar}, 129.0 $C_{ar,}$127.9 $C_{ar,}$125.4 $C_{ar,}$ 123.1 $C_{ar,}$ 122.1 $C_{ar,}$ 65.5 (-$\boldsymbol{C}H(CH_3)_2$), 25.3 (-$CH(\boldsymbol{C}H_3)_2$)17.8 (Ar-CH_3).

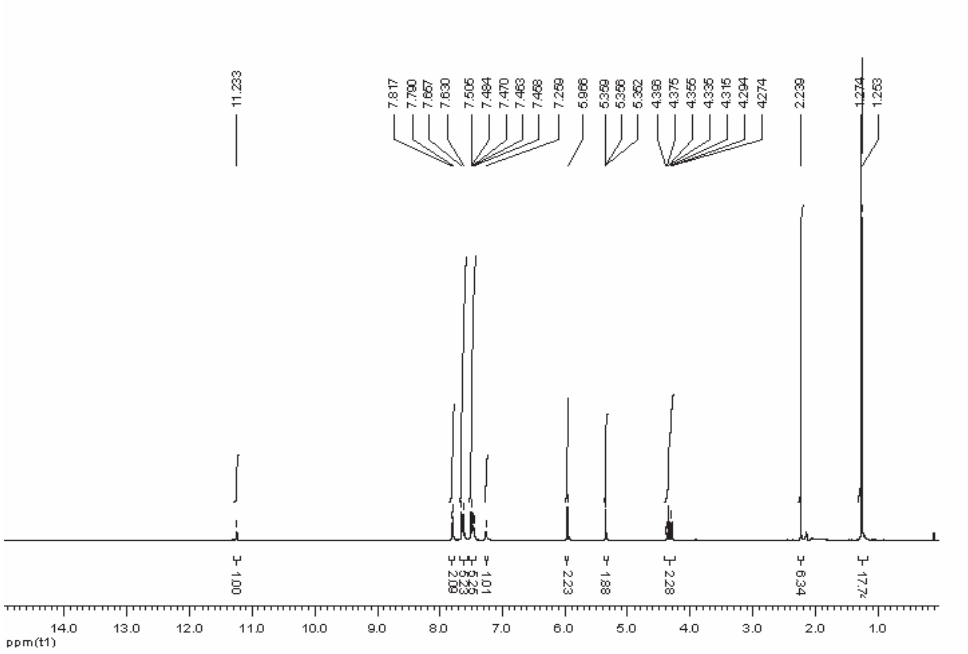

Figure 19: ^{1}H NMR of **PhMsIm$_{Si}$**.

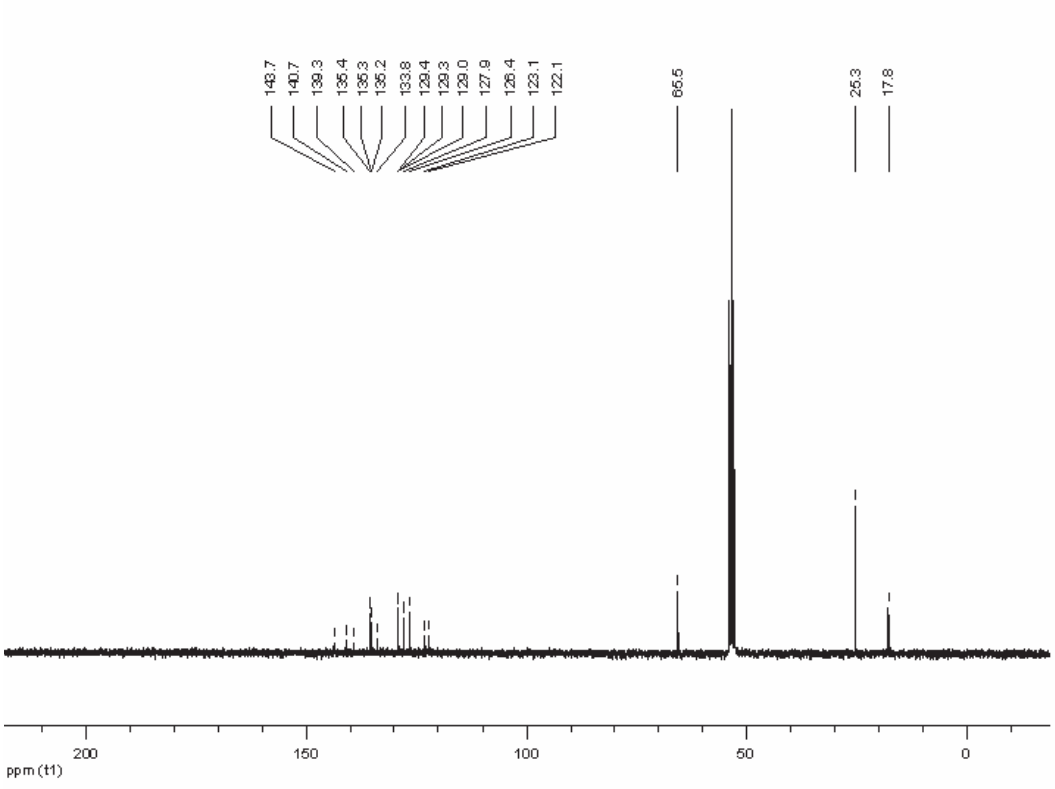

Figure 20: ^{13}C NMR of **PhMsIm**.

5.1.5.3. Synthesis of $RuPhMs_{Si}$

To 1- triisopropoxysilylphenylmesityl -3-benzyl imidazolium chloride (0.35 g, 0.60 mmol) in 5 mL of toluene, was added 1.45 mL (0.72 mmol) of a 0.5 M toluene solution of $[K(N(SiMe_3)_2]$. After stirring for 20 min, a solution of $Cl_2(PCy_3)_2Ru(=CHPh)$ (0.55, 0.66 mmol) in 10 mL of toluene was added. The reaction mixture was stirred for 3 h and filtered over celite. The solvent was removed under vacuum, and the residual solid product was crystallized in toluene and pentane giving 0.16 g of **$RuPhMs_{Si}$**. ^1H NMR (CD_2Cl_2, 300 MHz): δ (ppm) = 19.2 (s, 1H), 7.93 (br, 1H), 7.37 –7.47 (m,5H), 7.25 (t, 1H, *J* = 7.5 Hz), 6.88 – 6.99 (m, 5H), 6.85 (br, 2H), 5.9 (s, 2H), 4.32 (m, 1H, -*CH(*$CH_3)_2$) 2.4-2.3 (m, 4H), 2.0 (s, 6H), 1.64-1.53 (m, 18H), 1.24 (d, 18H, *J* = 6Hz) 1.11-0.9 (m, 14H), ^{31}P NMR (CD_2Cl_2, 300 MHz): δ (ppm) = 36.4 (s, 1P). ^{13}C NMR (CD_2Cl_2, 75 MHz): δ (ppm) = 163.2 (C_{NHC}=Ru, J_{P-C} = 75 Hz), 151.4 C_{ar}, 141.5 C_{ar}, 140.9 $C_{ar,}$ 138.1 C_{ar}, 136.9 C_{ar}, 135.3 C_{ar}, 135.0 C_{ar}, 131.8 C_{ar}, 129.9 C_{ar}, 129.4 C_{ar}, 128.8 $C_{ar,}$128.6 $C_{ar,}$128.2.4 $C_{ar,}$ 126.3 $C_{ar,}$ 123.8 $C_{ar,}$121.1 $C_{ar,}$ 121.0 $C_{ar,}$ 65.5 (-***C****H(*$CH_3)_2$), 55.1 (-NCH_2Ph), 31.4 (d, J_{P-C} = *16.5 Hz, ipso*-C_{Cy}), 29.5 (*meta*-C_{Cy}), 27.7 (d, J_{P-C} = *9.8 Hz ortho*-C_{Cy}), 26.5 (*para*-C_{Cy}), 25.3 (-C*H(****C****H*$_3)_2$)18.3 (Ar-CH_3). HRMS (ESI+)**:** m/z 1049.4478 $[M-Cl]^+$ *i.e.* calculated 1049.4493.

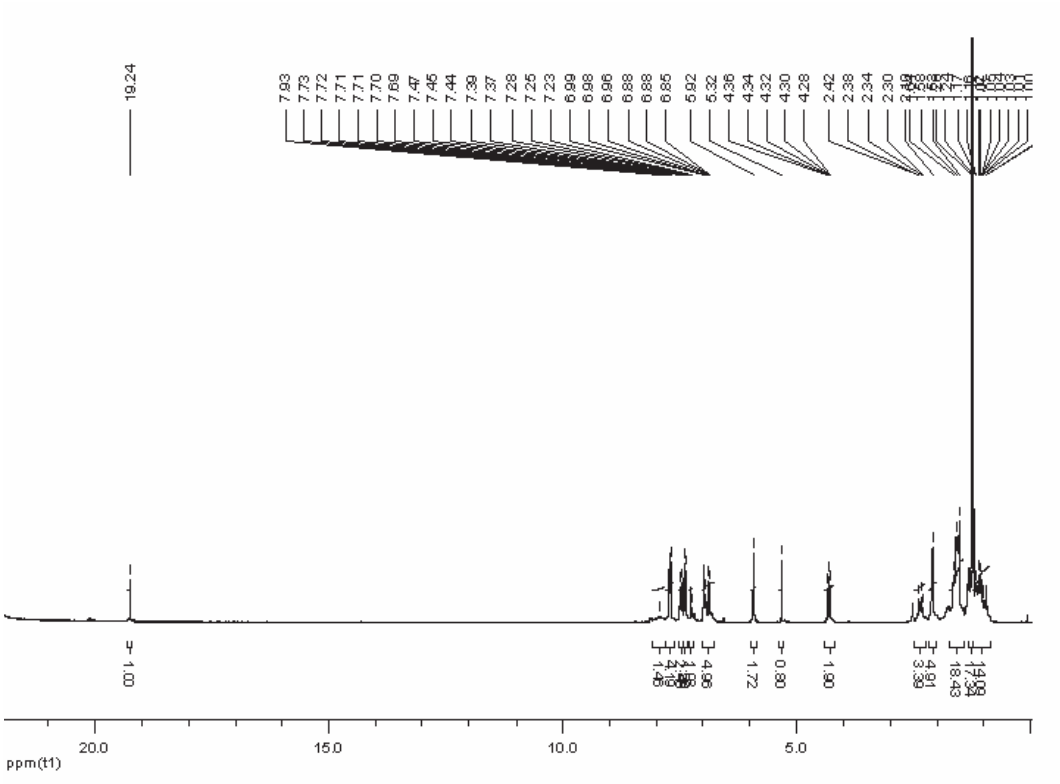

Figure 21: ^1H NMR of **$RuPhMs_{Si}$**.

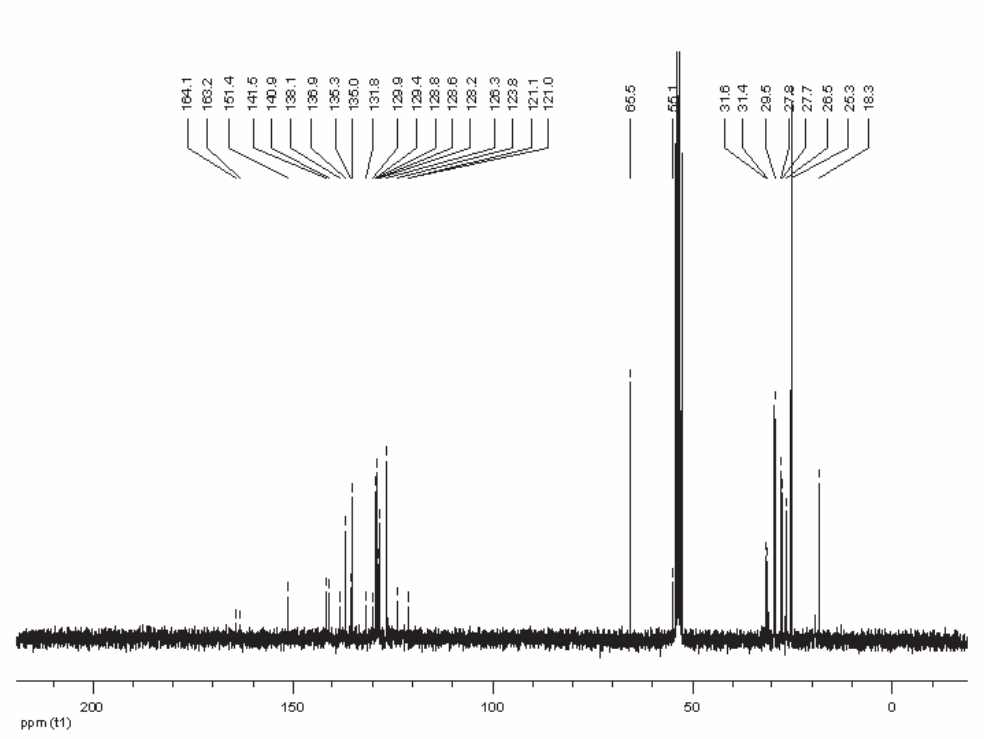

Figure 22: ^{13}C NMR of **RuPhMs$_{Si}$**.

a) High resolution mass spectrum (ESI+) of **RuPhMs$_{Si}$**

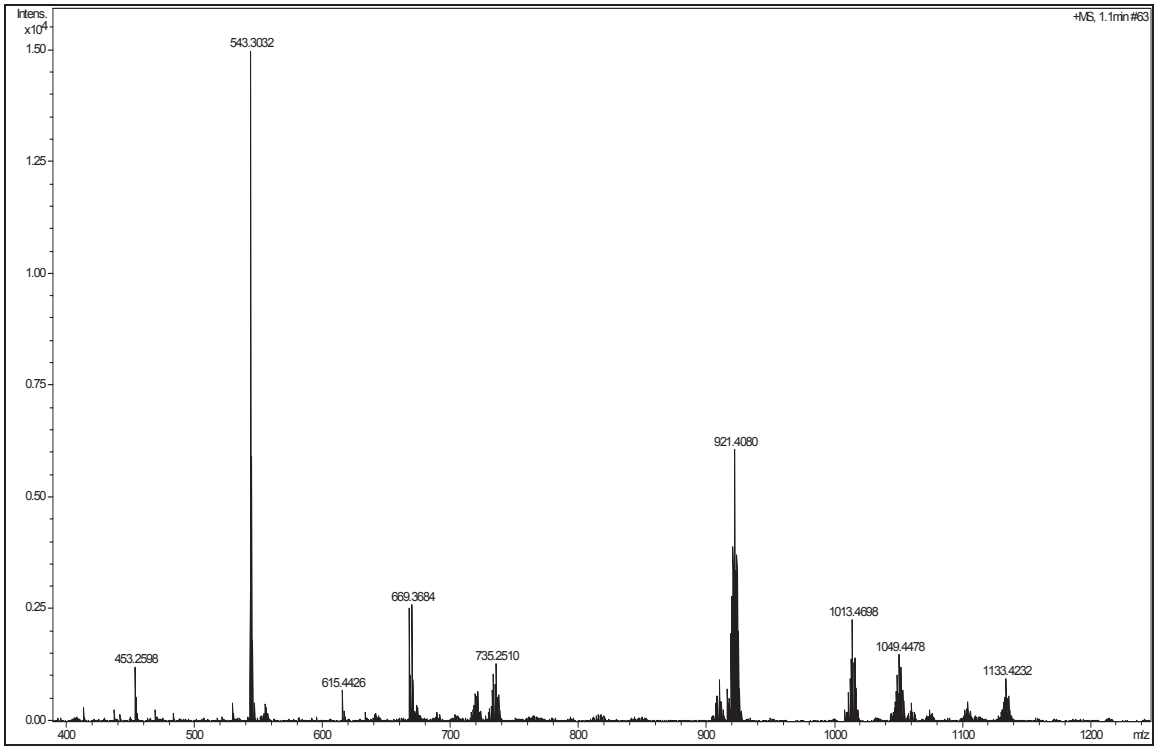

b) Experimental molecule ion spectrum c) Simulated spectrum.

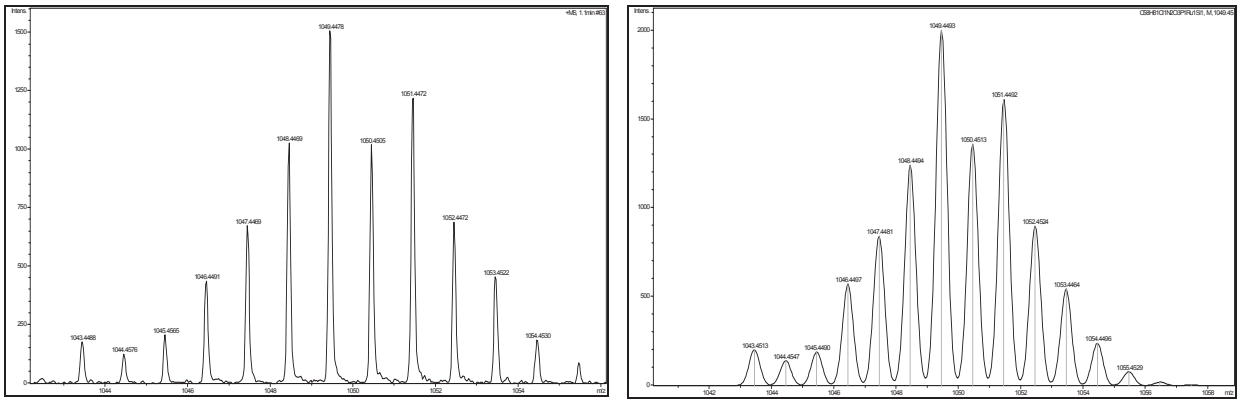

Figure 23: a) High resolution mass spectrum (ESI+) of **RuPhMs$_{Si}$** b) Experimental molecule ion spectrum. c) Simulated spectrum.

5.2. Catalytic performances

All metathesis experiments were carried out under an inert atmosphere, in a glove-box. Toluene was dried over NaK and distilled under nitrogen prior to use. Cyclooctene (*cis*-cyclooctene) was purchased from Aldrich, distilled over Na prior to use. Catalysts Grubbs second generation catalyst was purchased from Aldrich and Nolan catalyst was synthesized according to the literature procedures.

Cyclooctene metathesis experiments with homogeneous Ru-complexes

(*Ratio Cyclooctene/ Ru of ca. 10,000)*

Representative procedure for homogeneous catalysts: Eicosane was dissolved in ~20 mM toluene solution of cyclooctene. Sample was taken for GC analysis as a reference. Homogeneous Ru-catalyst was dissolved in toluene so as to obtain the initial stock solution. An aliquot of this stock solution was added to the aforementioned solution of cyclooctene, at room temperature. The progress of the metathesis reaction was monitored by sampling at suitable intervals. The samples were immediately quenched by an excess of ethyl acetate. The samples were analysed by GC with a HP5 column.

6. Appendix

6.1. $RuPr_{Si}$

Table 5: Catalytic performances of **$RuPr_{Si}$** in the RO-RCM of cyclooctene.

Time [h]	Conversion (%)	TON	Sel-dimer (%)	Sel-trimer (%)	Sel-tetra (%)	Sel-penta (%)	Mass balance (%)
0.5	2.1	211	**38**	13	6	0	57
1.0	10.9	1089	**54**	19	7	3	83
1.5	22.2	2221	**53**	22	9	4	87
2.0	33.2	3322	**51**	24	10	4	90
2.5	43.8	4383	**49**	25	12	5	91
3.0	51.9	5185	**47**	26	12	5	91
4.0	70.4	7035	**42**	27	14	6	90
5.0	80.3	8035	**39**	28	14	7	88
6.0	87.6	8756	**36**	29	15	7	88
7.0	91.1	9111	**34**	30	15	8	87
8.0	93.5	9350	**33**	30	16	8	86
24.0	97.4	9741	**28**	31	17	8	84
32.0	97.4	9741	**28**	31	16	8	83
50.0	97.4	9739	**28**	31	17	8	84

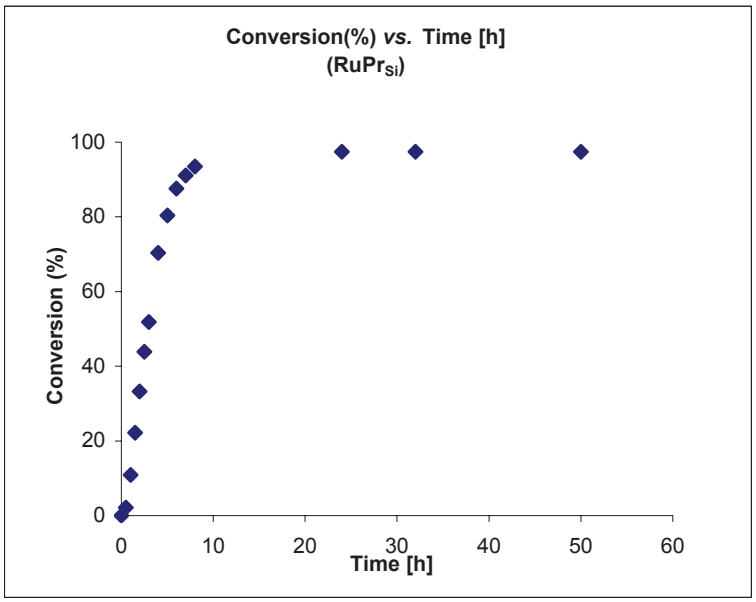

Figure 24: Conversion of cyclooctene (%) *vs.* time [h] using **$RuPr_{Si}$**.

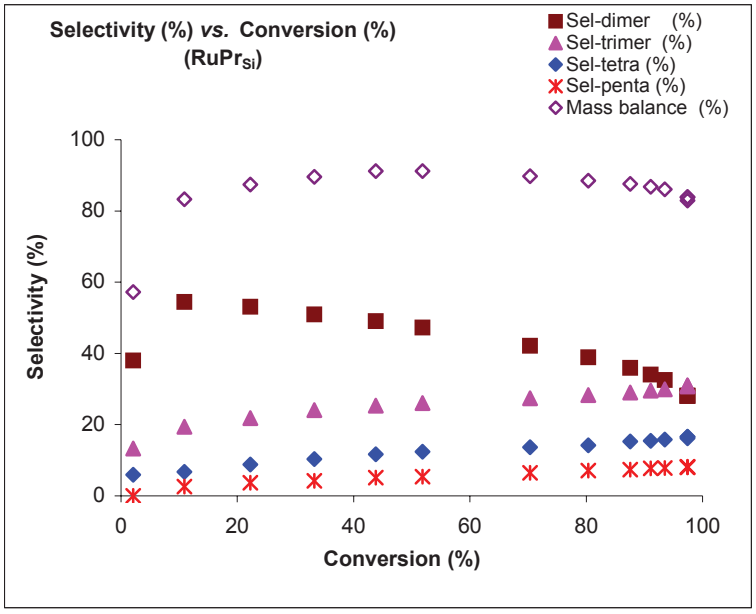

Figure 25: selectivity of cyclic oligomers (%) *vs.* Conversion of cyclooctene (%) using **RuPr$_{Si}$**.

6.2. $RuBn_{Si}$

Table 6: Catalytic performance of **$RuBn_{Si}$** in the RO-RCM of cyclooctene.

Time [h]	Conversion (%)	TON	Sel-dimer (%)	Sel-trimer (%)	Sel-tetra (%)	Sel-penta (%)	Mass balance (%)
0.5	4.7	475	**26**	8	2	0	36
1.0	7.7	769	**40**	13	4	2	59
1.5	14.2	1417	**49**	18	6	2	74
2.0	22.2	2218	**51**	20	7	3	80
3.0	38.3	3828	**51**	23	9	4	87
4.0	54.2	5425	**47**	25	11	5	89
5.0	67.2	6719	**43**	27	12	6	89
6.0	77.3	7726	**40**	28	13	7	87
7.0	82.5	8248	**38**	28	14	7	86
8.5	90.3	9027	**34**	29	15	8	86
24.0	97.2	9717	**28**	30	16	9	83
50.0	97.3	9727	**28**	30	15	8	80

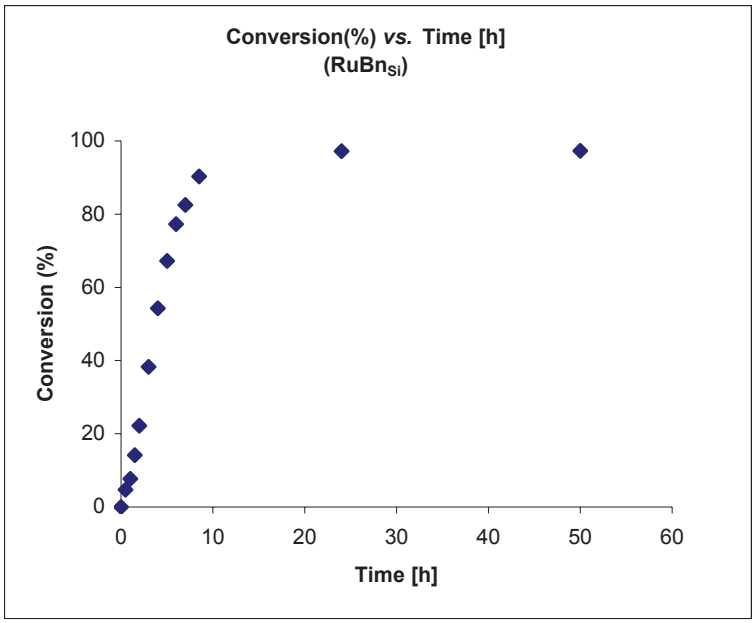

Figure 26: Conversion of cyclooctene (%) *vs.* time [h] using **$RuBn_{Si}$**

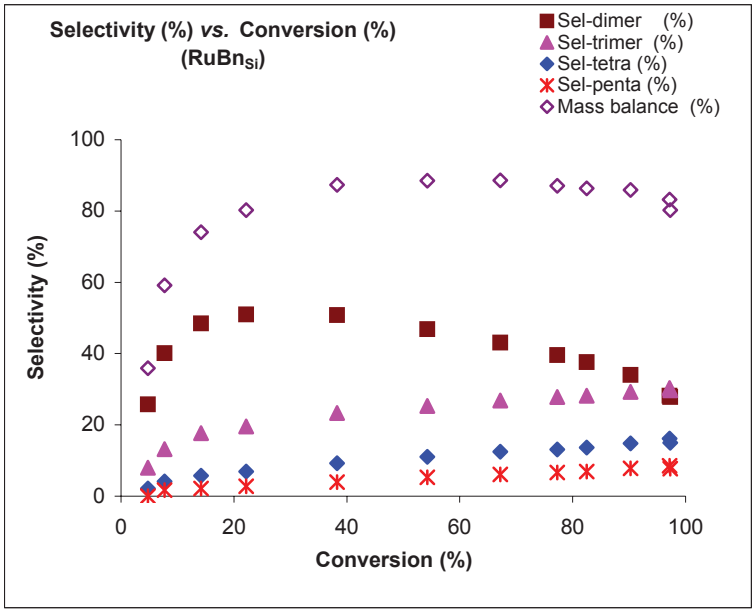

Figure 27: selectivity of cyclic oligomers (%) *vs.* Conversion of cyclooctene (%) using **RuBn$_{Si}$**.

6.3. $RuPhMs_{Si}$

Table 7: Catalytic performance of **$RuPhMs_{Si}$** in the RO-RCM of cyclooctene.

Time [h]	Conversion (%)	TON	Sel-dimer (%)	Sel-trimer (%)	Sel-tetra (%)	Sel-penta (%)	Mass balance (%)
0.5	2.1	211	**29**	8	2	0	39
1.0	5.1	513	**47**	13	4	0	64
1.5	9.0	898	**54**	16	4	2	77
2.0	12.4	1237	**58**	19	6	2	85
2.5	17.1	1711	**55**	21	7	3	84
3.0	20.0	1998	**57**	22	8	3	90
4.0	30.9	3093	**52**	23	9	3	88
5.0	38.2	3816	**52**	25	10	4	90
6.0	46.0	4603	**50**	26	11	5	92
7.0	53.0	5301	**48**	26	11	5	90
8.0	58.6	5858	**46**	27	12	5	91
24.0	95.3	9534	**30**	28	14	6	79
32.0	96.6	9659	**28**	25	11	5	69
50.0	97.2	9717	**26**	20	8	3	58

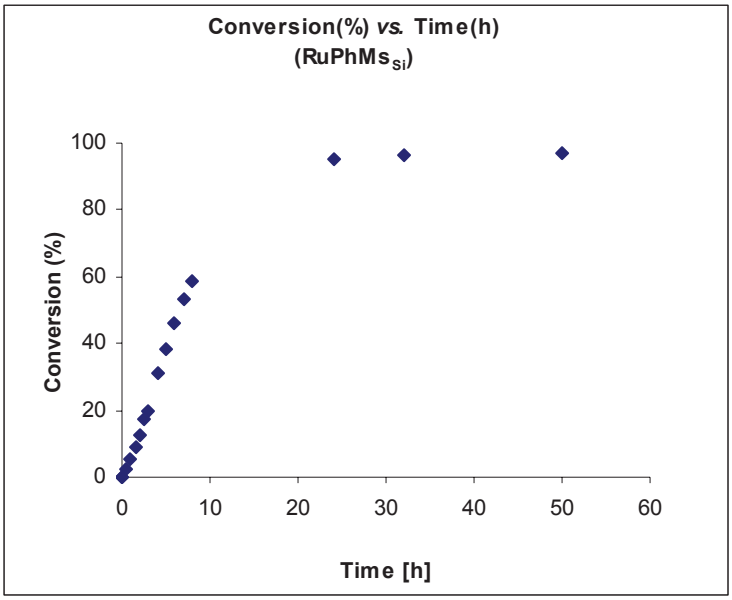

Figure 28: Conversion of cyclooctene (%) *vs.* time [h] using **$RuPhMs_{Si}$**.

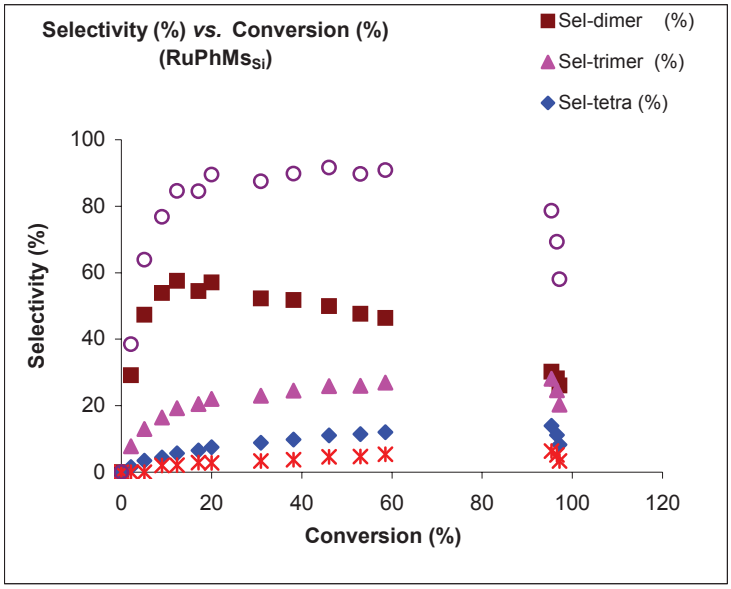

Figure 29: selectivity of cyclic oligomers (%) *vs.* Conversion of cyclooctene (%) using **RuPhMs$_{Si}$**

6.4. G-II

Table 8: Catalytic performance of **G-II** in the RO-RCM of cyclooctene.

Time [h]	Conversion (%)	TON	Sel-dimer (%)	Sel-trimer (%)	Sel-tetra (%)	Sel-penta (%)	Mass balance (%)
0.2	36.9	3692	**25**	3	1	1	29
0.3	91.0	9099	**20**	5	2	1	28
0.5	96.7	9675	**24**	17	7	3	52
1.0	97.2	9721	**28**	29	15	8	79
1.5	97.3	9730	**28**	30	16	8	82
2.0	97.3	9731	**28**	30	16	8	83
2.5	97.3	9729	**28**	30	16	8	82
3.5	97.3	9733	**28**	30	16	8	82
4.5	97.4	9737	**28**	30	16	8	83
5.5	97.4	9738	**28**	30	16	8	82
6.5	97.3	9734	**28**	30	16	8	82
7.5	97.4	9740	**28**	30	16	8	82
23.0	97.5	9745	**27**	30	16	8	81
32.0	97.4	9745	**27**	30	16	8	81
50.0	97.5	9747	**27**	30	16	8	81

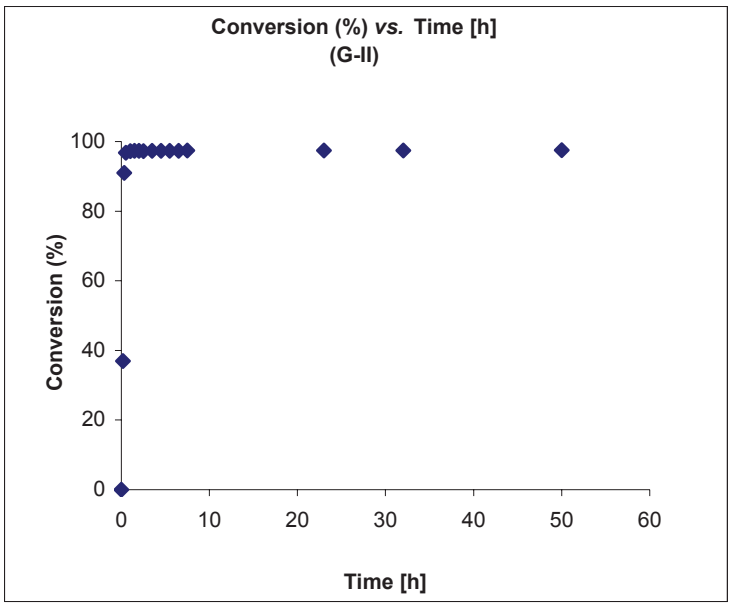

Figure 30: Conversion of cyclooctene (%) *vs.* time [h] using **G-II**.

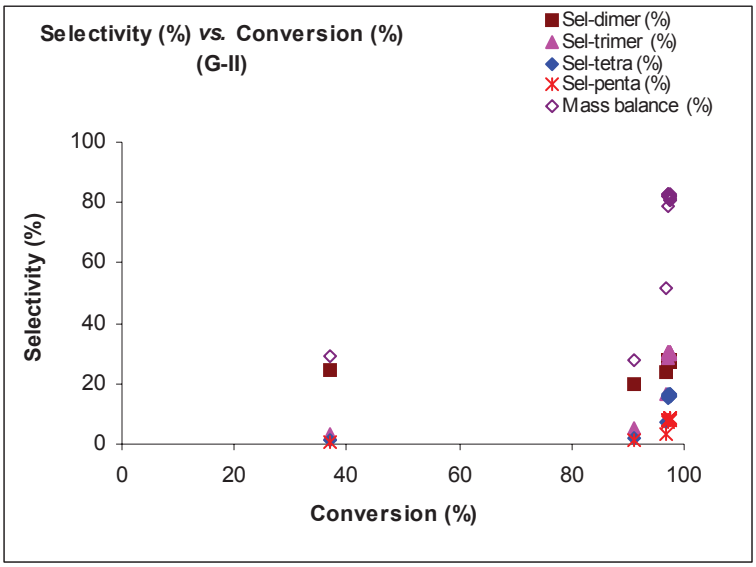

Figure 31: selectivity of cyclic oligomers (%) *vs.* Conversion of cyclooctene (%) using **G-II**.

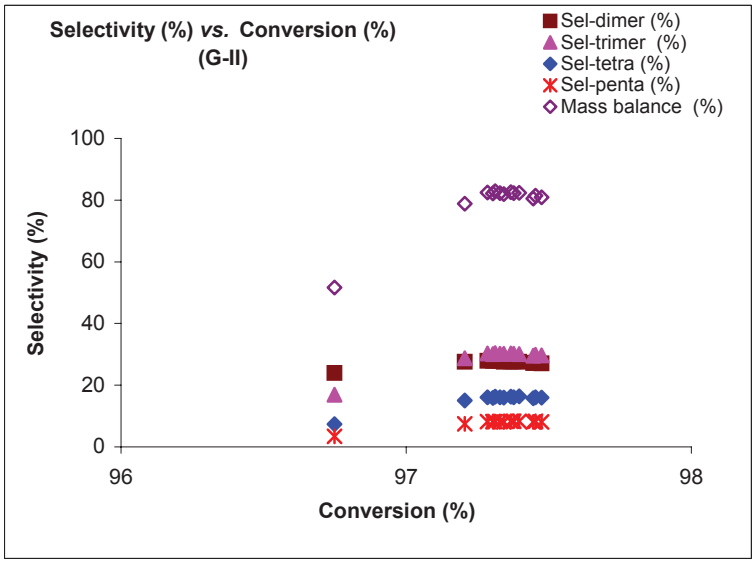

Figure 32: Zoom of selectivity of cyclic oligomers (%) *vs.* Conversion of cyclooctene (%) using **G-II**.

6.5. N-II

Table 9: Catalytic performance of **N-II** in the RO-RCM of cyclooctene.

Time [h]	Conversion (%)	TON	Sel-dimer (%)	Sel-trimer (%)	Sel-tetra (%)	Sel-penta (%)	Mass balance (%)
0.2	4.9	486	**41**	9	4	0	54
0.3	10.8	1084	**46**	8	2	1	57
0.5	18.6	1864	**38**	6	2	1	46
1.0	41.8	4181	**32**	5	2	1	40
1.5	61.6	6163	**30**	6	2	1	39
2.0	75.7	7574	**33**	14	5	2	55
2.5	85.5	8549	**31**	14	5	2	52
3.5	94.7	9473	**27**	13	5	2	48
4.5	97.0	9696	**28**	24	10	5	68
5.5	97.3	9730	**28**	28	14	7	76
6.5	97.3	9735	**28**	29	15	8	80
7.5	97.3	9734	**28**	28	15	7	78
23.0	97.1	9707	**26**	20	8	4	58
32.0	96.2	9618	**23**	10	4	2	39
50.0	96.7	9668	**23**	14	6	2	45

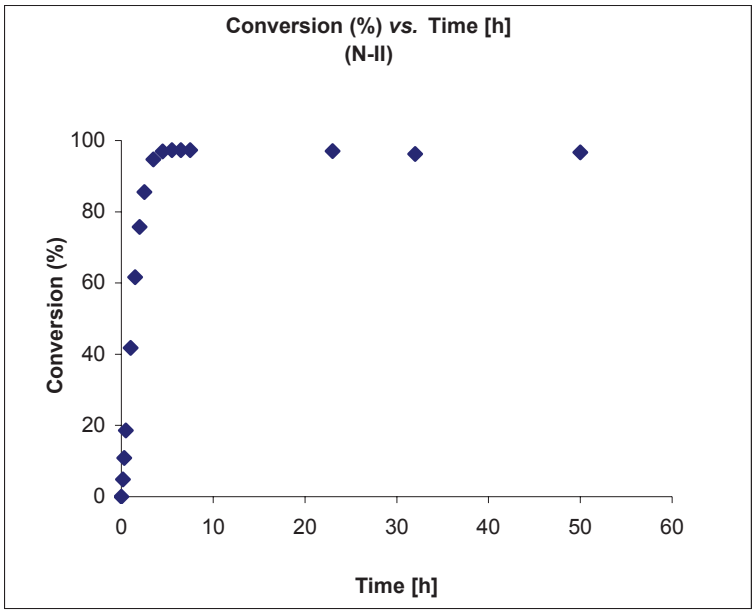

Figure 33: Conversion of cyclooctene (%) *vs.* Time [h] using **N-II**.

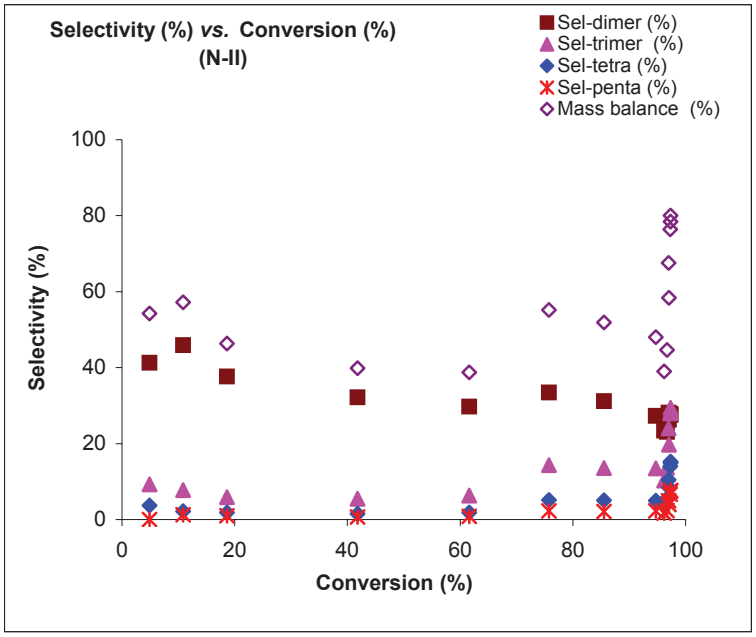

Figure 34: Selectivity of cyclic oligomers (%) *vs.* conversion of cyclooctene (%) using **N-II**.

6.6. RuPr

Table 10: Catalytic performance of **RuPr** in the RO-RCM of cyclooctene.

Time [h]	Conversion (%)	TON	Sel-dimer (%)	Sel-trimer (%)	Sel-tetra (%)	Sel-penta (%)	Mass balance (%)
0.5	9.9	989	**40**	16	7	4	67
1.0	23.4	2343	**50**	22	9	4	86
1.5	40.2	4025	**48**	24	11	5	88
2.0	55.3	5526	**45**	25	12	6	87
3.0	76.3	7627	**40**	27	13	7	87
4.0	88.0	8802	**35**	28	15	7	86
5.0	93.1	9313	**32**	29	15	8	85
6.0	95.4	9543	**31**	30	16	9	85
7.0	96.2	9618	**30**	30	16	9	84
8.5	96.9	9689	**29**	30	16	9	84
24.0	97.2	9724	**28**	30	16	8	83
50.0	97.2	9719	**28**	30	16	9	83

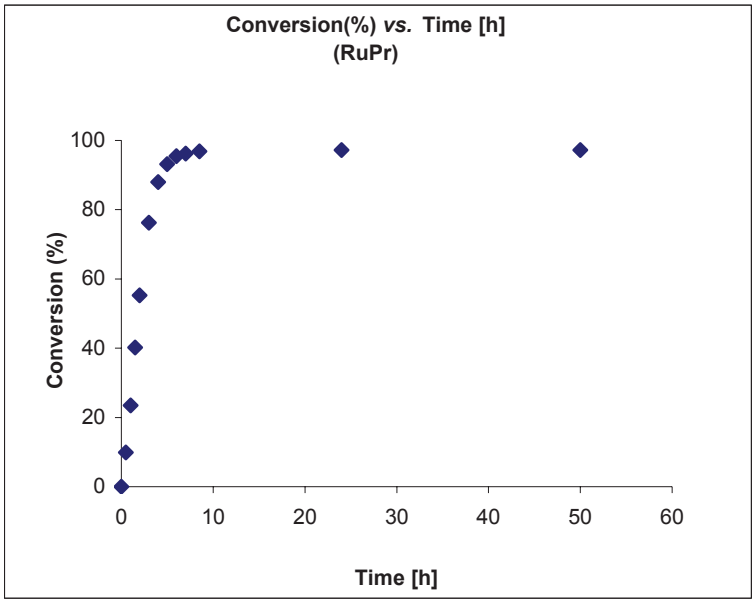

Figure 35: Conversion of cyclooctene (%) *vs.* time [h] using **RuPr**.

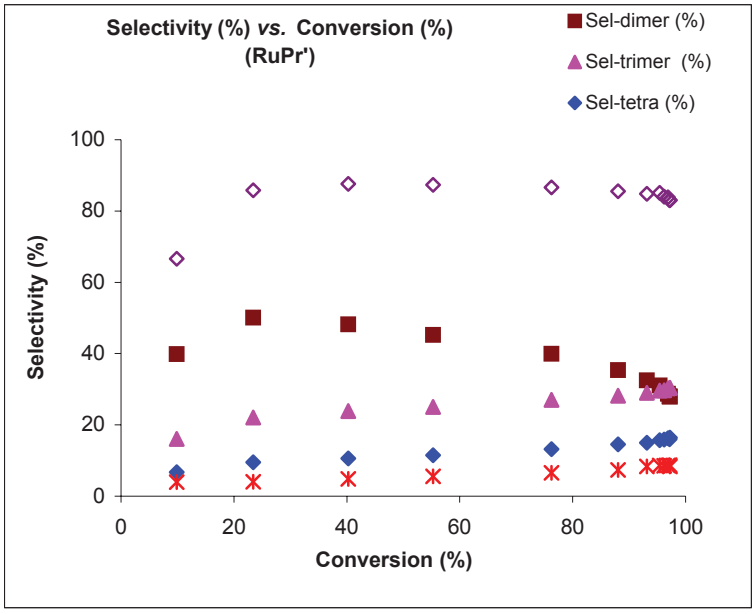

Figure 36: Selectivity of cyclic oligomers (%) *vs.* conversion of cyclooctene (%) using **RuPr**.

6.7. RuBn

Table 11: Catalytic performance of **RuBn** in the RO-RCM of cyclooctene.

Time [h]	Conversion (%)	TON	Sel-dimer (%)	Sel-trimer (%)	Sel-tetra (%)	Sel-penta (%)	Mass balance (%)
0.5	2.5	252	**13**	4	0	0	17
1.0	5.0	505	**42**	14	5	0	61
1.5	10.0	1005	**53**	17	5	2	78
2.0	16.9	1687	**53**	19	7	2	82
2.5	22.4	2237	**53**	21	8	3	85
3.0	28.1	2808	**52**	22	8	3	85
4.0	40.7	4072	**50**	24	10	4	88
5.0	51.2	5118	**47**	25	11	5	88
6.0	60.9	6090	**45**	26	12	5	87
7.0	68.1	6812	**42**	27	12	6	87
8.0	73.8	7376	**40**	27	13	6	87
23.0	96.7	9671	**29**	30	16	8	83
34.0	97.3	9730	**28**	30	16	8	81
52.0	97.5	9746	**27**	30	16	8	82

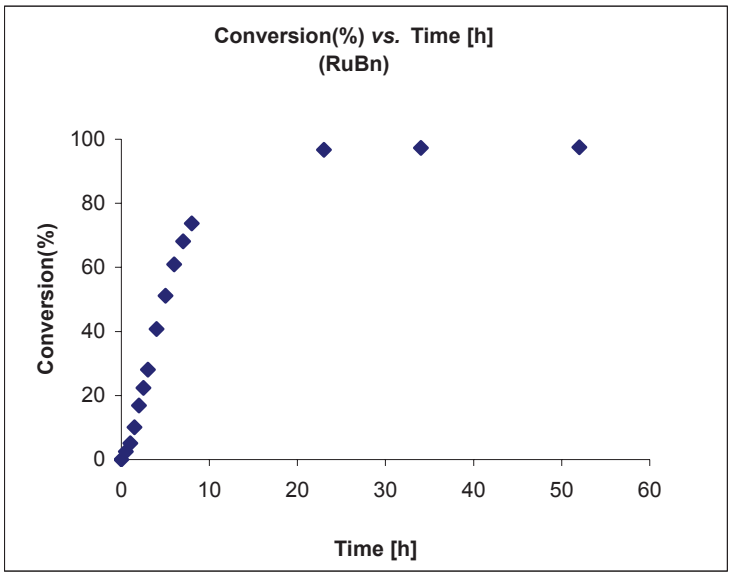

Figure 38: Conversion of cyclooctene (%) *vs.* time [h] using **RuBn**.

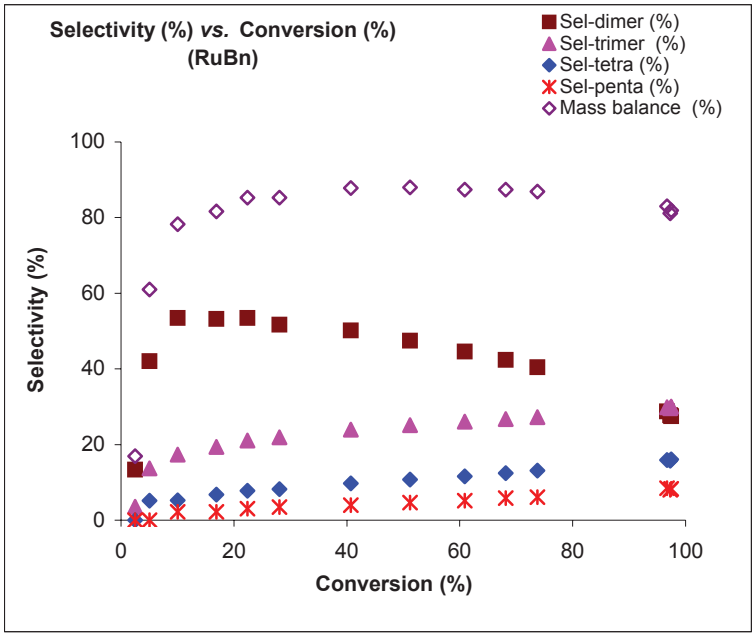

Figure 39: Selectivity of cyclic oligomers (%) *vs.* conversion of cyclooctene (%) using **RuBn**.

6.8. X-ray structure of RuBn

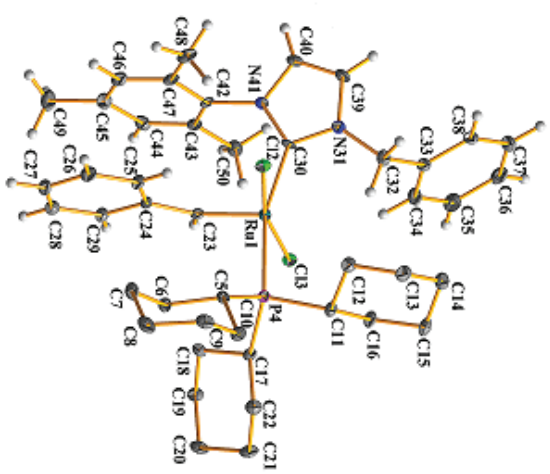

Figure 40: X-ray structure of **M-RuBn**.

Crystal data

$C_{44}H_{59}Cl_2N_2PRu$	$Z = 2$
$M_r = 818.91$	$F(000) = 860$
Triclinic, $P\bar{1}$	$D_x = 1.348$ Mg m^{-3}
Hall symbol: -P 1	Mo $K\alpha$ radiation, $\lambda = 0.7107$ Å
$a = 9.5221$ (6) Å	Cell parameters from 23423 reflections
$b = 13.8865$ (7) Å	$\theta = 3.3–29.6°$
$c = 17.1831$ (9) Å	$\mu = 0.59$ mm^{-1}
$\alpha = 96.169$ (4)°	$T = 110$ K
$\beta = 104.967$ (5)°	Block, dark brown
$\gamma = 109.769$ (5)°	0.25 × 0.18 × 0.09 mm
$V = 2017.7$ (2) Å^3	

Data collection

Xcalibur, Atlas, Gemini ultra diffractometer	10138 independent reflections
Radiation source: Enhance (Mo) X-ray Source	8696 reflections with $I > 2.0\sigma(I)$
graphite	$R_{int} = 0.082$
Detector resolution: 10.4685 pixels mm^{-1}	$\theta_{max} = 29.7°$, $\theta_{min} = 3.4°$
Absorption correction: analytical *CrysAlis PRO*, Oxford Diffraction Ltd., Version 1.171.34.40 (release 27-08-2010 CrysAlis171 .NET) (compiled Aug 27 2010,11:50:40) Analytical numeric absorption correction using a multifaceted crystal model based on expressions derived by R.C. Clark & J.S. Reid. (Clark, R. C. & Reid, J. S. (1995). Acta Cryst. A51, 887-897)	$h = -13\rightarrow13$
$T_{min} = 0.903$, $T_{max} = 0.954$	$k = -19\rightarrow18$
39857 measured reflections	$l = -23\rightarrow23$

Refinement

Refinement on F^2	Primary atom site location: structure-invariant direct methods
Least-squares matrix: full	Hydrogen site location: inferred from neighbouring sites
$R[F^2 > 2\sigma(F^2)] = 0.068$	Method, part 1, Chebychev polynomial, (Watkin, 1994, *P*rince, 1982) [*w*eight] = $1.0/[A_0*T_0(x) + A_1*T_1(x) \cdots + A_{n-1}]*T_{n-1}(x)]$ where A_i are the Chebychev coefficients listed belo*w* and x = *F* /*F*max Method = Robust Weighting (*P*rince, 1982) W = [*w*eight] * [1-(delta*F*/6*sigma*F*)^2]^2 A_i are: 0.102E + 04 0.159E + 04 828. 218.
$wR(F^2) = 0.168$	$(\Delta/\sigma)_{max} = 0.001$
$S = 0.98$	$\Delta\rangle_{max} = 1.75$ e Å^{-3}
10138 reflections	$\Delta\rangle_{min} = -1.98$ e Å^{-3}
452 parameters	Extinction correction: Larson (1970), Equation 22
0 restraints	Extinction coefficient: 52 (9)

Geometric parameters (Å, º)

Ru1—Cl2	2.3968 (10)	C22—H221	0.973
Ru1—Cl3	2.3959 (10)	C23—C24	1.471 (5)
Ru1—P4	2.4202 (11)	C23—H231	0.933
Ru1—C23	1.830 (4)	C24—C25	1.401 (6)
Ru1—C30	2.067 (3)	C24—C29	1.411 (6)
P4—C5	1.858 (4)	C25—C26	1.378 (6)
P4—C11	1.861 (4)	C25—H251	0.933
P4—C17	1.858 (4)	C26—C27	1.397 (7)
C5—C6	1.540 (6)	C26—H261	0.936
C5—C10	1.542 (6)	C27—C28	1.389 (7)
C5—H51	0.980	C27—H271	0.933
C6—C7	1.530 (6)	C28—C29	1.378 (6)
C6—H61	0.972	C28—H281	0.932
C6—H62	0.965	C29—H291	0.934
C7—C8	1.526 (7)	C30—N31	1.357 (5)
C7—H71	0.973	C30—N41	1.359 (5)
C7—H72	0.970	N31—C32	1.471 (6)
C8—C9	1.530 (7)	N31—C39	1.381 (5)
C8—H82	0.975	C32—C33	1.508 (6)
C8—H81	0.973	C32—H322	0.972
C9—C10	1.533 (6)	C32—H321	0.977
C9—H91	0.968	C33—C34	1.386 (6)

C9—H92	0.964	C33—C38	1.392 (6)
C10—H102	0.976	C34—C35	1.388 (7)
C10—H101	0.972	C34—H341	0.928
C11—C12	1.527 (6)	C35—C36	1.388 (8)
C11—C16	1.537 (6)	C35—H351	0.935
C11—H111	0.986	C36—C37	1.377 (8)
C12—C13	1.523 (6)	C36—H361	0.930
C12—H122	0.978	C37—C38	1.390 (7)
C12—H121	0.974	C37—H371	0.928
C13—C14	1.531 (7)	C38—H381	0.929
C13—H131	0.965	C39—C40	1.335 (7)
C13—H132	0.968	C39—H391	0.927
C14—C15	1.516 (7)	C40—N41	1.402 (5)
C14—H142	0.973	C40—H401	0.934
C14—H141	0.972	N41—C42	1.451 (5)
C15—C16	1.525 (6)	C42—C43	1.401 (6)
C15—H151	0.969	C42—C47	1.381 (6)
C15—H152	0.963	C43—C44	1.386 (6)
C16—H161	0.968	C43—C50	1.482 (6)
C16—H162	0.978	C44—C45	1.388 (7)
C17—C18	1.537 (6)	C44—H441	0.933
C17—C22	1.536 (6)	C45—C46	1.398 (8)
C17—H171	0.978	C45—C49	1.503 (7)
C18—C19	1.526 (6)	C46—C47	1.401 (7)
C18—H182	0.980	C46—H461	0.934
C18—H181	0.972	C47—C48	1.505 (7)
C19—C20	1.525 (6)	C48—H481	0.961
C19—H191	0.972	C48—H482	0.967
C19—H192	0.973	C48—H483	0.960
C20—C21	1.526 (7)	C49—H492	0.958
C20—H201	0.973	C49—H491	0.956
C20—H202	0.970	C49—H493	0.958
C21—C22	1.532 (6)	C50—H502	0.961
C21—H211	0.974	C50—H501	0.965
C21—H212	0.972	C50—H503	0.958
C22—H222	0.972		
Cl2—Ru1—Cl3	165.56 (4)	C21—C20—H202	108.8
Cl2—Ru1—P4	91.92 (4)	H201—C20—H202	109.0
Cl3—Ru1—P4	89.70 (4)	C20—C21—C22	112.3 (4)
Cl2—Ru1—C23	104.50 (13)	C20—C21—H211	108.5

Cl3—Ru1—C23	89.39 (13)	C22—C21—H211	108.1
P4—Ru1—C23	99.06 (13)	C20—C21—H212	109.5
Cl2—Ru1—C30	82.97 (11)	C22—C21—H212	109.2
Cl3—Ru1—C30	91.20 (11)	H211—C21—H212	109.2
P4—Ru1—C30	162.38 (12)	C17—C22—C21	109.9 (4)
C23—Ru1—C30	98.55 (17)	C17—C22—H222	109.5
Ru1—P4—C5	115.12 (14)	C21—C22—H222	108.9
Ru1—P4—C11	108.41 (14)	C17—C22—H221	110.1
C5—P4—C11	103.47 (19)	C21—C22—H221	109.6
Ru1—P4—C17	114.65 (14)	H222—C22—H221	108.8
C5—P4—C17	110.44 (19)	Ru1—C23—C24	135.4 (3)
C11—P4—C17	103.43 (19)	Ru1—C23—H231	112.7
P4—C5—C6	111.9 (3)	C24—C23—H231	111.9
P4—C5—C10	119.1 (3)	C23—C24—C25	125.9 (4)
C6—C5—C10	109.1 (3)	C23—C24—C29	116.8 (4)
P4—C5—H51	105.1	C25—C24—C29	117.3 (4)
C6—C5—H51	105.5	C24—C25—C26	121.2 (5)
C10—C5—H51	105.0	C24—C25—H251	118.7
C5—C6—C7	109.8 (3)	C26—C25—H251	120.0
C5—C6—H61	108.5	C25—C26—C27	120.6 (5)
C7—C6—H61	109.3	C25—C26—H261	119.2
C5—C6—H62	109.4	C27—C26—H261	120.2
C7—C6—H62	110.5	C26—C27—C28	119.2 (4)
H61—C6—H62	109.2	C26—C27—H271	120.6
C6—C7—C8	111.3 (4)	C28—C27—H271	120.2
C6—C7—H71	109.5	C27—C28—C29	120.2 (5)
C8—C7—H71	109.1	C27—C28—H281	119.5
C6—C7—H72	108.8	C29—C28—H281	120.3
C8—C7—H72	109.2	C24—C29—C28	121.5 (4)
H71—C7—H72	108.9	C24—C29—H291	119.2
C7—C8—C9	111.2 (4)	C28—C29—H291	119.3
C7—C8—H82	109.1	Ru1—C30—N31	123.2 (3)
C9—C8—H82	109.1	Ru1—C30—N41	132.0 (3)
C7—C8—H81	108.5	N31—C30—N41	104.1 (3)
C9—C8—H81	109.4	C30—N31—C32	125.2 (4)
H82—C8—H81	109.5	C30—N31—C39	111.6 (4)
C8—C9—C10	112.6 (4)	C32—N31—C39	123.2 (4)
C8—C9—H91	108.5	N31—C32—C33	112.6 (4)
C10—C9—H91	108.8	N31—C32—H322	107.3
C8—C9—H92	108.9	C33—C32—H322	108.8

C10—C9—H92	109.0	N31—C32—H321	109.7
H91—C9—H92	109.0	C33—C32—H321	109.4
C5—C10—C9	109.9 (4)	H322—C32—H321	108.9
C5—C10—H102	109.1	C32—C33—C34	121.2 (4)
C9—C10—H102	109.0	C32—C33—C38	120.0 (4)
C5—C10—H101	110.2	C34—C33—C38	118.8 (4)
C9—C10—H101	109.9	C33—C34—C35	120.4 (5)
H102—C10—H101	108.8	C33—C34—H341	119.6
P4—C11—C12	110.5 (3)	C35—C34—H341	120.0
P4—C11—C16	112.6 (3)	C34—C35—C36	120.2 (5)
C12—C11—C16	110.9 (4)	C34—C35—H351	119.5
P4—C11—H111	107.3	C36—C35—H351	120.3
C12—C11—H111	108.0	C35—C36—C37	120.0 (5)
C16—C11—H111	107.4	C35—C36—H361	120.4
C11—C12—C13	112.2 (4)	C37—C36—H361	119.6
C11—C12—H122	108.8	C36—C37—C38	119.7 (5)
C13—C12—H122	108.9	C36—C37—H371	120.1
C11—C12—H121	108.0	C38—C37—H371	120.2
C13—C12—H121	109.6	C33—C38—C37	120.9 (4)
H122—C12—H121	109.3	C33—C38—H381	119.6
C12—C13—C14	110.2 (4)	C37—C38—H381	119.5
C12—C13—H131	110.1	N31—C39—C40	107.0 (4)
C14—C13—H131	108.8	N31—C39—H391	125.9
C12—C13—H132	109.6	C40—C39—H391	127.1
C14—C13—H132	108.7	C39—C40—N41	106.6 (4)
H131—C13—H132	109.5	C39—C40—H401	127.6
C13—C14—C15	109.8 (4)	N41—C40—H401	125.8
C13—C14—H142	110.5	C40—N41—C30	110.7 (4)
C15—C14—H142	109.7	C40—N41—C42	122.4 (4)
C13—C14—H141	109.6	C30—N41—C42	126.6 (3)
C15—C14—H141	109.2	N41—C42—C43	117.2 (4)
H142—C14—H141	108.1	N41—C42—C47	119.2 (4)
C14—C15—C16	111.7 (4)	C43—C42—C47	123.5 (4)
C14—C15—H151	108.5	C42—C43—C44	117.0 (4)
C16—C15—H151	109.4	C42—C43—C50	121.6 (4)
C14—C15—H152	108.9	C44—C43—C50	121.4 (4)
C16—C15—H152	109.2	C43—C44—C45	122.4 (5)
H151—C15—H152	109.1	C43—C44—H441	118.3
C11—C16—C15	111.2 (4)	C45—C44—H441	119.4
C11—C16—H161	109.1	C44—C45—C46	118.2 (5)

C15—C16—H161	109.0	C44—C45—C49	120.7 (5)
C11—C16—H162	109.1	C46—C45—C49	121.1 (5)
C15—C16—H162	109.2	C45—C46—C47	121.9 (5)
H161—C16—H162	109.3	C45—C46—H461	118.9
P4—C17—C18	114.1 (3)	C47—C46—H461	119.2
P4—C17—C22	115.5 (3)	C46—C47—C42	117.0 (4)
C18—C17—C22	111.3 (4)	C46—C47—C48	121.8 (4)
P4—C17—H171	103.7	C42—C47—C48	121.3 (4)
C18—C17—H171	104.4	C47—C48—H481	109.4
C22—C17—H171	106.6	C47—C48—H482	110.4
C17—C18—C19	110.7 (4)	H481—C48—H482	108.8
C17—C18—H182	108.6	C47—C48—H483	110.1
C19—C18—H182	109.0	H481—C48—H483	108.7
C17—C18—H181	108.6	H482—C48—H483	109.3
C19—C18—H181	110.0	C45—C49—H492	110.1
H182—C18—H181	109.9	C45—C49—H491	111.3
C18—C19—C20	111.5 (4)	H492—C49—H491	108.3
C18—C19—H191	108.7	C45—C49—H493	110.5
C20—C19—H191	109.9	H492—C49—H493	108.1
C18—C19—H192	108.4	H491—C49—H493	108.5
C20—C19—H192	109.2	C43—C50—H502	110.7
H191—C19—H192	109.0	C43—C50—H501	110.1
C19—C20—C21	111.1 (4)	H502—C50—H501	108.8
C19—C20—H201	109.4	C43—C50—H503	110.2
C21—C20—H201	109.9	H502—C50—H503	108.7
C19—C20—H202	108.6	H501—C50—H503	108.3

7. References

1 . a) Fürstner, A.; Ackermann, L.; Gabor, B.; Goddard, R.; Lehmann, C. W.; Mynott, R.; Stelzer, F.; Thiel, O. R. *Chem. Eur. J.* **2001***, 7, No.15,* 3236. b) Prühs, S.; Lehmann, C. W.; Furstner, A. *Organometallics* **2004,** *23,* 280. c) Dinger, M. B.; Nieczypor, P.; Mol, J. C. *Organometallics* **2003,** *22,* 5291. d) Ledoux, N.; Allaert, B.; Pattyn, S.; Mierde, H. V.; Vercaemst, C.; Verpoort, F. *Chem. Eur. J.* **2006***, 12,* 4654. e) Vehlow, K.; Maechling, S.; Blechert, S. *Organometallics* **2006,** *25,* 25. f) Vougioukalakis, G. C.; Grubbs, R. H. *Chem. Eur. J.* **2008***, 14,* 7545.

2 . a) Bornand, M.; Chen, P. *Angew. Chem. Int. Ed.* **2005***, 44,* 7909. b) Bornand, M..; Torker, S.; Chen, P. *Organometallics,* **2007,** *26,* 3585.

3 .a) Vehlow, K.; Wang, D.; Buchmeiser, M. R.; Blechert, S. *Angew. Chem. Int. Ed.* **2008***, 47,* 2615. b) Lichtenheldt, M.; Wang, D.; Vehlow, K.; Reinhardt, I.; Kühnel, C.; Decker, U.; Blechert, S.; Buchmeiser, M. R. *Chem. Eur. J.* **2009***, 15,* 9451.

4 . Benhamou, L.; Chardon, E.; Lavigne, G.; Bellemin-Laponnaz, S.; Cesar; V. *Chem. Rev.* **2011***, 111,* 2705.

5. Karame, I.; Boualleg, M.; Camus, J. M.; Maishal, T. K.; Alauzun, J.; Basset, J. M.; Coperet, C.; Corriu, R. J. P.; Jeanneau, E.; Mehdi, A.; Reye, C.; Veyre, L.; Thieuleux, C. *Chem. Eur. J.* **2009**, 15, 11 820.

6. Huang, J.; Stevens, E. D.; Nolan, S. P.; Petersen, J. L. *J. Am. Chem. Soc.* **1999***, 121,* 2674.

7. (a) Fürstner, A.; Ackermann, L.; Gabor, B.; Goddard, R.; Lehmann,C. W.; Mynott, R.; Stelzer, F.; Thiel, O. R. *Chem. Eur. J.* **2001**, *7*, 3236. (b) Fürstner, A.; Krause, H.; Ackermann, L.; Lehmann, C. W.*Chem. Commun*. **2001**, 2240.

Chapter 4

Synthesis and Catalytic performances of homogeneous and supported symmetrical and unsymmetrical GH-II catalysts

In the BASF company, promising results for the selective formation of low cyclic oligomers in the RO-RCM of cyclooctene were observed using symmetrical **GH-II** complexes, immobilized on Grace SP silica.[1] To further investigate the role of the surface, we looked at the performances of symmetrical and unsymmetrical **GH-II** type homogeneous catalysts and their heterogeneous analogues prepared by adsorption on Grace SP silica support.

In the present chapter we will thus describe the following points:

1. The synthesis, characterization and catalytic properties of heterogeneous catalysts **RuGH-II/silica** (immobilized **GH-II** on silica).
2. The synthesis and catalytic performances of unsymmetrical **GH-II** type catalysts.
    a. Synthesis and characterization of unsymmetrical **GH-II** type catalysts (**RuPrGH-II** and **RuBnGH-II)**
    b. Immobilization on silica to obtain **RuPrGH-II/silica** and **RuBnGH-II/silica**
    c. Comparison of the catalytic performances of **RuPrGH-II/silica** and **RuBnGH-II/silica** heterogeneous catalysts with their homogeneous homologues, namely **RuPrGH-II** and **RuBnGH-II** catalysts.

1. Introduction

In recent years, several reports concerning the immobilization of olefin metathesis catalysts on various supports were investigated using different strategies.[2] The Grubbs-type catalysts were immobilized via (a) exchange of halide ligands[3] (b) exchange of phosphine and NHC ligands[4] (c) the functionalization of supports by alkylidene ligand.[5] In the latter case, the non-permanent grafting of the precatalyst to the support allowed the release of the active species into the reaction mixture after the initial catalytic cycle and the recapture of the resting state when the reaction was complete, this phenomenon being called the "boomrang effect". However, recent work by Pleino *et al.* has shown that it is probably not the case, and that the catalyst is purely homogeneous.[6] Besides, Sels *et al.* reported recently an alternative convenient method for the immobilization of Grubbs–Hoveyda catalyst: adsorption of molecular Ru-NHC complex on the silica support.[1] However, till today, the exact nature of the interaction between the molecular catalyst and the silica surface is still unknown. Yet, based on this strategy, BASF showed that higher performances in RO-RCM of cyclooctene under flow conditions could be obtained compared to those of homogeneous equivalents. Here, the goal is to obtain further insight into the structure of such catalysts through spectroscopy and reactivity studies. Further improvement of these catalysts activity/selectivity will also be attempted.

2. Results and discussion

2.1. Synthesis, characterization and catalytic performances of GH-II catalyst immobilized on silica (RuGH-II/silica)

2.1.1. Synthesis of immobilized catalyst RuGH-II/silica

A study concerning the "best" BASF system (**GH-II** adsorbed on Grace SP silica support calcined at 550 °C under 'Ar') was carried out.

The preparation of the supported catalyst required the following experimental procedure: a dichloromethane solution of Grubbs-Hoveyda catalyst was added to the suspension of the dehydroxylated Grace support in dichloromethane. After stirring for 2 h, the solvent was removed under vacuum yielding the targetted **RuGH-II/silica** catalyst (Scheme 1) as reported by BASF. Here, Ru loading was typically 0.064%$_{wt}$.

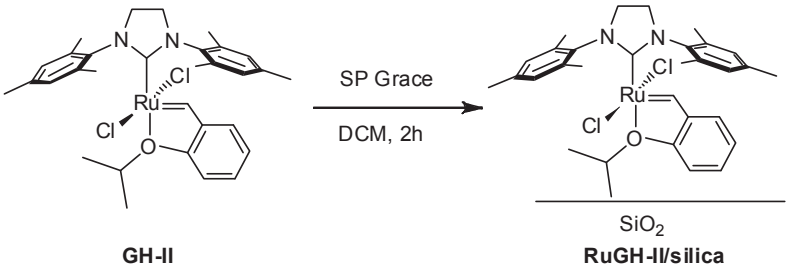

Scheme 1: Immobilization of the **GH-II** catalyst on Grace silica support.

However, the low Ru loading and thus the larger amount of support could represent a drawback for catalysis because of adsorption/desorption problems but also for catalyst characterization. Note that such loading is about 10 times lower than that of our hybrid heterogeneous catalyst **M-RuPr** as discussed in the previous chapter 2 (Table 1). For example, if 5 mg of **M-RuPr** are needed for a catalytic run, we need 50 mg of **RuGH-II/silica** to be in the same conditions.

Table 1: Loading ($\%_{wt}$) and surface density of Ru in the catalysts.

Catalysts	$\%_{wt}$ of Ru	Ru (mmol/g)	Surface area (m^2/g)	Ru ($mmol/m^2$)
RuGH-II/ silica	0.064	0.0064	550	0.000012
M-RuPr	0.63	0.0623	900	0.000069

2.1.2. Study of the acidity of support by pyridine adsorption using IR (DRIFT) technique

In order to understand the nature of the interaction of the molecular complex and silica, the acidity of the support was investigated by pyridine adsorption.[7]

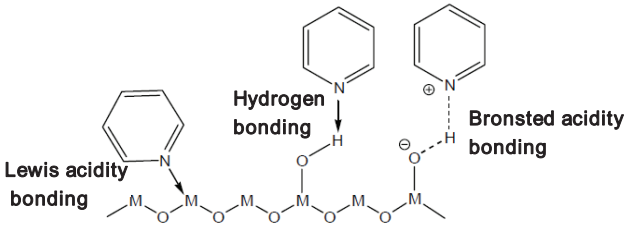

Figure 1: Representative figure describing type of pyridine bonding with the surface.

Table 2: IR bands for different type of pyridine bonding with the surface.

Position of bands ν(C=C) (cm^{-1})	Type of bonding	Temperature of desorption [°C]
1438 / 1485 / 1580	Physisorption	25
1444/1593	Hydrogen bonding	150
1490 / 1575 / 1606 / 1619	Lewis acidity	250-500
1544 / 1638	Bronsted acidity	400

The acidity was monitored by DRIFT technique, however the expected distinctive peaks corresponding to the C=C frequencies for the hydrogen bonded pyridine (in the region around 1600 cm^{-1}) were not observed, indicating that pyridine desorbed at 150 °C (Figure 3, Table 2) and therefore that the support presented very little acidity. The observed difference in the intensity of Si-OH at 3750 cm^{-1} was not significant, in particular because of the use of DRIFT technique, which is not quantitative (Figure 2).

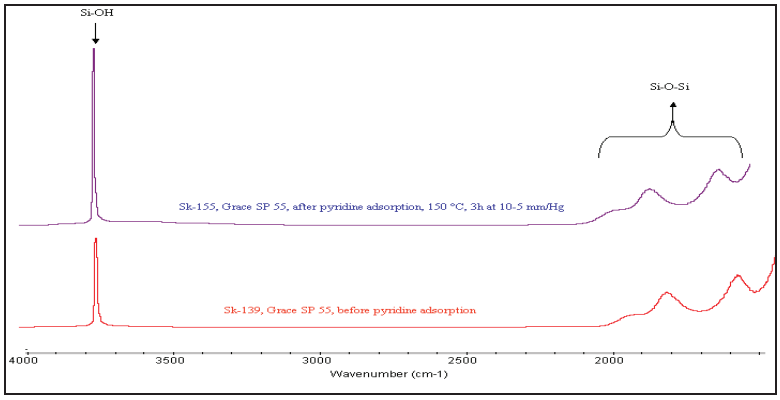

Figure 2: Comparison of DRIFT spectra for Grace SP 55 support before and after the adsorption of pyridine

2.1.3. Study of the immobilized catalyst (RuGH-II/silica) by IR (DRIFT) technique

Investigation of the immobilized catalyst itself by solid state NMR gave no further clue because only very broad signals were observed. Similarly, IR spectroscopy (DRIFT) did not show any evidence for the presence of adsorbed **GH-II** complex either (signals corresponding to the C-H frequencies expected around 3000 cm^{-1}) (Figure 3). This is probably due to the very high dilution of **GH-II** complex in the **RuGH-II/silica** catalyst. IR spectroscopy is thus not the technique of choice to investigate such systems, despite its higher sensitivity compared to NMR spectroscopy. Overall no structural information could be obtained by usual spectroscopic techniques; one alternative option being the use of solid state NMR using DNP.

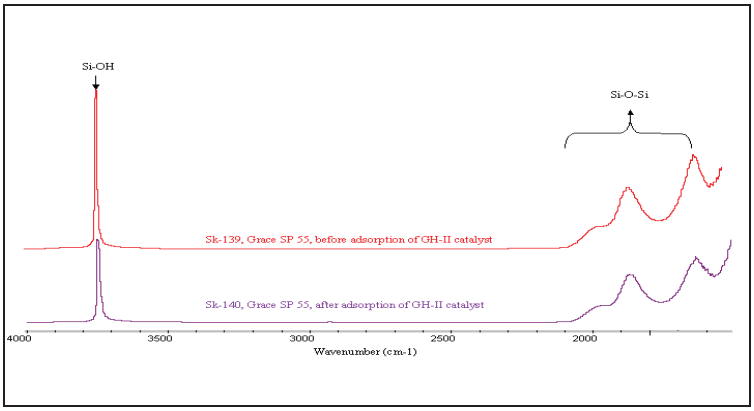

Figure 3: Comparison of DRIFT spectra for Grace SP 550 support before and after the adsorption of catalyst

2.1.4. Comparison of catalytic performance of supported heterogeneous catalysts (RuGH-II/silica) *vs.* homogeneous analogue (GH-II)

Catalytic tests using **RuGH-II/silica** was carried out under the standard conditions, as described earlier for RO-RCM of cyclooctene using hybrid materials: cyclooctene : Ru ratio of 10,000 using 20 mM cyclooctene solution. The **RuGH-II/silica** catalytic performances were studied and further compared with those of **GH-II**, to have understanding of the silica surface effect for the selective formation of cyclic oligomers in the present reaction. The details for individual performances can be found in the appendix section.

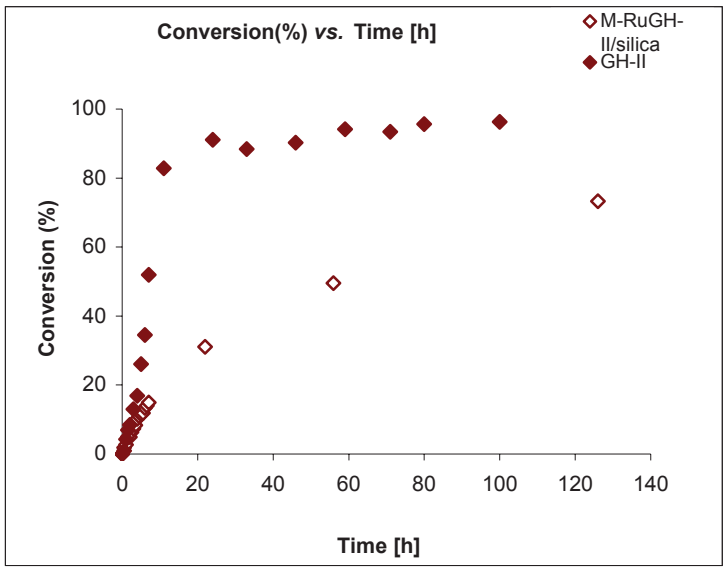

Figure 4: Conversion of cyclooctene (%) *vs.* time [h] using **GH-II** and **RuGH-II/silica**.

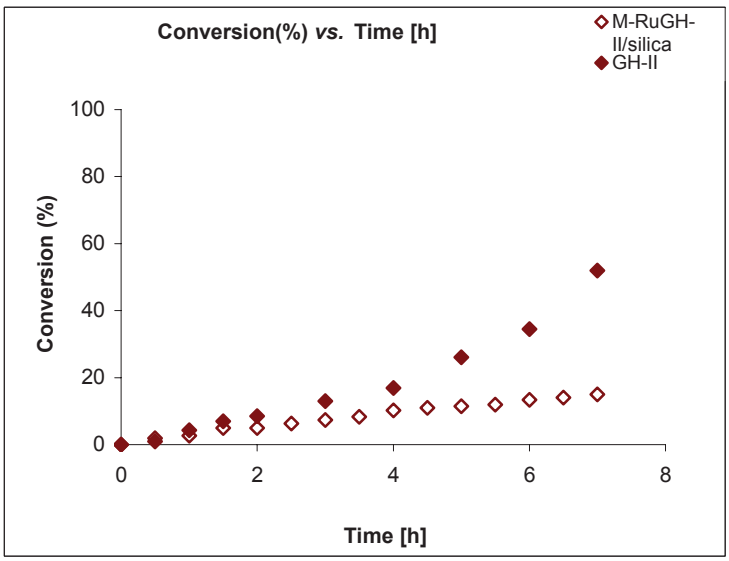

Figure 5: Zoom of initial 8h for conversion of cyclooctene (%) *vs.* time [h] using **GH-II** and **RuGH-II/silica**.

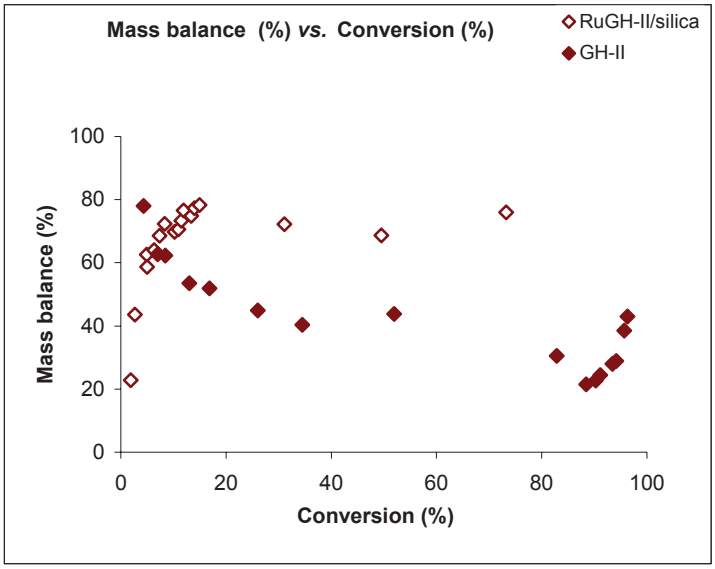

Figure 6: Dimer selectivity (%) *vs.* conversion of cyclooctene (%)using **GH-II** and **RuGH-II/silica**.

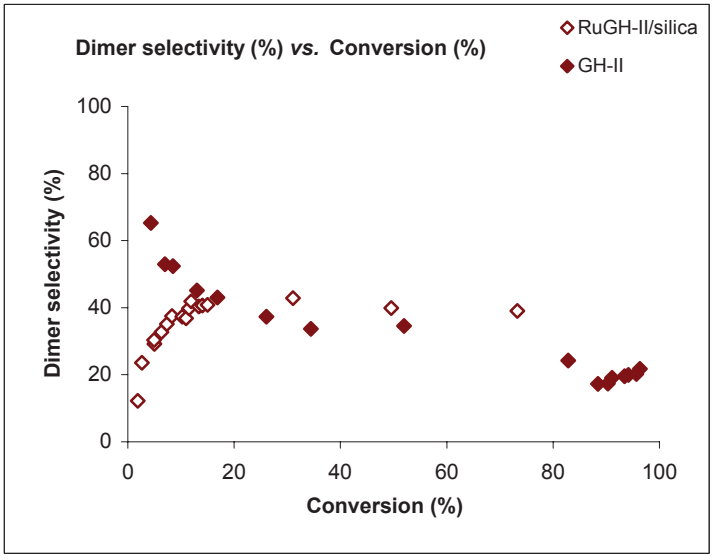

Figure 7: Mass balance (%) *vs.* conversion of cyclooctene (%)using **GH-II** and **RuGH-II/silica**.

In RO-RCM of cyclooctene, the **RuGH-II/silica** displayed very low reaction rate, allowing 15% conversion in 7 h *vs.* 52% conversion in 7 h for the molecular catalyst **GH-II.** Although, the reaction was slow, there was no initiation period in contrast to what was observed for **GH-II** (Figure 4, 5)**.** This could indicate that **RuGH-II/silica** active sites were different than those of **GH-II**, and it brings the question on what is the role of the silica surface (Grace SP 550, calcined at 550 °C) and the OH groups on **RuGH-II/silica**.

It is also important to note that, in terms of mass balance and selectivity, the observed trend for **RuGH-II/silica** was exactly the opposite to **GH-II**, *i.e.* increasing mass balance and increasing selectivities for dimer (Figure 6, 7) and cyclic oligomers up to pentamer (appendix section) with a maximum mass balance of 75-77% and a dimer selectivity up to 39% (Figure

6, 7). The low mass balance at low conversions could be due to a problem of adsorption/desorption of the reagents because of the presence of large amount of support.

Note however that the **RuGH-II/silica** displayed almost similar catalytic performances in terms of selectivity of dimer and mass balance than those of **M-RuPr**.

Table 3: Comparison of selectivity of cyclic products and mass balance at 30-40% conversion of cyclooctene.

Catalyst	Initial rate [mol/mol Ru/h]	Selectivity (%)				Mass balance (%)
		Dimer	Trimer	Tetramer	Pentamer	
RuGH-II/silica	267	43	20	7	3	72
M-RuPr	1350	53	22	10	4	89
GH-II	431	**34**	5	1	1	40

More importantly, in chapter 3, we have seen that the unsymmetrical nature of NHC ligand was the key factor for the observed selectivity towards low cyclic oligomers (dimer and trimer). Thus it was possible to propose that upon adsorption of **GH-II**, dissymmetrisation of the NHC ligand occured, with one mesityl substituent more strongly interacting with the silica surface than the other (Figure 8). Finally, comparison of the catalytic performances (**RuGH-II/silica** *vs.* **GH-II)**, clearly showed that the catalysts had different active sites and thus that, in **RuGH-II/silica**, the reaction does not take place in the homogeneous phase (*i.e.* no release of molecular **GH-II** in the solution which performed catalysis).

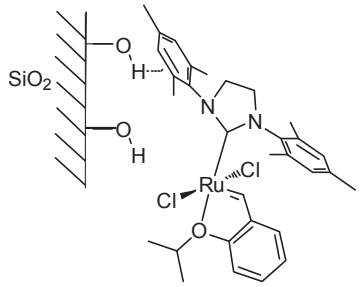

Figure 8: One putative dissymmetrisation of the NHC ligand by the silica surface.

To further investigate these observations and with the hope to generate improved catalysts, we prepared unsymmetrical **GH-II** type complexes **RuPrGH-II** and **RuBnGH-II** and they were further adsorbed on SP Grace silica support, yielding **RuPrGH-II/silica** and **RuBnGH-II/silica**. The preparation and the comparison of the catalytic performances for these systems are discussed in the following section.

2.2. Homogeneous and silica-immobilized unsymmetrical NHC-GH-II type complexes

2.2.1. Synthesis of homogeneous catalysts

To determine the influence of the disymmetry of the NHC ligand, we have developed the synthesis of unsymmetrical molecular **GH-II** type complexes and further adsorbed them on

Grace silica. For the synthesis of unsymmetrical **GH-II** type catalysts, a two-step process was used. First, the imidazolium salt was treated with the Ag_2O in dichloromethane at RT to generate the silver carbene. The silver carbene was further reacted with the **GH-I** complex in the presence of CuCl in toluene at 50°C. The targetted Ru-NHC compound was isolated in 65-70% yield *via* column chromatography. It is noteworthy that synthesis of **GH-II** type catalysts *via* this route typically provides low yields of *ca.* 30-35% and was thus optimized here.[8]

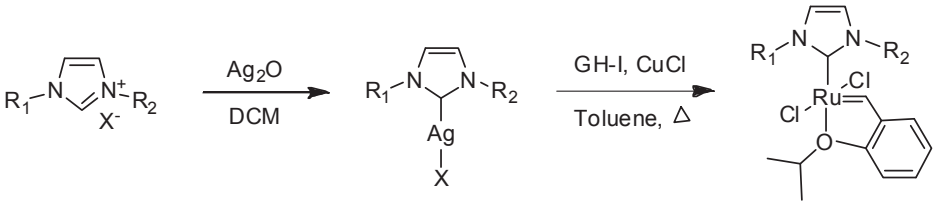

Scheme 2: Methodology for the synthesis of Ru-NHC GH-II type homogeneous catalysts.

Two unsymmetrical catalysts **RuPrGH-II** and **RuBnGH-II** (Figure 9) were prepared and their detailed synthesis is described in the experimental section.

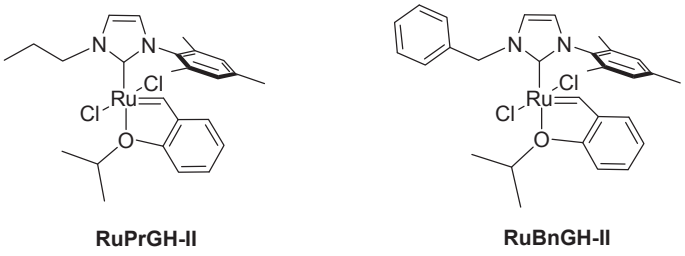

Figure 9: Unsymmetrical **GH-II** type catalysts.

2.2.2. Structural feature of homogeneous catalysts

Suitable crystals for X-ray crystallography were obtained for both **RuPrGH-II** and **RuBnGH-II** (Figure 9). Structural analysis of **RuPrGH-II** and **RuBnGH-II** showed shorter bond lengths for the Ru-C of the NHC ligand, bond distance (1.985 Å for both the catalysts) than that observed for **GH-II** (1.978 Å). An increase in the (C-N-C) bond angles (4-5°) for the NHC substituents with respect to NHC backbone carbons was observed as compared to **GH-II**, thus indicating an increased steric hindrance around the metal center. Note that, an increase of the Ru-benzylidene bond distance was observed for **RuBnGH-II** (1.840 Å) compared to that obtained for **GH-II** (1.831 Å), the effect being smaller in the case of **RuPrGH-II** (1.832 Å). The benzylidene protons were located under the mesityl group as reported already on similar compounds.[9]

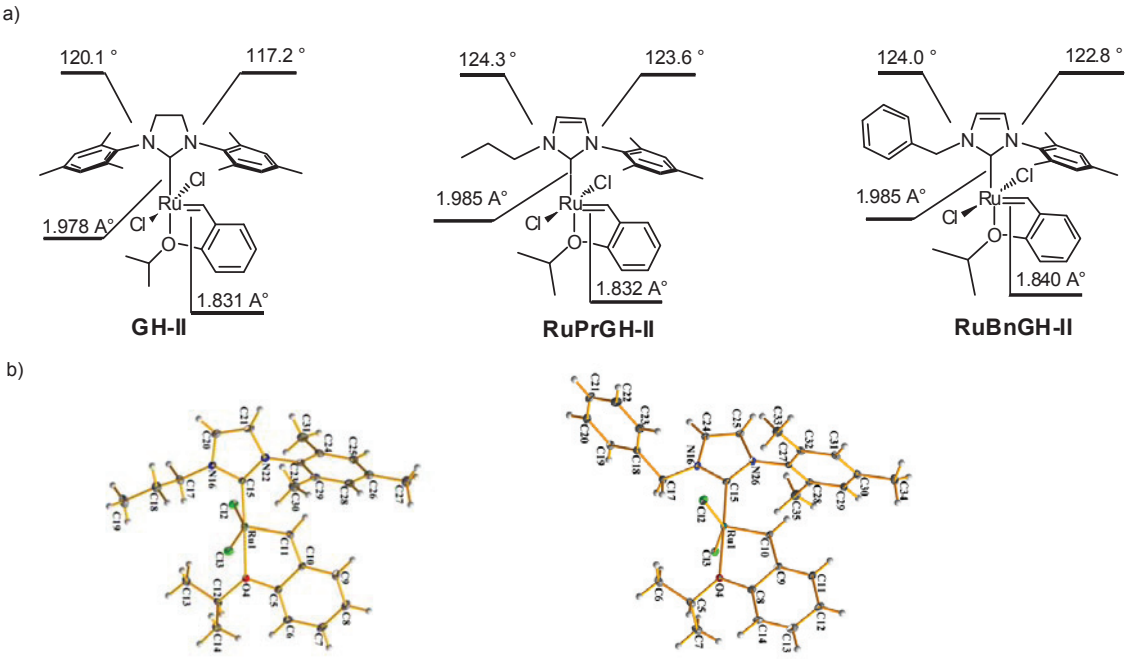

Figure 10: a) Selected geometrical features of unsymmetrical GH-II type complexes, b) Ortep X-ray crystal structure of **RuPrGH-II** (left) and **RuBnGH-II** (right).

2.2.3. Immobilization of unsymmetrical GH-II type catalysts

The immobilization of unsymmetrical **GH-II** type catalysts was carried out by adsorption on Grace SP 550 – 10020 pretreated at 550 °C under 'Ar'. The same procedure as described in section 2.1.1 was used for the synthesis of immobilized catalysts **RuPrGH-II** and **RuBnGH-II** (Figure 11). Note that the loading of the Ru (0.064%$_{wt}$) is kept constant and identical to that of **RuGH-II/silica**. For time reasons and because of the failure of **RuGH-II/silica** characterization by spectroscopic methods, no further characterization of **RuPrGH-II/silica** and **RuBnGH-II/silica** were undertaken.

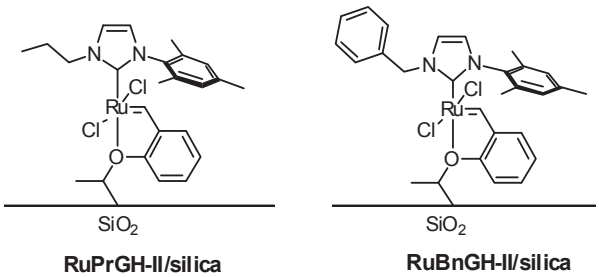

Figure 11: Unsymmetrical immobilized **GH-II** type catalysts **RuPrGH-II/silica** and **RuBnGH-II/silica**.

2.2.4. Catalytic performances of homogeneous and immobilized catalysts

As the selectivity for low cyclic products was attributed to the unsymmetrical nature of NHC (see chapter 3) and as the grace silica surface further induced similar trend when adsorbing

GH-II complex, we attempted to increase the selectivity towards low cyclic oligomers by adsorbing unsymmetrical NHC-GH-II type molecular complexes on silica. We thus carried out the catalytic tests using homogeneous and immobilized catalysts based on **RuPrGH-II** and **RuBnGH-II** under our standard conditions and their catalytic performances were compared to those of previously studied **RuPr** and **RuBn** catalysts and **RuGH-II/silica** immobilized catalyst**.**

2.2.4.1. Comparison of catalytic performances of unsymmetrical catalysts RuPrGH-II and RuBnGH-II *vs.* RuPr and RuBn

In RO-RCM of cyclooctene, **RuPrGH-II** and **RuBnGH-II** displayed low reaction rate with a long initiation period of 24-40 h, allowing only 10-12% conversion in 48 h *vs.* 95-96% conversion for **RuPr** and **RuBn** catalysts, in 6 h and 23 h respectively (Figure 12). However, the mass balance and selectivity in dimer for these unsymmetrical catalysts **RuPrGH-II** and **RuBnGH-II** were similar to those of **RuPr** and **RuBn** catalysts (Figure 13, 14 and Table 4). This result further confirmed that the selectivity for cyclic oligomers in RO-RCM of cyclooctene is indeed due to the unsymmetrical nature of NHC. It also shows that changing from Grubbs-type catalysts to Grubbs-Hoveyda type catalysts, mainly affected initiation as expected (replacement of PCy_3 *via* a RO-tether alkylidene).

Table 4: Comparison of selectivity of cyclic products and mass balance at 30-40% conversion of cyclooctene.

Catalyst	Initial rate [mol/mol Ru/h]	Selectivity (%)				Mass balance (%)
		Dimer	Trimer	Tetramer	Pentamer	
RuPr	2343	48	24	11	5	88
RuBn	505	50	24	10	4	88
RuPrGH-II	310 / 24 h	49	20	6	2	78
RuBnGH-II	821 / 33 h	53	22	7	3	84

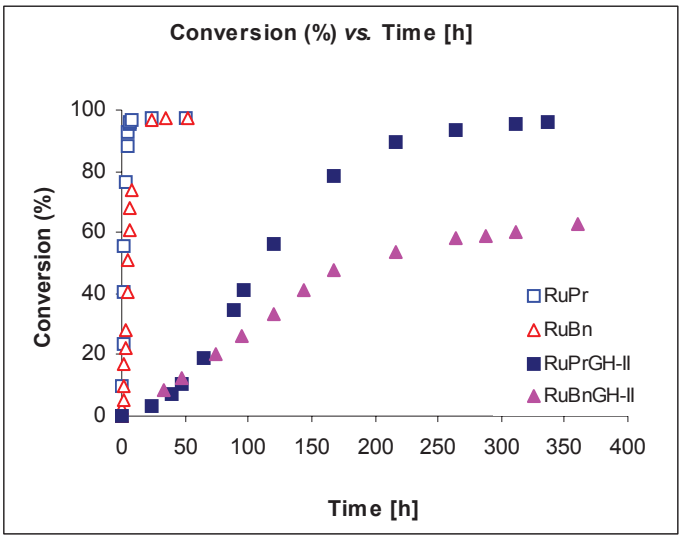

Figure 12: Conversion of cyclooctene (%) *vs.* time [h].

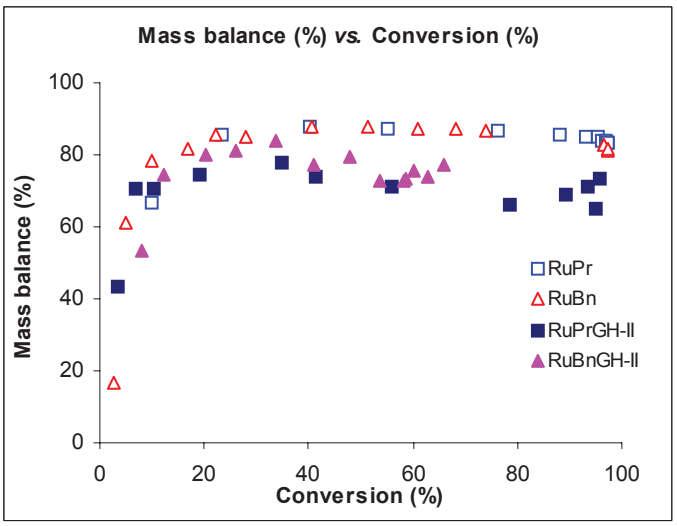

Figure 13: Mass balance (%) *vs.* conversion of cyclooctene (%).

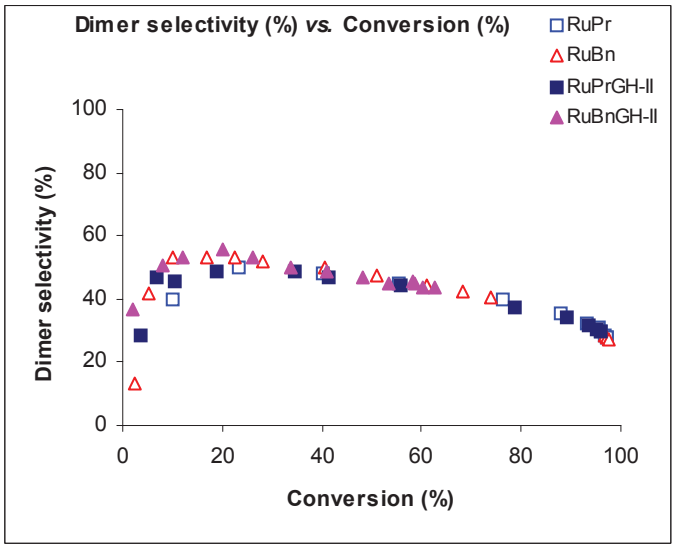

Figure 14: Dimer selectivity (%) *vs.* conversion of cyclooctene (%).

2.2.4.2. Comparison of catalytic performances of unsymmetrical homogeneous *vs.* immobilized GH-II type catalysts

Furthermore, the immobilized **RuPrGH-II/silica** (6-8% conversion) and **RuBnGH-II/silica** (5-6% conversion) displayed much lower initiation rate with almost no conversion within 250 h in sharp contrast to the molecular complexes **RuPrGH-II** (95-96% conversion) and **RuBnGH-II** (60-65% conversion) (Figure 15). This result shows that the surface was detrimental to the reaction rate, as previously observed when comparing **RuGH-II/silica** and **GH-II**. Note that this detrimental effect was not observed for the hybrid mesostructured catalysts and for which the surface has a stabilising effect.

It is also noteworthy that the mass balance and the selectivity in dimer for **RuPrGH-II** and **RuBnGH-II** were almost similar to those of their immobilized counterparts for the observed minimum conversion, indicating that there is probably no modification of the active sites (Figure 16, 17). Furthermore, all the immobilized catalysts showed similar mass balance and selectivity of dimer (Table 5). However, no improvement in the selectivity of cyclic oligomers after immobilization of unsymmetrical catalysts was observed, indicating that the surface did not influence the selectivity in RO-RCM of cyclooctene and that here the catalytic TON could be attributed to homogeneous "active sites" (in sharp contrast with what was observed with **RuGH-II/silica**).

Table 5: Comparison of selectivity of cyclic products and mass balance at 5-8% conversion of cyclooctene.

Catalyst	Conversion (%)	Selectivity (%)				Mass balance (%)
		Dimer	Trimer	Tetramer	Pentamer	
RuPrGH-II	7	**47**	17	5	2	71
RuBnGH-II	8	**36**	12	5	0	53
RuPrGH-II/silica	6	**39**	17	6	3	66
RuBnGH-II/silica	5	**29**	12	5	2	47
RuGH-II/silica	7	**35**	20	9	4	69

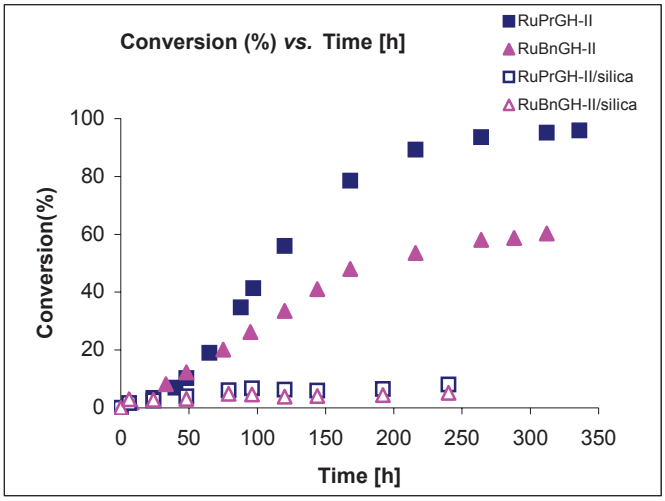

Figure 15: Conversion of cyclooctene (%) *vs.* time [h].

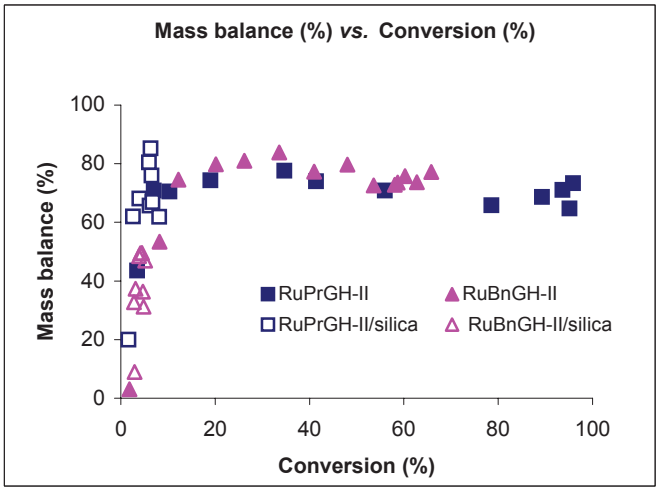

Figure 16: Mass balance (%) *vs.* conversion of cyclooctene (%).

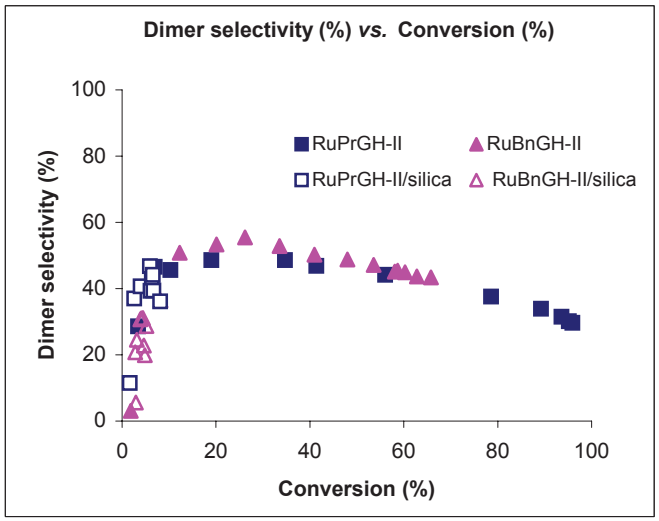

Figure 17: Dimer selectivity (%) *vs.* conversion of cyclooctene (%).

3. Conclusion

- The adsorption of **GH-II** complex on silica induced the reversal of products selectivity (*i.e.* here small cyclic oligomers are formed), if compared to **GH-II** complex which produces mainly polymers and/or higher oligomers.
- Immobilized unsymmetrical catalysts (**RuPrGH-II/silica** and **RuBnGH-II/silica)** showed little activity if compared to **RuGH-II/silica** with no improvement in the selectivity of cyclic oligomers.
- In all cases, while surface could bring selectivity, it is detrimental to the reaction rate, probably through retardation of catalyst initiation. Such an effect was further enhanced in case of unsymmetrical **GH-II** type catalysts because of the initiation mechanism that involved a rotation of the alkylidene ligand in place.
- The catalytic performances of unsymmetrical catalysts **RuPrGH-II** and **RuBnGH-II** were found to be similar to those of **RuPr** and **RuBn** catalysts, in terms of dimer selectivity and mass balance, thus confirming that the unsymmetrical nature of NHC was a key for low cyclic oligomers selectivity in RO-RCM of cyclooctene.

4. Experimental section

4.1. General procedure for the synthesis of adsorbed heterogeneous catalysts using GH-II type catalysts

4.1.1. Reaction scheme

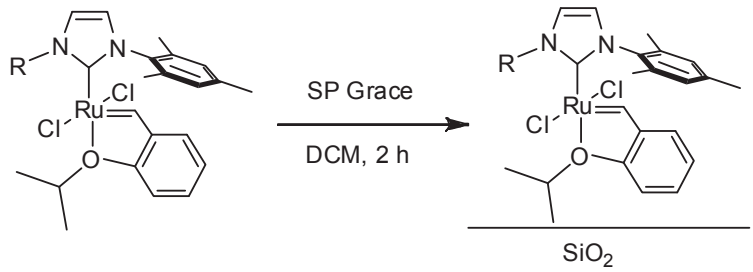

GH-II , R = Mesityl
RuPrGH-II, R = propyl
RuBnGH-II, R = benzyl

RuGH-II/silica , R = Mesityl
RuPrGH-II/silica, R = propyl
RuBnGH-II/silica, R = benzyl

4.1.2. Synthesis

The "best" BASF catalyst (optimized loading and support) was prepared using Grace SP 550 – 10020 support pretreated at 550 °C under 'Ar', with a heating ramp of 5 °C/min and plateau kept at 550 °C for 5 h (this support was characterized by pyridine adsorption, see section 3.1.2). To 1.0 g of this "activated" support in dichloromethane (10 mL), was added a dichloromethane solution of GH II type catalyst (4 mg, 0.064%$_{wt}$ of Ru), and the resulting suspension was stirred for 2 h. After removal of dichloromethane at 50 °C under vacuum, the obtained catalysts were stored in the glove box.

4.2. Synthesis of homogeneous catalysts

4.2.1. Synthesis of RuPrGH-II

4.2.1.1. Reaction scheme

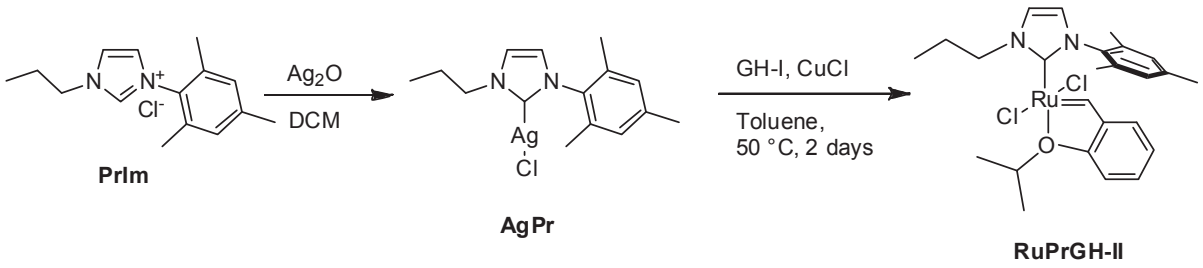

4.2.1.2. Synthesis of RuPrGH-II

To a solution of (1-mesityl-3-propyl-imidazol-2-ylidene) AgI (0.42 g, 0.9 mmol) in 10 mL of toluene, were added CuCl (0.089 g, 0.9 mmol) and GH-I (0.46 g, 0.77 mmol). The reaction mixture was stirred for 2 days at 50 °C. The reaction mixture was filtered over Celite. The solvent was removed under vacuum and the solid product was purified by column chromatography using acetone and pentane mixture (25:75) yielding 0.4 g of **RuPrGH-II**.

^{1}H NMR (CD_2Cl_2, 300 MHz): δ (ppm) = 16.39 (s, 1H, (-*H*C=Ru)), 7.62 (m, 1H), 7.33 (d, 1H, J = 2.1 Hz), 7.17 (brs, 2H, z), 7.05 (m, 2H), 7.03 (s, 1H), 6.95 (d, 1H, J = 2.1 Hz), 5.22 (m, 1H), 4.87 (m, 2H), 2.54 (s, 3H), 2.26 (m, 2H), 2.02 (s, 6H), 1.79 (d, 6H, J = 6.0Hz), 1.21 (t, 3H, J = 7.5Hz). ^{13}C NMR (CD_2Cl_2, 75 MHz): δ (ppm) = 288.5 (-HC=Ru), 172.7 (C_{NHC}=Ru), 153.2 C_{ar}, 145.1 C_{ar}, 140.6 C_{ar}, 138.2 C_{ar}, 130 C_{ar}, 129.8 C_{ar}, 125.4 C_{ar}, 123.5 C_{ar}, 122.6 C_{ar}, 122.2 C_{ar}, 76.09 (-***C***H(CH_3)$_2$), 54.4 (CH_2-N), 25.1 (-CH_2), 22.6 (Ar-CH_3), 21.9 (CH(***C***H_3)$_2$) , 18.5 (Ar-CH_3), 12 (-CH_3) . HRMS (ESI+): 513.1229 m/z $[M-Cl]^+$ *i.e.* 513.1244 m/z calculated.

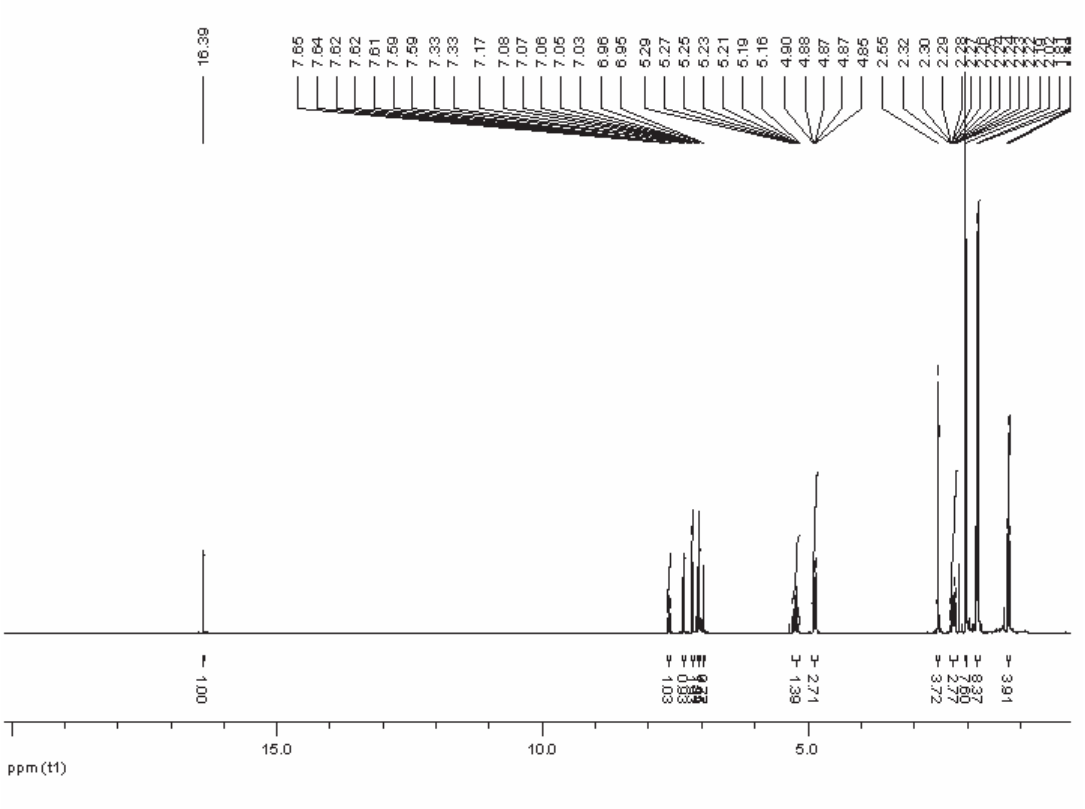

Figure 18: ^{1}H NMR of **RuPrGH-II**.

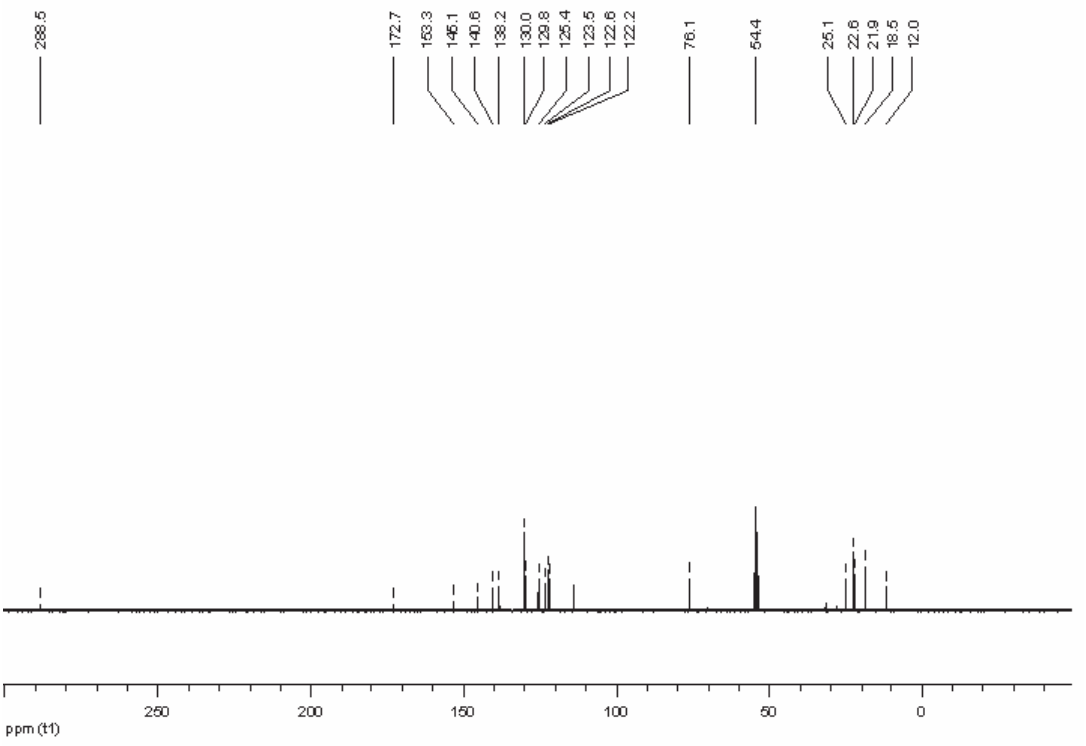

Figure 19: ^{13}C NMR of **RuPrGH-II**.

a) High resolution mass spectrum (ESI+) of **RuPrGH-II**.

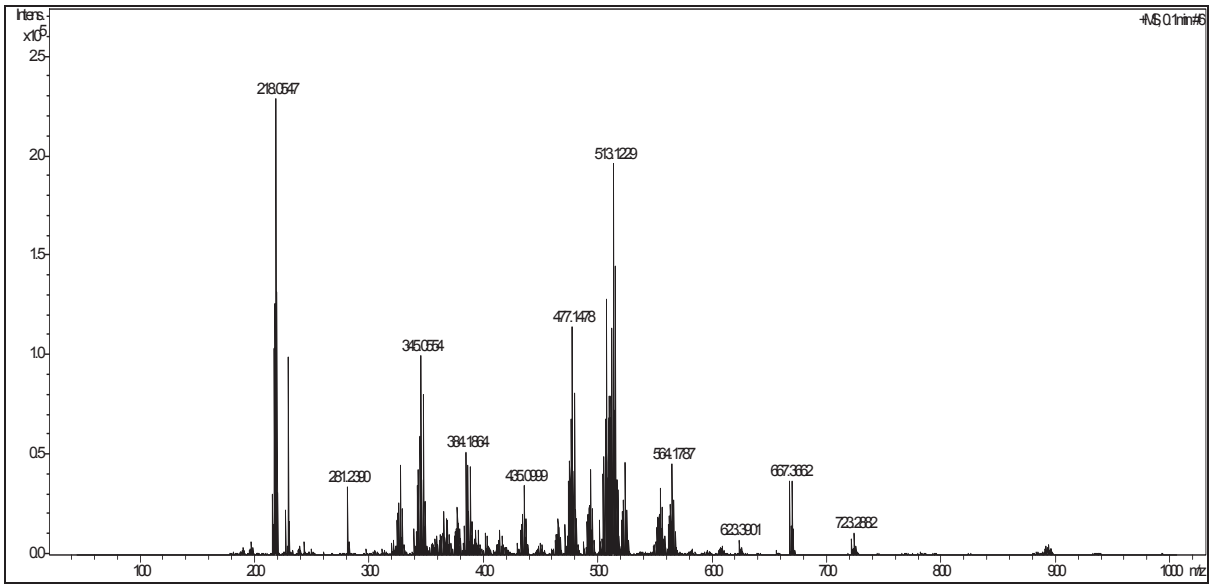

b) Experimental molecule ion spectrum and simulated spectrum.

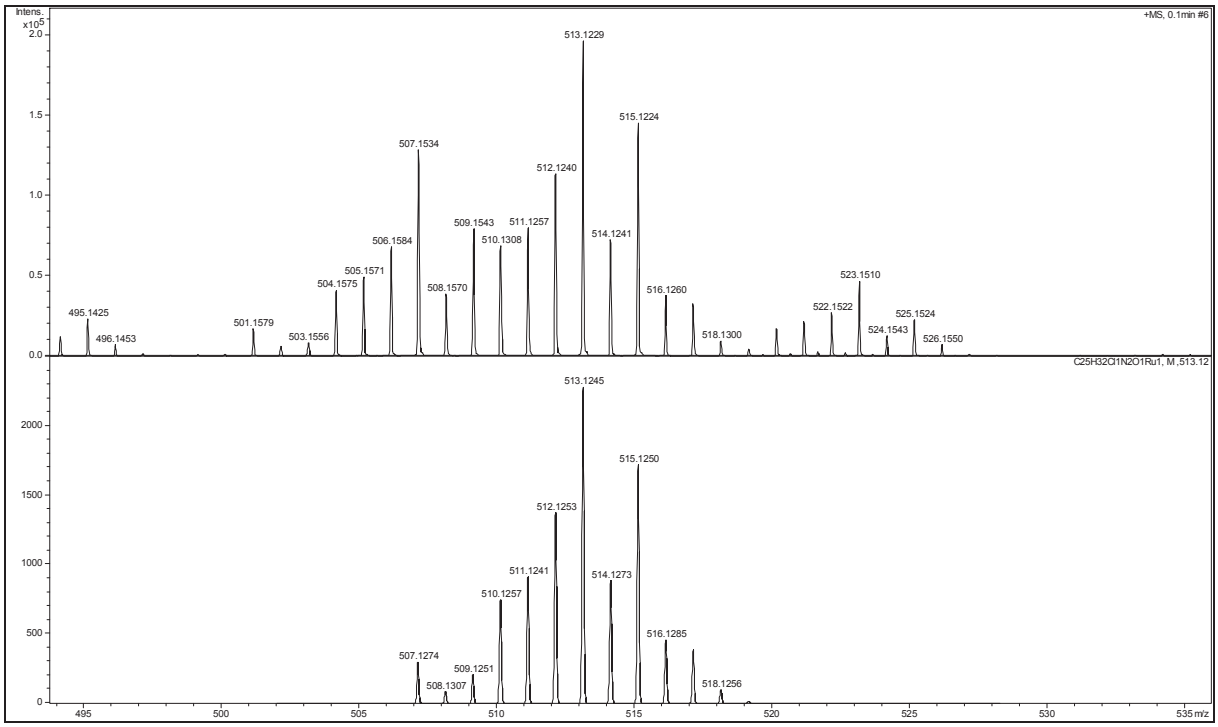

Figure 20: a) High resolution mass spectrum (ESI+) of RuPrGH-II b) Experimental molecule ion spectrum. c) Simulated spectrum.

4.2.2. Synthesis of RuBnGH-II

4.2.2.1. Reaction scheme

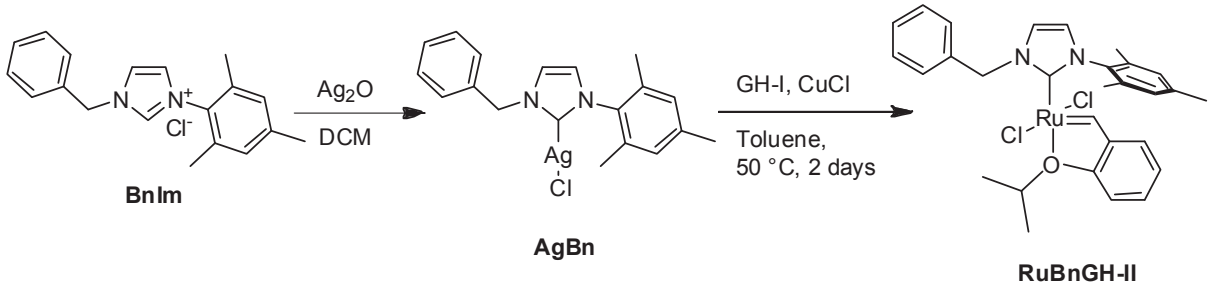

4.2.2.2. Synthesis of RuBnGH-II

To a solution of (1-mesityl-3-benzyl-imidazol-2-ylidene) AgCl (0.42 g, 1.0 mmol) in 10 mL of toluene, were added CuCl (0.098 g, 1.0 mmol) and GH-I (0.51 g, 0.85 mmol). The reaction mixture was stirred for 2 days at 50°C. The reaction mixture was filtered over Celite. The solvent was removed under vacuum and the solid product was purified by column chromatography using acetone and pentane mixture (25:75) yielding 0.38 g of **RuBnGH-II**.

^{1}H NMR (CD_2Cl_2, 300 MHz): δ (ppm) = 16.37 (s, 1H, (-*H*C=Ru)), 7.60-7.70 (m, 3H), 7.50 (m, 2H, J = 2.1 Hz), 7.19 (brs, 2H), 7.05 (m, 3H), 6.90 (d, 1H, J = 2.1 Hz), 6.94 (d, 1H, J = 2.1 Hz), 6.17 (s, 2H), 5.22 (m, 1H), 4.87 (m, 2H), 2.56 (s, 3H), 2.07 (s, 6H), 1.77 (d, 6H, J = 6.0Hz). ^{13}C NMR (CD_2Cl_2, 75 MHz): δ (ppm) = 287.7 (-HC=Ru), 173.6 (C_{NHC}=Ru), 153.3 C_{ar}, 144.9 C_{ar}, 140.7 C_{ar}, 138.0 C_{ar}, 136.8 C_{ar}, 130.3 C_{ar}, 130.0 C_{ar}, 129.8 C_{ar}, 128.7 C_{ar}, 129.4 C_{ar}, 125.4 C_{ar}, 123.5 C_{ar}, 122.5 $C_{ar,}$ 122.3 $C_{ar,}$ 113.8 $C_{ar,}$ 76.2 (-*C*H(CH_3)$_2$), 56.2 (Ph*C*H_2-N), 26.8 (-CH_2), 22.6 (Ar-CH_3), 21.8 (CH(*C*H_3)$_2$) , 18.5 (Ar-CH_3). HRMS (ESI+): 557.1721 m/z [M-2Cl + CHO^-]$^+$ *i.e.* 557.1744 m/z calculated.

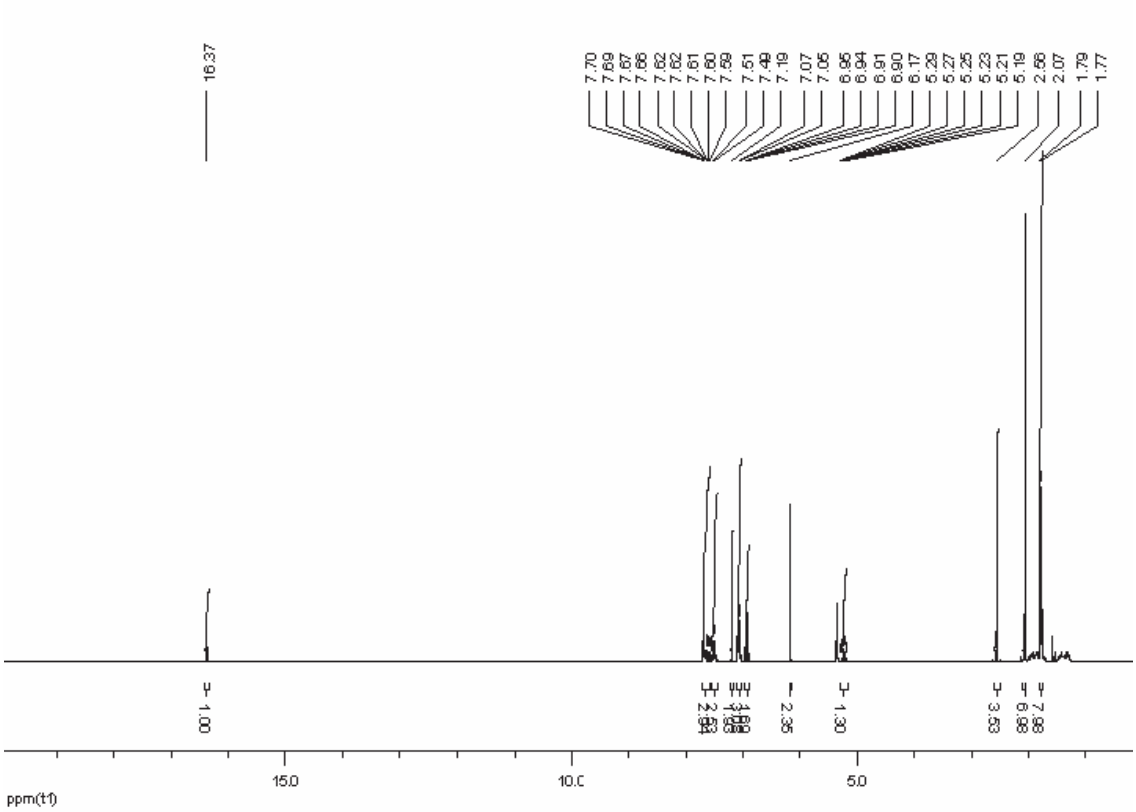

Figure 21: ^{1}H NMR of **RuBnGH-II**.

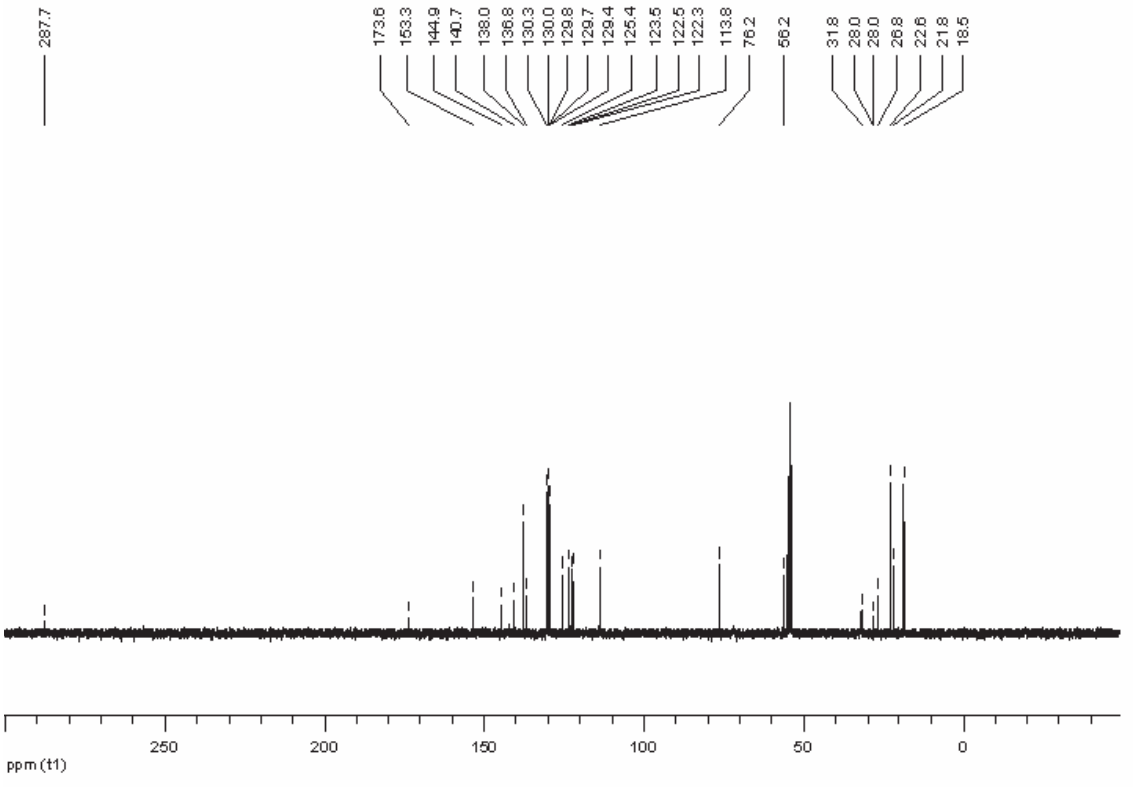

Figure 22: ^{13}C NMR of **RuBnGH-II**.

a) High resolution mass spectrum (ESI+) of **RuBnGH-II**.

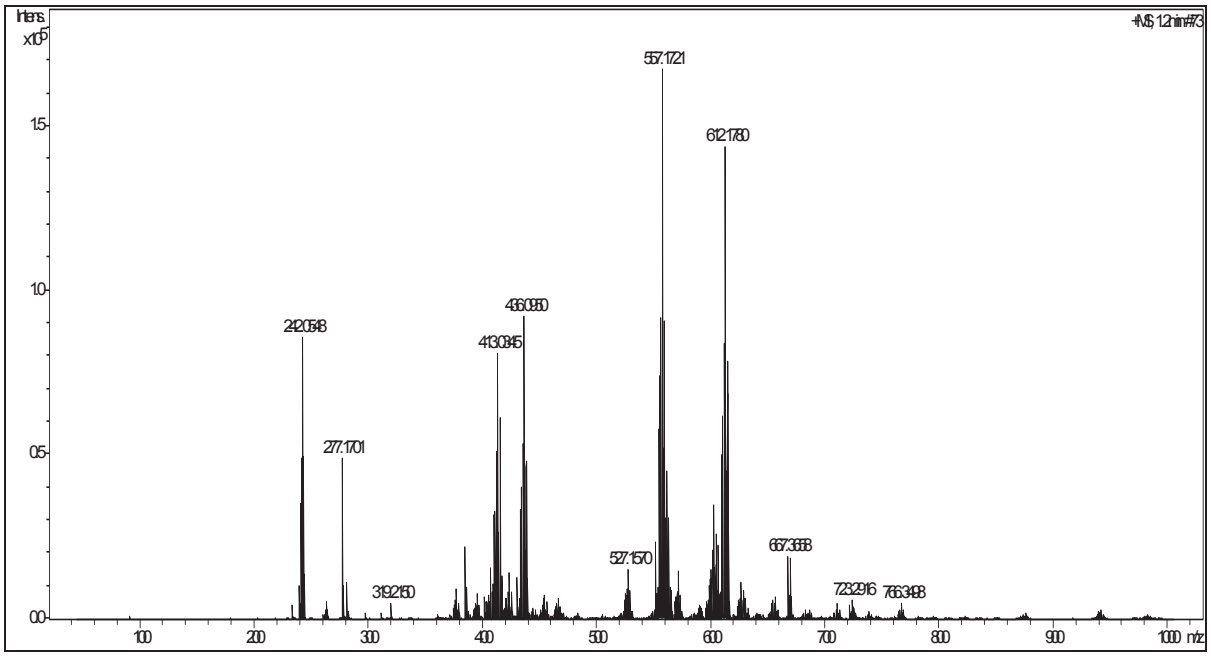

b) Experimental molecule ion spectrum and Simulated spectrum.

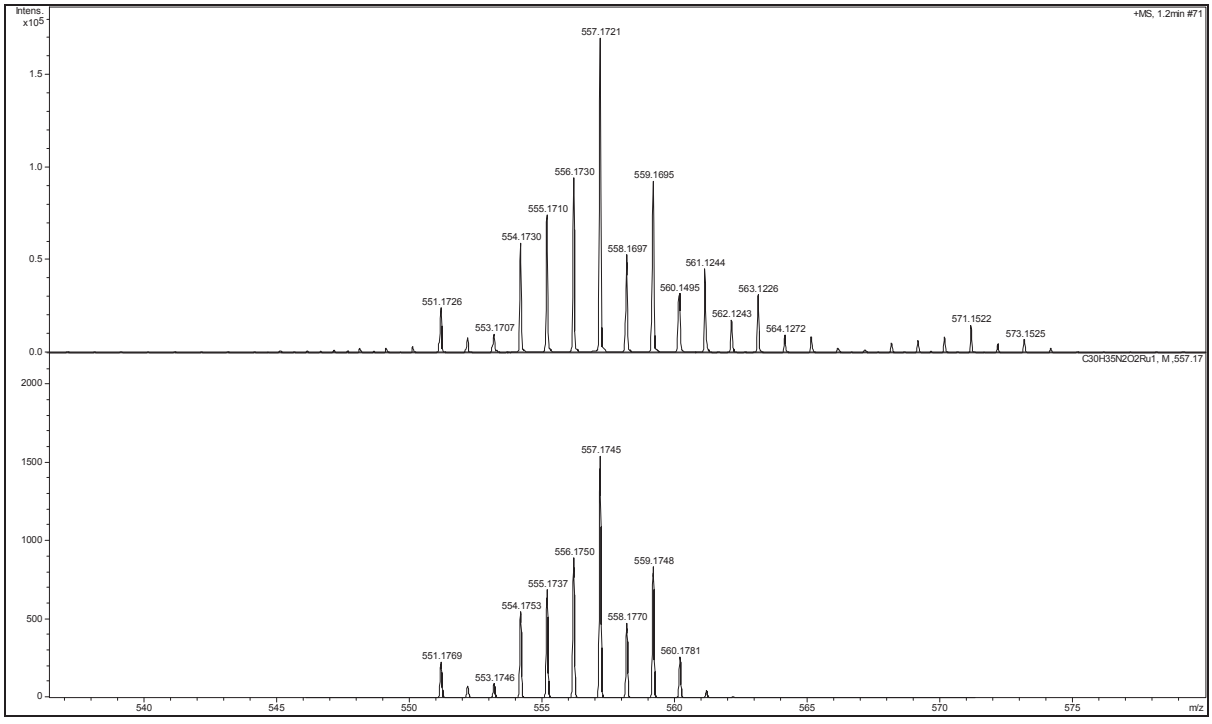

Figure 23: a) High resolution mass spectrum (ESI+) of **RuBnGH-**II b) Experimental molecule ion spectrum and simulated spectrum.

4.3. Catalytic performances

Catalytic tests:

All metathesis experiments were carried out under an inert atmosphere, in a glove-box. Toluene was dried over NaK and distilled under nitrogen prior to use. Cyclooctene (*cis*-cyclooctene) was purchased from Aldrich, distilled over Na prior to use. Catalysts Grubbs second generation catalyst was purchased from Aldrich and catalyst (Nolan) was synthesized according to the literature procedures.

Representative procedure for heterogeneous catalysts: Eicosane was dissolved in ~20 mM toluene solution of cyclooctene. Sample was taken for GC analysis as a reference. Heterogeneous Ru-catalyst was added to the solution of cyclooctene, at room temperature. The progress of the metathesis reaction was monitored by sampling at suitable intervals. The samples were immediately quenched by an excess of ethyl acetate. The samples were analysed by GC with a HP5 column

5. Appendix

5.1. Catalytic performances

5.1.1. GH-II

Table 6: Catalytic performances of **GH-II** in the RO-RCM of cyclooctene.

Time [h]	Conversion (%)	Sel-dimer (%)	Sel-trimer (%)	Sel-tetra (%)	Sel-penta (%)	Mass balance (%)
1.0	4.3	**65**	10	3	0	78
1.5	7.0	**53**	8	2	0	63
2.0	8.5	**52**	8	2	0	62
3.0	13.0	**45**	7	1	0	54
4.0	16.9	**43**	6	2	1	52
5.0	26.1	**37**	6	1	0	45
6.0	34.5	**34**	5	1	1	40
7.0	52.0	**35**	7	2	1	44
11.0	82.8	**24**	4	1	1	31
24.0	91.1	**19**	4	1	1	24
33.0	88.4	**17**	3	1	0	22
46.0	90.3	**17**	4	1	1	23
59.0	94.2	**20**	6	2	1	29
71.0	93.4	**20**	6	2	1	28
80.0	95.7	**20**	11	5	2	39
100.0	96.3	**22**	13	5	3	43

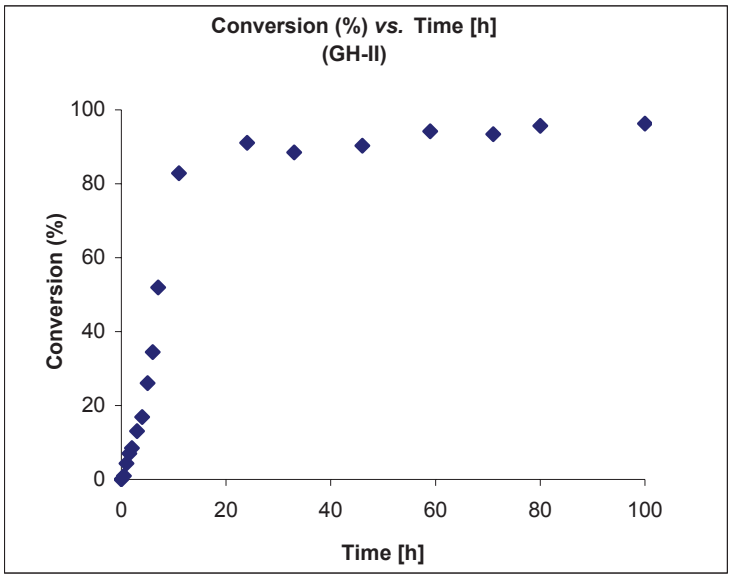

Figure 24: Conversion of cyclooctene (%) *vs.* time [h] using **GH-II**.

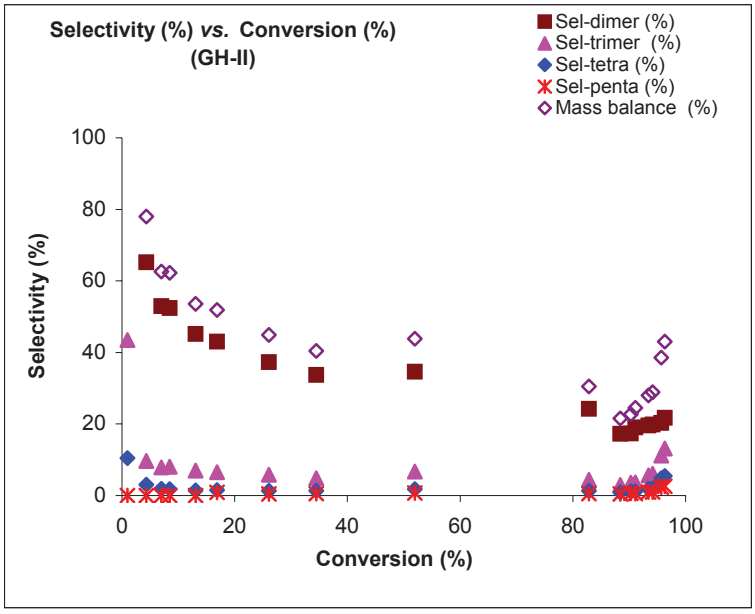

Figure 25: Selectivity of cyclic oligomers (%) *vs.* conversion of cyclooctene (%) using **GH-II**.

5.1.2. RuPrGH-II

Table 7: Catalytic performances of **RuPrGH-II** in the RO-RCM of cyclooctene.

Time [h]	Conversion (%)	TON	Sel-dimer (%)	Sel-trimer (%)	Sel-tetra (%)	Sel-penta (%)	Mass balance (%)
24.0	3.4	310	**29**	12	3	0	44
40.0	7.0	628	**47**	17	5	2	71
48.0	10.3	926	**46**	18	5	2	71
65.0	19.0	1712	**49**	18	6	2	74
88.0	34.7	3121	**49**	20	6	2	78
97.0	41.4	3725	**47**	19	6	2	74
120.0	56.0	5040	**44**	19	6	2	71
168.0	78.6	7073	**38**	20	6	2	66
216.0	89.2	8032	**34**	23	8	4	69
264.0	93.6	8423	**31**	25	10	5	71
312.0	95.1	8562	**30**	23	8	3	65
336.0	95.9	8630	**30**	27	12	5	73

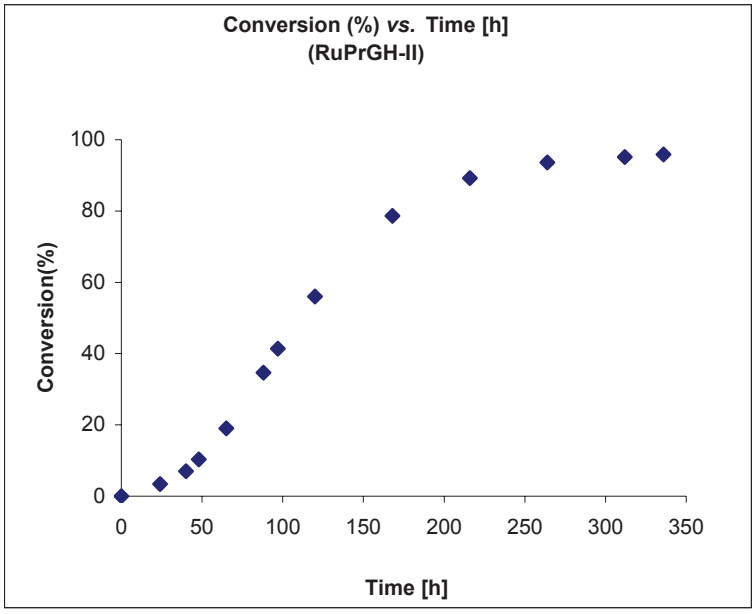

Figure 26: Conversion of cyclooctene (%) *vs.* time [h] using **RuPrGH-II**.

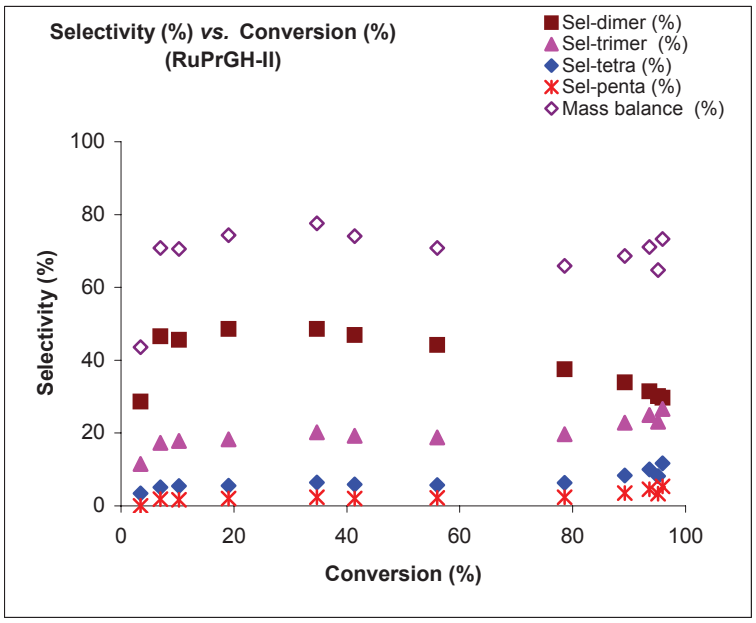

Figure 27: Selectivity of cyclic oligomers (%) *vs.* conversion of cyclooctene (%) using **RuPrGH-II**.

5.1.3. RuBnGH-II

Table 8: Catalytic performances of **RuBnGH-II** in the RO-RCM of cyclooctene.

Time [h]	Conversion (%)	TON	Sel-dimer (%)	Sel-trimer (%)	Sel-tetra (%)	Sel-penta (%)	Mass balance (%)
33.0	8.2	821	**36**	12	5	0	53
48.0	12.2	1224	**51**	18	4	1	75
75.0	20.1	2014	**53**	19	5	2	80
95.0	26.2	2620	**55**	19	5	1	81
120.0	33.6	3355	**53**	22	7	3	84
144.0	41.0	4100	**50**	19	6	2	77
168.0	48.0	4802	**49**	21	7	3	80
216.0	53.6	5359	**47**	17	6	2	73
264.0	58.1	5806	**45**	20	6	2	73
288.0	58.7	5870	**45**	20	6	2	74
312.0	60.2	6023	**45**	21	7	2	76
360.0	62.8	6279	**44**	21	7	2	74
432.0	65.8	6577	**43**	23	8	3	77

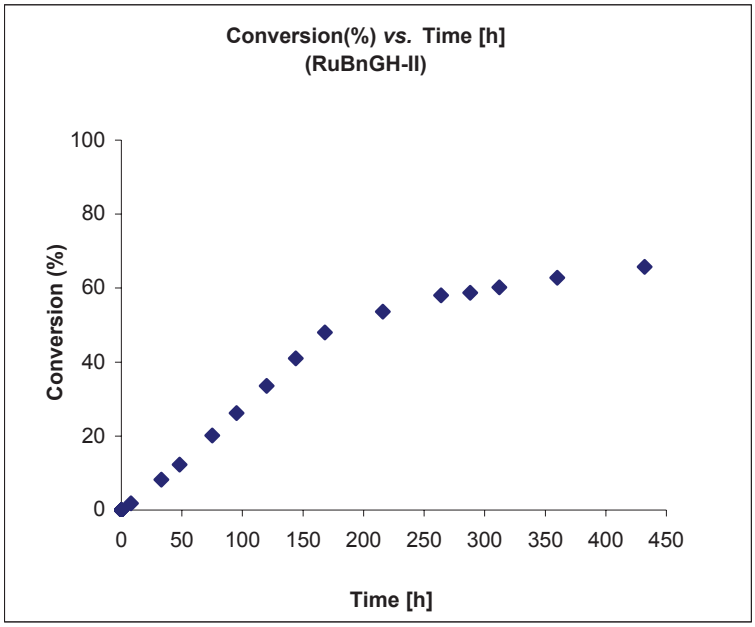

Figure 28: Conversion of cyclooctene (%) *vs.* time [h] using **RuBnGH-II**.

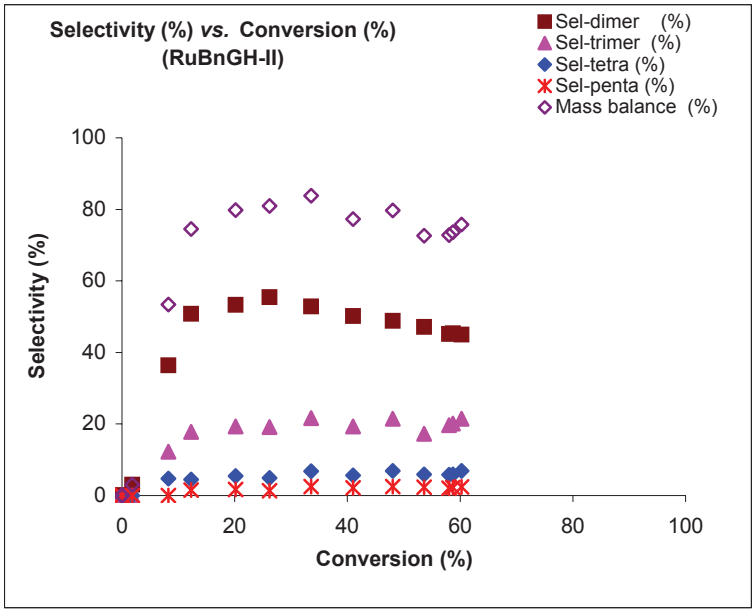

Figure 29: selectivity of cyclic oligomers (%) *vs.* Conversion of cyclooctene (%)using **RuBnGH-II**.

5.1.4. RuGH-II/silica

Table 9: Catalytic performances of **RuGH-II/silica** in the RO-RCM of cyclooctene.

Time [h]	Conversion (%)	TON	Sel-dimer (%)	Sel-trimer (%)	Sel-tetra (%)	Sel-penta (%)	Mass balance (%)
0.5	1.9	187	**12**	7	4	0	23
1.0	2.7	267	**24**	14	6	0	44
1.5	5.0	501	**29**	18	8	3	59
2.0	4.9	493	**30**	19	9	4	63
2.5	6.3	632	**33**	20	9	3	64
3.0	7.4	737	**35**	20	9	4	69
3.5	8.3	831	**38**	21	10	4	72
4.0	10.2	1021	**37**	21	8	3	70
4.5	11.0	1095	**37**	21	9	4	71
5.0	11.5	1150	**40**	21	9	3	73
5.5	11.9	1189	**42**	23	9	3	77
6.0	13.4	1336	**40**	22	9	3	75
6.5	14.0	1402	**41**	23	10	4	77
7.0	15.0	1498	**41**	23	10	4	78
22.0	31.1	3105	**43**	20	7	3	72
56.0	49.5	4952	**40**	19	7	3	69
126.0	73.2	7324	**39**	25	6	6	76

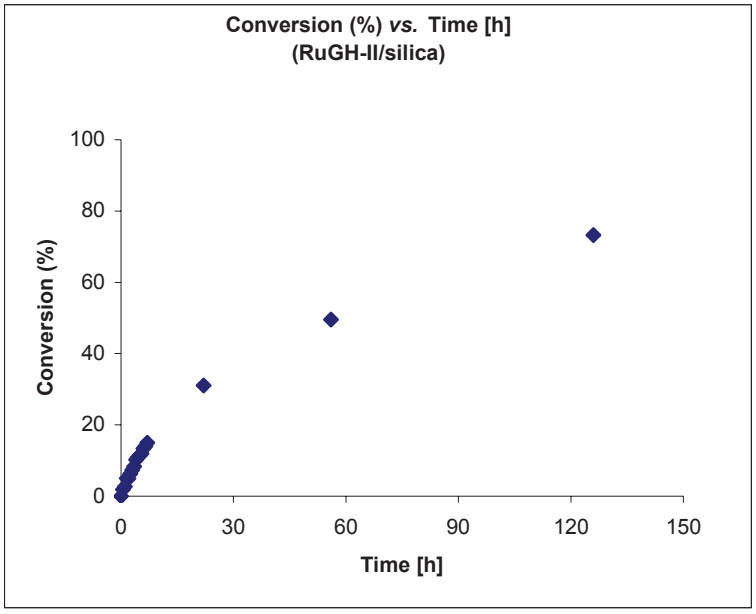

Figure 30: Conversion of cyclooctene (%) *vs.* time [h] using **RuGH-II/silica**.

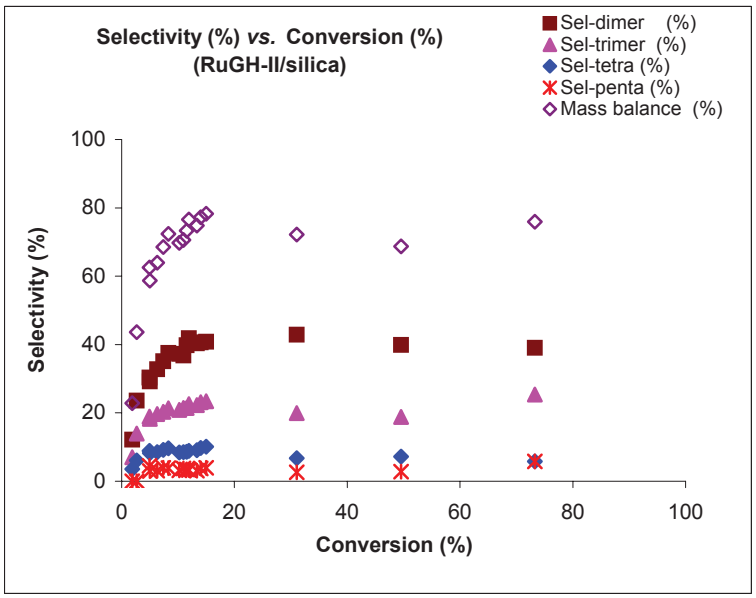

Figure 31: Dimer selectivity (%) *vs.* conversion of cyclooctene (%) using **RuGH-II/silica**.

5.1.5. RuPrGH-II/silica

Table 10: Catalytic performances of **RuPrGH-II/silica** in the RO-RCM of cyclooctene.

Time [h]	Conversion (%)	TON	Sel-dimer (%)	Sel-trimer (%)	Sel-tetra (%)	Sel-penta (%)	Mass balance (%)
6.0	1.6	164	**11**	5	4	0	20
24.0	2.6	259	**37**	16	7	2	62
48.0	3.9	394	**41**	18	7	3	68
79.0	6.1	609	**39**	17	6	3	66
96.0	6.7	670	**39**	17	7	3	67
120.0	6.3	634	**43**	19	20	3	85
144.0	5.9	594	**47**	21	8	4	81
192.0	6.5	653	**44**	20	8	4	76
240.0	8.1	812	**36**	16	7	3	62

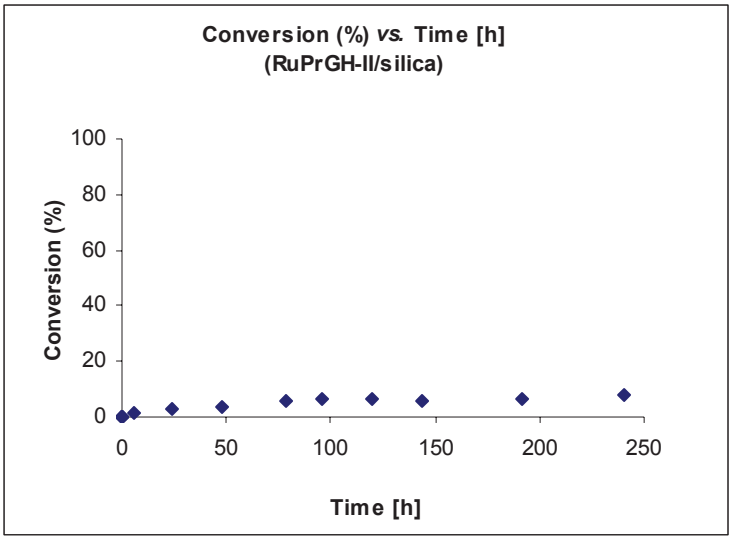

Figure 32: Conversion of cyclooctene (%) *vs.* time [h] using **RuPrGH-II/silica**.

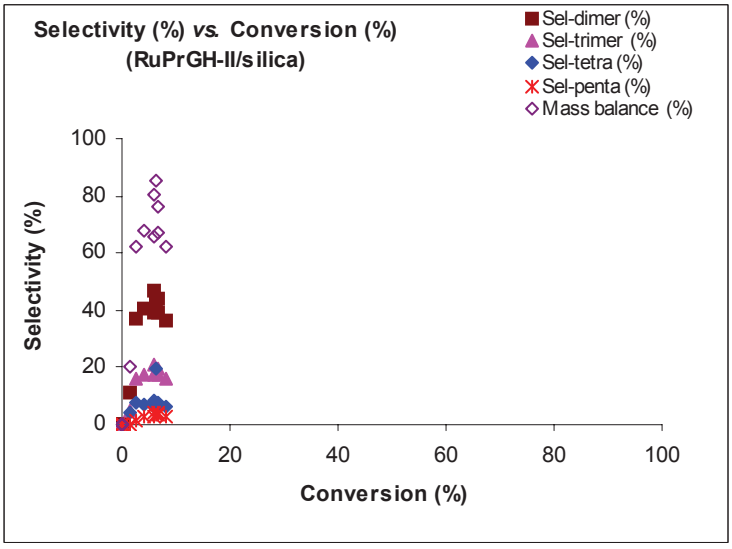

Figure 33: Dimer selectivity (%) *vs.* Conversion of cyclooctene (%) using **RuPrGH-II/silica**.

5.1.6. RuBnGH-II/silica

Table 11: Catalytic performances of **RuBnGH-II/silica** in the RO-RCM of cyclooctene.

Time [h]	Conversion (%)	TON	Sel-dimer (%)	Sel-trimer (%)	Sel-tetra (%)	Sel-penta (%)	Mass balance (%)
6.0	2.9	295	**6**	2	2	0	9
24.0	2.8	279	**21**	8	4	0	33
48.0	3.1	315	**24**	9	4	0	37
79.0	4.8	483	**20**	8	3	0	31
96.0	4.7	467	**23**	9	3	1	36
120.0	3.9	388	**31**	12	5	1	48
144.0	4.1	411	**31**	12	5	2	49
192.0	4.5	446	**31**	12	5	2	50
240.0	5.2	515	**29**	12	5	2	47

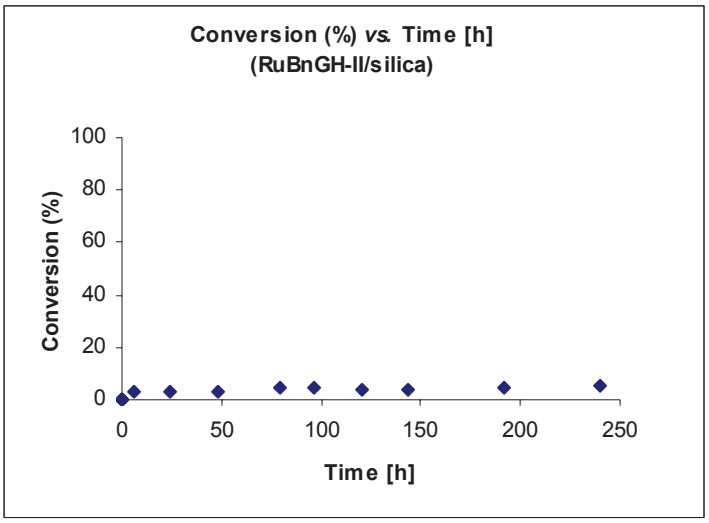

Figure 34: Conversion of cyclooctene (%) *vs.* time [h] using **RuBnGH-II/silica**.

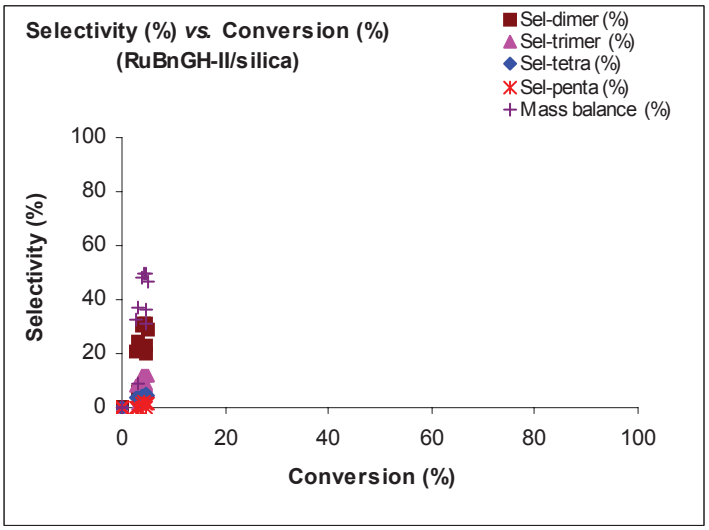

Figure 35: Dimer selectivity (%) *vs.* Conversion of cyclooctene (%) using **RuBnGH-II/silica**

5.1.7. X-ray crystal structures

5.1.7.1. X-ray structure of RuPrGH-II

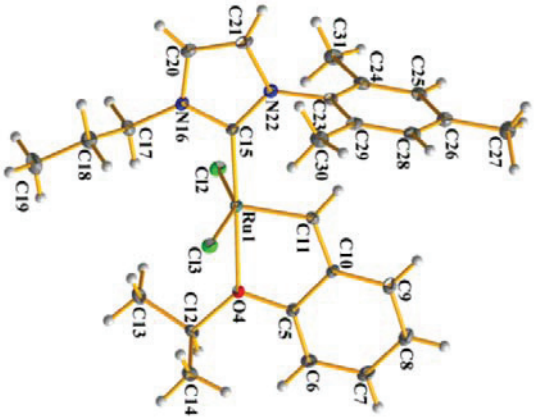

Figure 36: X-ray crystal structure of **RuPrGH-II**.

Crystal data

$C_{25}H_{32}Cl_2N_2ORu$	$F(000) = 1128$
$M_r = 548.52$	$D_x = 1.413$ Mg m^{-3}
Orthorhombic, $P2_12_12_1$	Mo $K\alpha$ radiation, $\lambda = 0.7107$ Å
Hall symbol: P 2ac 2ab	Cell parameters from 8534 reflections
$a = 10.684$ (1) Å	$\theta = 3.5–29.5°$
$b = 15.195$ (1) Å	$\mu = 0.83$ mm^{-1}
$c = 15.885$ (1) Å	$T = 100$ K
$V = 2578.8$ (3) Å^3	Plate, dark brown
$Z = 4$	0.56 × 0.20 × 0.09 mm

Data collection

Xcalibur, Atlas, Gemini ultra diffractometer	6404 independent reflections
Radiation source: Enhance (Mo) X-ray Source	5725 reflections with $I > 2.0\sigma(I)$
graphite	$R_{int} = 0.045$
Detector resolution: 10.4685 pixels mm^{-1}	$\theta_{max} = 29.6°$, $\theta_{min} = 3.5°$
ω scans	$h = -14 \rightarrow 14$
Absorption correction: analytical *CrysAlis PRO*, Agilent Technologies, Version 1.171.35.11 (release 16-05-2011 CrysAlis171 .NET) (compiled May 16 2011,17:55:39) Analytical numeric absorption correction using a multifaceted crystal model based on expressions derived by R.C. Clark & J.S. Reid. (Clark, R. C. & Reid, J. S. (1995). Acta Cryst. A51, 887-897)	$k = -20 \rightarrow 19$
$T_{min} = 0.853$, $T_{max} = 0.934$	$l = -21 \rightarrow 19$
26520 measured reflections	

Refinement

Refinement on F^2	H-atom parameters constrained
Least-squares matrix: full	Method, part 1, Chebychev polynomial, (Watkin, 1994, *P*rince, 1982) [*w*eight] = $1.0/[A_0*T_0(x) + A_1*T_1(x) \cdots + A_{n-1}]*T_{n-1}(x)]$ where A_i are the Chebychev coefficients listed below and x = *F* /*F*max Method = Robust Weighting (*P*rince, 1982) W = [*w*eight] * [1-(delta*F*/6*sigma*F*)^2]^2 A_i are: 357. 449. 278. 112. 25.5
$R[F^2 > 2\sigma(F^2)] = 0.038$	$(\Delta/\sigma)_{max} = 0.001$
$wR(F^2) = 0.090$	$\Delta\rangle_{max} = 1.24$ e Å^{-3}
$S = 0.93$	$\Delta\rangle_{min} = -1.49$ e Å^{-3}
6404 reflections	Extinction correction: Larson (1970), Equation 22
282 parameters	Extinction coefficient: 117 (15)
0 restraints	Absolute structure: Flack (1983), 2660 Friedel-pairs
Primary atom site location: structure-invariant direct methods	Flack parameter: -0.06 (4)
Hydrogen site location: difference Fourier map	

Geometric parameters (Å, º)

Ru1—Cl2	2.3330 (10)	C17—H172	0.977
Ru1—Cl3	2.3377 (10)	C17—H171	0.969
Ru1—O4	2.246 (3)	C18—C19	1.508 (7)
Ru1—C11	1.832 (4)	C18—H182	0.976
Ru1—C15	1.985 (4)	C18—H181	0.970
O4—C5	1.373 (5)	C19—H191	0.964
O4—C12	1.469 (5)	C19—H192	0.959
C5—C6	1.381 (5)	C19—H193	0.965
C5—C10	1.414 (6)	C20—C21	1.347 (6)
C6—C7	1.393 (6)	C20—H201	0.927
C6—H61	0.926	C21—N22	1.389 (5)
C7—C8	1.382 (7)	C21—H211	0.932
C7—H71	0.935	N22—C23	1.440 (5)
C8—C9	1.376 (6)	C23—C24	1.398 (6)
C8—H81	0.941	C23—C29	1.386 (6)
C9—C10	1.398 (5)	C24—C25	1.390 (6)
C9—H91	0.936	C24—C31	1.501 (6)
C10—C11	1.444 (5)	C25—C26	1.384 (7)
C11—H111	0.932	C25—H251	0.930
C12—C13	1.510 (6)	C26—C27	1.518 (7)
C12—C14	1.521 (6)	C26—C28	1.394 (7)

C12—H121	0.987	C27—H271	0.962
C13—H132	0.952	C27—H273	0.965
C13—H131	0.957	C27—H272	0.967
C13—H133	0.964	C28—C29	1.388 (7)
C14—H141	0.963	C28—H281	0.936
C14—H143	0.961	C29—C30	1.508 (7)
C14—H142	0.966	C30—H303	0.966
C15—N16	1.354 (5)	C30—H302	0.968
C15—N22	1.364 (5)	C30—H301	0.963
N16—C17	1.458 (5)	C31—H311	0.961
N16—C20	1.377 (5)	C31—H312	0.964
C17—C18	1.519 (6)	C31—H313	0.958
Cl2—Ru1—Cl3	153.15 (4)	N16—C17—H171	108.5
Cl2—Ru1—O4	88.09 (8)	C18—C17—H171	108.1
Cl3—Ru1—O4	90.34 (8)	H172—C17—H171	109.3
Cl2—Ru1—C11	102.64 (13)	C17—C18—C19	110.1 (4)
Cl3—Ru1—C11	103.41 (13)	C17—C18—H182	109.6
O4—Ru1—C11	79.44 (15)	C19—C18—H182	108.9
Cl2—Ru1—C15	90.22 (12)	C17—C18—H181	109.2
Cl3—Ru1—C15	90.58 (12)	C19—C18—H181	109.9
O4—Ru1—C15	177.87 (14)	H182—C18—H181	109.1
C11—Ru1—C15	102.21 (17)	C18—C19—H191	110.7
Ru1—O4—C5	110.7 (2)	C18—C19—H192	110.2
Ru1—O4—C12	129.0 (2)	H191—C19—H192	109.0
C5—O4—C12	119.0 (3)	C18—C19—H193	110.1
O4—C5—C6	125.8 (4)	H191—C19—H193	108.4
O4—C5—C10	112.8 (3)	H192—C19—H193	108.4
C6—C5—C10	121.4 (4)	N16—C20—C21	107.1 (4)
C5—C6—C7	118.4 (4)	N16—C20—H201	125.4
C5—C6—H61	121.2	C21—C20—H201	127.5
C7—C6—H61	120.4	C20—C21—N22	106.3 (4)
C6—C7—C8	121.3 (4)	C20—C21—H211	127.6
C6—C7—H71	119.5	N22—C21—H211	126.0
C8—C7—H71	119.3	C21—N22—C15	111.0 (4)
C7—C8—C9	120.0 (4)	C21—N22—C23	123.6 (4)
C7—C8—H81	120.3	C15—N22—C23	125.4 (3)
C9—C8—H81	119.7	N22—C23—C24	117.7 (4)
C8—C9—C10	120.8 (4)	N22—C23—C29	118.8 (4)
C8—C9—H91	119.3	C24—C23—C29	123.4 (4)

C10—C9—H91	119.9	C23—C24—C25	117.0 (4)
C5—C10—C9	118.1 (4)	C23—C24—C31	121.1 (4)
C5—C10—C11	118.0 (3)	C25—C24—C31	121.9 (4)
C9—C10—C11	123.9 (4)	C24—C25—C26	121.6 (4)
C10—C11—Ru1	119.0 (3)	C24—C25—H251	119.5
C10—C11—H111	119.8	C26—C25—H251	118.9
Ru1—C11—H111	121.1	C25—C26—C27	120.2 (5)
O4—C12—C13	106.0 (3)	C25—C26—C28	119.3 (4)
O4—C12—C14	110.0 (3)	C27—C26—C28	120.5 (5)
C13—C12—C14	112.2 (4)	C26—C27—H271	109.3
O4—C12—H121	108.8	C26—C27—H273	109.3
C13—C12—H121	110.4	H271—C27—H273	109.4
C14—C12—H121	109.3	C26—C27—H272	109.1
C12—C13—H132	107.6	H271—C27—H272	109.1
C12—C13—H131	109.4	H273—C27—H272	110.6
H132—C13—H131	110.0	C26—C28—C29	121.4 (4)
C12—C13—H133	109.5	C26—C28—H281	118.9
H132—C13—H133	109.7	C29—C28—H281	119.7
H131—C13—H133	110.6	C28—C29—C23	117.3 (4)
C12—C14—H141	109.1	C28—C29—C30	121.4 (4)
C12—C14—H143	109.4	C23—C29—C30	121.3 (4)
H141—C14—H143	109.2	C29—C30—H303	110.5
C12—C14—H142	110.3	C29—C30—H302	110.0
H141—C14—H142	109.3	H303—C30—H302	108.6
H143—C14—H142	109.4	C29—C30—H301	109.9
Ru1—C15—N16	120.7 (3)	H303—C30—H301	109.3
Ru1—C15—N22	135.2 (3)	H302—C30—H301	108.5
N16—C15—N22	104.1 (3)	C24—C31—H311	110.5
C15—N16—C17	124.2 (3)	C24—C31—H312	110.7
C15—N16—C20	111.4 (4)	H311—C31—H312	108.1
C17—N16—C20	124.3 (3)	C24—C31—H313	110.1
N16—C17—C18	114.1 (4)	H311—C31—H313	108.4
N16—C17—H172	108.2	H312—C31—H313	109.0
C18—C17—H172	108.6		

5.1.7.2. X-ray structure of RuBnGH-II

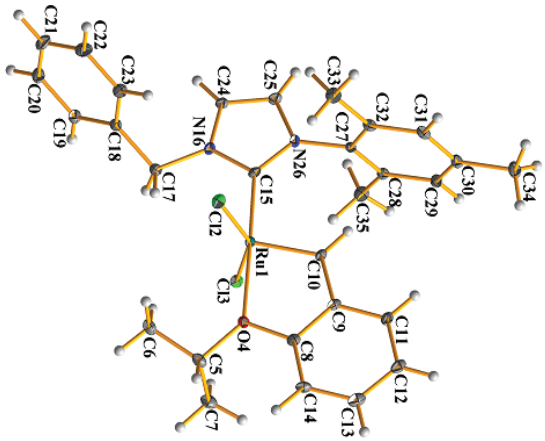

Figure 37: X-ray crystal structure of **RuBnGH-II**.

Crystal data

$C_{29}H_{32}Cl_2N_2ORu$	$F(000) = 1224$
$M_r = 596.56$	$D_x = 1.467$ Mg m^{-3}
Monoclinic, $P2_1/n$	Mo $K\alpha$ radiation, $\lambda = 0.7107$ Å
Hall symbol: -P 2yn	Cell parameters from 16912 reflections
$a = 11.9793$ (7) Å	$\theta = 3.4–29.5°$
$b = 14.2782$ (8) Å	$\mu = 0.80$ mm^{-1}
$c = 15.8058$ (8) Å	$T = 100$ K
$\beta = 92.238$ (5)°	Needle, dark brown
$V = 2701.4$ (3) Å^3	0.72 × 0.27 × 0.12 mm
$Z = 4$	

Data collection

Xcalibur, Atlas, Gemini ultra diffractometer	7089 independent reflections
Radiation source: Enhance (Mo) X-ray Source	5958 reflections with $I > 2.0\sigma(I)$
graphite	$R_{int} = 0.070$
Detector resolution: 10.4685 pixels mm^{-1}	$\theta_{max} = 29.6°$, $\theta_{min} = 3.4°$
ω scans	$h = -16 \rightarrow 16$
Absorption correction: analytical *CrysAlis PRO*, Agilent Technologies, Version 1.171.35.11 (release 16-05-2011 CrysAlis171 .NET) (compiled May 16 2011,17:55:39) Analytical numeric absorption correction using a multifaceted crystal model based on expressions derived by R.C. Clark & J.S. Reid. (Clark, R. C. & Reid, J. S. (1995). Acta Cryst. A51, 887-897)	$k = -19 \rightarrow 19$
$T_{min} = 0.733$, $T_{max} = 0.929$	$l = -21 \rightarrow 21$
58855 measured reflections	

Refinement

Refinement on F^2	Primary atom site location: structure-invariant direct methods
Least-squares matrix: full	Hydrogen site location: inferred from neighbouring sites
$R[F^2 > 2\sigma(F^2)] = 0.047$	Method, part 1, Chebychev polynomial, (Watkin, 1994, *P*rince, 1982) [*w*eight] = $1.0/[A_0*T_0(x) + A_1*T_1(x) \cdots + A_{n-1}]*T_{n-1}(x)]$ where A_i are the Chebychev coefficients listed belo*w* and x = *F* /*F*max Method = Robust Weighting (*P*rince, 1982) W = [*w*eight] * [1-(delta*F*/6*sigma*F*)^2]^2 A_i are: 0.153E + 04 0.229E + 04 0.128E + 04 361.
$wR(F^2) = 0.122$	$(\Delta/\sigma)_{max} = 0.001$
S = 1.06	$\Delta\rangle_{max} = 1.49$ e Å^{-3}
7089 reflections	$\Delta\rangle_{min} = -2.23$ e Å^{-3}
317 parameters	Extinction correction: Larson (1970), Equation 22
0 restraints	Extinction coefficient: 24 (4)

Geometric parameters (Å, º)

Ru1—Cl2	2.3393 (10)	C18—C23	1.392 (5)
Ru1—Cl3	2.3310 (9)	C19—C20	1.388 (6)
Ru1—O4	2.255 (3)	C19—H191	0.929
Ru1—C10	1.840 (4)	C20—C21	1.375 (6)
Ru1—C15	1.985 (4)	C20—H201	0.933
O4—C5	1.472 (5)	C21—C22	1.386 (6)
O4—C8	1.383 (4)	C21—H211	0.926
C5—C6	1.513 (6)	C22—C23	1.382 (6)
C5—C7	1.522 (6)	C22—H221	0.932
C5—H51	0.985	C23—H231	0.934
C6—H62	0.958	C24—C25	1.340 (5)
C6—H61	0.967	C24—H241	0.933
C6—H63	0.957	C25—N26	1.388 (5)
C7—H71	0.965	C25—H251	0.930
C7—H73	0.966	N26—C27	1.442 (4)
C7—H72	0.964	C27—C28	1.389 (5)
C8—C9	1.393 (5)	C27—C32	1.387 (5)
C8—C14	1.387 (5)	C28—C29	1.393 (5)
C9—C10	1.453 (5)	C28—C35	1.503 (5)
C9—C11	1.405 (5)	C29—C30	1.383 (5)
C10—H101	0.938	C29—H291	0.931
C11—C12	1.390 (6)	C30—C31	1.389 (6)

C11—H111	0.931	C30—C34	1.507 (5)
C12—C13	1.389 (6)	C31—C32	1.397 (5)
C12—H121	0.933	C31—H311	0.936
C13—C14	1.399 (6)	C32—C33	1.509 (5)
C13—H131	0.937	C33—H331	0.957
C14—H141	0.932	C33—H333	0.963
C15—N16	1.360 (4)	C33—H332	0.955
C15—N26	1.363 (5)	C34—H341	0.962
N16—C17	1.464 (5)	C34—H343	0.958
N16—C24	1.395 (5)	C34—H342	0.960
C17—C18	1.509 (5)	C35—H351	0.965
C17—H172	0.969	C35—H352	0.965
C17—H171	0.978	C35—H353	0.966
C18—C19	1.389 (5)		
Cl2—Ru1—Cl3	151.61 (3)	C17—C18—C19	121.4 (3)
Cl2—Ru1—O4	88.83 (7)	C17—C18—C23	120.1 (3)
Cl3—Ru1—O4	91.54 (7)	C19—C18—C23	118.5 (4)
Cl2—Ru1—C10	104.15 (12)	C18—C19—C20	121.1 (4)
Cl3—Ru1—C10	103.84 (12)	C18—C19—H191	119.0
O4—Ru1—C10	79.75 (13)	C20—C19—H191	120.0
Cl2—Ru1—C15	92.16 (11)	C19—C20—C21	119.4 (4)
Cl3—Ru1—C15	86.88 (11)	C19—C20—H201	120.4
O4—Ru1—C15	178.21 (13)	C21—C20—H201	120.3
C10—Ru1—C15	101.44 (16)	C20—C21—C22	120.7 (4)
Ru1—O4—C5	128.0 (2)	C20—C21—H211	119.8
Ru1—O4—C8	110.1 (2)	C22—C21—H211	119.5
C5—O4—C8	119.2 (3)	C21—C22—C23	119.6 (4)
O4—C5—C6	106.0 (3)	C21—C22—H221	120.0
O4—C5—C7	110.3 (3)	C23—C22—H221	120.4
C6—C5—C7	113.4 (3)	C18—C23—C22	120.8 (4)
O4—C5—H51	108.4	C18—C23—H231	119.6
C6—C5—H51	109.0	C22—C23—H231	119.6
C7—C5—H51	109.5	N16—C24—C25	106.5 (3)
C5—C6—H62	108.6	N16—C24—H241	125.6
C5—C6—H61	109.5	C25—C24—H241	127.9
H62—C6—H61	109.7	C24—C25—N26	107.3 (3)
C5—C6—H63	109.9	C24—C25—H251	127.2
H62—C6—H63	109.7	N26—C25—H251	125.5
H61—C6—H63	109.4	C25—N26—C15	110.9 (3)

C5—C7—H71	108.9	C25—N26—C27	122.8 (3)
C5—C7—H73	109.6	C15—N26—C27	126.1 (3)
H71—C7—H73	109.6	N26—C27—C28	118.9 (3)
C5—C7—H72	109.4	N26—C27—C32	118.0 (3)
H71—C7—H72	109.7	C28—C27—C32	123.0 (3)
H73—C7—H72	109.6	C27—C28—C29	117.5 (3)
O4—C8—C9	113.0 (3)	C27—C28—C35	121.0 (3)
O4—C8—C14	125.0 (4)	C29—C28—C35	121.4 (3)
C9—C8—C14	122.0 (4)	C28—C29—C30	121.7 (4)
C8—C9—C10	119.3 (3)	C28—C29—H291	119.2
C8—C9—C11	118.6 (3)	C30—C29—H291	119.1
C10—C9—C11	122.1 (4)	C29—C30—C31	118.7 (4)
C9—C10—Ru1	117.9 (3)	C29—C30—C34	120.7 (4)
C9—C10—H101	120.6	C31—C30—C34	120.6 (4)
Ru1—C10—H101	121.5	C30—C31—C32	121.9 (4)
C9—C11—C12	120.4 (4)	C30—C31—H311	119.5
C9—C11—H111	119.3	C32—C31—H311	118.6
C12—C11—H111	120.3	C31—C32—C27	117.1 (3)
C11—C12—C13	119.6 (4)	C31—C32—C33	121.5 (3)
C11—C12—H121	120.0	C27—C32—C33	121.4 (3)
C13—C12—H121	120.4	C32—C33—H331	110.4
C12—C13—C14	121.2 (4)	C32—C33—H333	110.3
C12—C13—H131	119.4	H331—C33—H333	109.6
C14—C13—H131	119.4	C32—C33—H332	109.1
C13—C14—C8	118.2 (4)	H331—C33—H332	109.1
C13—C14—H141	120.7	H333—C33—H332	108.4
C8—C14—H141	121.1	C30—C34—H341	110.1
Ru1—C15—N16	120.4 (3)	C30—C34—H343	110.5
Ru1—C15—N26	135.1 (3)	H341—C34—H343	108.7
N16—C15—N26	104.2 (3)	C30—C34—H342	109.9
C15—N16—C17	124.7 (3)	H341—C34—H342	108.8
C15—N16—C24	111.1 (3)	H343—C34—H342	108.8
C17—N16—C24	124.0 (3)	C28—C35—H351	110.0
N16—C17—C18	111.0 (3)	C28—C35—H352	109.4
N16—C17—H172	109.1	H351—C35—H352	109.4
C18—C17—H172	109.7	C28—C35—H353	109.6
N16—C17—H171	108.9	H351—C35—H353	109.4
C18—C17—H171	109.4	H352—C35—H353	109.1
H172—C17—H171	108.6		

6. References

1. Berlo, B. V.; Houthoofd, K.; Sels, B. F.; Jacobs, P. A. *Adv. Synth. Catal.* **2008**, *350*, 1949.

2. (a) Buchmeiser, M. R. *New J. Chem*. **2004**, *28*, 549-557. (b) Coperet, C.; Basset, J.-M.*Adv. Synth. Catal.* **2007**, *349*, 78. (c) Clavier, H.; Grela, K.; Kirschning, A.; Mauduit, M.; Nolan, S. P. *Angew. Chem. Int.Ed.* **2007**, *46*, 6786. b) Sommer, W. J.; Weck, M. *Coord. Chem. Rev.* **2007**, *251*, 860. (d) Buchmeiser, M. R. *Chem. Rev.* **2009,** *109,* 303. (e) Rendón, N.; Blanc, F.; Coperet, C. *Coord. Chem. Rev.* **2009**, *253*, 2015. (f) Marciniec, B.; Rogalski, S.; Potrzebowski, M. J.; Pietraszuk, C. *ChemCatChem.* **2011**, *3*, 904.

3. (a) Nieczypor, P.; Buchowicz, W.; Meester, W. J. N.; Rutjes, F. P. J. T.;Mol, J. C. *Tetrahedron Lett.* **2001,** *42,* 7103. (c) Krause, J. O.; Wurst, K.;Nuyken, O.; Buchmeiser, M. R. *Chem.Eur. J.* **2004**, *10*, 778. (d) Halbach, T. S.; Mix, S.; Fischer, D.; Maechling, S.; Krause, J. O.;Sievers, C.; Blechert, S.; Nuyken, O.; Buchmeiser, M. R. *J. Org. Chem.* **2005,** *70,* 4687. (e) Vehlow, K.; Maechling, S.; Köhler, K.; Blechert, S. *J. Organomet. Chem.* **2006,** *691,* 5267. (f) Bek, D.; Žilková, N.; Dědeček, J.; Sedláček, J.; Balcar, H. *Top. Catal.* **2010,** *53,* 200.

4. (a) Nguyen, S. T.; Grubbs, R. H. *J. Organomet. Chem.* **1995**, *497*, 195. (b) Schürer, S. C.; Gessler, S.; Buschmann, N.; Blechert, S. *Angew. Chem., Int. Ed.***2000**, *39*, 3898. (c) Melis, K.; De Vos, D.; Jacobs, P.; Verpoort, F. *J. Mol. Catal. A: Chem.***2001**, *169,* 47. (d) Mayr, M.; Buchmeiser, M. R.; Wurst, K. *Adv. Synth. Catal.* **2002**, *344,*712. (e) Prühs, S.; Lehmann, C. W.; Fürstner, A. *Organometallics* **2004**, *23*, 280. (f) Li, L.; Shi, J. *Adv. Synth. Catal.* **2005**, *347*, 1745. (g) Allen, D. P.; Van Wingerden, M. M.; Grubbs, R. H. *Org. Lett.* **2009**, 11, 1261. (h) Karame, I.; Boualleg, M.; Camus, J. M.; Maishal, T. K.; Alauzun, J.; Basset, J. M.; Coperet, C.; Corriu, R. J. P.; Jeanneau, E.; Mehdi, A.; Reye, C.; Veyre, L.; Thieuleux, C. *Chem. Eur. J.* **2009**, 15, 11 820.

5. (a) Nguyen, S. T.; Grubbs, R. H. *J. Organomet. Chem.* **1995**, *497*, 195. (b) Jafarpour, L.; Nolan, S. P. *Organic Letters* **2000**, *2*, 4075. (c) Kingsbury, J. S.; Garber, S. B.; Giftos, J. M.; Gray, B. L.; Okamoto, M. M.; Farrer, R. A.; Fourkas, J. T.; Hoveyda, A. H. *Angew. Chem., Int. Ed.* **2001,** *40,* 4251. (d) Jafarpour, L.; Heck, M. P.; Baylon, C.; Man Lee, H.; Mioskowski, C.; Nolan, S. P. *Organometallics* **2002**, *21*, 671. (e) Yao, Q.; Motta, A. R. *Tetrahedron Lett.* **2004,** *45,* 2447. (f) Zarka, M. T.; Nuyken, O.; Weberskirch, R. *Macromol. Rapid Commun.* **2004,** *25,* 858. (g) Fischer, D.; Blechert, S. *Adv. Synth. Catal.* **2005,** *347,* 1329. (h) Elias, X.; Pleixats, R.; Man, M. W. C. *Tetrahedron* **2008,** *64,* 6770. (i) Lim, J.; Lee, S. S.; Ying, J. Y. *Chem. Commun.* **2010**, *46,* 806.

6. (a) Vorfalt, T.; Wannowius, K. J.; Thiel, V.; Plenio, H. *Chem. Eur. J.* **2010**, *16*, 12312. (b) Vorfalt, T.; Wannowius, K. J.; Thiel, V.; Plenio, H. *Angew. Chem. Int. Ed.* **2010**, *49*, 5533.

7 . Parry, E. P. *J. Catal.* **1963**, *2,* 371.

8 . Hoveyda, A. H.; Gillingham, D. G.; Van Veldhuizen, J. J.; Kataoka, O.; Garber, S. B.; Kingsbury, J. S.; Harrity, J. P. A. *Org. Biomol. Chem.,* **2004***, 2,* 8.

9. Vehlow, K.; Maechling, S.; Blechert, S. *Organometallics* **2006,** *25,* 25.

Chapter 5
General conclusion
and
Perspectives

1. General conclusion

The main objective of the study was to selectively form lower cyclic oligomers (in particular cyclooctene dimer) in RO-RCM of cyclooctene. The strategy was to develop well-defined, single-site mesostructured heterogeneous materials containing regularly distributed Ru-NHC units along the pore channels of their silica matrix and to use the pore confinement to constrain the formation of cyclic structures over polymers, *i.e.* to favor backbiting over polymerization.

Towards this goal, we prepared and characterized hybrid, heterogeneous Ru-NHC based catalysts with different tether lengths and flexibilities: **M-RuPr** *(short-flexible tether)*, **M-RuBn** *(semi-rigid tether)*, **M-RuHex** *(long-flexible tether)*, **M-RuPhMs** *(long-rigid tether)* and **M-RuMs** *(short-rigid tether).*

The structural investigation of these catalysts by ^{31}P NMR revealed that the active sites of catalysts having shorter and flexible tethers do not contain a coordinated PCy_3, but are stabilized by surface functionalities. Increasing the length and the rigidity of the tether shows an increasing amount of PCy_3 coordinated to Ru as evidence that surface functionalities can no longer stabilize these systems.

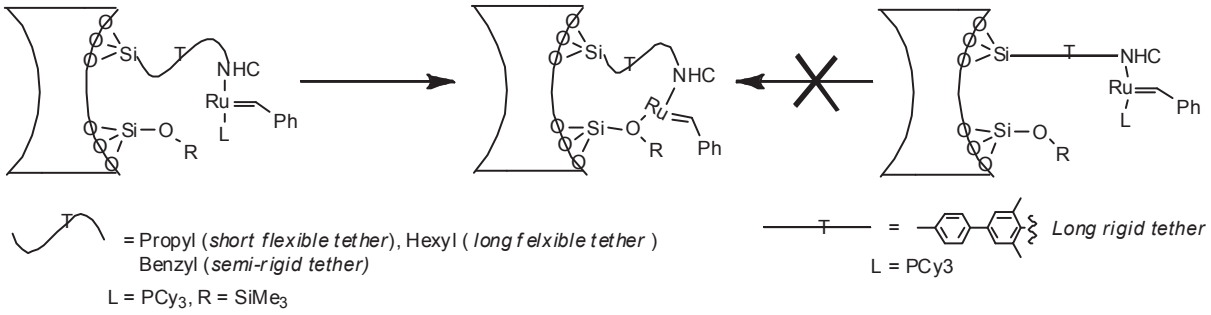

Scheme 1: Interaction of surface functionality with Ru-NHC active site.

We also showed that these catalysts displayed unprecedented high mass balance and selectivity for low cyclic oligomers (dimer and trimers) compared to those of symmetrical **G-II** and **GH-II** homogeneous catalysts. In particular, the mass balance was 85-90% and remained constant throughout the reaction with dimer and trimer selectivities of 50% and 25%, respectively. These data clearly show the preference for the cyclic oligomers formation over polymers, in other words backbiting is favoured over polymerization. Furthermore, among these highly selective catalysts, those with short-flexible tethers (**M-RuPr** and **M-RuBn**) are the best ones in particular in terms of rate and stability, thus further illustrating the

influence of Ru-NHC interactions with the surface functionalities. Further kinetic investigation on the **M-RuPr** catalyst showed that RO-RCM reaction was 1st order in cyclooctene, and that the dimer and trimer were found to be primary products, while the tetramer and pentamer were secondary products.

To understand the origin of this selectivity towards low cyclic oligomers, we prepared the isostructural homogeneous Ru-NHC complexes with unsymmetrical NHC ligands. We showed that their reactivity and selectivity are similar to those of previously prepared heterogeneous homologues and that the main factor influencing the dimer and trimer selectivity was the unsymmetry on the NHC ligand and not pore confinement.

The collected data allowed us to propose an hypothetical mechanism explaining the observed selectivity towards cyclic oligomers and fitting the experimental observations (the prefered formation of dimers and trimers and their 2:1 ratio, Table 1).This mechanism is based on the catalyst architecture which exhibits dual site configuration (see Scheme 1).

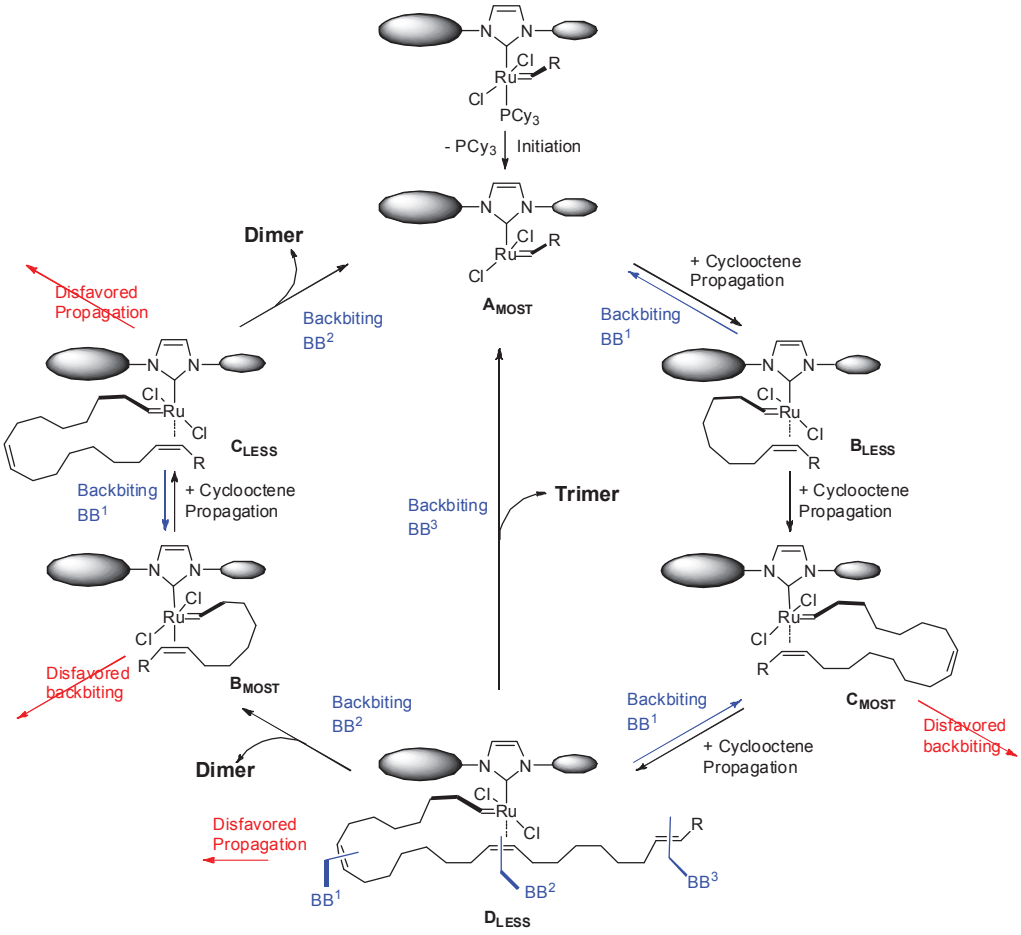

Scheme 1: Proposed mechanism for the tandem Ring Opening-Ring Closing Metathesis of cis-cyclooctene, selective formation of dimer and trimer. (Mesityl represents the small group while Propyl or Benzyl represent the bulky group, BB^n = backbiting, n = position of alkene from the carbene carbon).

Table 1: Ratio of dimer to trimer in RO-RCM of cyclooctene using homogeneous/heterogeneous catalysts.

Catalyst	Selectivity (%)		Ratio of dimer/trimer	
	Dimer	Trimer	Experimental	Expected
RuPr	**48**	**24**	2	2
$RuPr_{Si}$	**51**	**24**	2.1	2
M-RuPr	**53**	**22**	2.4	2
RuBn	**50**	**24**	2.1	2
$RuBn_{Si}$	**51**	**23**	2.1	2
M-RuBn	**54**	**20**	2.7	2
RuPhMs	**52**	**25**	2.1	2
M-RuPhMs	**45**	**19**	2.4	2
M-RuMs	**34**	**17**	2	2
M-RuHex	**54**	**24**	2.2	2

Finally, we also showed that for the BASF catalyst the selectivity was very similar to that of unsymmetrical systems, and we thus proposed that adsorbing **GH-II** on silica promotes the disymmetrization of the complex. Attempts to further increase the selectivity of these systems by adsorbing unsymmetrical precursors was carried out, but such systems displayed unfortunately very little activity and no improvement of selectivity.

Overall, we have successfully developed both well-defined single site Ru-NHC based heterogeneous catalysts and their homogeneous analogues for the selective formation of cyclic oligomers. The Ru-NHC alkylidene metathesis catalysts were found to require unsymmetrical NHC ligands to generate a dual catalytic site configuration: one site favors intramolecular backbiting while the other one coordinates an additional substrate (intermolecular) and favors propagation. This original catalyst architecture provided selectivity for the formation of small cyclic oligomer (dimer and trimer) – over polymers from cyclooctene *via* a tandem RO-RCM reaction. These new results open perspectives in forming selectively macrocycles from other cyclic alkenes *via* metathesis.

2. Perspectives

Knowing that the unsymmetrical nature of NHC is key for the selective formation of low cyclic oligomers in the tandem RO-RCM of cyclooctene, it would be interesting to test these catalysts with other cycloolefins (cycloheptene, cyclopentene *etc.*) as substrates for the formation of the corresponding low cyclic oligomers (dimer, trimer and tetramers), because these molecules are key intermediates in the flavor and perfume industry (synthesis of macrocyclic musks).

With the catalyst architecture having dual-site configuration, it would also be worth looking at the alternating co-RO-RCM for various mixture of cyclic alkenes. For example cyclohexene does not undergo metathesis and thus cannot be used to generate cyclic C_{12} diene. However, co-RO-RCM of cycloheptene and cyclopentene could be an attractive solution for this product. Moreover, generation of odd numbered cyclic systems like C_{13} (cyclooctene + cyclopentene) and C_{15} (cyclooctene + cycloheptene) could also be generated by this approach, taking into account that these reactions depend on several factors like reactivity differences of substrates.

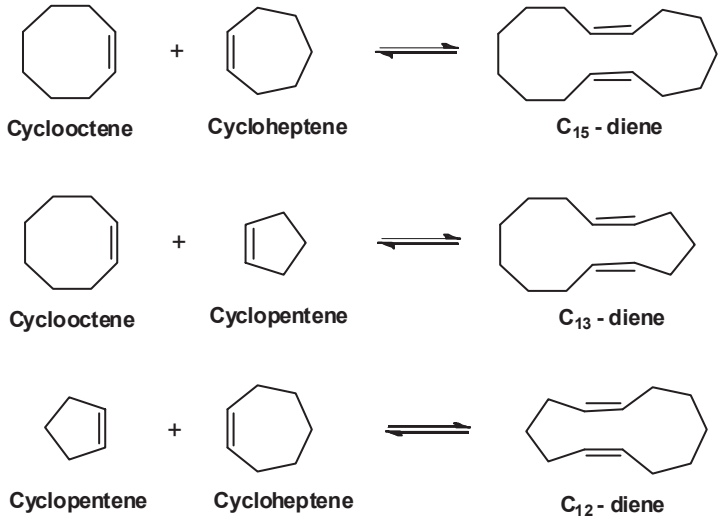

Scheme 1: Alternating co-RO-RCM reaction.

Finally, it would also be important to investigate in more details the structure (in particular, how the molecular complex interacts with the surface) of the BASF catalyst (**RuGH-II/silica**) to obtain deeper understanding of the observed reactivity and selectivity in RO-RCM of cyclooctene. Structure investigation by surface enhanced NMR spectroscopy using dinuclear polarization technique (DNP) could be the way forward.[1-2]

3. References

1. Lesage, A.; Lelli, M.; Gajan, D.; Caporini, M. A.; Vitzthum, V.; Miéville, P.; Alauzun, J.; Roussey, A.; Thieuleux, C.; Mehdi, A.; Bodenhausen, G.; Copéret, C.; Emsley, L. *J. Am. Chem. Soc.* **2010**, *132*, 15459.

2. Lelli, M.; Gajan, D.; Lesage, A.; Caporini, M. A.; Vitzthum, V.; Miéville, P.; Héroguel, F.; Rascón, F.; Roussey, A.; Thieuleux, C.; Boualleg, M.; Veyre, L.; Bodenhausen, G.; Copéret, C.; Emsley, L. *J. Am. Chem. Soc.* **2011**, *133*, 2104.